Late Quaternary palaeoenvironmental change in the northeastern Mediterranean: a diatom-based reconstruction from lacustrine sediments

A thesis submitted to the University of Hull

for the degree of

Doctor of Philosophy

Robyn Francesca Seymour-Jones

January 2022

Abstract

Much of our understanding of Quaternary palaeoenvironmental change has been generated from long, continuous marine sediment and ice core sequences. These records span multiple glacial–interglacial cycles, providing an essential long-term perspective on natural climate variability that sets the context for recent anthropogenic climate change. However, to develop resilience to future climatic changes, it is crucial to understand the manifestation of global climatic change over terrestrial regions and the environmental response to such changes. This is especially critical in hydrologically sensitive, semi-arid regions such as the northeastern Mediterranean, where anthropogenic climate change is already having a detrimental impact on water security. This region is remarkable for its high density of ancient lakes, and long sediment cores of good stratigraphic continuity have been recovered from Lake Ioannina (Greece) and Lake Ohrid (North Macedonia/Albania). These have been used to produce reconstructions of environmental change spanning multiple glacial–interglacial cycles.

This thesis generates new diatom assemblage records from these two lakes to fill the gap in our knowledge about MIS 7–9, an interval of particular interest given the relatively weak glacial–interglacial changes at this time. These lakes are only c. 150 km apart, so are subject to the same climatic forcing, but shallow, eutrophic Lake Ioannina experiences significant lake-level fluctuations, while deep, oligotrophic Lake Ohrid is renowned for its long-term stability. By comparing the diatom assemblages of these two lakes and their differing response to the same climatic forcing, changes in hydroclimate and temperature can be better disentangled. Meanwhile, existing palynological and geochemical data enable the separation of the palaeoclimate signal from other drivers of limnological change.

The results reveal a diatom response at Lake Ioannina that is driven by variations in lake level and mixing regime and is remarkably subtle, with the persistence of a relatively deep lake throughout most of MIS 7–9. In contrast, the response at Lake Ohrid during MIS 7 reflects temperature changes, which become more variable on the approach towards the penultimate glacial inception.

Acknowledgements

Contents

List of figures

List of tables

Abbreviations

AP	Arboreal pollen
AP–PJB	Arboreal pollen minus *Pinus*, *Juniperus* and *Betula*
bSi	Biogenic silica
CONISS	Constrained incremental sum of squares
DAZ	Diatom assemblage zone
DCA	Detrended correspondence analysis
EMPT	Early–Middle Pleistocene Transition
GHG	Greenhouse gas
GMST	Global mean surface temperature
IDZ	Ioannina diatom zone
IPCC	Intergovernmental Panel on Climate Change
IRD	Ice-rafted debris
ITCZ	Intertropical convergence zone
ka	Kilo-annum (used in this thesis to refer to thousands of years ago)
kyr	Thousand years (used in this thesis to refer to duration in thousands of years)
NAO	North Atlantic oscillation

NAP	Non-arboreal pollen
ODZ	Ohrid diatom zone
Ma	Mega-annum (used in this thesis to refer to millions of years ago)
MIS	Marine isotope stage
P–B ratio	Planktonic to benthic ratio
PCA	Principal component analysis
SBER	Southern Balkan extensional region
SEM	Scanning electron microscopy
SST	Sea surface temperature
$\delta^{18}O$	Ratio of ^{18}O to ^{16}O
$\delta^{13}C$	Ratio of ^{13}C to ^{12}C

Chapter 1 | Introduction

This thesis examines lacustrine sediments from the northeastern Mediterranean in the context of past environmental change. Specifically, it investigates diatom responses to changing environmental conditions in two proximal but contrasting ancient lakes: Lake Ioannina (Greece) and Lake Ohrid (Albania/North Macedonia). The data generated are used to establish the palaeolimnological histories of the lakes during the glacial–interglacial cycles equivalent to marine isotope stages (MIS) 7–9 and subsequently to contribute to our knowledge of northeastern Mediterranean palaeoclimate. The rationale and context of the research is provided in this chapter before an outline of the aims and objectives of the thesis. The chapter concludes with a summary of the thesis structure.

1.1 Research context

1.1.1 Contemporary climate change

It is now considered unequivocal that greenhouse gas (GHG) emissions resulting from human activities are causing widespread and rapid changes in the climate system on a scale that is unprecedented over many centuries to many thousands of years (IPCC, 2021). Global mean surface temperatures (GMST) are estimated to have increased by approximately 1°C since the nineteenth century (Gulev et al., 2021), and further warming is projected for the twenty-first century, the severity of which depends on the trajectory of future anthropogenic GHG emissions (Lee et al., 2021). Hydroclimate changes are expected to accompany twenty-first-century warming, with the hydrological cycle anticipated to intensify (Douville et al., 2021) and annual global land precipitation projected to increase (Lee et al., 2021). However, these global averages hide substantial regional and seasonal differences, as well as climate extremes.

Temperature increases are expected to be greater over land than over the oceans (Sutton et al., 2007) with both warm and cold temperature extremes over land projected to increase at a faster pace than mean global temperature (Seneviratne et al., 2016). Warming is likely to be particularly pronounced over the Arctic, a phenomenon known as the Arctic amplification (Pithan & Mauritsen, 2014). At these high northern latitudes, winter warming is expected to be stronger than summer warming, resulting in a reduced amplitude of the seasonal cycle of surface temperatures (Dwyer et al., 2012; Bintanja & van der Linden, 2013). In contrast, the subtropics and mid-latitudes are expected to experience stronger summer warming with an amplification of the seasonal surface temperature cycle (Dwyer et al., 2012; Santer et al., 2018). The hydroclimate response to warming will exhibit substantial spatial variation, with mean annual precipitation expected to increase over large parts of the middle to high latitudes, decrease over parts of the subtropics and display contrasting responses between different parts of the tropics (Lee et al., 2021). The characteristics of precipitation over most land areas are expected to change in a similar way and include an increase in the intensity of precipitation events, the occurrence of extreme events of unprecedented magnitude and an increase in the number of dry days with increased dry spell length (Giorgi et al., 2014; Giorgi et al., 2019).

The Mediterranean has long been identified as a region with a climate that is particularly responsive to global change, and it has consequently been labelled a climate change "hot spot" with projected warming and drying over the twenty-first century, especially during summers (Giorgi, 2006). This remains evident in more recent climate models, which predict regional warming at a pace 20% higher than the global mean and marked decreases in regional precipitation as a function of GMST increase during the twenty-first century (Lionello & Scarascia, 2018). On parts of the Balkan Peninsula, summer temperatures are expected to warm at a rate twice that of GMST (Figure 1.1a) and annual precipitation is expected to decrease by 50 mm per degree of GMST

increase (Figure 1.1b). The reduced precipitation and increased evaporative demand will make the region drier, reduce soil moisture and increase drought occurrence, intensity and severity (Douville et al., 2021). Existing environmental problems are likely to be exacerbated, with reduced freshwater availability putting additional pressure on increasingly in-demand water resources (Cramer et al., 2018). An improved understanding of the responses of the regional climate and freshwater systems to changes in GMST will enable us to better prepare for future change and assist in the sustainable management of water resources in this highly responsive and vulnerable region. One way this can be accomplished is to investigate earlier such responses within the geological record.

1.1.2 Quaternary palaeoclimatology

Palaeoclimate records provide an essential long-term perspective on natural climate variability that sets the context for recent anthropogenic climate change (Chen, D. et al., 2021). Natural archives left behind by geological, chemical and biological processes can be exploited to reconstruct past environmental and climatic change in the absence of human impact and over a range of temporal scales and resolutions. One of the most convenient and rewarding time periods to focus on is the Quaternary, which is the current geological period and spans the last 2.58 million years (Gibbard & Head, 2009a). It has exhibited characteristic cycles associated with large variations in global ice volume (the glacial–interglacial cycles; Lowe & Walker, 2015). Changes that have operated over shorter millennial timescales are increasingly being identified in regional and local records of past change (Fletcher et al., 2010). This range of variability provides an abundance of natural experiments within which past limnetic and regional climatic responses to global change can be investigated (Tzedakis et al., 2009a).

The majority of studies have focused on the late glacial and Holocene (the end of the last glacial period to the current interglacial) as natural archives
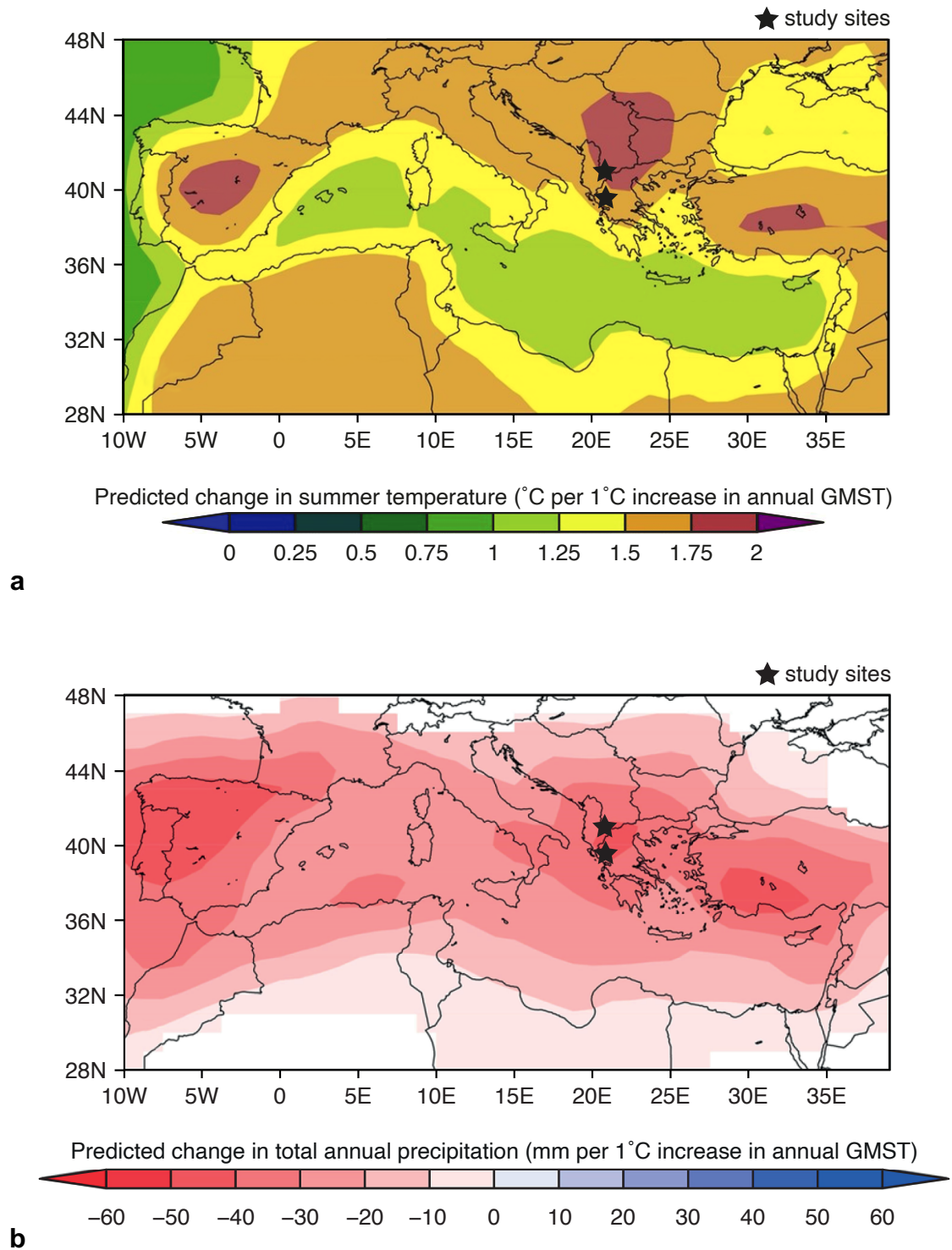
Figure 1.1: Spatial distribution of predicted changes in summer (June, July and August) temperature (**a**) and total annual precipitation (**b**) as a function of change in annual GMST (modified from Lionello & Scarascia, 2018). The locations of the study sites on the Balkan Peninsula are indicated. They are predicted to experience summer temperature increases that are 1.5–2 times greater than any increase in annual GMST and a decline of 30–50 mm per degree of annual GMST increase.

containing sediments from this period are more widespread and easier to retrieve for study than those of earlier glacial–interglacial cycles. Many records have been published that show in detail how the climate of the Mediterranean region has changed during this time (e.g. Roberts et al., 2011a; Dean et al., 2015; Finné et al., 2019). At a basic level, glacials in the Mediterranean region are drier and interglacials wetter, although as these published palaeoclimate reconstructions demonstrate, there can be significant variability in moisture availability through time whilst a glacial or interglacial progresses. The availability of such a large number of records spanning this time period has also enabled spatial contrasts in moisture availability to be identified across the Mediterranean. Magny et al. (2013) proposed a north–south contrast either side of c. 40°N, while other studies have suggested the existence of east–west contrasts (Roberts et al., 2008; Roberts et al., 2011b; Roberts et al., 2012).

Due to the smaller number of studies, the potential to establish a similar level of knowledge for earlier glacial–interglacial cycles is more limited. More records spanning earlier intervals are needed if we are to take advantage of the wide range of natural experiments offered by the Quaternary Period to improve our understanding of how Mediterranean climates and environments respond to global change. Earlier intervals of focus have included the interglacials equivalent to MIS 5e, which is also relatively well represented in natural archives, and MIS 11, due to its potential as an analogue for future climate trajectories (Candy et al., 2014). In comparison, relatively little attention has been paid to the intervening climatic cycles of MIS 7–9 (c. 190–340 ka), which have been identified as weak in marine sediment and ice core records (Lang & Wolff, 2011).

1.1.3 The value of ancient lakes in palaeoclimate research

The dynamic nature of Earth's surface, especially the erosional effects of the Pleistocene ice sheets, limits the age of terrestrial records so that those spanning multiple glacial–interglacial cycles are rare (Lang & Wolff, 2011; Past

Interglacials Working Group of PAGES, 2016). As a consequence, much of our understanding of Quaternary climate change preceding the last glacial–interglacial cycle has been generated from long, continuous marine sediment and ice core sequences. However, these are not able to provide an accurate account of climatic and environmental change over the terrestrial regions we inhabit (Gibbard & Hughes, 2021). Long records from terrestrial archives are required.

In addition to being a region where it is critical to understand the effects of future climate change (section 1.1.1), the Mediterranean is located south of the southern limit of the northern hemisphere Pleistocene ice sheets. Therefore, conditions in the region have been favourable for the accumulation of relatively undisturbed, thick sedimentary sequences of Quaternary climatic and environmental change that can be used to address such needs (Tzedakis et al., 1997). Rare terrestrial records spanning multiple glacial–interglacial cycles have been obtained from sites around the Mediterranean region including the Velay mountains (France; e.g. Reille et al., 1998), Valle di Castiglione (Italy; e.g. Follieri et al., 1988), Tenaghi Philippon (Greece; e.g. Tzedakis et al., 2006; Pross et al., 2015), Lake Van (Turkey; e.g. Litt et al., 2014) and the two sites investigated in this thesis: Lake Ioannina (Greece; e.g. Tzedakis et al., 2002a; Roucoux et al., 2008; Roucoux et al., 2011; Wilson et al., 2021) and Lake Ohrid (North Macedonia/Albania; e.g. Wagner et al., 2017; Wagner et al., 2019).

The thick sedimentary sequences retrieved from Lake Ioannina and Lake Ohrid originate from a type of lacustrine system known as an ancient lake. This is a term that is applied to long-lived continental water bodies that have persisted for tens of thousands to millions of years (Wilke et al., 2016; Albrecht et al., 2020). It differentiates the small proportion of the world's lakes that are long-lived from the numerous shorter-lived lakes that have formed since the last glacial maximum and are therefore no older than around 18 kyr (Albrecht et al., 2006). In addition to a location away from the influence of the erosional Pleistocene ice sheets, many ancient lakes are situated in tectonic basins where

subsidence counteracts sedimentation, allowing the accumulation of thick sediment sequences, some of which are hundreds of meters thick, without the lake filling in completely (Wilke et al., 2016). In contrast to other depositional environments, the sedimentation in lakes is relatively rapid and uninterrupted, so these sediment sequences can provide highly resolved records of past climate and environmental change (Cohen, 2012). Such records are generated from a variety of biotic components (e.g. pollen, diatoms, ostracods, chironomids, cladocerans, plant microfossils, etc.) and abiotic properties (e.g. organic and inorganic geochemistry, magnetic properties, stable isotopes, grain size, etc.) that are sensitive to climatic and catchment processes and therefore act as indicators of palaeoenvironmental conditions (Cohen, 2003).

1.1.4 Diatoms as indicators of past environmental and climatic change

Lake sediments are derived from various organic and inorganic materials delivered from the catchment and atmosphere (allochthonous material) or produced within the lake itself (autochthonous material; Figure 1.2). One organic component of lake sediments is a group of microscopic algae known as the diatoms (Class Bacillariophyceae; Round et al., 1990). These single-celled, photosynthetic eukaryotes are an abundant and diverse group, distributed ubiquitously in most aquatic environments where they tend to occur in large numbers, both as solitary cells and in colonies (Julius & Theriot, 2010). A very large number of diatom species are ecologically sensitive, which has encouraged their use in biological monitoring and palaeoenvironmental investigations (Smol & Stoermer, 2010).

Diatom records have proven value in the Mediterranean region, especially when analysed alongside other proxies (indicators of past change). Those spanning the late glacial and Holocene have contributed to our understanding of hydroclimate changes during the most recent glacial–interglacial cycle. Shifts in the dominance of different diatom taxa have tended to reflect changes
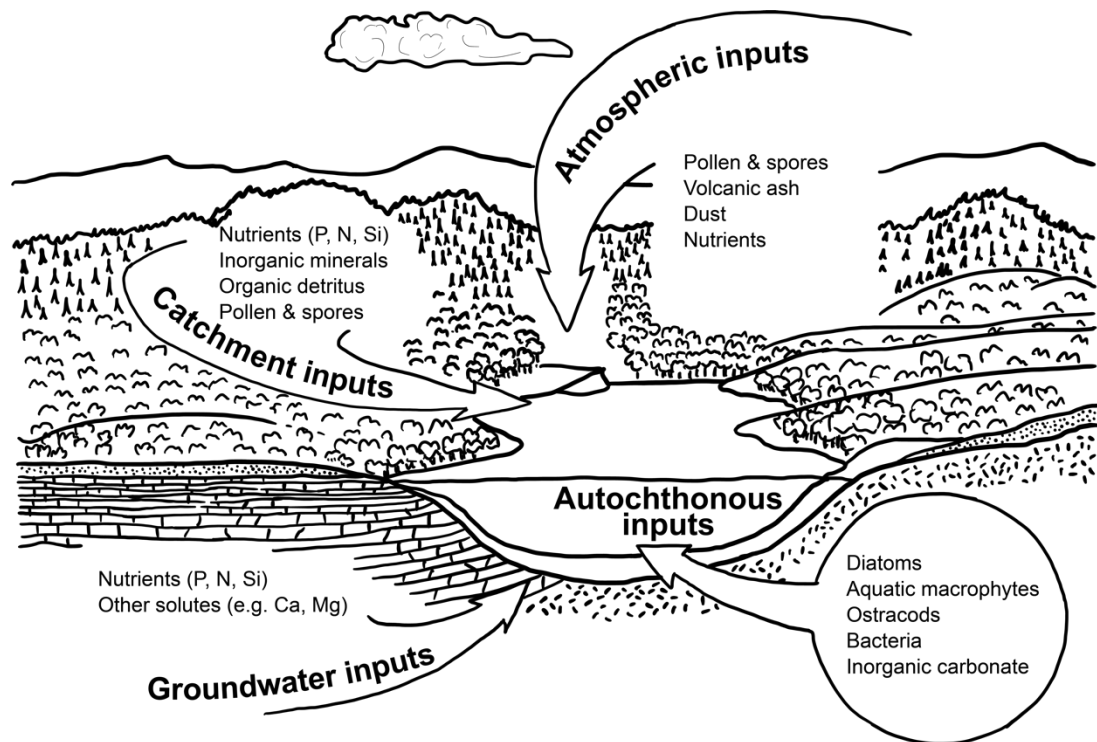
Figure 1.2: Diagram illustrating some of the various allochthonous and autochthonous components that would have been deposited in lacustrine sediments prior to anthropogenic influences (modified from Smol et al., 2001).

in lake levels as moisture availability varied (e.g. Jones et al., 2013; Cvetkoska et al., 2014a; Vossel et al., 2018). Other diatom community shifts have the ability to inform on past temperature changes where they are the result of temperature-driven productivity changes (e.g. Zhang et al., 2016). These diatom community responses are extremely sensitive so have been able to demonstrate the occurrence of abrupt climate changes in the Mediterranean (e.g. Wilson et al., 2008). Diatoms are therefore an ideal proxy to use when investigating past limnetic and regional climatic responses to global change over a range of timescales.

1.2 Aims and objectives

This chapter has demonstrated that the response of the Mediterranean region during the late glacial and Holocene are well documented, but less is known

about how the Mediterranean responded during glacial–interglacial cycles further back in time. Of particular interest is the interval spanning MIS 7–9, within which global records have suggested weak glacials and interglacials, but for which few records exist from the Mediterranean region.

This project uses long sedimentary sequences from Lake Ioannina and Lake Ohrid to address this gap in our knowledge. Diatom records from these lakes spanning recent glacial–interglacial cycles have demonstrated a high sensitivity to climatic change compared to other proxies. In particular, comparing the diatom records from Ioannina (where they have previously been seen to respond more to lake level; Jones et al., 2013) and Ohrid (where they have previously been seen to respond more to temperature; Zhang et al., 2016) should allow for a robust palaeoclimate reconstruction.

This project aims to:

1. Improve our understanding of how diatoms respond to changing environmental conditions at Lake Ioannina and Lake Ohrid;
2. To produce a reconstruction of palaeoclimatic change during MIS 7–9 in the northeastern Mediterranean.

These aims will be achieved by completing the following objectives:

1. The creation of a high-resolution record of diatom assemblage change within the I-284 core from Lake Ioannina, focusing on MIS 7–9.
2. The creation of a high-resolution record of diatom assemblage change within the DEEP core from Lake Ohrid, focusing on MIS 7.
3. A comparison between the new diatom assemblage records from the two lakes. The interpretation of these records will be assisted by other proxy records that have already been produced.
4. A comparison of the new records covering MIS 7–9 with previously published records.

1.3 Thesis outline

The structure of this thesis is outlined in Figure 1.3.

Introduction
Chapter 1

Introduces the research
context, aims and objectives.

Literature review
Chapter 2

Quaternary climate variability
Section 2.1

Details the characteristics and forcing mechanisms of
Quaternary climate variability before summarising our
current knowledge of palaeoclimate during MIS 7–9.

Diatom responses to environmental change
Section 2.2

Outlines the features that make diatoms suitable for
palaeoenvironmental reconstructions before
summarising our current knowledge of diatom
responses at Ioannina and Ohrid.

Study region and sites
Chapter 3

Introduces the tectonic and climatic settings of the northeastern Mediterranean.
Subsequently details the physical geography of each study site before comparing them.

Methodology
Chapter 4

Provides details of the methods used to create
and analyse both of the new diatom records.

Results
Chapter 5 and Chapter 6

Lake Ioannina
Chapter 5

Details the results and palaeolimnological
interpretation for Lake Ioannina during MIS 7–9.

Lake Ohrid
Chapter 6

Details the results and palaeolimnological
interpretation for Lake Ohrid during MIS 7.

Discussion
Chapter 7

Examines palaeoclimate in the northeastern Mediterranean during
MIS 7–9, making use of the new data generated in chapters 5 and 6.

Conclusions
Chapter 8

Summarises the findings of the research whilst considering
the aims outlined in the introduction.

Figure 1.3: Diagram illustrating the structure of this thesis.

Chapter 2 | Literature review

Having established the two aims of this thesis, it is clear that achievement of each aim would contribute knowledge to a different topic: diatom responses to environmental change and climate variability during the Quaternary. Our current understanding of these two broad topics is reviewed in this chapter. The first section of this literature review (section 2.1) details our current understanding of Quaternary climatic variability. It begins with a broad focus, looking at changes that have occurred over long then short timescales. Subsequently, the focus narrows to summarise our current knowledge of palaeoclimate during MIS 7–9. The second section of the literature review (section 3.4) outlines the features that make diatoms suitable for reconstructing palaeoenvironmental change and describes how diatoms are known to respond to changes in different limnological variables. Once again, the section finishes by narrowing the focus, this time summarising our current knowledge of diatom responses specifically in the lakes under investigation in this thesis.

2.1 Characteristics and forcing mechanisms of Quaternary climatic variability

Geologically recent sediments of the Quaternary Period (c. 2.58 Ma to present) have the potential to contain highly resolved records of palaeoenvironmental change, having not been subjected to millions of years of erosion and deep burial. In addition, the nature of the Quaternary's climatic variability makes the period particularly valuable for palaeoclimate studies. This climatic variability has operated over a range of temporal scales and as a result of different forcing mechanisms. Characteristic cycles associated with large variations in global ice volume have occurred over long timescales spanning tens of thousands of years and are overprinted by changes that have occurred

over shorter millennial timescales. The subsections that follow introduce the characteristics and forcing mechanisms of Quaternary climate variability over these long and short timescales before examining the current state of knowledge of this variability over the time period investigated in this thesis (MIS 7–9).

2.1.1 Climatic variability over long temporal scales—the glacial–interglacial cycles

Initiation of the glacial–interglacial cycles

By convention, the base of the Quaternary is marked by a point on a stratigraphic section with a specific age (a Global Stratotype Section and Point), however the changes that mark the initiation of the conditions that characterise the Quaternary Period took place over a few hundred thousand years with no single global event emerging as the trigger (Gibbard & Head, 2009b). Ice sheets began to develop over the northern hemisphere continents as part of a long-term cooling trend that began around 50 million years ago and is attributed to declining atmospheric CO_2 concentrations and tectonic movements (Zachos et al., 2001; Zachos et al., 2008). This is evident in oxygen isotope ($\delta^{18}O$) records of benthic foraminifera from marine sediment cores, which primarily reflect global ice volume (Figure 2.1; Shackleton, 1967). Between 2.8 Ma and 2.4 Ma, multiple major cooling phases resulted in the onset of a pattern of glacial–interglacial cycles paced by Earth's orbital parameters (Pillans & Naish, 2004; Gibbard & Head, 2009b).

Characteristics of the glacial–interglacial cycles

The glacial–interglacial cycles are associated with frequent, high amplitude oscillations in Earth's climate between cold intervals associated with the expansion of the continental ice sheets (glacials) and warm intervals, during which temperatures have occasionally exceeded those of the present day (interglacials; Lowe & Walker, 2015). Their structure is evident in $\delta^{18}O$ records
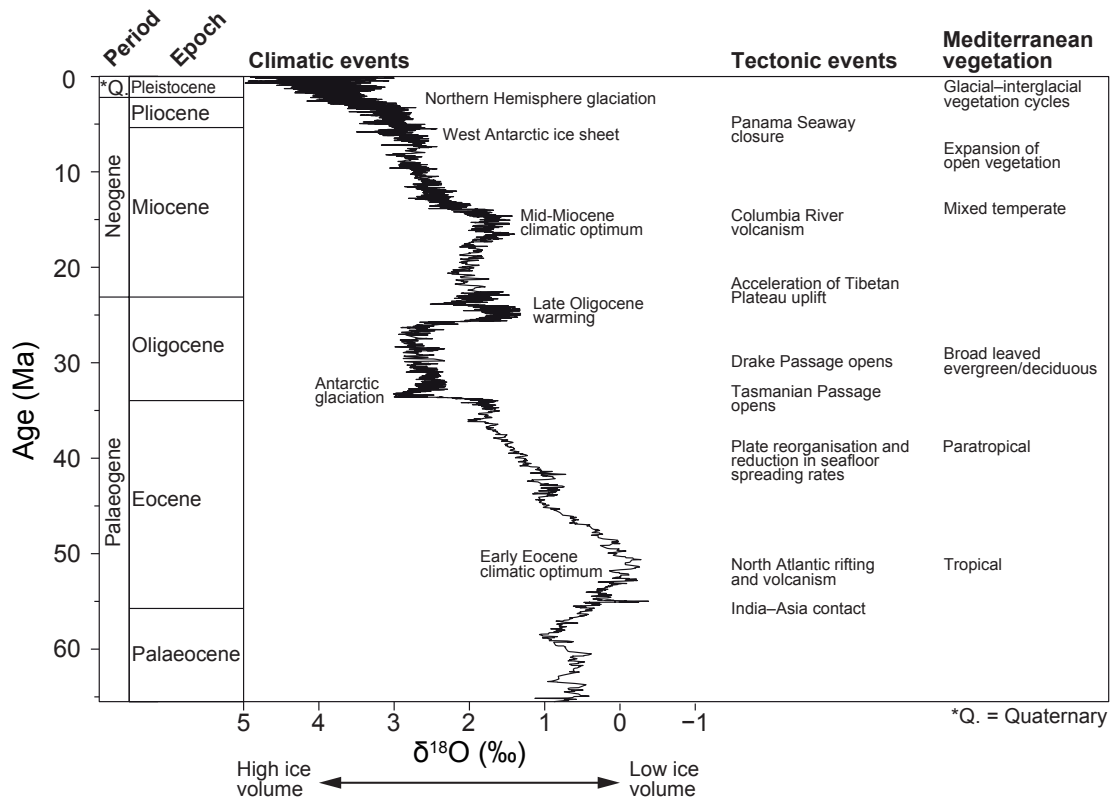
Figure 2.1: $\delta^{18}O$ record of benthic foraminifera from marine sediment cores recovered from more than 40 sites. The data are five-point running means and reflect global ice volume. Major climatic events and vegetation changes in the Mediterranean region are also shown. A trend of increasing global ice volume is evident from around 50 Ma. Modified from Zachos et al. (2001) and Tzedakis (2009).

and has changed over the Quaternary (Lisiecki & Raymo, 2005; Figure 2.2). The early glacial–interglacial cycles were roughly symmetrical with a periodicity of about 41 kyr. Compared to later cycles, ice volumes were lower during these early cycles and demonstrated less variation between glacial and interglacial intervals. During the Early–Middle Pleistocene Transition (EMPT; previously known as the Mid-Pleistocene Transition or Revolution), there was an intensification in the amplitude of the cycles, a lengthening of the dominant period of the cycles from c. 41 kyr to c. 100 kyr and a shift to more asymmetrical cycles with abrupt glacial terminations (Maslin & Brierley, 2015). This transition was gradual and took place over several hundred thousand years, although there is a disagreement about its exact timing with different

studies providing various age ranges for the EMPT (Berends et al., 2021). The widest range encountered in the literature spans from an onset as early as c. 1400 ka to a termination as late as c. 424 ka, although the greatest changes took place near the midpoint of this interval at around 900 ka (Head & Gibbard, 2015). The disagreement on timings partly results from differences in the benthic δ^{18}O records used (as each can carry a regional signal; Clark et al., 2006), the statistical techniques used to analyse the data (e.g. wavelet analysis, change-point analysis, moving window Fourier transforms) and the different timing criteria chosen to mark the onset or termination (e.g. δ^{18}O threshold, peaks in wavelet spectrograms; Berends et al., 2021).
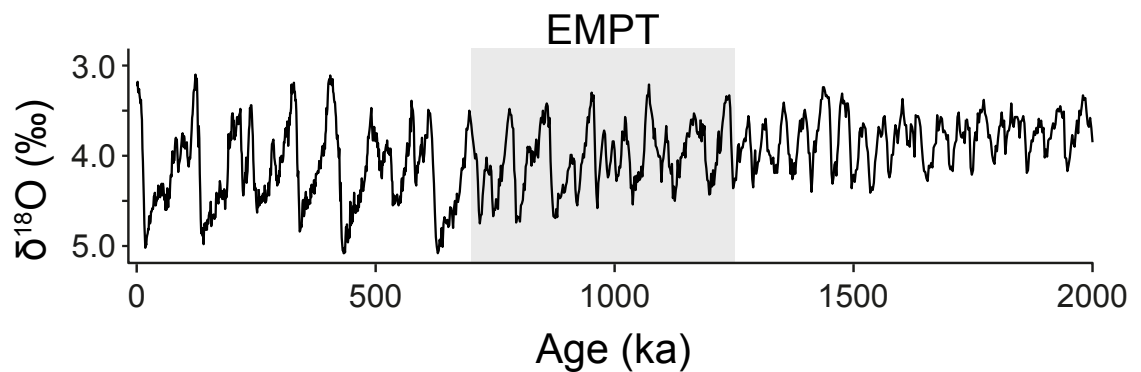
Figure 2.2: Benthic δ^{18}O record of the LR04 benthic stack spanning the last two million years and demonstrating the change in the structure of the glacial–interglacial cycles during the EMPT (Lisiecki & Raymo, 2005). Low δ^{18}O values reflect low ice volumes and high ocean temperatures. The EMPT is marked as spanning from 1250 ka to 700 ka after Clark et al. (2006).

The climatic changes over glacial–interglacial cycles are a global phenomenon and do not only affect the high and middle latitudes where the ice sheets advance and retreat. The changes in ice volume and ocean temperatures associated with these glacial–interglacial cycles have resulted in large changes in sea level over a vertical range of approximately 130 m (Spratt & Lisiecki, 2016). Over land, shifts in climatic zones have led to continental-scale reorganisations of landscapes and ecosystems, one example being the spread of trees from refugia during interglacials and their *in-situ* degradation during glacials (Bennett et al., 1991; Figure 2.3).
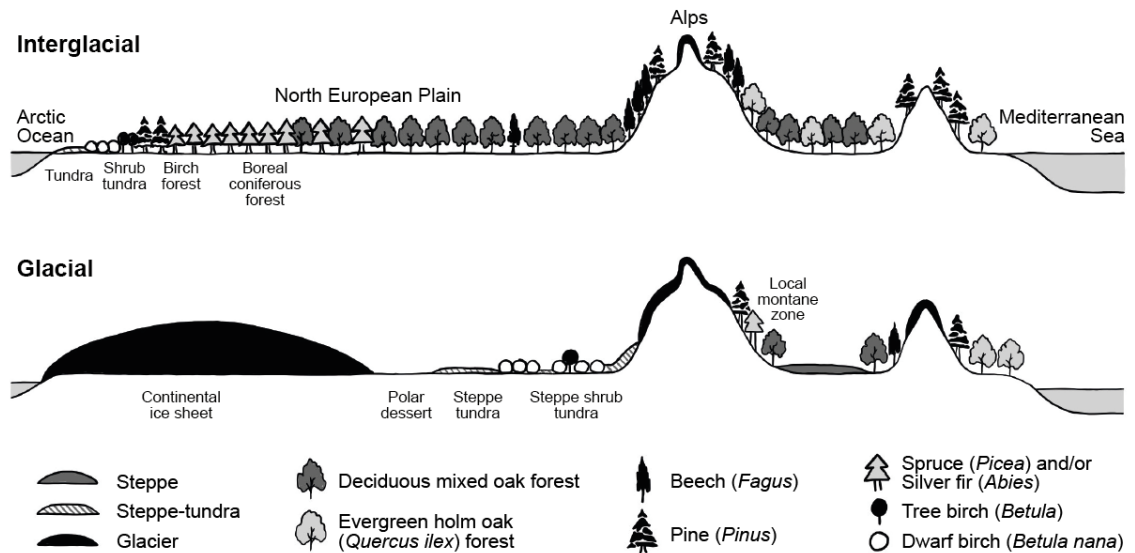
Figure 2.3: Schematic representation of vegetational belts across a north–south transect of Europe during interglacial and glacial stages. Modified from van der Hammen et al. (1971) and Woodward (2014).

Forcing mechanisms of the glacial–interglacial cycles

In the first half of the twentieth century, Milutin Milanković proposed that the intensity of summer insolation at 65°N, as determined by the quasi-periodic variations in Earth's orbital parameters, dictated whether ice could survive the warmer season in order to gradually accumulate into an ice sheet and thus enter Earth into a glacial period (Maslin, 2016). It was not until several decades later that geological evidence supporting this theory was published. In their seminal paper, Hays et al. (1976) identified frequencies of the orbital cycles in the geological record by performing spectral analyses on an oxygen isotope record from a marine sediment core, a proxy for global ice volume. They uncovered spectral peaks at periods of approximately 23 kyr, 42 kyr and 100 kyr, which were correlated with precession, obliquity and eccentricity respectively. Whilst the 100-kyr cycle was the most dominant, eccentricity variation induces too small a change in insolation to account for this (Imbrie et al., 1993). Explaining the 100-kyr cycle become one of the biggest challenges in the astronomical theory of climate (Elkibbi & Rial, 2001). Various explanations

were proposed with the view that there is either a non-linear amplification of the eccentricity signal or that eccentricity merely acts as a pacing mechanism for other drivers, although it has also been recognised that the 100-kyr cycle could be completely unrelated to eccentricity (Maslin & Brierley, 2015).

However, since advancements have been made in chronologies and demarcating interglacial periods, it has been recognised that interglacials since the EMPT do not actually occur at regular 100 kyr intervals, and a robust model incorporating insolation and ice-sheet dynamics has been proposed to explain the quasi-periodicity of interglacial onset both prior to, and since, the EMPT (Tzedakis et al., 2017). The theory suggests that deglaciation has been triggered when energy related to precession- and obliquity-driven summer insolation at 65°N (caloric summer half-year insolation) exceeds a simple threshold. Prior to 1 Ma, this threshold was exceeded on every other insolation peak (approximately every 41 kyr), which was boosted by high obliquity. A gradual increase in the threshold, starting around 1.55 Ma, led to some of these peaks being skipped, allowing the build-up of larger ice sheets. From around 1 Ma, the larger size of the ice sheets started to influence the threshold itself. Larger ice sheets are more unstable and therefore more sensitive to insolation. As the time since the last deglaciation increases, the ice sheets get bigger, which leads to an increase in their instability and sensitivity to insolation, thereby lowering the deglaciation threshold.

2.1.2 Climatic variability over short temporal scales—millennial-scale variability

Characteristics of millennial-scale climatic variability

The climatic oscillations of the Quaternary are not limited to the glacial–interglacial cycles, with variations also occurring over shorter timescales. Millennial-scale climatic variability has long been recognised as a feature of the last glacial period (c. 115–11.6 ka) with Dansgaard et al. (1984) linking large amplitude $\delta^{18}O$ oscillations in Greenland ice cores to quasi-periodic cycles in

North Atlantic climate. The $\delta^{18}O$ of the ice reflects local air temperature (Johnsen et al., 1972), and it records fluctuations between cold glacial conditions (stadials) and mild interstadial conditions in Greenland during the last glacial period (Johnsen et al., 1992; Dansgaard et al., 1993). A total of twenty-five Greenland interstadials, with intervening Greenland stadials, have been identified during this period (Figure 2.4; North Greenland Ice Core Project members, 2004; Rasmussen et al., 2014). Each one starts with an abrupt increase in temperature (5°C to 16.5°C over a few decades). This is followed by gradual and then abrupt cooling back to stadial conditions (Wolff et al., 2010; Kindler et al., 2014). These variations are now known as Dansgaard–Oeschger (D–O) events, although this term has seen a confusing range of uses in the literature, having at times been used to refer to just the abrupt interstadial onsets, the interstadial periods or each cycle of abrupt warming then gradual cooling (Rasmussen et al., 2014). What Rasmussen et al. (2014) highlight is that regardless of the precise terminology, the characteristic feature of these events is the abrupt climatic warming.
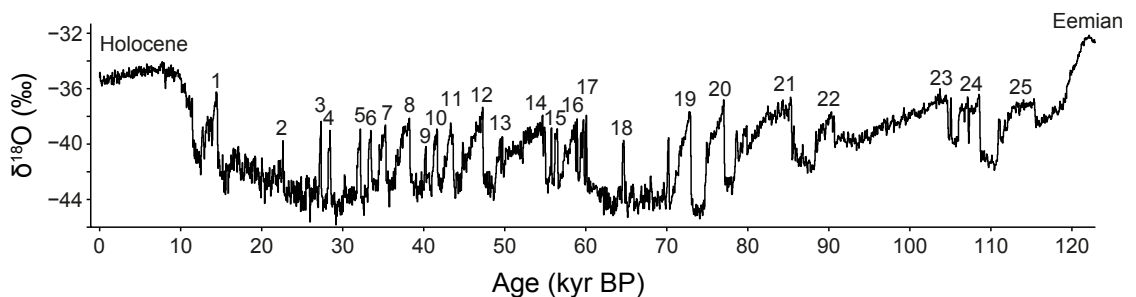
Figure 2.4: $\delta^{18}O$ record of the NGRIP ice core showing the climatic fluctuations of the last glacial period. The 25 interstadials are numbered, and the pattern of abrupt warming followed by gradual cooling that characterises the D–O events is evident. The data are 50 year means (North Greenland Ice Core Project members, 2007).

The D–O climatic variability is not limited to Greenland and is seen in a range of northern hemisphere climate records (Voelker, 2002; Menviel et al., 2020). Records from North Atlantic marine sediment cores indicate that sea surface temperature (SST) has varied in phase with Greenland air temperature changes

(Waelbroeck et al., 2019). Some of the Greenland stadials are associated with thick layers of ice-rafted debris (IRD), which is terrigenous sediment that was transported over the ocean by ice and deposited upon the melting of the ice. These thick IRD layers are believed to be the result of large discharges from the Laurentide Ice Sheet and are termed Heinrich Events (Heinrich, 1988; Bond et al., 1992; Bond et al., 1993). Weaker, higher frequency discharges have also been noted from the European ice sheets (Elliot et al., 2001). In Europe, there is cooling and drying during Greenland stadials, which is evident both in terrestrial (e.g. Margari et al., 2009) and marine (e.g. Martrat et al., 2004; Martrat et al., 2007) records. At low latitudes, D–O variability is associated with changes in monsoon intensity (Schulz et al., 1998; Cheng et al., 2012). Millennial-scale variability is also expressed further south in Antarctica, but its expression is more muted and gradual (Wolff et al., 2010). Synchronised ice core records demonstrate that whilst every D–O event has an Antarctic counterpart, Antarctica warms when Greenland is cold and then cools during Greenland interstadials (EPICA Community Members, 2006). Furthermore, the changes in Antarctica are offset from those in Greenland, with lags of around 200 years from Greenland warming to the onset of Antarctic cooling and from Greenland cooling to Antarctic warming (WAIS Divide Project Members, 2015).

Millennial-scale climate variability is not limited to the last glacial period. It has been acknowledged as a ubiquitous feature of glacial climates from ice core and speleothem records of the last 800 kyr (Jouzel et al., 2007; Barker et al., 2011). Marine sediment cores from various regions including the North Atlantic (McManus et al., 1999) and Iberian margin (Birner et al., 2016; Rodrigues et al., 2017) also contain records of millennial-scale climate variability prior to the last glacial period. Whilst this type of climatic variability is suppressed in interglacials (Past Interglacials Working Group of PAGES, 2016), there is still evidence for abrupt events during these periods (e.g. Bond et al., 1997; Oppo et al., 2006; Zielhofer et al., 2019).

Forcing mechanisms of millennial-scale climate variability

Various forcing mechanisms have been proposed for millennial-scale climate variability, although there is no consensus on its cause, and no single mechanism can account for all of its observed characteristics (Menviel et al., 2020; Kageyama et al., 2021; Landais et al., 2022). However, strong evidence from proxy records and climate modelling experiments suggests it is linked to variations in the strength of the Atlantic meridional overturning circulation (AMOC; Menviel et al., 2020). The strength of the AMOC is related to salinity-driven changes in water density; reduced surface water salinity in the Nordic Seas impedes the sinking of surface waters, slowing or shutting off the AMOC, while an increase in the salinity of surface waters in the Nordic Seas encourages the sinking of the surface waters, which strengthens or restarts the AMOC (Broecker et al., 1990; Rahmstorf, 2002). These changes impact the climate of the high northern latitudes as the AMOC transports heat from the tropics. If the AMOC weakens or shuts down, warm waters are not able to penetrate as far north, encouraging sea ice to advance, increasing albedo, perpetuating cooling and triggering stadial conditions (Menviel et al., 2020). Atmospheric and oceanic teleconnections propagate these North Atlantic changes to the continents (Fletcher et al., 2010) and southern hemisphere (WAIS Divide Project Members, 2015). However, the drivers of change in the strength of the AMOC are still debated. With some exceptions (e.g. Peltier & Vettoretti, 2014), most theories implicate increased meltwater input from the northern ice sheets in the freshening of the Nordic Seas and the weakening of the AMOC. Hypotheses for the triggering of meltwater increases include self-regulating internal oscillations in the atmosphere-ocean-sea-ice system (the "salt oscillator"; Broecker et al., 1990), changes in the height of the Laurentide Ice Sheet that alter wind stress over the Atlantic (Zhang et al., 2014a), changes in atmospheric CO_2 concentrations (Zhang et al., 2017) and direct forcing by insolation variations (Yin et al., 2021; Zhang et al., 2021).

2.1.3 Current understanding of MIS 7–9 palaeoclimate

The glacial–interglacial cycles of the last c. 450 kyr are generally stronger than the preceding cycles (section 2.1.1). MIS 9 fits this general pattern, especially in Antarctica where ice cores record the highest Antarctic surface air temperatures of the last 800 kyr within MIS 9e, as well as the highest CO_2 and CH_4 concentrations (Past Interglacials Working Group of PAGES, 2016). In contrast, MIS 8 and MIS 7 have been highlighted as exceptions to the general pattern and described as weak (Lang & Wolff, 2011). Benthic $\delta^{18}O$ values from marine sediment cores are relatively low during MIS 8, indicating low ice volumes for a glacial interval (Lang & Wolff, 2011). However, whilst most glacial intervals reach their maximum intensity just prior to the termination (Past Interglacials Working Group of PAGES, 2016), MIS 8 is unusual in that in some records, particularly those from Antarctica, it reaches peak glacial conditions earlier, around 15–20 kyr before the glacial termination (Lang & Wolff, 2011). The characteristic, abrupt, high amplitude variations in marine sediment core proxies of the last glacial period (section 2.1.2) are also present throughout MIS 8, with true Heinrich events (of the same provenance as those of the last glacial) occurring at c. 263 ka, c. 249 ka and c. 243 ka (Obrochta et al., 2014). MIS 7 stands out amongst the interglacial periods of the last 450 kyr. In many records it contains three peaks, which have been assigned the substages 7e, 7c and 7a. MIS 7e is usually considered representative of full, but weak, interglacial conditions, and it is separated from 7c by an interval of close to full glacial conditions (substage 7d) that were at least as strong as those of MIS 14 (Lang & Wolff, 2011). MIS 7c also represents weak, full interglacial conditions in many records. In some it is separated from substage 7a by the more glacial conditions of substage 7b, but in many, MIS 7c to 7a represents a long period of weak interglacial character (Lang & Wolff, 2011). In the LR04 benthic stack, MIS 7e and MIS 7c to 7a are of comparable strength to the weaker, earlier intervals prior to 450 ka (Lisiecki & Raymo, 2005; Past Interglacials Working Group of PAGES, 2016).

In the northeastern Mediterranean specifically, MIS 9 was cooler than the preceding interglacial (MIS 11) and relatively wet (Francke et al., 2016; Lacey et al., 2016). In the Ohrid record, the onset of full interglacial conditions during MIS 9e is relatively rapid (Lacey et al., 2016) and is consistent with warming at the start of MIS 9 seen in pollen records from Tenaghi Philippon (Fletcher et al., 2013). Colder and drier conditions are seen during the stadial conditions of MIS 9d, before warmer and wetter conditions during the MIS 9c interstadial, colder and drier condition during MIS 9b stadial and warmer and wetter conditions during MIS 9a interstadial (Fletcher et al., 2013; Lacey et al., 2016). In the Ohrid record, MIS 8 is seen as being somewhat warmer than many other glacials, with some times during this interval seeing interglacial-like conditions (Francke et al., 2016). The first half of the MIS 8 glacial saw the coolest and driest conditions according to the Tenaghi Philippon pollen record, with less severe conditions later in this interval (Fletcher et al., 2013). MIS 7 at Lake Ohrid is characterised by warmer and wetter conditions that likely correspond to MIS substages 7e, 7c and 7a (Lacey et al., 2016), at which times pollen data from Ioannina also indicate warmer and wetter conditions (Roucoux et al., 2006).

2.2 The use of diatoms in palaeolimnology

First introduced in section 1.1.4, diatoms are unicellular algae that contribute to the organic component of lake sediments. They possess a number of features that enable their use in palaeolimnological investigations. Their robust cell walls can preserve well in sediment and are morphologically distinct between species. The latter allows identification to species level through visual features alone. Furthermore, many species are ecologically sensitive, so the presence and abundance of certain species can be indicative of specific palaeolimnological conditions. These features that enable the use of diatoms in palaeolimnological investigations are discussed in more detail within the sections that follow.

2.2.1 The diatom frustule

Critical to their application in palaeolimnology, diatoms possess a distinctive siliceous cell wall known as a frustule, which can preserve well in accumulated sediments. Composed of rigid opaline silica ($SiO_2 \cdot nH_2O$), the function of the frustule is to protect and constrain the internal organic part of the cell—the protoplast (Cox, 2011). A frustule consists of two halves (thecae) of slightly different sizes that slot together to form a pillbox-like structure (Figure 2.5a). It is perforated to allow the protoplast to interact with the environment through various processes such as nutrient intake and the excretion of cellular products (Cox, 2011). These perforations, along with other wall structures and the overall frustule shape, vary between diatoms such that the morphological variation of the frustule can be used for taxonomic identification down to the subspecies level (Figure 2.5b). The size of the diatom frustule must be considered with caution when performing taxonomic identifications as diatoms reproduce via vegetative cell division with a successive reduction in size until sexual reproduction occurs (Cox, 2014). Sexual reproduction involves production of an auxospore with a different morphology to the vegetative cells (Pérez-Martínez & Cruz-Pizarro, 1992).

2.2.2 Diatom habitats

Due to the light requirements of photosynthesis, diatoms typically inhabit the parts of a lake where light penetrates (the photic zone), including the lake margins (littoral zone) and within the open water column (pelagic zone). To survive in this range of environments, different diatom taxa have adopted planktonic, facultative planktonic and benthic existences (Battarbee et al., 2001), which are referred to as "life modes" throughout this thesis. The photic region of the pelagic zone is occupied by planktonic taxa, which typically possess centric valve shapes with large surface area to volume ratios that aid buoyancy while floating in the open water (e.g. *Pantocsekiella ocellata* in Figure 2.5b; Serôdio, 2021). In the littoral zone, benthic taxa grow attached to a variety

a

Pantocsekiella ocellata   *Placoneis balcanica*

b
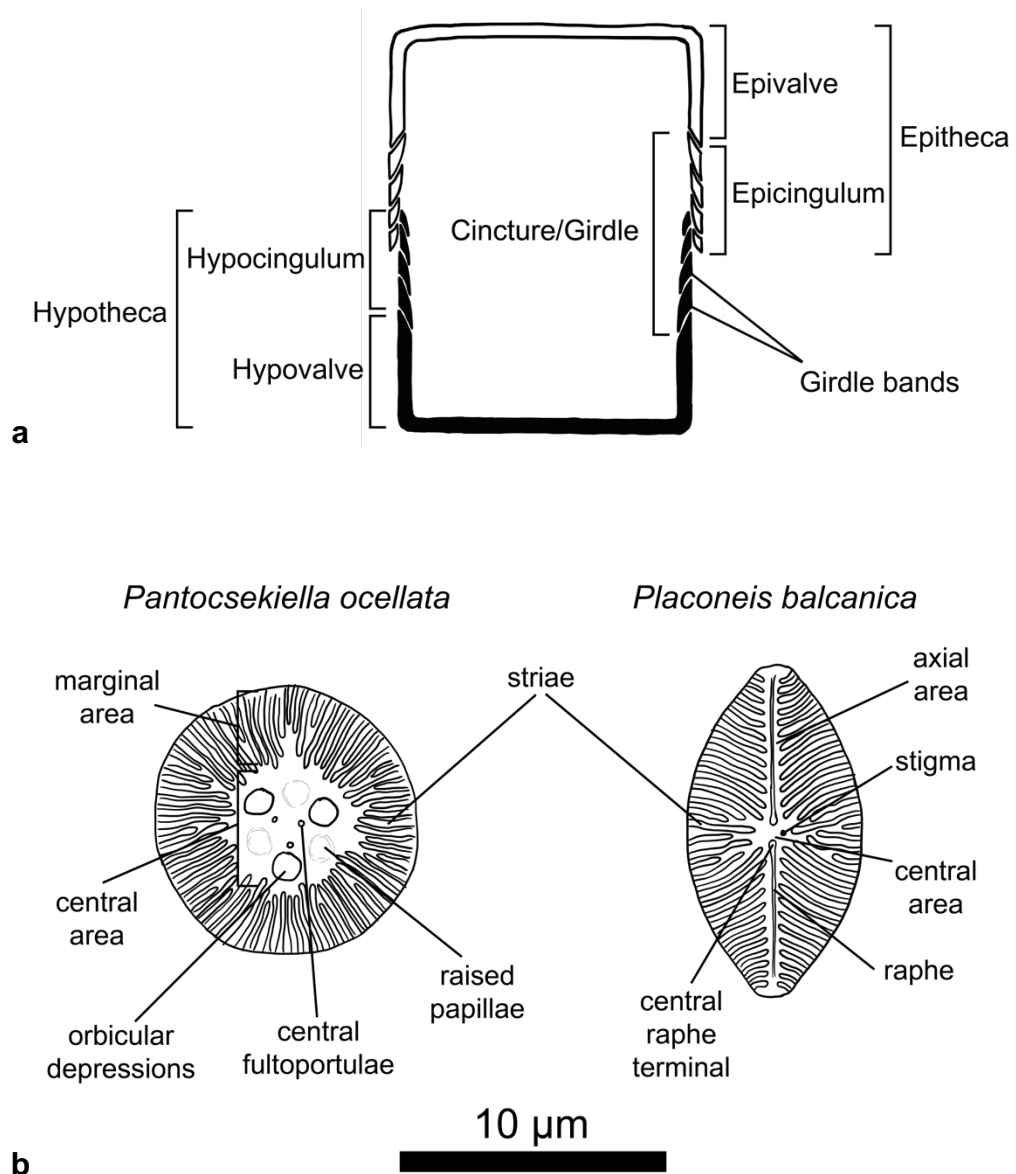
Figure 2.5: Diagrams of diatom frustules: a schematic cross-section through a frustule illustrating the structure and arrangement of the two thecae (**a**; modified from Round et al., 1990) and illustrations of some of the morphological features encountered on the valve faces of two diatom species, which can be used for diatom identification (**b**).

of substrates including stones (epilithic), sand (epipsammic), mud (epipelic) and plants (epiphytic; Battarbee et al., 2001). Some even grow attached to larger diatoms (Tiffany & Lange, 2002) and animals (epizoic; Tiffany, 2011). Benthic taxa typically have elongated valve shapes (e.g. *Placoneis balcanica* in Figure 2.5b), although they have evolved highly diverse morphologies, partly due to the range of substrates they inhabit. Many possess a raphe system (seen

on *Placoneis balcanica* in Figure 2.5b), which allows some motility (Serôdio, 2021). Facultative planktonic (tychoplanktonic) taxa usually live in benthic habitats but can also survive if entrained in the water column through turbulence and mixing (Battarbee et al., 2001).

2.2.3 Controls on diatom assemblages

The ecological sensitivity of many diatom taxa is another key factor in their application to palaeolimnology (Smol & Stoermer, 2010). A summary of the ecological and environmental associations of the main taxa that appear in this thesis is provided in Table 2.1. It demonstrates that some are able to tolerate a wide range of conditions, while others tend to occur under specific physical and chemical limnological conditions. Changes in these limnological variables can therefore lead to shifts in the specific taxa that inhabit the lake and their abundances (the diatom assemblage).

The physical and chemical limnological variables that influence diatom assemblages include lake level, nutrient availability, mixing regime, ice cover, temperature, light availability, pH and salinity (Battarbee et al., 2001). These variables reflect changing limnological conditions in response to changes in the climate (e.g. temperature, wind patterns, solar radiation/cloudiness; Rühland et al., 2015) and the catchment (e.g. vegetation cover and erosion rates). Furthermore, these variables are interrelated, with changes in one often leading to a change in another (e.g. a climate-induced increase in water mixing can increase nutrient availability by the release of nutrients from disturbed sediments). There is therefore a complex range of limnological variables to which diatom assemblages can respond. To complicate matters further, similar diatom responses can occur as a result of changes in different variables. Some of the key factors influencing the composition of the lacustrine diatom assemblages encountered in this thesis are now discussed.

Table 2.1: Details of the ecological and environmental associations of the most abundant taxa encountered in this thesis. Taxa present at ≥4% in at least one sample of the Lake Ioannina record and ≥1% in at least one sample of the Lake Ohrid record are included.

Taxon and authority	Details
Actinocyclus normanii (Gregory ex Greville) Hustedt 1957	*Actinocyclus normanii* is large planktonic taxon that is also encountered in benthic environments (Vidaković et al., 2016). It is cosmopolitan and often considered an invasive species (e.g. Kaštovský et al., 2010; Kiss et al., 2012; Vidaković et al., 2016).
	A. normanii is associated with nutrient enriched conditions (Kaštovský et al., 2010). It is tolerant of a wide range of salinities, occurring in both marine and freshwater environments with potentially larger valves as salinity increases (Kiss et al., 1990; Vidal et al., 2018). It is considered stenothermic as its highest abundances have been observed in summer and autumn (Kiss et al., 1990; Kiss et al., 2012).
Amphora pediculus (Kützing) Gunrow 1880	*Amphora pediculus* is a small benthic taxon. It is documented as one of the taxa dominating the littoral zone of the present-day Lake Prespa (Levkov et al., 2007a). In Lake Ohrid it is associated with very shallow areas of the littoral zone (0.5–1 m water depth) and sandy substrates (Cvetkoska et al., 2018). It is tolerant of oligotrophic to eutrophic conditions (Kelly et al., 1995; Zhang et al., 2014b).
Aneumastus minor Lange-Bertalot 1993	*Aneumastus minor* is widespread, at least throughout the northern hemisphere (Glushchenko et al., 2017). However, the literature provides little further information on this specific taxon.
	The freshwater genus Aneumastus is only a small group but is relatively diverse in ancient lakes (Levkov et al., 2007a; Glushchenko et al., 2017) with recent evidence from Lake Ohrid demonstrating that rapid in situ speciation can occur within a single lake (Stelbrink et al., 2018). In Lake Prespa, Aneumastus taxa are found in the littoral zone where there is organic sediment and carbonate geology but not where there is a sandy substrate and silicate geology (Levkov et al., 2007a).
Asterionella formosa Hassall 1850	*Asterionella formosa* is a freshwater planktonic taxon (Round et al., 1990). It is relatively well studied in comparison to many of the other taxa included here, probably because it is widely distributed and becoming increasingly common in modern-day lakes (Sivarajah et al., 2016).
	It has often been considered an indicator of nutrient enrichment and is associated with high nitrogen and silica supplies (Saros et al., 2005). For example, its increase in alpine lakes of the western US has been attributed to an increased delivery of atmospheric nitrogen related to human activity (e.g. Hobbs et al., 2010; Saros et al., 2011), and in Lake Prespa, it was present after tephra deposition, which is known to increase the silica content of water (Cvetkoska et al., 2015).
	A. formosa has also been found in oligotrophic conditions (e.g. Rimet et al., 2009), demonstrating that it is tolerant of a wide range of nutrient levels (Rühland et al., 2015). Its abundance has been observed to increase even as nutrient levels decline, so there are clearly other controls on its abundance than just nutrient availability (Sivarajah et al., 2016).

Table 2.1 (continued)

Taxon and authority	Details
Asterionella formosa Hassall 1850 (continued)	It has been reported to bloom in spring and autumn when lakes are well mixed and nutrients are distributed throughout the water column, and it can also bloom during summer when lakes are thermally stratified (Rühland et al., 2015). Its elongated valves form star-shaped colonies (Round et al., 1990), which are resistant to sinking and make it competitive in stratified waters (Sivarajah et al., 2016). There are some reports it might reside in deeper waters during stratification to take advantage of the hypolimnetic nutrients (Rühland et al., 2015).
	It is also associated with longer ice-free periods (Rühland et al., 2015) such as during the Holocene at Lake Moon (NE China; Chen, J. et al., 2021).
Aulacoseira granulata (Ehrenberg) Simonsen 1979	*Aulacoseira granulata* is considered a species complex that is common in shallow lakes, rivers and the marginal areas of larger lakes (Kilham & Kilham, 1975; Stone et al., 2011). It can be abundant in well mixed, shallow waters as *Aulacoseira* species have heavy valves that require circulating water to keep them suspended (Spooner et al., 2002). Although dominance of this taxon is usually associated with shallow and wind-stressed eutrophic waters (Cvetkoska et al., 2014a), it has also been inferred to occur in deep water provided there is enough mixing to keep their valves suspended (Zhang et al., 2014b).
	It is widespread in mesotrophic and eutrophic conditions, dominating the planktonic habitat of the present-day Lake Ioannina, which is currently hyper-eutrophic (Wilson et al., 2013).
Cavinula scutelloides (Smith) Lange-Bertalot 1996	This is a benthic species and has been found as part of epipsammic communities (Jewson et al., 2006). In Lake Ohrid it dominates benthic communities on sand substrate and silicate bedrock (Levkov et al., 2007a; Cvetkoska et al., 2014a).
	Based on its abundance in the Ancylus Lake stage of the Baltic Sea, Ampel et al. (2010) suggest it could be considered a cold-adapted taxon.
Cocconeis placentula Ehrenberg 1838	*Cocconeis placentula* is a common cosmopolitan taxon (Jahn et al., 2009). It is considered a pioneer species that can grow on a variety of substrates but prefers an epiphytic habitat. (Müller, 1999). It can be found in shallow, eutrophic environments that are dominated by macrophytes (Zalat & Vildary, 2005). In Lake Ohrid, it is present in the shallow, sandy littoral area (0.5–1 m water depth) and is also one of the few dominant taxa in the lower part of the littoral zone (5–10 m water depth), which is characterised by the dense growth of macrophytic algae (of the genus *Chara* Linnaeus) that forms submerged meadows (Cvetkoska et al., 2018).
Cyclotella cavitata Tofilovska, Cvetkoska, Jovanovska, Ognjanova-Rumenova & Levkov 2016	Planktonic *Cyclotella cavitata* is an extinct endemic taxon of Lake Ohrid (Tofilovska et al., 2016). It demonstrates remarkable morphological variability through time and probably represents a species complex (Cvetkoska et al., 2021; Zaova et al., 2021). Their valves disappear from the Lake Ohrid record c. 213 ka, around the same time as an increase in the abundance of a novel variety of *Cyclotella fottii* (Cvetkoska et al., 2021), which is referred to as *C. fottii* var. 1 in this thesis. The morphological similarities and presence of intermediate forms between the two taxa could be indicative

Table 2.1 (continued)

Taxon and authority	Details
Cyclotella cavitata Tofilovska, Cvetkoska, Jovanovska, Ognjanova-Rumenova & Levkov 2016 (continued)	of evolutionary processes and suggests they probably share similar niches (Wagner et al., 2014). See *C. fottii* for further details. Note that *C. cavitata* was included within *Cyclotella iris* in earlier investigations (e.g. Wagner et al., 2014; Zhang, 2015).
Cyclotella fottii Hustedt 1942	*Cyclotella fottii* is an extant planktonic taxon that is endemic to Lake Ohrid. It is hypolimnetic with viable populations occurring below a water depth of 100 m where temperatures are low and light availability is far below optimum for photosynthesis (Stanković, 1960). Cvetkoska et al. (2016) suggest that temperature, rather than light availability, is the main control on its vertical distribution and abundance. The taxon exhibits a wide range of morphological variability (Cvetkoska et al., 2021) such as the elliptical variety (*C. fottii* var. 1).
Cyclotella fottii var. 1 Undescribed	*Cyclotella fottii* var. 1 is an extinct morphological variety that existed in Lake Ohrid c. 213–183 ka (Cvetkoska et al., 2021). It differs from *C. fottii* mainly in its outline, which is elliptical rather than circular. It probably shares the same oligotrophic, oligothermic and oligophotic affinities as *C. fottii.* Note that *C. fottii* var. 1 was included within *Cyclotella iris* in some earlier investigations (e.g. Wagner et al., 2014; Zhang, 2015) and referred to as *C. fottii* var. 2. nov. by Cvetkoska et al. (2021).
Diatoma ehrenbergii Kützing 1844	Taxa of the genus Diatoma are generally epiphytic. They have been found on stones and macrophytes in the shallow littoral regions (0–4 m water depth) of Lake Prespa and Lake Ohrid (Levkov & Williams, 2006). Their highest abundances in Lake Prespa and Lake Ohrid occur during winter and spring, reaching a peak in January and February (Levkov & Williams, 2006). However, they have also been noted in Lake Prespa in the summer months when macrophytes are abundant (Levkov et al., 2007a). They appear to prefer low temperatures with their highest abundances in Lake Ohrid occurring at 4°C to 8°C (Levkov & Williams, 2006). This preference for cold conditions is also documented elsewhere (e.g. Potapova & Snoeijs, 1997; Liu et al., 2010). Their valves can join at the poles to form star-like or zig-zag colonies, which enables them to also adopt a planktonic existence (Round et al., 1990).
Diploneis marginestriata Hustedt 1922	*Diploneis marginestriata* is a benthic taxon and is morphologically similar to *Diploneis submarginestriata* and *Diploneis oculata*. These taxa have been found in shallow to deep epilithic and epipsammic habitats (Jovanovska et al., 2015), including at a water depth of 18 m in Lake Ohrid (Jovanovska & Levkov, 2020). Their water depth optima at Lake Lugu (SW China) has been estimated at c. 22 m (Wang et al., 2012).
Diploneis mauleri (Brun) Cleve 1894	*Diploneis mauleri* is widespread and is found in the sediments of several lakes on the Balkan Peninsula including Lake Dojran (Zhang et al., 2014b), Lake Prespa (Cvetkoska et al., 2014a; Cvetkoska et al., 2015) and Lake Ohrid (Jovanovska et al., 2013).

Table 2.1 (continued)

Taxon and authority	Details
Diploneis mauleri (Brun) Cleve 1894 (continued)	*Diploneis* frustules are usually heavily silicified (Round et al., 1990), and *D. mauleri* is no exception. It requires a sufficient silica supply for their large and complex frustules to form (Cvetkoska et al., 2015).
	It is a benthic taxon and in the present day Lake Prespa, it is found as part of deep benthic communities in the pelagic zone (15–17 m depth) alongside other heavily silicified benthic taxa (Levkov et al., 2007a; Levkov et al., 2007b). It has been inferred to occur during times of high water transparency (Cvetkoska et al., 2015). It also seems to be associated with winter and spring (Levkov et al., 2007b).
Encyonopsis microcephala (Grunow) Krammer 1997	*Encyonopsis microcephala* is an epiphytic taxon. In Lake Ohrid it is associated with both the shallow sandy littoral area (0.5–1 m water depth) and is one of the few taxa to dominate the lower littoral area (5–10 m water depth) that is characterised by dense macrophytes (Cvetkoska et al., 2018). This distribution across the shallow and mid-depths is also evident at Lake Tovel (Italy; Angeli & Cantonati, 2005; Cantonati et al., 2009).
Fallacia lucinensis (Hustedt) Mann 1990	*Fallacia* is a genus of benthic species. There is some evidence that *Fallacia lucinensis* prefers relatively deep benthic habitats. It has been recorded, albeit at very low abundances, at a water depth of 19 m (Li et al., 2010), and in Lake Lugu, its water depth optima has been estimated as being similar to the planktonic taxa *Pantocsekiella ocellata* and *Asterionella formosa* at around 30 m (Wang et al., 2012).
(Small) Fragilariaceae taxa including: *Pseudostaurosira brevistriata* (Grunow) Williams & Round 1987 *Staurosira construens* var. *venter* (Ehrenberg) Hamilton 1992 *Staurosirella pinnata* (Grunow) Williams & Round 1987	These small Fragilariaceae taxa have been found to inhabit stable sediment surfaces at the base of emergent macrophytes where they form only loose attachments so are easily transported into the water column as tychoplankton (Sayer, 2001). They are associated with relatively shallow water depths. At Lugu Lake (China), they have an estimated depth optimum of c. 10 m (Wang et al., 2012).
	They have a large surface area to volume ratio and high growth rates, which makes them competitive under low nutrient conditions (Lotter et al., 2010), although they demonstrate broad nutrient tolerances, having also been found in eutrophic lakes (e.g. Bennion et al., 2001).
	These taxa are characteristic of unstable environments and physical disturbance, being common in cold, ice-covered Arctic and alpine lakes and increasing in abundance with increasing latitude and altitude (Lotter et al., 2010). They have been described as pioneering taxa and are often the most abundant taxa following deglaciation (Haworth, 1976). At Lake Ioannina, they have been associated with cool, arid conditions and extended seasonal ice cover (Wilson et al., 2021), while at Lake Ohrid, they are associated with intensified lake circulation as a result of low water temperature and strong winds (Zhang et al., 2016).
	There is not much information on the individual ecologies of each of these taxa, and they tend to be treated as a group throughout the literature. They are often included in references to the *Fragilaria,* as they were previously assigned to this genus.

Table 2.1 (continued)

Taxon and authority	Details
Gomphonema pseudotenellum Lange-Bertalot 1985	This is a small-celled *Gomphonema* species. *Gomphonema* taxa are colonial and form branched mucilage stalks attached to solid substrata in the littoral zone (Round et al., 1990). In the present-day Lake Ohrid, taxa in this genus have been found in the sandy upper littoral area at a water depth of 0.5–1.0 m (Cvetkoska et al., 2018).
Gomphonema pumilum (Gunrow) Reichardt & Lange-Bertalot 1991	*Gomphonema pumilum* is widely distributed in regions with a carbonate geology (Lange-Bertalot et al., 2017). There are many taxa that are morphologically similar to *G. pumilum* so it is often referred to as a species complex (e.g. Levkov & Williams, 2011). See *Gomphonema pseudotenellum* form more information on the *Gomphonema* genus.
Gyrosigma sciotoense (Sullivant & Wormley) Cleve 1894	A large benthic taxon. *Gyrosigma* taxa are epipelic, and there is evidence they prefer relatively deep water. They are associated with the pelagic zone (15–17 m depth) alongside other heavily silicified taxa in the modern-day Lake Prespa (Levkov et al., 2007a). In Lake Tovel (Italy), they are found at water depths of 24–30 m.
Pantocsekiella minuscula (Jurilj) Kiss & Ács 2016	*Pantocsekiella minuscula* is a small (2–7 µm) planktonic taxon that probably occupies a similar niche to other small-celled *Cyclotella sensu lato* species (Saros & Anderson, 2015). Their small size results in a high surface area to volume ratio, making them efficient at nutrient uptake and resulting in low sinking velocities (Winder et al., 2009). For these reasons, they can often be found when lake water is stratified and there is less redistribution of nutrients to the surface waters (e.g. during the early Holocene in Lake Ohrid, Zhang et al., 2016). They are also competitive under low light availability and have been associated with detrital input in Lake Prespa and Lake Ohrid (Cvetkoska et al., 2014b; Cvetkoska et al., 2016), where their tolerance for low nutrient and light supplies has also seen them outcompete other taxa following tephra deposition (Jovanovska et al., 2016).
Pantocsekiella ocellata (Panktocsek) Kiss & Ács 2016	*Pantocsekiella ocellata* is a cosmopolitan, planktonic taxon with tolerances for a broad range of temperatures and nutrient levels. At Lake Ioannina they have been associated with oligotrophic–mesotrophic conditions (Wilson et al., 2015). At Lake Ohrid they reside in the epilimnion where they dominate during spring and summer (Stanković, 1960; Zhang et al., 2016). They are considered to be indicative of mesotrophic conditions in Lake Ohrid (Lorenschat et al., 2014).
	Large valves of this taxon are present in the sediments of Lake Ioannina but have no modern analogue. They are probably indicative of deep, open-water conditions based on their life–habit characteristics (Wilson et al., 2008; Jones et al., 2013). Morphologically similar taxa have been found in modern Lake Prespa (Levkov et al., 2007b) and in the lake's fossil assemblages (Cvetkoska et al., 2014b). They are associated with low levels of detrital input (Cvetkoska et al., 2015) and low nutrient levels (Cvetkoska et al., 2014a; Cvetkoska et al., 2015).
	See section 4.3.2 for more detailed information on this taxon and how it is treated in this thesis.

Table 2.1 (continued)

Taxon and authority	Details
Pantocsekiella sp. 1	This is an undescribed taxon from Lake Ioannina that does not resemble any taxon currently described in the literature. It shares some morphological similarities with *Pantocsekiella ocellata,* and its centric valve shape suggests it is planktonic. It is noticeably more heavily silicified than *Pantocsekiella ocellata*. This could indicate a requirement for circulating or turbulent water to keep it suspended.
Placoneis balcanica (Hustedt) Lange-Bertalot, Metzeltin & Levkov 2005	*Placoneis balcanica* is a benthic taxon and has been found in the shallow sandy littoral area of Lake Ohrid (Cvetkoska et al., 2018). Low abundances are also noted from the pelagic zone of Lake Prespa at a water depth of 15–17 m (Levkov et al., 2007a).
Sellaphora rotunda (Hustedt) Wetzel, Ector, Van de Vijver, Compère & Mann 2015	This benthic taxon has been found in specific parts of the littoral zone of Lake Prespa that are covered in organic sediment and have a carbonate geology (Levkov et al., 2007a). Its growth appears to be associated with the summer months (Levkov et al., 2007b).
Stephanodiscus medius Håkansson 1986	Planktonic *Stephanodiscus medius* has been described as mesotrophic (Zhang et al., 2014b). *Stephanodiscus* species can tolerate low light and silica availability, but they do require a high phosphorus supply (Kilham et al., 1986).
Stephanodiscus minutulus (Kützing) Cleve & Möller 1882 *Stephanodiscus parvus* Stoermer & Håkansson 1984	These planktonic taxa have been associated with high nutrient conditions (Chen, J. et al., 2021). They specifically require a high phosphorus supply (Kilham et al., 1986; Bennion, 1995). Despite being planktonic, they do not necessarily reflect deep water conditions. Small *Stephanodiscus* species have been found in shallow (mean water depth 3.7 m) Lake Juusa (Estonia) where their distribution does not seem to be connected to water depth (Punning & Puusepp, 2007). In the modern-day Great Lakes, *S. parvus* is associated with disturbed environments (Reavie & Cai, 2019).

Lake level

Lake level can vary as a result of geological, biological and climatic processes. In terms of geological processes, tectonic movements and sedimentary infilling can alter the depth of the water column (Dearing & Foster, 1986), whilst biological processes that influence lake level include changes in vegetation that alter drainage patterns and groundwater flow (Wolin & Stone, 2010). Although these are important considerations to make during any interpretation of potential lake level changes, the most important factor in controlling lake level is hydrology (Wolin & Stone, 2010).

Lake levels are a balance between inputs (stream inflow, groundwater inflow, surface runoff and precipitation) and outputs (stream outflow, groundwater outflow and evaporation). In lakes without a major outflow (closed-basin lakes), variations in lake level reflect changes in the balance between precipitation and evaporation (Fritz et al., 2010). Records of lake level change from such lakes can therefore reflect past changes in hydroclimate. Diatom records have the potential to reveal this information as lake level changes alter the availability and distribution of their different habitat types.

Changes in lake level alter the size of the different planktonic and benthic diatom habitats as well as their proximity to the deep central regions of the lake, from which sediment cores are typically recovered (Wolin & Stone, 2010). This has an impact on the ratio of planktonic to benthic (P–B) diatom taxa that become incorporated into the sediment at that location. When lake level is high, the depth of the photic zone limits the diatom assemblage at the core site so that it primarily consists of planktonic taxa that have sunk from the water column above, with a small component of benthic taxa that have been transported from the distal lake margins (Figure 2.6a). This results in a diatom assemblage with a high P–B ratio. Following a lake level decrease, the littoral zone is larger (due to the reduced slope angle of the lakebed) and closer to the core site (Figure 2.6b). This results in a larger number of benthic diatoms

reaching the core site. There is also a reduced lake area that is suitably deep for planktonic diatoms. The combined result is a reduction in the P–B ratio of the diatom assemblage at the core site. There are some exceptions to this typical behaviour as complex bathymetries can result in non-linear P–B ratio responses to changing lake levels (Stone & Fritz, 2004).
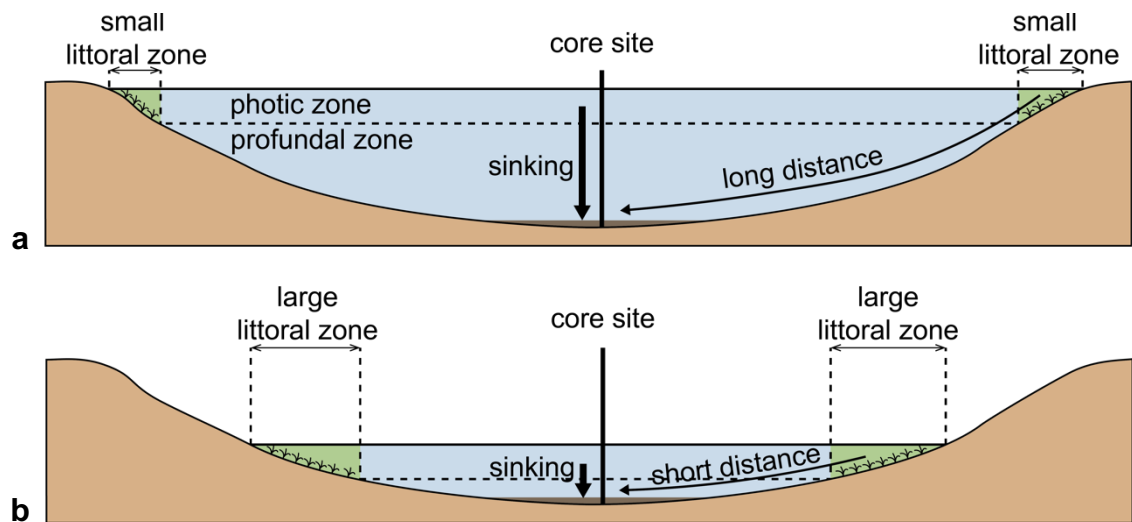
Figure 2.6: Schematic diagram demonstrating the size and location of the photic region of the pelagic zone (primarily inhabited by planktonic diatoms) and the littoral zone (primarily inhabited by benthic diatoms) under high (**a**) and low (**b**) lake levels.

Nutrient availability

Nutrients are the various elements and simple compounds that are critical for metabolic processes and the growth of lacustrine autotrophs (Cohen, 2003). Those that are important for diatom growth, but are of limited supply in lake waters, include phosphorus, nitrogen and silicon. These nutrients have complex cycles and numerous potential supply sources within lakes and their catchments (Wetzel, 2001). Of key relevance for this thesis is the detrital input of these nutrients from the catchment, which can be modified by changes in climate and vegetation cover (e.g. Francke et al., 2019), and the recycling of nutrients from the hypolimnion and lake sediments, where nutrients accumulate due to the settling of organic matter and decomposition (Cohen,

2003). This process is influenced by the mixing regime, which can be driven by changes in the climate such as temperature and wind strength (see below).

As demonstrated in Table 2.1, diatom taxa have various nutrient tolerances and optima, so they can be sensitive to changes in the concentration, supply rates and ratios of different nutrients (Hall & Smol, 2010). Phosphorus supply is usually the main variable responsible for driving change in diatom productivity and species composition, although it tends to cause more alteration to planktonic communities than benthic ones (Battarbee et al., 2001). If planktonic productivity increases as a result of increased nutrient availability, light transmission to the benthic habitats can be reduced, further intensifying this contrast (Scheffer & van Nes, 2007). The result is an increase in the P–B ratio. This clearly complicates diatom interpretations as the same response that might be expected if lake level had increased.

Ice cover

Once surface lake water has cooled below the temperature at which it reaches its maximum density (c. 4°C), convection is reduced and the surface water can continue to cool until ice forms (Kirillin et al., 2012). This can lead to the seasonal development of solid ice sheets or unconsolidated ice accumulations (Michel & Ramseier, 1971). The timing of ice formation, which is mainly controlled by air temperature and local wind strength, can demonstrate considerable variation from year to year, whilst the timing of ice break-up is mainly controlled by solar radiation so demonstrates less variation (Kirillin et al., 2012). Ice decay occurs at the top, bottom and edges of the ice pack, which can result in the littoral areas becoming ice-free first (Brown & Duguay, 2010). In some lakes of the high Arctic, ice can be present perennially, perhaps with some limited summer melting at the lake margins (Smol, 1988).

Ice cover can have various impacts on lacustrine diatom assemblages. Light is typically the limiting factor for photosynthesis under ice, although light transmission will vary with ice type and snow accumulation (Hampton et al.,

2017). Clear, snow-free ice, which has similar light transmission properties to water, can form on lakes in cold, dry climates or towards the end of the ice-cover period (Kirillin et al., 2012). The light availability under this ice is adequate for diatom growth (Battarbee et al., 2001). The penetration of the solar radiation through the ice generates convective currents (Kirillin et al., 2012), and these conditions favour heavy tychoplanktonic diatoms, such as *Aulacoseira* taxa (Rühland et al., 2015). Light transmission is greatly reduced if the ice contains occlusions, such as air bubbles and organic matter, or if snow accumulates over the ice (Wetzel, 2001). This type of ice cover can greatly reduce diatom productivity (Battarbee et al., 2001). The extent of the ice cover is also important; the thawing that can occur around the lake margins enables diatom growth in the littoral zone (typically small Fragilariaceae taxa; see their entry in Table 2.1), and if the lake becomes ice-free in summer, planktonic taxa will become more abundant (Douglas & Smol, 2010). The length of the ice-free period can also impact diatom assemblages, as it can encourage moss and macrophyte growth, allowing more complex diatom communities to develop in the littoral zone (Douglas & Smol, 2010).

Light availability

Light availability in lacustrine environments is controlled by various factors. Depending on latitude, the photoperiod will vary with the seasonal pattern of insolation. This is especially acute in lakes at high latitudes (Douglas & Smol, 2010). The light availability in such lakes can be further impacted by ice and snow cover, as discussed above. Water column transparency is an important modulator on light availability and is itself controlled by many factors. Reduced water column transparency can occur during times of high lake mixing or turbulence, which can resuspend sediment from the bottom of the lake (Hellström, 1991). The addition of detrital material from the catchment during times of higher erosion can have the same impact. High plankton productivity can also reduce water column transparency and impact benthic communities; this is a key process in eutrophication (Hall & Smol, 2010).

Due to the interconnected nature of the various controls on diatom assemblages, some of the impact of light availability on diatom assemblages has already been elucidated. As mentioned in section 2.2.2, diatoms typically inhabit the photic zone as they require light for photosynthesis. It has already been demonstrated that changes in lake level can have an impact on which regions of a lake basin lie within the photic zone, as has the impact this can have on diatom assemblages. Water transparency is also implicated in this process as it modifies the depth of the photic zone. Increased water transparency can enlarge the areas suitable for benthic habitats and therefore lower P–B ratios (Battarbee et al., 2001). Variations in light availability can also impact the specific taxa that reside in a lake as some are better able to adapt to low light conditions than others (e.g. *Cyclotella fottii*; Table 2.1).

Temperature

Solar radiation is the greatest contributor of heat to lakes (smaller contributions come from the lake sediments and the air) and is absorbed in the surface waters, from where it is distributed throughout the lake by internal mixing (Wetzel, 2001). Heat is lost from lakes by a variety of processes (e.g. thermal radiation, specific conduction, evaporation and outflow) and mainly occurs at the surface (Wetzel, 2001). The temperature of lacustrine environments can therefore be impacted by a range of factors including variations in insolation, air temperature, ice cover and mixing regime.

There have been extensive studies on the impact of temperature on algal growth, including laboratory culture experiments that demonstrate the direct influence of temperature on diatoms (e.g. Hania et al., 2021). However, temperature has such a large influence over so many lacustrine variables (e.g. stratification, mixing regime and nutrient availability) that recorded diatom responses to temperature are either indirect or difficult to disentangle from the myriad of variables it influences (Lotter et al., 2010). Despite this complicated response, palaeoclimate studies are still able to take advantage of both the

direct and indirect influences of temperature on diatom assemblages, for example in Lake Ohrid (Zhang et al., 2016).

Mixing regime and stratification

As discussed in the previous subsection, heat primarily enters a lake through the surface. This results in a temperature and density gradient (the thermocline, which occurs within the metalimnion) between the warm, light surface waters (the epilimnion) and the cool, dense deep waters (the hypolimnion). In this situation, the lake is said to be thermally stratified (Figure 2.7a). As winds blow over the surface, the frictional stress can generate mixing and currents in the epilimnion (Wetzel, 2001). Depending on the intensity of the turbulent mixing and the strength of the density gradient, the turbulence can propagate to the vertically adjacent water masses and stratification can be lost (Cohen, 2003; Figure 2.7b). This mixing of the water column is most likely to occur when the density contrast is reduced, which is encouraged by the loss of heat from the surface waters in the colder months (Cohen, 2003). If ice develops over the lake surface, air currents cannot induce surface mixing, and stratification can occur again (Figure 2.7c), although the water density profiles can be dynamic and are sometimes inversed (e.g. Bruesewitz et al., 2015). The density contrasts under ice are usually minimal (Figure 2.7c), so when the ice melts, mixing can occur rapidly, and as the density contrast increases into the warmer months, stratification can occur again (Cohen, 2003). Lakes with this mixing regime are characteristic of temperate regions and are termed dimictic. Other mixing regimes will result under different climatic settings. In addition to the climate-related variables of temperature, wind and ice cover, lake depth is important in determining the mixing regime of a lake, with some shallow lakes able to mix several times a year (polymictic), while deep lakes might mix very rarely (oligomictic) or only partially (meromictic).
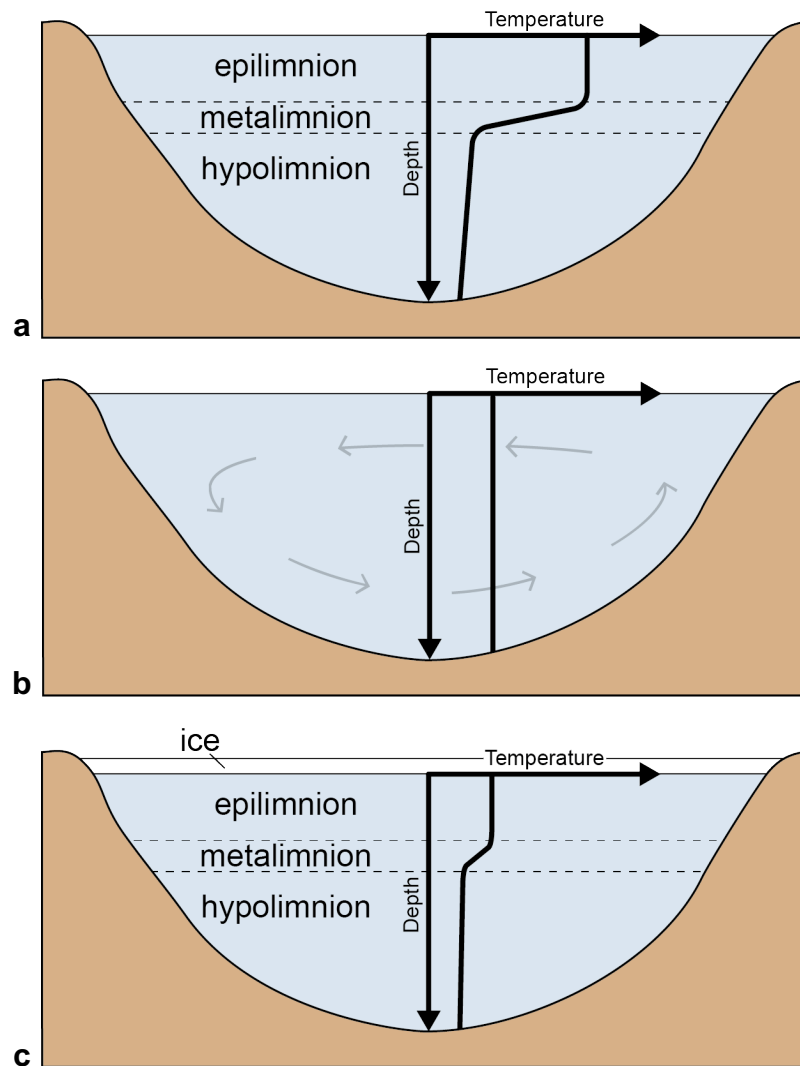
Figure 2.7: Cross-sectional diagrams of a lake illustrating temperature–depth profiles for a thermally-stratified lake with a large temperature gradient (**a**), a lake with no temperature gradient undergoing mixing (**b**) and a thermally-stratified lake under ice cover with a small temperature gradient (**c**).

The mixing regime of a lake can impact both the planktonic and benthic diatom communities with varying results. Turbulent mixing is responsible for suspending facultative planktonic and benthic taxa in the water column (Battarbee et al., 2001), which could reduce the P–B ratio at profundal coring sites. In shallow lakes, mixing can resuspend sediments from the bottom of the lake into in the water column. Clay particles can remain suspended for long periods of time and reduce light availability for benthic communities (Hellström, 1991; Schallenberg & Burns, 2004), thereby increasing the P–B

ratio. However, this process can also release nutrients and increase algal productivity if it was previously nutrient-limited (Schallenberg & Burns, 2004).

Planktonic taxa are generally more abundant during times of lake mixing as diatoms have a specific gravity greater than 1.0, which means they should sink through the water column (Battarbee et al., 2001). This is especially true for those with heavily silicified valves such as *Aulacoseira* species. Periods of intense mixing can be characterised by the presence of such taxa (Wolin & Stone, 2010). Others have developed a range of coping strategies to remain successful despite this tendency to sink. During times of limited water mixing and stratification, small valves are more easily kept suspended in the water column (e.g. *Pantocsekiella minuscula*; Table 2.1), so they can dominate assemblages (Winder et al., 2009). Others, such as *Asterionella formosa*, form stellate colonies that are more resistant to sinking than individual cells (Table 2.1; Rühland et al., 2015). There is also evidence that some are able to survive and grow as part of the benthic community if they sink (Yehoshua & Alster, 2011). This could explain why *Actinocyclus normanii*, a large planktonic taxon, has been documented within both planktonic and benthic communities (Table 2.1).

2.2.4 Difficulties and limitations

In addition to the difficulties in disentangling the influence of the various competing controls on diatom assemblages (section 2.2.3), other problems can arise with diatom-based reconstructions. A lack of ecological data for extinct taxa with no modern analogues can be problematic, particularly in ancient lakes with their older fossil assemblages and high degrees of endemism (Mackay et al., 2010; Wilke et al., 2016). In such situations, some inferences can be made from the morphological features they share with extant taxa such as valve size (Winder et al., 2009).

The accuracy with which the fossil diatom assemblage reflects the living diatom assemblage is an important consideration in any diatom

reconstruction. Various taphonomic processes can affect diatoms within the water column and in sediments. Complete or partial dissolution of their silica valves can occur in waters that are undersaturated with silica, particularly if temperature, pH or salinity is high (Flower & Ryves, 2009). Interspecific variations in valve thickness, ornamentation and surface area to volume ratio can result in differential dissolution between diatom taxa and lead to bias in the fossil assemblage towards robust species such as small Fragilariaceae and those of the genus *Aulacoseira* (Barker et al., 1994; Ryves et al., 2003; Battarbee et al., 2005). Valve breakage can occur in high energy environments such as shallow lakes, which can encourage dissolution through the exposure of a larger surface area upon which dissolution can act (Ryves et al., 2006). It can also result from grazing (Haberyan, 1985) and the compaction or desiccation of sediments (Flower, 1993; Reed, 1998). Hassan (2015) demonstrated that the taxonomic composition of diatom death assemblages can significantly differ from living assemblages as a result of the differential preservation of diatom taxa and the long periods of time represented by death assemblages. In this particular instance the death assemblage was still able to faithfully reflect environmental conditions, but it does highlight the need to understand the preservation potential of the specific taxa in the diatom assemblage that is being investigated and the taphonomic processes likely to be occurring in the specific lake under investigation.

2.2.5 Diatoms as part of a multiproxy approach

In light of the difficulties associated with the use of diatoms in palaeolimnology, it is prudent to analyse them alongside other lines of evidence. It is well recognised that studying multiple proxies within a record strengthens palaeoenvironmental interpretations (Birks & Birks, 2006). Some proxy records have previously been obtained from the sedimentary material that is analysed within this thesis (see section 4.1). In order to make use of these existing data, it is necessary to understand the proxies from which they were obtained. These palaeoenvironmental indicators are now introduced.

Pollen

Pollen analysis (palynology) is one of the most widely adopted methods in the reconstruction of past environments (Lowe & Walker, 2015) and has a long history in Quaternary Science (Birks & Berglund, 2018). It is used to understand past vegetational change on local to continental scales (e.g. Magri et al., 2017). It is also useful for the correlation of stratigraphic sequences (e.g. Tzedakis, 1994), including between marine and terrestrial records (e.g. Roucoux et al., 2005).

Pollen grains and spores (collectively known as sporomorphs) are the reproductive propagules of seed-producing (angiosperms or gymnosperms) and lower (cryptogams) plants respectively (Lowe & Walker, 2015). They are dispersed through a range of means but primarily via the wind (anemophilous) or insects (entomophilous; Bennett & Willis, 2001). Pollen that settles on sites where sediment is accumulating (e.g. lakes) can become embedded and preserved within the sediment, a process that is aided by the highly resistant material (a biopolymer known as sporopollenin) that makes up their outer walls (exine; Jardine et al., 2021). As the pollen grains of different taxa possess different morphologies, they are able to be identified to genus or family level from their visual features alone. The identification of pollen grains throughout a sedimentary sequence allows the reconstruction of vegetation communities in the area around the site of deposition and their development through time (Birks & Birks, 1980).

There are some key considerations to make when interpreting pollen records. A preserved pollen assemblage does not necessarily reflect the exact vegetation composition of the local environment at the time of pollen deposition as biological, chemical and environmental processes influence the production, dispersal and preservation of pollen grains (Chevalier et al., 2020). The amount of pollen released by a plant varies according to the dispersal mechanism employed by the plant species. Anemophilous taxa produce much higher

pollen quantities than entomophilous taxa, which are consequentially underrepresented in pollen records. Furthermore, wind-borne pollen can travel large distances so their taxa can be overrepresented in pollen records, even when they are not prominent in the local environment (e.g. Campbell et al., 1999). The size of the lake is also an important consideration, with pollen assemblages from smaller lakes more likely to capture local changes and those from larger lakes tending to reflect changes on a more regional scale (Prentice, 1985). Such contrasts have even been detected within a single lake basin; at Ioannina, pollen records from a smaller sub-basin reflect more local changes in vegetation than those from a larger sub-basin (Jones, 2010). The differential preservation of various taxa can lead to taxonomic bias in the pollen assemblage and tends to be related to the sporopollenin content of the exine (Havinga, 1967). As well as examining the pollen assemblage, it can be useful to consider the pollen concentration as it can reflect vegetation biomass (Magri, 1994). However, its interpretation is often complicated by changes in sedimentation rate (Roucoux et al., 2008).

Pollen data are usually expressed as percentage relative abundances based on a sum that excludes the pollen of obligate aquatic plants, moss, spores and unidentifiable grains (Bennett & Willis, 2001). In this way, percentages represent a proportion of only the terrestrial vascular plants. These pollen data are often summarised into two groups reflecting the percentage of arboreal pollen (AP) and the percentage of non-arboreal pollen (NAP). This can indicate the extent of any woodland nearby with high AP percentages representing periods of extensive woodland. It is sometimes useful to exclude pioneer taxa such as *Pinus*, *Juniperus* and *Betula* (AP–PJB) to reflect the extent of the temperate tree population only (e.g. Roucoux et al., 2008).

Organic content

Most organic matter in lake sediments originates from plants (Meyers & Teranes, 2001). This plant material can be allochthonous, derived from

different components of catchment vegetation (e.g. leaves, pollen grains, woody material, etc.) or it can autochthonous, derived from algae and aquatic macrophytes within the lake itself (Dean, 1981). Therefore, an estimate of the percentage of organic content within lake sediments can provide an indication of the combined productivity of the lake and its catchment with a higher organic content associated with higher productivity. Caution is required in its interpretation as several processes, such as benthic respiration and decay, affect the amount of organic material that is eventually preserved in the sediment (Dean, 1981).

Carbonate content

There are numerous possible sources of carbonate material in lacustrine sediments, complicating its interpretation. These include the input of detrital carbonate from the catchment as well as precipitation, both organic and inorganic, of carbonate within the lake itself (Kelts & Hsü, 1978). For lakes situated in carbonate bedrock catchments, the amount of detrital carbonate in their sediments can provide an indication of catchment erosion with more erosion of the catchment bedrock resulting in the delivery of more detrital carbonate to the lake. In contrast, carbonate precipitated within the lake can provide an indication of productivity. Many lacustrine organisms produce carbonate skeletal material such as shells, with larger volumes of this material indicating higher productivity levels. However, this type of carbonate tends to be concentrated in the littoral zone and only forms a small component of the carbonate sedimentation in hardwater lakes (Kelts & Hsü, 1978). Of more importance is the primary precipitation of inorganic carbonate induced by the removal of CO_2 from the water by photosynthetic macrophytes and algae (Dean, 1981). A greater accumulation of inorganic carbonate produced in this way could indicate greater within-lake productivity, although it is important to consider that other factors, such as warming temperatures or a lowering of the precipitation to evaporation ratio, can also encourage carbonate precipitation (Dean, 1981). To complicate matters further, carbonate is susceptible to

dissolution, meaning the volume preserved in the sediment is not necessarily a reflection of the volume that was present in the lake. It is clear that both the source of the carbonate and any dissolution must be considered in order to make a reliable interpretation.

Magnetic mineral properties

Lake sediments can contain a variety of iron-bearing, magnetic minerals such as magnetite, haematite and goethite. By applying a temporary, weak magnetic field to the sediment, these minerals become magnetised. The ratio of the intensity of the applied magnetic field to the resulting magnetisation of the sediment sample can be used to calculate its mass specific magnetic susceptibility (χ), which reflects the size, shape, concentration and chemical composition of the magnetic minerals in the sample (Thompson & Oldfield, 1986). As magnetic minerals in lake sediments are often derived from detrital material washed in from the catchment (eroded bedrock and soil), magnetic susceptibility measurements can be used as an indicator of inwash to the lake (e.g. Thompson et al., 1975) and are therefore useful in making interpretations about past vegetation cover and erosion rates (Thompson et al., 1980).

However, there are numerous sources of magnetic minerals and various controls on their transportation and transformation, complicating interpretations of magnetic susceptibility measurements (Verosub & Roberts, 1995). The original source of magnetic minerals is the bedrock, within which they are known as primary magnetic minerals (Thompson & Oldfield, 1986). The processes of weathering and soil formation (pedogenesis) act upon the bedrock and can result in the production of secondary magnetic minerals with different chemical compositions, and therefore magnetic susceptibilities, to the primary magnetic minerals (Thompson & Oldfield, 1986). Furthermore, the climatic conditions during pedogenesis can influence the type of magnetic minerals that form (Maxbauer et al., 2016). In summary, this means that variations in the magnetic susceptibility of lake sediments might not simply

represent a change in the rate of inwash to the lake but could also reflect changes in the source of the magnetic minerals, the rate of soil formation or the climate during soil formation. It is important, therefore, to consider the type and source of the magnetic minerals present in lake sediments when making palaeoenvironmental interpretations from magnetic susceptibility measurements.

2.2.6 Diatom responses in lakes of the northeastern Mediterranean

Within the northeastern Mediterranean, Quaternary palaeoenvironmental records based on diatom analyses have been published from very few sites but include the two investigated in this thesis, Lake Ioannina and Lake Ohrid, as well as Lake Prespa (Albania/Greece/North Macedonia) and Lake Dojran (Greece).

Lake Ioannina

In the early 1990s, palaeoenvironmental analyses of a long core from Lake Ioannina (I-249) enabled the reconstruction of vegetational changes over multiple glacial–interglacial cycles and identified the area as a glacial refugium for temperate tree species (Tzedakis, 1993; 1994). This established Ioannina as a key site for Quaternary research, and numerous palaeoenvironmental studies ensued on a proximal, but higher resolution, core (I-284; detailed in section 4.1.1). Palynological data from the I-284 core for the Lateglacial and early Holocene demonstrated a subdued response during the Younger Dryas, a time when SSTs in the Adriatic Sea and other parts of the Mediterranean Sea exhibit a decline (Lawson et al., 2004). This prompted the first diatom investigation of the site, which aimed to establish whether climate change was truly muted at Ioannina during the Younger Dryas or if local factors such as topographic variability modulated the vegetational response (Wilson et al., 2008). The analyses revealed a diatom assemblage dominated by eurytopic taxa (those able to tolerate a wide range of environmental conditions) but one that was highly sensitive to climate change, with planktonic taxa dominating during

warmer, wetter intervals and small Fragilariaceae dominating during cold, arid phases. It provided the first strong evidence for a Younger Dryas event in northwest Greece, although the dominance of the eurytopic taxa meant it was not possible to confidently separate the extent to which lake level or productivity changes were driving the variation in the record. This data was re-examined as part of multicore study, which established that the diatom assemblage change during the Lateglacial and Holocene was primarily a response to changing lake levels (Jones et al., 2013).

Following the identification of a response more sensitive than that represented by the pollen, diatom analyses were performed on earlier sections of the I-284 core for which pollen records had already been published, namely the penultimate deglaciation (MIS 6 to MIS 5e transition, Termination II; Wilson et al., 2015) and penultimate glacial (MIS 6; Wilson et al., 2013; Wilson et al., 2021). The diatoms consistently demonstrated incredible sensitivity to abrupt climate variability.

During the penultimate deglaciation, an abrupt increase in the P–B ratio reflected an increase in lake levels c. 2.7 kyr before regional forest expansion and peak precipitation (Wilson et al., 2015). It was suggested that the early onset of high lake levels could have been due to the input of snow melt and glacial meltwater into the subterranean karst system. The contrast of the diatom response between the penultimate deglaciation (Wilson et al., 2015) and the last deglaciation (Wilson et al., 2008; Jones et al., 2013) highlighted the potential of investigating earlier glacial–interglacial cycles with different boundary conditions.

The diatoms also demonstrate that abrupt climate variability at Ioannina is not confined to the glacial terminations. High amplitude millennial-scale oscillations in the diatom assemblage persisted throughout the entirety of the penultimate glacial and were interpreted as representing a series of discrete warmer/wetter intervals versus cooler/drier intervals (Wilson et al., 2021). This

variation was associated with variability in the AMOC with the warmer/wetter intervals coinciding with strong Asian Monsoon events and North Atlantic interstadials, and the cooler/drier intervals coinciding with weaker Asian Monsoon events and North Atlantic stadials. Once again, the diatoms demonstrated a strong response in comparison to the relatively subdued response exhibited by the pollen.

The diatom record spanning MIS 6 represents the oldest section of the I-284 core for which diatom data have so far been published. The published pollen record extends through the penultimate interglacial (MIS 7), which contains four forested intervals separated by periods of more open vegetation (Roucoux et al., 2008). The evidence indicates that the forested intervals had cooler winters and wetter summers than those of the last interglacial or the Holocene, and it also suggests that millennial-scale climatic variability persisted through the very cold and very dry conditions of the interval equivalent to MIS 7d. This variability and contrast with earlier intervals highlights the potential of a diatom record from this interval to add to our understanding of limnological responses to various climatic conditions.

Lake Ohrid

The first palaeolimnological investigation of the Lake Ohrid diatoms related changes observed in a 8.85 m core from the central region of the lake to variations in climate (Roelofs & Kilham, 1983). A more recent analysis of a sediment core from the northeast part of the lake basin, and with a basal age of approximately 136 ka (Co1202; Vogel et al., 2010), demonstrated the sensitivity of the Lake Ohrid diatoms to climate change and revealed a response to glacial–interglacial climate variability (Reed et al., 2010). Shifts between the dominant planktonic taxa of hypolimnetic *Cyclotella fottii* and epilimnetic *Pantocsekiella ocellata* were interpreted as reflecting temperature-driven productivity shifts.

Subsequent analyses were performed on a higher resolution core from the western part of the lake (Co1262) for the Lateglacial and Holocene (Zhang et al., 2016). This provided support for the interpretation of a direct diatom response to temperature-driven lake productivity but revealed that indirect responses to temperature-related lake stratification or lake mixing and epilimnetic nutrient availability also occurred. The contrast between the temperature-driven diatom response in Lake Ohrid and the moisture-driven diatom responses in shallower Mediterranean lakes was also highlighted. Lake Ohrid is unusual in its great depth (section 3.2.2) so does not demonstrate the large Quaternary fluctuations in lake level that are observed as the dominant control on diatom assemblages in shallower lakes such as Lake Ioannina (Jones et al., 2013), Lake Prespa (Cvetkoska et al., 2014a) and Lake Dojran (Zhang et al., 2014b). While these lake level changes can provide insight into past variations in moisture availability, Lake Ohrid is able to provide information on past changes in temperature. Utilising these contrasting responses can therefore lead to more robust regional palaeoclimate interpretations.

High-resolution analyses of core 5045-1 from the DEEP site (henceforth referred to as the DEEP core; section 4.1.2) once again demonstrated diatom responses to climate change over the most recent glacial–interglacial cycle (Cvetkoska et al., 2016). The responses were compared with those of Lake Prespa, and it was concluded that Lake Ohrid demonstrated more resistance to climate change than Lake Prespa. Other diatom-based research at Lake Ohrid has further contrasted these two hydrologically connected lakes through an investigation into their contrasting resilience to environmental disturbance by focusing on responses after a volcanic eruption (Jovanovska et al., 2016). Both lakes demonstrated a high resilience, although the diatom assemblages of Lake Ohrid recovered more quickly than those of shallower Lake Prespa.

Most recently, a long, low-resolution diatom record was published for the entire DEEP sequence, which investigated the influence of global/regional-versus local-scale environmental change on diatom communities over the past

1.36 Ma (Cvetkoska et al., 2021). The results indicated that long stable periods in diatom community composition were punctuated by relatively rapid turnover in species composition, and three distinct diatom communities characterised by specific taxa were identified. Local-scale environmental change (e.g. water column mixing, nutrient availability and precipitation) had some influence on diatom community composition throughout the whole record, but its influence diminished over time. Global/regional environmental change (e.g. orbital parameters, global ice volume and atmospheric CO_2 concentrations) was important only once the lake had deepened c. 1 Ma. These results highlighted the importance of considering lacustrine, catchment and climate dynamics in diatom record interpretations.

Chapter 3 | Study region and sites

Lake Ioannina (also known as Lake Pamvotis or Lake Pamvotida) and Lake Ohrid are located approximately 150 km apart on the Balkan Peninsula in the northeastern Mediterranean (Figure 3.1). They are both ancient lakes that formed within tectonic basins of the Dinaride-Albanide-Hellenide mountain belt. Being situated in such close proximity, Lake Ioannina and Lake Ohrid have evolved under similar tectonic and climatic settings. As a result, they share many catchment and limnological characteristics. They differ mainly in depth and trophic status; Lake Ioannina is currently shallow and eutrophic whilst Lake Ohrid is deep and oligotrophic. This chapter discusses their regional setting, their individual characteristics and concludes with a summary of their contrasts and similarities.
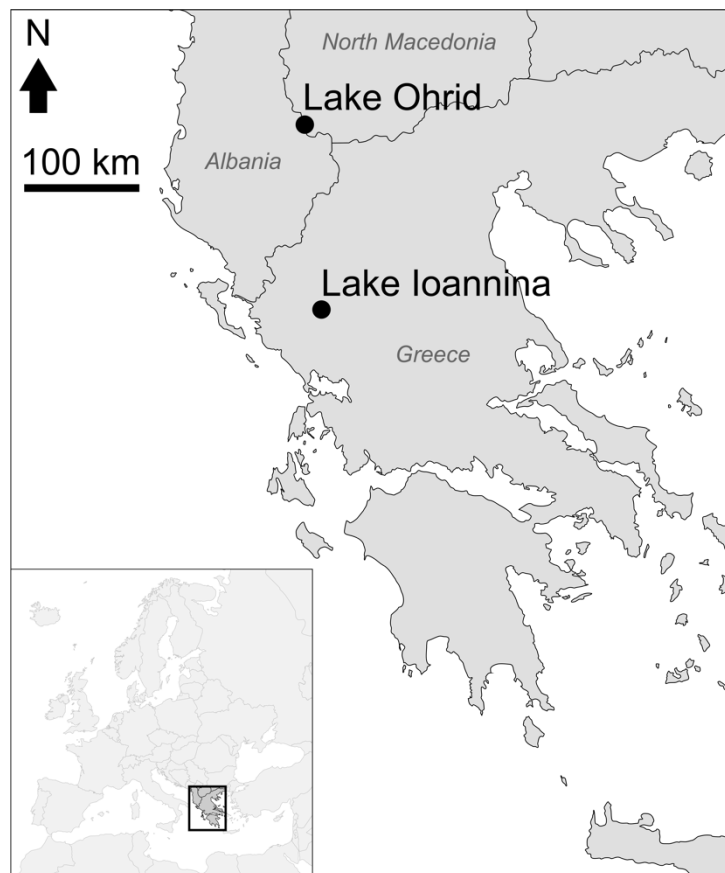
Figure 3.1: Map showing the locations of Lake Ioannina and Lake Ohrid on the Balkan Peninsula with an inset map showing the location of the Balkan Peninsula within Europe.

3.1 Study region

3.1.1 Tectonic setting

The land around the Mediterranean basin is dominated by the high relief of the Alpine orogenic belt (Figure 3.2), which is a product of the complex convergence of the African and European plates. It consists of connected fold and thrust belts, which differ in timing and tectonic setting and are associated with the closure of several oceanic basins of varying age and size (Cavazza & Wezel, 2003).

Figure 3.2: Map of the Mediterranean region illustrating the high relief and simplified tectonics of the Alpine orogenic belt. The SBER is highlighted in white. (after Cavazza & Wezel, 2003 and Dumurdzanov et al., 2005).

Of relevance to the northeastern Mediterranean is the closure of the Vardar Ocean during the latest Cretaceous to earliest Cenozoic (c. 65 Ma), which accreted several continental fragments onto the Balkan Peninsula and initiated an extensional regime over an area known as the southern Balkan extensional region (SBER; Figure 3.2; Burchfiel et al., 2008). Extension was able to develop within this convergent setting due to a process known as slab rollback. As the oceanic lithosphere subducted eastwards beneath the Balkan Peninsula, rollback of the subducted slab caused the subduction zone to migrate

westwards, stretching the area of land to the east of the subduction zone (Figure 3.3). The associated east–west extension resulted in the formation of sedimentary basins initially in the east and later in the west as the subduction zone migrated (Dumurdzanov et al., 2004). These are the basins within which the study sites are location.
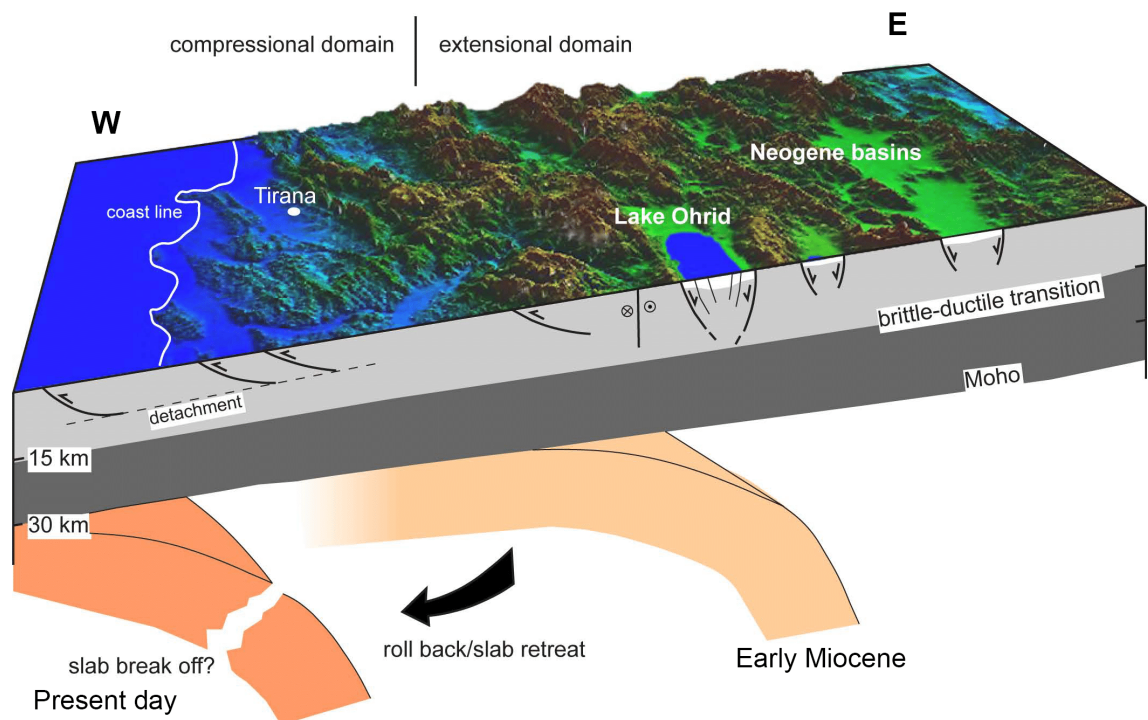
Figure 3.3: Structural cross-section of the Adriatic coast showing the subduction rollback that enables extension in the SBER despite the convergent setting of oceanic lithosphere subducting beneath. Slightly modified from Hoffmann et al. (2010).

Although no crust is actively being subducted in the northern Hellenic trench today (Hoffmann et al., 2010), GPS studies indicate it is still under compressional stress (Dumurdzanov et al., 2005). Recent earthquake data and field observations indicate that the area is still tectonically active with some areas, such as the Ohrid basin, undergoing active extension (Hoffmann et al., 2010; Reicherter et al., 2011; Lindhorst et al., 2015). Other lines of evidence, such as river terraces and archaeological evidence, suggest that tectonic uplift is still active in northwestern Greece (King & Bailey, 1985).

3.1.2 Climatic setting

At 30–45 °N, the Mediterranean region is situated in a transitional zone between the mid-latitude westerly wind belt to the north and the subtropical high pressure systems to the south (Harding et al., 2009). The seasonal migration of the Intertropical Convergence Zone (ITCZ) is associated with latitudinal shifts in the pressure and wind belts of the global atmospheric circulation and therefore brings the Mediterranean region under the dominance of the mid-latitude westerly wind belt during winter and the sub-tropical high pressure belt during summer. This causes pronounced seasonality in Mediterranean precipitation (Figure 3.4). Warm, dry conditions ensue when the high pressure belt resides over the Mediterranean region during the summer. In contrast, winters are cool and wet as the mid-latitude westerlies generate low pressure systems across the Mediterranean (Tzedakis et al., 2009b).
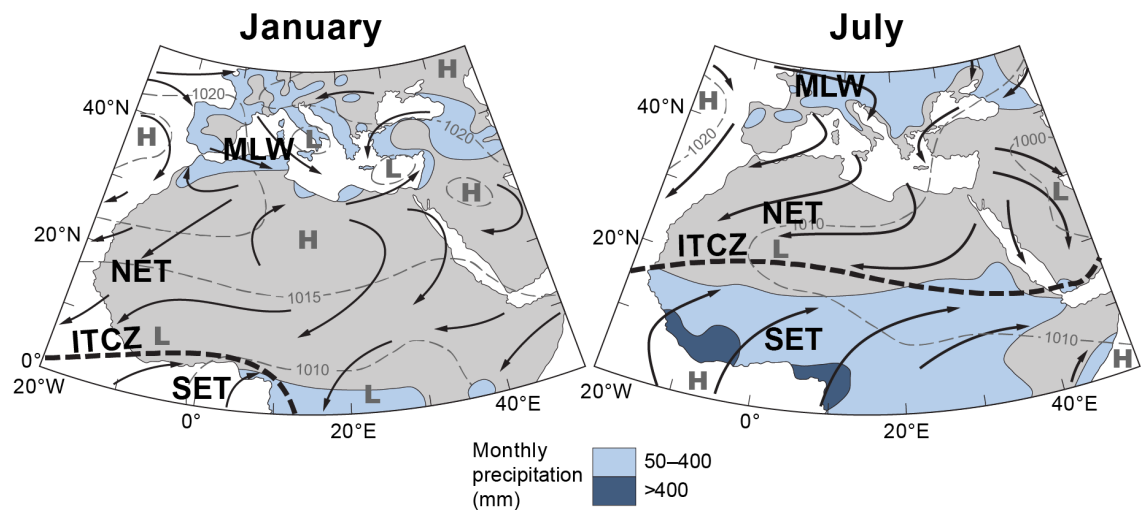
Figure 3.4: Maps of the Mediterranean region and North Africa illustrating the contrasting positions of the wind and pressure belts between winter (January) and summer (July). The seasonal contrasts in precipitation as a result of the different atmospheric configurations is evident. (ITCZ—Intertropical Convergence Zone; MLW—Mid-Latitude Westerly winds; NET—North-Easterly Trade winds; SET—South-Easterly Trade winds). Modified from Harding et al. (2009).

Winter conditions are further modulated by large-scale pressure patterns over the North Atlantic. The North Atlantic Oscillation (NAO) is a variation in the north–south sea level pressure contrast between a low pressure system to the north (the Icelandic low) and a high pressure system to the south (the Azores high). During positive NAO phases, there is a large pressure contrast between the Icelandic low and the Azores high (Hurrell et al., 2002). This strengthens the mid-latitude westerlies and shifts them northwards, resulting in drier conditions in the Mediterranean (Magny et al., 2013; Figure 3.5a). During negative NAO, the contrast between the Icelandic low and the Azores high is much smaller. The westerly winds move southwards resulting in increased storm activity and precipitation in the Mediterranean (Hurrell & Deser, 2009; Figure 3.5b).
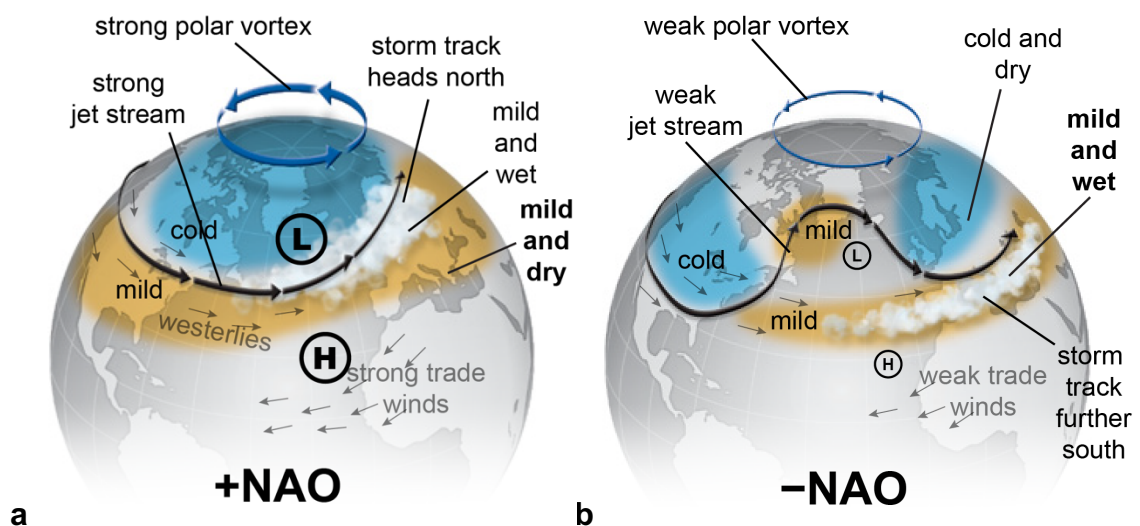
Figure 3.5: Diagrams illustrating the impact of positive (**a**) and negative (**b**) NAO phases on the prevailing weather patterns in Europe. During positive phases, the Mediterranean is mild and dry. During negative phases, the Mediterranean is mild and wet. Modified from Greene (2012).

The climate also varies between different parts of the Mediterranean region. There is a general trend of decreasing precipitation and an increase in extreme temperatures towards the south and east (Harding et al., 2009). These trends are further modified by variation in local climate as a result of extreme

topographic variability, which is especially true on the Balkan Peninsula (Figure 3.6; Lolis & Kotsias, 2020).
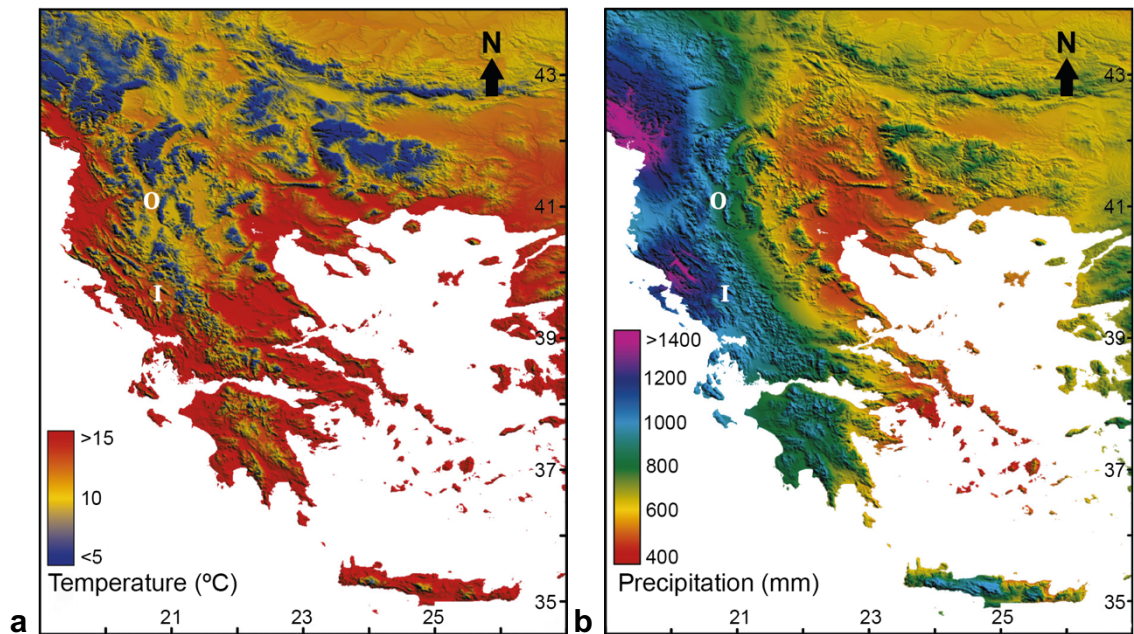
Figure 3.6: Contrasts in mean annual temperature (**a**) and precipitation (**b**) across the Balkan Peninsula. The locations of Lake Ioannina (I) and Lake Ohrid (O) are marked. Modified from Panagiotopoulos (2013), which is based on data from Hijmans et al. (2005).

There are few other regions in the world where the resulting temperature contrasts are as strong as on the Balkan Peninsula (Reed et al., 2004). These contrasts are greatest in winter when mean January temperatures are typically high in the Mediterranean coastal regions (+12°C in northern Crete), due to the protection of the Dinaride, Pindus and Rhodopes mountains from the invasion of cold air from the north, but drop to below freezing in northeastern areas along the coast of the Black Sea (−0.8°C around the Danube delta), which remain exposed (Reed et al., 2004). Local topographic variation across the Balkan Peninsula also results in strong differences in mean annual precipitation, with marked differences between the west and east coasts (<1000 mm yr^{-1} on the Adriatic coast and around 350–400 mm yr^{-1} on the Black Sea coast) and between the mountainous and lowland regions (Furlan, 1977; Reed et al., 2004). The southern peaks of the Dinarides experience some of the

highest values of mean annual precipitation in Europe (>4,600 mm yr^{-1} at Crkvice, Montenegro) with values decreasing in all directions from here (Reed et al., 2004). The local topography also influences the timing of precipitation maxima across the region. The south of the Balkan Peninsula experiences typical Mediterranean precipitation maxima during the winter in association with the westerlies. Across the Mediterranean, local orography modifies the path of these westerlies (Raicich et al., 2003), and on the Balkan Peninsula it prevents their penetration into the northern lowlands. This area remains open to Central and Eastern Europe and so experiences a more continental climate, exposed to anticyclones in winter and experiencing precipitation maxima in spring and summer when the westerlies shift northwards (Furlan, 1977; Reed et al., 2004).

3.2 Study sites

3.2.1 Lake Ioannina

Location and topography

Lake Ioannina (39°40´ N, 20°53´ E) is located in Epirus, northwest Greece, at an altitude of 470 m above sea level. The lake is surrounded by the high topography of the Pindus Mountains (Figure 3.7). Along the northeastern edge of the Ioannina basin, the steep slopes of the Mitsikeli mountain range rise to a summit of 1810 m. The gentler slopes of the Tomarochoria mountain range rise to the 1173 m summit of Megali Tsouka along the basin's southwestern edge. With a surface area of 22.8 km^2 (Kagalou et al., 2008), the present day lake occupies only a small part of the Ioannina basin (Figure 3.7). Whilst the basin is 35 km long and has a variable width of 3–10 km, the lake only has a maximum length of 11 km and a maximum width of 5 km. The lake once filled the larger basin area but has been subjected to several artificial drainage schemes since 1600, including the construction of a canal and tunnel in 1944 (Higgs et al., 1967). By the 1950s, two lakes occupied the basin, separated by a

peaty marsh. The more northerly Lake Lapsista, with a depth of 1–3 m, was drained in 1959 to create agricultural land, leaving the southerly Lake Ioannina as the only remaining remnant of the once larger water body (Kagalou et al., 2001; Romero et al., 2002).
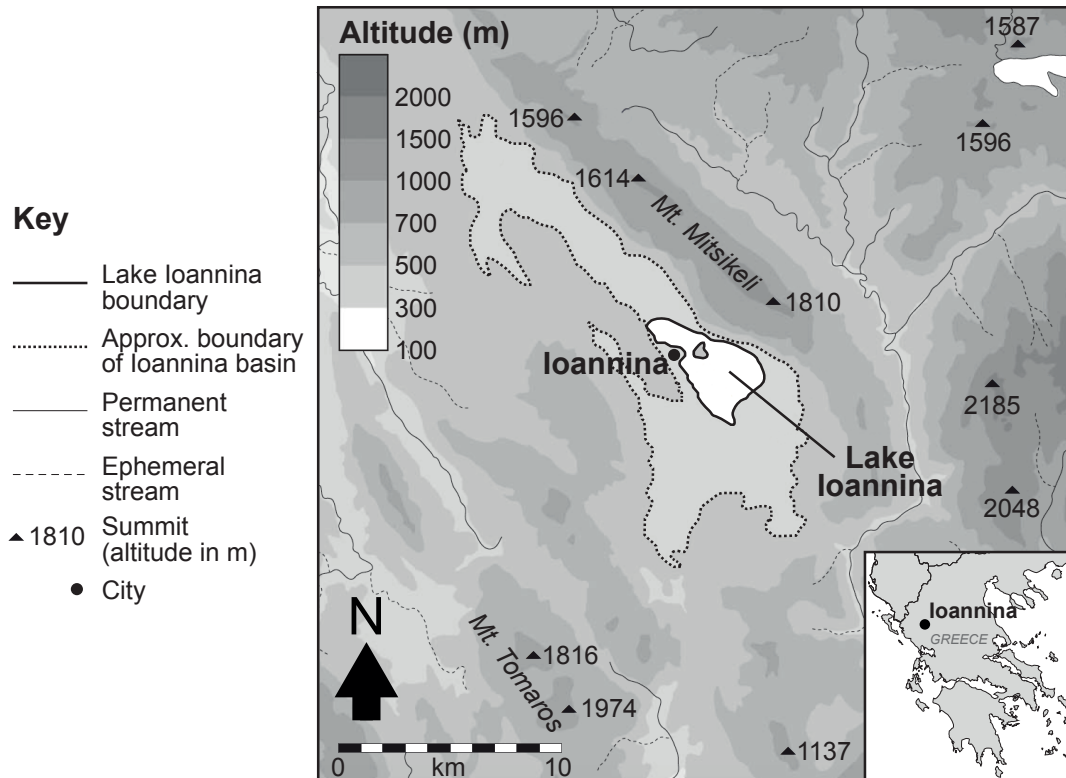
Figure 3.7: Map illustrating the topographic setting of Lake Ioannina with an inset set map showing the location of Ioannina within Greece (modified from Lawson et al., 2004). The 500 m contour that encircles the present-day Lake Ioannina is delineated by the thicker dotted line and approximates to the basin margin, which represents the maximum extent of the larger lake that once occupied the basin.

Geological setting

Formed on a syncline of the Alpine orogenic belt, the Ioannina basin is a *polje*, which is a large flat depression formed as a result of karst solution of the limestone bedrock. These Mesozoic to early Cenozoic limestones comprise the majority of the bedrock with flysch (interbedded, marine sandstone and mudstone) also outcropping towards the south of the basin (King et al., 1994;

Tzedakis, 1994). Slow tectonic subsidence has led to the accumulation of a thick sequence of Quaternary sediments (Clews, 1989).

Physical and chemical limnological characteristics

The lake forms the base level of a karstic aquifer within the Mitsikeli Mountain. It is fed only by karstic springs and drains intermittently through a series of sink holes to the Arachthos, Louros and Kalamas rivers (Kagalou et al., 2001). There are no major fluvial inputs or outputs. Although it appears to be hydrologically closed and the isotopic composition of the lake water demonstrates enrichment by evaporative concentration (Frogley, 1997), the lake water remains fresh with a conductivity of 393 µS cm^{-1} and a pH range of 6.7–8.9 (Kagalou et al., 2008). This freshness indicates some form of subsurface outflow, although the degree to which subterranean springs influence its hydrology, either now or in the past, is poorly understood (Wilson et al., 2008). The lake is currently shallow, with a mean depth of 4.3 m and a maximum depth of 7.5 m (Kagalou et al., 2008). It is dimictic, mixing twice a year as a result of changes in water density (Zacharias et al., 2002), although based on its depth and area, Jones (2010) suggested it might even be polymictic. It has a hydraulic residence time of 0.84–0.90 years (Kagalou et al., 2008). Summer temperatures are approximately +25°C in the epilimnion and +20°C in the hypolimnion, whilst winter surface water temperatures can drop to below +4°C with ice formation sometimes occurring over the lake surface (Kagalou et al., 2008).

Nutrient status

Agricultural, industrial and urban expansion has led to severe nutrient enrichment of the lake, and it is now considered hypereutrophic. It had an average total phosphorus content of 0.11 mg l^{-1} and a Secchi depth of 60–80 cm during 1998–1999 (Romero et al., 2002). This status had persisted since at least the 1980s, and whilst restoration attempts have been made (focussing on reducing external phosphorus loading and biomanipulation), phosphorus

levels in the lake remain high enough to maintain eutrophic conditions; by 2004–2005, there was still an average orthophosphate concentration of 0.19 mg l^{-1} (Kagalou et al., 2008). Due to its shallow depth and polymictic status, nutrients are readily released from the sediment. This internal phosphorus loading is slowing the lake's response to the attempts to reduce external phosphorus loading (Kagalou et al., 2008). Throughout 2016 to 2018, eutrophication monitoring of the lake using remote sensing techniques to estimate chlorophyll–a concentration, an indicator of phytoplankton productivity, demonstrates that the lake has remained eutrophic in more recent times (Peppa et al., 2020). Due to all of this anthropogenic impact, the diatom assemblage of the modern-day lake is unlikely to be a good analogue for those of its Quaternary past.

Climate

The Ioannina basin experiences a sub-Mediterranean climate with cool, wet winters and warm, dry summers (Figure 3.8). The basin experienced a mean annual precipitation of 1158 mm over the period 1915–1998 (Romero et al., 2002), a relatively high value due to the orographic uplift of warm, moist air from the nearby Ionian sea. Values are much lower for sites further east due to the rain shadow effect of the mountain ranges (Frogley, 1997). January is the coldest month, with a mean temperature of +4.9°C, and July is the warmest month, with a mean temperature of +24.9°C (Tzedakis, 1994). Due to its elevation, frosts and snowfall are common. This has impacts on the vegetation of the basin which lacks some of the usual Mediterranean species such as *Olea* (Lawson et al., 2004).

Vegetation

Due to intense grazing and agricultural pressures, little of the natural vegetation remains within the Ioannina basin (Frogley, 1997) with open scrub (*Juniperus communis*) and grassland dominating (Roucoux et al., 2008). The nearby nature reserve of Zagoria is less grazed and better preserves the natural
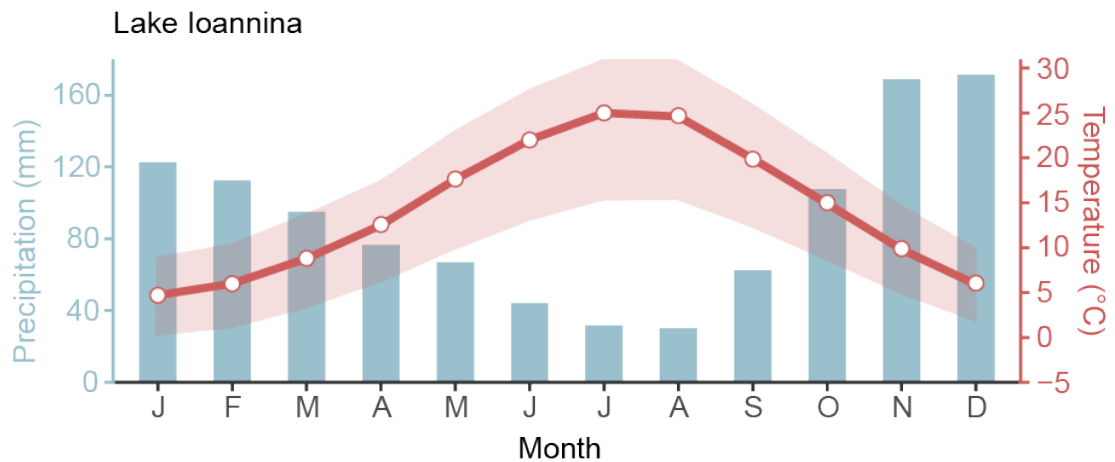
Figure 3.8: Mean monthly temperature and precipitation for Lake Ioannina. Additionally, the range between minimum and maximum monthly temperatures is shaded in red. Based on observed data from the Ioannina meteorological station over the period 1956–2010 (Hellenic National Meteorological Service, 2020).

vegetation expected at Ioannina: mixed deciduous woodland dominates below 1500 m; *Pinus* and *Juniperus* increase in abundance with altitude, often forming the tree line at 1900 m; and *Fagus* and *Abies* grow at 1000–1800 m, particularly in wetter and cooler areas, where they sometimes form the tree line (Roucoux et al., 2011). Around the lake itself, free-standing reeds, such as *Phragmites australis,* surround the margins (Higgs et al., 1967; Frogley, 1997). A decline in the abundance and diversity of the aquatic vegetation, in particular the submerged macrophytes, has been recorded since 1970 with the present day vegetation being primarily located in the northern littoral zone of the lake and covering only 5% to 10% of the lake surface (Stefanidis & Papastergiadou, 2007). This has been attributed to the cultural eutrophication of the lake and to the stocking of the lake with carp species (since 1986), which are known to destroy submerged aquatic vegetation (Alexakis et al., 2013).

3.2.2 Lake Ohrid

Location and topography

Located at an altitude of 694 m above sea level, Lake Ohrid (40°54´–41°10´ N,

20°38´–20°48´ E) spans the border of the Republic of North Macedonia and the Republic of Albania (Figure 3.1). Of its 358 km^2 surface area (Stanković, 1960), 251 km^2 lies within Macedonia and 107 km^2 lies within Albania (Popovska & Bonacci, 2007). The lake is situated within a graben basin surrounded by the mountain ranges of the Dinaride mountain belt (Figure 3.9). The Mokra Mountains rise to 1500 m in the west, and the Galičica and Mali i Thatë Mountains rise to more than 1750 m in the east (Wagner et al., 2008).
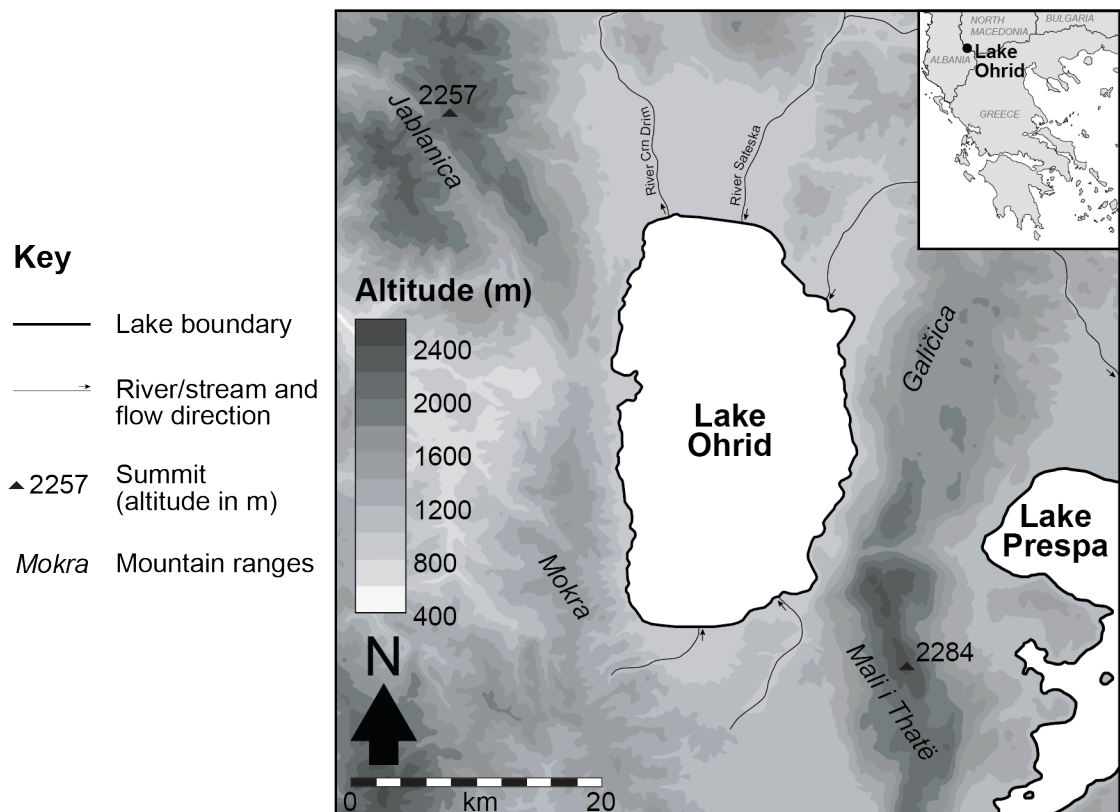
Figure 3.9: Map illustrating the topographic setting of Lake Ohrid with an inset set map showing the location of Lake Ohrid on the border of Albania and North Macedonia.

Geological setting

The geological contact between the Mirdita Zone and the Korabi Zone trends NW–SE through the Ohrid graben and outcrops south of the Lini Peninsula on the western edge of Lake Ohrid (Hoffmann et al., 2010). The Mirdita Zone consists of Jurassic ophiolites overlain by Upper Cretaceous carbonates, which outcrop within the Mokra Mountains to the SW of the lake, while the Korabi

Zone consists of Palaeozoic metamorphic rocks overlain by Mesozoic (Triassic to Early Jurassic) carbonates, which are widely exposed to the NW and SE of the lake (Hoffmann et al., 2010).

Physical and chemical limnological characteristics

Extensive karstification has affected the Mesozoic carbonates and resulted in a network of karst aquifers that supply around 50% (20.2 $m^3 s^{-1}$) of the total inflow (37.9 $m^3 s^{-1}$) to Lake Ohrid through numerous surface and lacustrine springs (Matzinger et al., 2006a). Direct precipitation on the lake surface and riverine inflow contribute about 25% each to the remaining input. The diverted River Sateska comprises the main riverine inflow. The River Crn Drim is the only surface outflow and thought to account for a substantial proportion (c. 60%) of the total output (37.9 $m^3 s^{-1}$), the remainder leaving the lake through evaporation (Matzinger et al., 2006a). Although missing from water balance models, it is probable that groundwater outflow also occurs (Lacey, 2016). The lake has a maximum length of 30.8 km and a maximum width of 14.8 km (Stanković, 1960). It has a bathtub-like morphology; mean water depth is 151 m, it is 289 m at its deepest, and it contains 50.7 km^3 of water (Popovska & Bonacci, 2007). Due to the small size of the drainage basin and the large volume of the lake it has a long hydraulic residence time, which is estimated at 70–80 years (Popovska & Bonacci, 2007). Complete overturn of the lake water is rare, occurring approximately every 7 years (Matzinger et al., 2006a). The top 150–200 m is mixed each winter, being thermally stratified during the summer months (Matzinger et al., 2007).

The karstic carbonates to the SE of the lake form the horst structure of the Galičica and Mali i Thatë Mountains between the Ohrid and Prespa graben basins and are of particular significance as they provide a groundwater connection with neighbouring lakes (Matzinger et al., 2006b). The water level elevation of neighbouring Lake Prespa is 150–159 m above that of Lake Ohrid, establishing a hydraulic gradient down which water from Lake Prespa can flow

through the aquifers (Figure 3.10; Popovska & Bonacci, 2007). First proposed by Cvijic (1906), this connection with Lake Prespa has been confirmed using stable isotopes (Anovski et al., 1991; Eftimi et al., 2002) and through an artificial tracer experiment (Amataj et al., 2007). Whilst the aquifers are partly recharged by precipitation infiltrating through the mountains, it is estimated that water originating from Lake Prespa comprises 42% of the aquifer inflow at the Sveti Naum spring (Anovski et al., 1991) and 52% of the inflow at the Tushemisht spring (Eftimi et al., 2002). It is estimated that about 20% of the total water inflow to Lake Ohrid originates from Lake Prespa (Matzinger et al., 2006b).
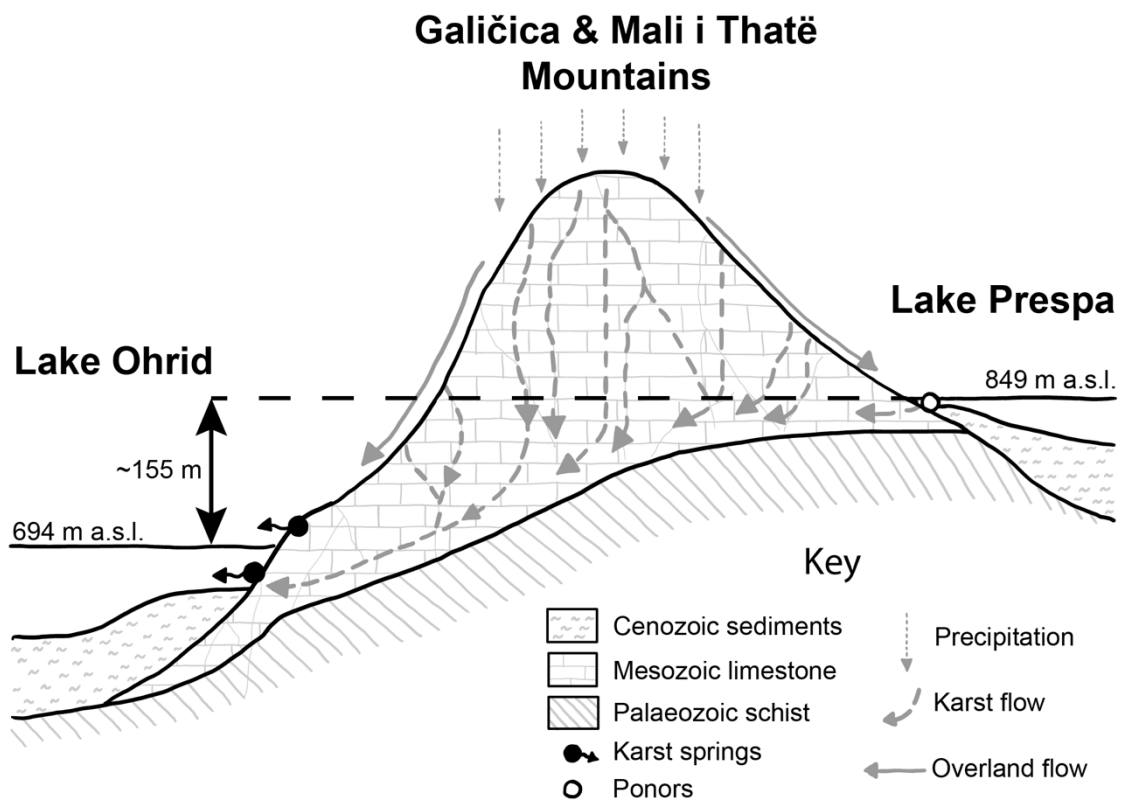
Figure 3.10: Schematic cross-section through the Galičica mountain range showing groundwater movement and the connection between Lake Ohrid and Lake Prespa (modified from Popovska & Bonacci, 2007).

The karstic geology also has implications for the lake's water chemistry. Whilst it contains freshwater, Lake Ohrid is carbonate-dominated and alkaline.

Surface waters have a pH range of 8.6–8.9 and a specific conductivity of about 200 μS cm⁻¹ (Wagner et al., 2017). Although it is regarded as oligotrophic, there are concerns over its trophic state, especially under the increasing pressures of tourism and a rising population (Matzinger et al., 2006b). Sediment cores suggest there has been an increase in phosphorus input to Lake Ohrid over the last century, resulting in a slow eutrophication (Matzinger et al., 2004). There is a need to conserve the oligotrophic state of Lake Ohrid in order to protect the endemic species that have evolved within it (Matzinger et al., 2004). Although the threat to Lake Ohrid is not immediate, the karst connection with Lake Prespa is particularly worrying as Lake Prespa has a total phosphorus concentration seven times that of Lake Ohrid (Matzinger et al., 2006b).

Climate

With cool, wet winters and hot, dry summers (Figure 3.11), the Ohrid basin experiences a Mediterranean climate but is influenced by the European continental climate. Mean annual precipitation was 907 mm over the period 1961–1990 (Popovska & Bonacci, 2007). This is relatively high and is due to the basin's moderate altitude and its close proximity to the Ionian and Adriatic seas.

Vegetation

The vegetation in the Lake Ohrid catchment has been categorised into altitudinal belts: lowlands are dominated by grasslands and agricultural land; deciduous and semi-deciduous forests, comprised of oak and hornbeam, dominate the lower altitudes up to 1600 m; mesophilous/montane species dominate the higher altitudes up to 1800 m; and above 1900 m, alpine pastures and grasslands are present (Matevski et al., 2011; Sadori et al., 2016; Wagner et al., 2017). Pollen analysis has shown the area to have been a refugium for temperate and montane trees during glacial periods and some relic Tertiary species are still present in the wider region (Sadori et al., 2016). The
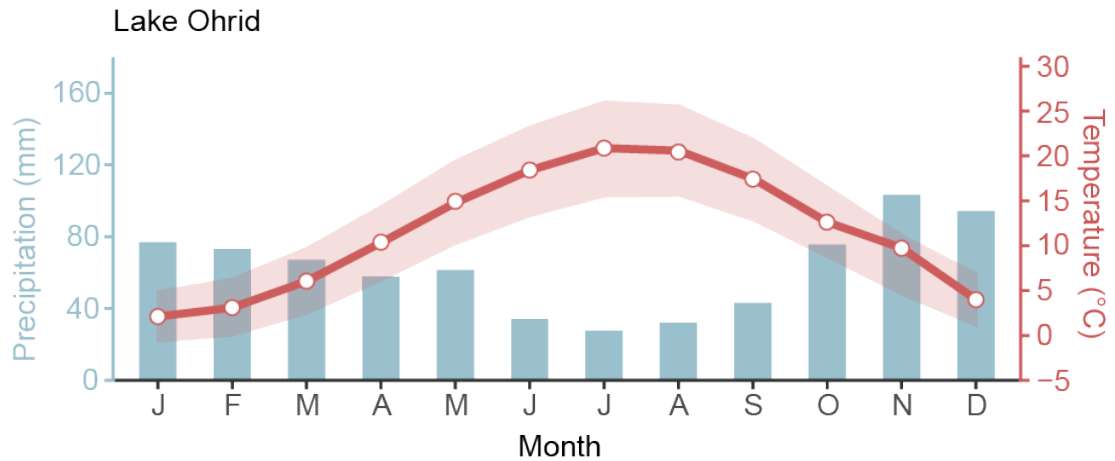
Figure 3.11: Mean monthly temperature and precipitation for Lake Ohrid. Additionally, the range between minimum and maximum monthly temperatures is shaded in red. Based on observed data from the Pogradec (Albania) meteorological station over the period 1961–1990 (Watzin et al., 2002 in Lacey & Jones, 2018).

macrophytic flora of Lake Ohrid is distributed across successive vegetational zones within the littoral region of the lake: the deepest parts of the littoral region, between 3 m and 30 m water depth, are occupied by *Chara* species; species of the submerged macrophyte *Potamogeton* are found in shallow waters of up to 2.5 m water depth; and a discontinuous reed belt, dominated by *Phragmites australis*, is found along the shore at depths of up to 1.5 m (Talevska et al., 2009; Imeri et al., 2010; Wagner et al., 2017). The discontinuous nature of macrophyte occurrence is due to the narrowness of the lake's littoral region, a consequence of the steep-sided topography of the basin.

3.3 Comparison of the study sites

Similarities

The main characteristics of Lake Ioannina and Lake Ohrid are summarised in Table 3.1. Both are ancient lakes situated on carbonate strata and surrounded by high topography on the Balkan Peninsula. The carbonate geology has had the same implications for both lakes. In terms of lake water chemistry, they exhibit alkaline pH ranges, and in terms of hydrology, the karstification of the

carbonates has resulted in karstic springs supplying the main inputs to both lakes. Neither lake has a major riverine inflow, but both remain relatively fresh, possibly due to subsurface outflows. The lack of any major inflows or outflows has important implications for this thesis as any climatic change affecting the precipitation–evaporation ratio has the potential to affect lake level, which in turn could affect the lake ecosystems and the diatom assemblage responses that are under investigation (Fritz et al., 2010).

Located approximately 150 km apart and at similar altitudes, the climate and vegetation of the Ioannina and Ohrid basins are relatively similar. In terms of their vegetation, both lake basins have been altered from their natural states through the development of agricultural and grazing land with the arboreal species composition on the catchment slopes also controlled by altitude. There is evidence that both areas served as arboreal refugia during Quaternary glacials (Tzedakis, 1993; Donders et al., 2021). Both experience a sub-Mediterranean climate, with the mild winter months being the wettest. They receive relatively high amounts of annual precipitation in comparison to sites further east in the Mediterranean region. Slight contrasts between the climates occur. Ohrid, with its more northerly location, is more influenced by the cooler European continental climate, and the slightly wetter conditions at Ioannina are possibly a result of the basin's more coastal position, at only c. 60 km inland compared to Ohrid's position c. 100 km inland. This similarity in climate is likely to have persisted throughout the Quaternary, thus making the lakes suitable for a comparison of their different responses to the same climatic change.

Differences

Although both lakes are situated in tectonic basins of the same extensional regime, the different ways in which the lake basins formed (graben-constrained Lake Ohrid versus the *polje* solution depression of Lake Ioannina) has resulted in contrasting lake bathymetries. This is responsible for the major

differences between the lakes. Being shallow with a gentle bathymetry, Lake Ioannina has a greater potential to support benthic communities, while Lake Ohrid, with its steep-sided basin and great depth, has a relatively small littoral zone with discontinuous macrophyte vegetation. The depth also influences lake mixing with Lake Ioannina experiencing complete overturn twice a year (Zacharias et al., 2002) and Lake Ohrid only experiencing this around every seven years (Matzinger et al., 2006a). Hydraulic residence times differ hugely. Although neither lake has a major outflow, the large volume of Lake Ohrid results in a much longer residence time of 70–80 years (Popovska & Bonacci, 2007) in comparison with just less than a year in Lake Ioannina (Kagalou et al., 2008). These volume and depth differences also have implications for anthropogenic eutrophication. Lake Ioannina is impacted to a much greater extent than Lake Ohrid, which remains oligotrophic for now (Romero et al., 2002; Matzinger et al., 2006b). The greater depth and volume of Lake Ohrid has provided a greater resilience to these modern pressures, and it is predicted it will also demonstrate a greater resilience to past changes in climate.

Table 3.1: Key characteristics of Lake Ioannina and Lake Ohrid.

Characteristic	Ioannina	Ohrid	References
Location			
Latitude; longitude	39°40´N; 20°53´E	40°54´–41°10´N; 20°38´–20°48´E	–
Lake surface altitude	470 m	694 m	–
Max. catchment altitude	1810 m	2288 m	–
Geology			
Catchment geology	Flysh and karstic carbonates	Ophiolites, metamorphics and karstic carbonates	Tzedakis, 1994; Hoffmann et al., 2010
Genesis	Polje	Tectonic graben	Tzedakis, 1994; Hoffmann et al., 2010
Climate			
Mean July temperature	+24.9°C	+20.6°C	Tzedakis, 1994; Merkel, 2018
Mean January temperature	+4.9°C	+2.0°C	Tzedakis, 1994; Merkel, 2018
Mean annual precipitation	1158 mm	907 mm	Romero et al., 2002; Popovska & Bonacci, 2007
Size			
Lake surface area	23 km^2	358 km^2	Stanković, 1960; Conispoliatis et al., 1986
Catchment area	510 km^2	1002 km^2 (excluding Lake Prespa catchment)	Popovska & Bonacci, 2007; Kagalou et al., 2008
Max. lake length; width	11 km; 5 km	31 km; 15 km	Stanković, 1960; Conispoliatis et al., 1986
Lake volume	0.1 km^3	50.7 km^3	Zacharias et al., 2002; Popovska & Bonacci, 2007
Maximum water depth	7.5 m	289 m	Popovska & Bonacci, 2007; Kagalou et al., 2008
Mean water depth	4.3 m	151 m	Popovska & Bonacci, 2007; Kagalou et al., 2008
Physical Limnology			
Inflows	Springs and minor ephemeral streams	Springs; River Sateska	Kagalou et al., 2001; Matzinger et al., 2006a
Outflows	Sinkholes drain to rivers	River Crn Drim; subsurface outflow?	Kagalou et al., 2001; Matzinger et al., 2006a; Lacey, 2016
Hydraulic residence time	0.8–0.9 years	70–80 years	Popovska & Bonacci, 2007; Kagalou et al., 2008
Mixing	Dimictic/polymictic	Once every c. 7 years	Zacharias et al., 2002; Matzinger et al., 2006b; Jones, 2010
Chemical Limnology			
pH range	6.7–8.9	8.6–8.9	Kagalou et al., 2008; Wagner et al., 2017
Conductivity	393 µS cm^{-1}	200 µS cm^{-1}	Kagalou et al., 2008; Wagner et al., 2017
Trophic status	Hypereutrophic	Oligotrophic	Romero et al., 2002; Matzinger et al., 2006b

Chapter 4 | Methodology

This chapter outlines the methodological approaches followed. It begins by describing the recovery of the sediment cores and the establishment of their chronological frameworks, both of these being steps that were taken prior to the commencement of the research that forms this thesis. The subsequent sections detail the processes followed to create microscope slides and to generate and analyse the diatom data.

4.1 Materials and chronologies

The analyses in this thesis have been carried out on the I-284 core from Lake Ioannina and the DEEP-5045-1 core from Lake Ohrid. These were recovered a number of years ago and have already been the subject of numerous palaeoenvironmental investigations. Sections corresponding to MIS 7–9 in the I-284 core and MIS 7 in the DEEP-5045-1 core have been made available for this study.

4.1.1 Lake Ioannina I-284 core

The I-284 core was recovered from an area immediately to the southeast of the modern Lake Ioannina in 1989 (Figure 4.1). It was one of approximately 280 boreholes drilled by the Greek Institute of Geology and Mineral Exploration (IGME) when prospecting for lignite deposits in the basin between 1977 and 1989 (Tzedakis, 1994; Frogley, 1997). With the aid of stratigraphical information from these IGME cores, it was possible to identify areas of the basin with the greatest potential in palaeoenvironmental investigations: those with continuous sedimentation and subsidence that did not show any evidence of uplift or major disturbance (Tzedakis, 1994). This resulted in some cores from the southeastern area of the basin (I-249 and I-284; Figure 4.1) being archived for palaeoenvironmental analyses (Tzedakis, 1994; Frogley, 1997).

With an unbottomed length of 319 m, core I-284 was one of the longer cores recovered from the Ioannina basin (Frogley, 1997). This meant it had the potential to provide one of the most temporally extensive or stratigraphically detailed records (Tzedakis, 1994). Although the I-284 core site is now located to the southeast of the lake margin, unpublished stratigraphical reports from the IGME indicate it is situated in one of the deepest sub-basins, and the sediments appear to have been deposited continuously in an area that, prior to artificial drainage schemes (see section 3.2.1), was always submerged (Frogley, 1997). Furthermore, no distinct lithological breaks were detected in the core with any lithological changes occurring across apparently conformable and gradual boundaries (Frogley, 1997).
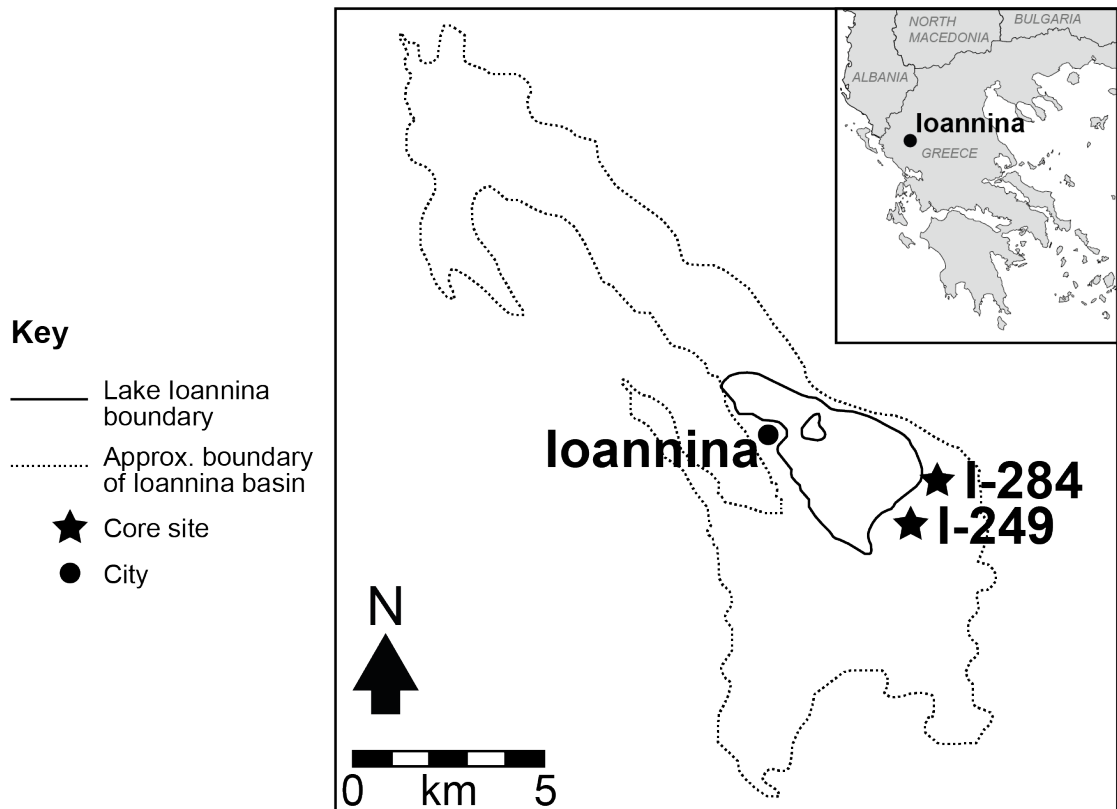
Figure 4.1: Map showing the locations of the I-284 and I-249 core sites in the Ioannina basin with an inset map showing the location of Ioannina within Greece (modified from Lawson et al., 2004). The dotted line represents the 500 m altitude contour line, which approximates to the basin boundary. The lake boundary represents the extent of the modern-day lake within the larger basin area that it once filled.

The chronostratigraphic framework for I-284 has been developed using a variety of methods. Initial attempts to date the core focused on correlating I-284 with I-249 (Frogley, 1997; Frogley et al., 1999). The latter possesses a tentative chronology based on the correlation of the pollen record (which is devoid of migrational lags due to the presence of refugial populations in the area) with other European pollen records and marine oxygen isotope records (Tzedakis, 1993). Although the sediments of many lake basins in the region contain tephra layers (layers of ash from volcanic eruptions) that have been accurately dated and used to establish very precise age control points (e.g. Vogel et al., 2010; Giaccio et al., 2019), none have been identified in the sediments of core I-284 (Frogley, 1997). Despite this, palaeomagnetic evidence and U-series dates were able to provide age control points and establish a broad chronological context for I-284 (Frogley, 1997).

Since those early investigations, much progress has been made in developing a more accurate chronology. The current chronology is based on analyses of the pollen content of core I-284 (Tzedakis et al., 2002b; Roucoux et al., 2008; Roucoux et al., 2011) and utilises two complementary techniques. The first is pollen astronomical tuning (Magri & Tzedakis, 2000), in which peaks in Mediterranean tree and shrub pollen are aligned with the timing of northern hemisphere June perihelion. The second is the alignment of the temperate tree pollen in the I-284 core to that of marine cores from the western Iberian Margin. These marine cores were recovered from an area that is sufficiently close to the continent to contain regional pollen signals whilst also being deep enough to provide high-quality isotopic and SST data that are reflective of basin-wide conditions (Margari et al., 2014). The pollen data of such cores reflect immediate vegetation responses to rapid climate variability without substantial migrational lags (Margari et al., 2010), which justifies their suitability for alignment with other lag-free pollen records. Meanwhile the isotopic and SST data have been used to develop robust age models for these marine cores through the alignment of these data with Antarctic ice cores (e.g.

Tzedakis et al., 2009b) and the synthetic Greenland record of Barker et al. (2011; e.g. Margari et al., 2014).

The progress in chronology development has resulted in a revised age for the unbottomed base of the I-284 core, from over 620 ka (MIS 16) to c. 350 ka (MIS 10; Roucoux and Tzedakis, unpublished data; Jones, 2010); however, the published age model currently extends to only 255 ka (Roucoux et al., 2008). For this reason, the I-284 data discussed within this thesis are plotted by depth and discussed within the context of published age control points, which are presented in Table 4.1.

Table 4.1: Age control points for the I-284 core.

Depth (m)	Age (ka)	Source of age control point
141.0	193.7	Base of the MIS 6 age model of Wilson et al. (2021), the most recently published chronology for the I-284 core. It is based on the alignment of the temperate tree pollen record of I-284 to that of Iberian Margin core MD01-2444 (Margari et al., 2010), the latter of which is on an updated age model based on the alignment of its SST record to the synthetic Greenland record (Margari et al., 2014).
149.5	198.0	Alignment of the I-284 pollen record to northern hemisphere June perihelion (Roucoux et al., 2008).
160.5	215.9	I-284 AP expansion (Roucoux et al., 2008) aligned with that at the MIS 7d–7c boundary in Iberian Margin core MD01-2443 (Roucoux et al., 2006), the latter core having a chronology based on the alignment of its benthic foraminiferal δ18O record with the Antarctic Vostok deuterium record of Petit et al., 1999.
192.5	242.0	Alignment of the I-284 pollen record to northern hemisphere June perihelion (Roucoux et al., 2008).
224.0	262.0	I-284 AP expansion (Roucoux, unpublished data) aligned with marine isotope event 8.3 in Iberian Margin core MD01-2443 (Roucoux et al., 2006), as stated by Roucoux et al. (2008).

As mentioned earlier, multiple palaeoenvironmental investigations have already been carried out on the I-284 core. These investigations have each focused on specific proxies and time periods. No part of the record has been published in its entirety, so a summary of all the individual analyses has been collated in Table 4.2.

Table 4.2: Summary of existing analyses and data from the I-284 core.

Analysis	Core depth (m)	Age (MIS equivalent)[a]	Resolution (cm)	First presented	Subsequent analyses
Lithology	0–319	1–10	–	Frogley, 1997	–
Particle size	0–20	1–2	15	Lawson et al., 2004	Wilson et al., 2008
	75–110	5–6	100	Frogley, 1997	–
Magnetic susceptibility	0–319	1–10	100	Frogley, 1997	Roucoux et al., 2008
	0–20	1–2	20 (10 between 10–20 m)	Lawson et al., 2004	Wilson et al., 2008
	124–141	6–7 transition	20	Wilson et al., 2013	–
Loss-on-ignition	0–319	1–10	20 (10 for top 100 m)	Frogley, 1997	Lawson et al., 2004; Roucoux et al., 2008; Wilson et al., 2013
Palaeomagnetism	0–319	1–10	100	Frogley, 1997	–
Stable isotopes (authigenic)	83–100	5d–5e	10–20	Frogley, 1997	Frogley et al., 1999; Frogley et al., 2001; Tzedakis et al., 2002c; 2003; Wilson et al., 2015
	124–141	6–7 transition	20	Wilson et al., 2013	Wilson et al., 2021
	95-141	6	20	Wilson et al., 2021	–
Stable isotopes (ostracod)	0–25	1–2	20	Frogley, 1997	–
			10	Frogley et al., 2001	Lawson et al., 2004; Wilson et al., 2008
Mollusc fauna	0–145	1–6	20	Frogley, 1997	–
Ostracod fauna	0–25	1–2	20	Frogley, 1997	Frogley et al., 2001; Lawson et al., 2004
	83–100	5d–5e	20	Frogley, 1997	–
Pollen	0–102	1–5	?	Tzedakis et al., 2002b	Roucoux et al., 2011
	0–25	1–2	10–30	Lawson et al., 2004	Roucoux et al., 2008; Wilson et al., 2008; Roucoux et al., 2011
	83–102	5d–5e	20	Frogley et al., 1999	Tzedakis, 2000; Tzedakis et al., 2002b; Tzedakis et al., 2002c; Tzedakis et al., 2003; Roucoux et al., 2008; Roucoux et al., 2011; Wilson et al., 2015
	95–145	6	20	Roucoux et al., 2011	Wilson et al., 2013; Wilson et al., 2021
	135–210	7	20	Roucoux et al., 2008	Wilson et al., 2013
Diatoms	10–17	1–2 transition	10	Wilson et al., 2008	Jones et al., 2013
	124–141	6–7 transition	20	Wilson et al., 2013	Wilson et al., 2021
	95–102	5–6 transition	10	Wilson et al., 2015	Wilson et al., 2021
	95–141	6	20	Wilson et al., 2021	–

[a] Based on current age model.

4.1.2 Lake Ohrid DEEP-5045-1 core

The DEEP-5045-1 core is one of several recovered from Lake Ohrid as part of the Scientific Collaboration on Past Speciation Conditions in Lake Ohrid (SCOPSCO) project, a multi-disciplinary, international research endeavour that is part of the International Continental Drilling Program (ICDP). Hydro-acoustic and multichannel seismic surveys were carried out between 2004 and 2009 (Reicherter et al., 2011; Lindhorst et al., 2015). These established the DEEP site, which is in the central area of the lake basin, as a coring target (Figure 4.2). In 2013, a 545 m composite sediment core was recovered from six boreholes at the site from beneath a water depth of 243 m (Wagner et al., 2014).
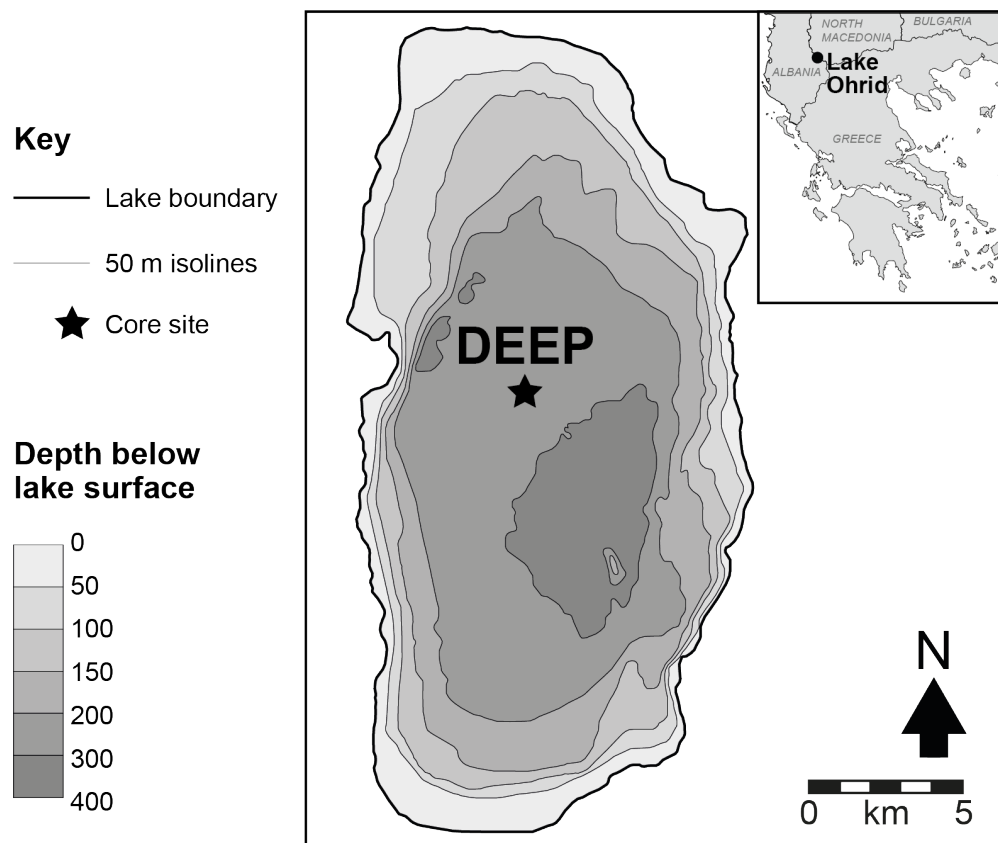
Figure 4.2: Bathymetric map showing the location of the DEEP core site within Lake Ohrid, and an inset map showing the location of Lake Ohrid on the border of Albania and North Macedonia (modified from Lacey, 2016).

The chronological framework for the upper 247.8 m composite depth of the DEEP site sequence (which covers the section under investigation in this thesis) was initially developed around 11 tephrostratigraphic age control points (Leicher et al., 2016) and tuned to orbital parameters using the total organic carbon (TOC) and total nitrogen (TN) contents (Francke et al., 2016). The resulting age model is in agreement with the palaeoclimate record from Tenaghi Philippon (Tzedakis et al., 2006) and the U–Th dated Soreq Cave speleothem record (Grant et al., 2012). The DEEP age model was later revised and extended, and it demonstrates that the core contains a record spanning to 1.36 Ma (Wagner et al., 2019).

4.2 Laboratory techniques for sample preparation

Samples of sediment were collected at regularly spaced intervals along each core prior to the start of this research project. After the project commenced, samples were selected and placed onto microscope slides. The preparation of sediment samples and the creation of diatom microscope slides followed the standard techniques of Battarbee (1986). For each sample, 0.1g of dry sediment was digested in 30% hydrogen peroxide (H_2O_2) to remove any organic content before a few drops of hydrochloric acid (HCl) were added to remove any carbonates. The sample residues were subsequently washed by adding distilled water, centrifuging and then decanting the supernatant. This wash process was repeated three more times, removing any remaining HCl and clay minerogenic material. The remaining residues were diluted with distilled water to an appropriate concentration before known quantities of plastic microspheres were added to allow calculation of absolute diatom concentration. To make the microscope slides, 0.4 ml of the diatom suspension was placed on a coverslip and left to evaporate overnight at room temperature. Finally, the dried coverslips were mounted onto slides using Naphrax.

4.3 Light microscopy

4.3.1 Counting procedure

Diatom valves were identified and counted with a Zeiss Axioscop 2 Plus light microscope under oil immersion and at a magnification of ×1000. A minimum of 300 diatom valves were counted per slide. This minimum count is within the range recommended by Battarbee et al. (2001). Exploratory analysis of preliminary count data from Lake Ioannina demonstrated this number was sufficient for the purposes of the analyses carried out in this thesis (Appendix A). As the Lake Ohrid diatom assemblages have a low diversity, this number is also sufficient for those samples (Reed et al., 2010). The microspheres present in each field of view were also counted in order to calculate diatom concentration using Equation 4.1 (Battarbee & Kneen, 1982).

$$\text{concentration} = \frac{\text{number of microspheres introduced} \times \text{diatoms counted}}{\text{microspheres counted}}$$

<div align="right">Equation 4.1</div>

4.3.2 Taxonomy

Diatoms were identified using standard texts based on central European diatoms (Krammer & Lange‑Bertalot, 1986; 1988; 1991a; 1991b; 2000; Lange-Bertalot et al., 2017) and the dedicated work on Lake Ohrid (Levkov et al., 2007a). Although the latter is indispensable for identifying diatoms from Lake Ohrid, it was also used to identify the taxa from Lake Ioannina as diatom taxa can be region-specific and those encountered in Lake Ioannina frequently bear a closer resemblance to those described from Lake Ohrid than those described from central Europe. A wide range of journal articles was also used to aid in the identification of taxa that were not included in the texts mentioned above. Diatoms were generally identified to species level. Where this was not possible

(e.g. if valves were poorly preserved), they were identified to genus level with the species designated as "spp." (e.g. *Sellaphora* spp.).

Morphological variability of Pantocsekiella ocellata

Special attention was paid to *Pantocsekiella ocellata* as this is a notoriously problematic taxon and preliminary examinations of the prepared microscope slides demonstrated it was abundant throughout the records of both lakes. It was first described under the name *Cyclotella ocellata* from Lake Balaton (Hungary) by Pantocsek (1902) as a centric diatom with a valve face characterised by a radially-striated marginal area and a central area containing a small number (usually three arranged in a triangle) of what would later become known as orbicular depressions or ocelli (Figure 4.3). Although the original description alludes to some potential variation in the number of ocelli on the valve face, it did not encapsulate the wide range of morphological variability that had been observed by the end of the last century in both natural (e.g. Kiss et al., 1996; Schlegel & Scheffler, 1999) and laboratory-cultured (e.g. Hegewald & Hindáková, 1997) populations. There was also immense taxonomic confusion due to a number of potentially conspecific taxa with similar morphological features and the occurrence of intermediate forms. Numerous studies have sought to re-examine the type material (Håkansson, 1990; 1993; Kiss et al., 1999; Håkansson, 2002; Houk et al., 2010) and to further examine the extent of the morphological variation (e.g. Cremer et al., 2005; Genkal & Popovskaya, 2008; Cvetkoska et al., 2014b). These investigations documented a wide range of morphological variation and, along with the occurrence of heterovalvar frustules where the two valves of a single diatom have different morphologies that could be identified as separate species (e.g. Teubner, 1995; Hegewald & Hindáková, 1997; Schlegel & Scheffler, 1999), have led to the general consensus that *P. ocellata* is part of a species complex consisting of morphologically diverse and related species.

The taxon is cosmopolitan and demonstrates broad ecological preferences, being found in both shallow and deep lakes across the full spectrum of trophic states from ultra-oligotrophic (e.g. Lake El'gygytgyn, Siberia; Cremer & Wagner, 2003) to eutrophic (e.g. Lake Dagow, Germany; Schlegel & Scheffler, 1999). For this reason, it proves problematic in palaeoenvironmental investigations. Resorting to documenting changes in the different morphotypes of *P. ocellata* that are present (on the assumption that different morphotypes have different environmental preferences) is one way to overcome this. Although Cherepanova et al. (2010) demonstrated that exploring valve morphology can provide additional information for palaeoenvironmental investigations, Reed et al. (2010) warns that multiple studies have found morphological variability to also occur independently of environmental change. With the possibility that morphological variation could provide additional information when interpreting the diatom record in terms of past environmental change, it was deemed sensible to capture any changes in the morphology of *P. ocellata*.

In Lake Ioannina specifically, previous palaeolimnological investigations have identified two distinct morphotypes within the sediments: the more dominant "classic" morphotype, which is relatively small and typically has three ocelli, and the less frequent "non-classic" morphotype, which is larger (30–50 μm) and can have a more complex central area structure. The latter was originally known as *Cyclotella* af. *fottii* (Wilson et al., 2008) due to its morphological resemblance to *Cyclotella fottii*, an endemic of Lake Ohrid. It was later referred to as *Cyclotella ocellata* morphotype 2 (Jones et al., 2013; Wilson et al., 2013) as the Ohrid taxonomists believed it might be within the range of morphological variability seen within *P. ocellata* (Jones, 2010). More recent work has not attempted to provide the large forms with a designation, referring to them descriptively as "large, non-classic forms with complex central area structure" (Wilson et al., 2015:819) or not mentioning them at all (Wilson et al., 2021).

A similar cautious approach is adopted here with no attempt made to split the forms strictly into two distinct morphotypes. Preliminary investigations of the material to be used in this study found that the morphologies of individual valves seem to sit along a spectrum with no definitive boundary between the two morphotypes and that to class transitional valves as one morphotype or the other was impossible. Therefore, in this investigation, the "classic" and "non-classic" morphotypes are considered two end members along a spectrum of morphological variation (Figure 4.3). To classify the valves along this spectrum, they have been counted in 5 μm valve diameter size classes and according to their central area morphology. The latter includes the number of orbicular depressions or puncta (it was not always possible to distinguish between the two under light microscope) on the valve surface, which tend to be arranged in a regular pattern resulting in a corresponding order of rotational symmetry. For valves with multiple depressions or puncta arranged in rows, the number of rows was counted rather than each individual punctum. Twinned orbicular depressions, such as those occasionally found in *Pantocsekiella paraocellata* (Cvetkoska et al., 2014b), were counted as a single orbicular depression (see Figure 4.3b).
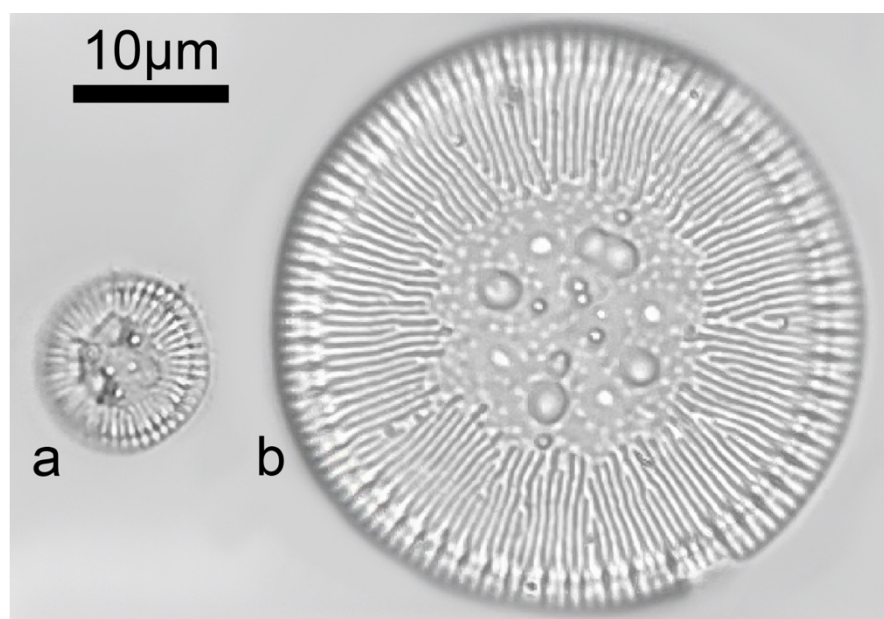
Figure 4.3: Photographs of the "classic" (**a**) and "non-classic" (**b**) morphotypes of *Pantocsekiella ocellata* from the Lake Ioannina sediments.

4.3.3 Diatom preservation

In order to track the preservation quality of the diatoms, each valve counted was classified as either pristine or not pristine. These data were then used to calculate the **F** index using Equation 4.2:

$$F_i = \frac{\sum_{j}^{m} n_{ij}}{\sum_{j}^{m} N_{ij}}$$

<div align="right">Equation 4.2</div>

where F_i is the **F** index of sample i, n_{ij} is the number of pristine valves of species j (of all species m) that were counted in sample i and N_{ij} is the total number of classifiable valves of species j (Ryves et al., 2001).

As discussed in section 2.2.4, some diatom taxa are more susceptible to dissolution than others. This can buffer the preservation signal provided by the **F** index. For example, during the Last Glacial Maximum (LGM) and Holocene at Lake Ioannina, the **F** index reflects variations in the abundance of the robust small Fragilariaceae taxa rather than true changes in dissolution (Jones et al., 2013). For this reason, the dissolution of the records was also estimated from the degree of dissolution exhibited by the valves of specific, abundant planktonic taxa. These valves are typically more susceptible to dissolution due to their high surface area to volume ratio.

In Lake Ioannina, valves of *Pantocsekiella ocellata* were classified into three categories: pristine, with the striae exhibiting some degree of dissolution, or with the marginal area dissolved to the point that only the central area remains (Figure 4.4). In Lake Ohrid, valves of *Cyclotella fottii* (including *C. fottii* var. 1) and *Cyclotella cavitata* were classified as either pristine or dissolving to

calculate the **F** index of the *Cyclotella* taxa. These taxa are morphologically similar (Table 2.1) so are believed to be impacted by dissolution to the same extent.
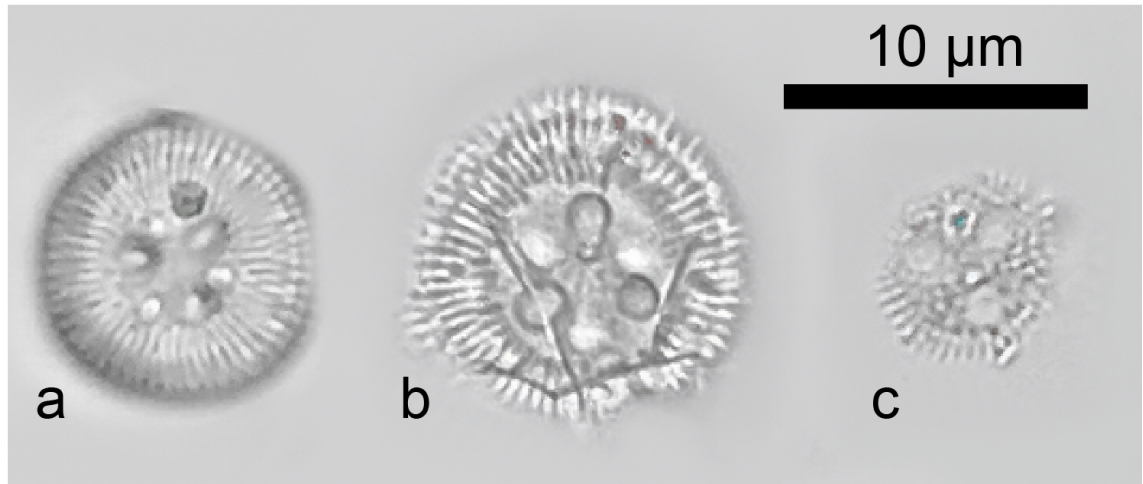
Figure 4.4: Valves of *Pantocsekiella ocellata* at different stages of dissolution: pristine (**a**), with striae dissolving (**b**) and with only the central area remaining (**c**). The valve with dissolving striae is also starting to fragment.

4.4 Numerical techniques

4.4.1 Zonation

Stratigraphical sequences of palaeoecological data are usually divided into assemblage zones (sections characterised solely by a particular assemblage of taxa) in order to aid the description and correlation of records (Birks, 2012). This approach was first applied to pollen sequences with the zones originally designated by eye (Cushing, 1963), and it was later achieved by numerical techniques, which provided methods that were repeatable and greatly reduced the subjectivity of zone delineation (Gordon & Birks, 1972; Birks & Gordon, 1985). Since they were first applied, the basic principles of these numerical techniques have remained largely unchanged (Birks, 2012). They are hierarchical clustering methods, grouping similar samples together into

clusters. The results of this type of analysis can be displayed with a tree-like diagram known as a dendrogram.

The cluster analyses in this thesis were performed using R (R Core Team, 2021) with the aid of several tidyverse packages (Wickham et al., 2019). Raw diatom counts were converted to relative abundances with the vegan package (Oksanen et al., 2019). Only abundant taxa present over a particular threshold (specific to each analysis) were included in the analysis and the relative abundances were calculated from a sum comprising of only those abundant taxa. This is recommended by the pioneers of the technique due to the low numerical importance of very rare taxa (Gordon & Birks, 1972). In addition, the inclusion of very rare taxa would be statistically dubious because their abundances are poorly estimated unless very large counts are undertaken and thus have a high relative error (Birks, 1986). The relative abundances were subsequently square-root transformed. This two-step process of calculating the relative abundances before taking the square-root is known as the Hellinger transformation and can be summarised with Equation 4.3:

$$y'_{ij} = \sqrt{\frac{y_{ij}}{y_{i+}}}$$

Equation 4.3

where y_{ij} is the number of diatom valves counted of species j in sample i and y_{i+} is the sum of all diatom valves counted in sample i. It has the effect of reducing the importance of very abundant taxa within each sample, which can multiply exponentially under favourable environmental conditions. After transforming the data, the vegan package was used to calculate the squared Euclidean distances between all samples, generating a dissimilarity matrix upon which the Constrained Incremental Sum of Squares (CONISS) clustering algorithm (Grimm, 1987) was run with the rioja package (Juggins, 2020). The

squared Euclidean distance between two samples is calculated with Equation
4.4:

$$D_{Euclidean^2}(\mathbf{x'}_1\mathbf{x'}_2) = \sum_{j=1}^{p} \left(y'_{1j} - y'_{2j}\right)^2$$

<div align="right">Equation 4.4</div>

where $\mathbf{x'}_1$ and $\mathbf{x'}_2$ are two row vectors (i.e. two samples) in the Hellinger-
transformed species abundance data table and y'_{1j} and y'_{2j} are the Hellinger-
transformed abundances of species j in those two samples. Although many
distance functions are available, using this one maintains consistency with the
original CONISS algorithm, which was written to operate on dissimilarity
matrices of squared Euclidean distances (Grimm, 1987) and remained this way
when it was built into popular software used by palaeoecologists such as Tilia
(Grimm, 2011). The squared Euclidean distance exaggerates the dissimilarities
between samples—the greater the dissimilarity, the greater the exaggeration.
The effect is lessened somewhat by the preceding square-root transformation.
This combination has proved particularly satisfactory for percentage
abundance data (Grimm, 1987). It ensures that the absence of a species in two
samples is not considered an indication of similarity between them, a
phenomenon known as the double zero problem, which is discussed within
section 7.2.2 of Legendre and Legendre (2012).

The CONISS algorithm uses an agglomerative (bottom up) approach, beginning
by considering each sample in the dissimilarity matrix as an individual cluster
and merging similar clusters together into larger and larger clusters (as
opposed to a divisive approach where all samples are considered as one cluster
that is split into successively smaller clusters). A full description of the
algorithm is provided by Grimm (1987). Essentially, it searches through the
dissimilarity matrix and merges the pair of clusters with the smallest
dissimilarity value into a single new cluster, reducing the number of clusters

by one and increasing both the within-cluster and total dispersion (sum of squares). New dissimilarities are then calculated between this new cluster and all of the other clusters. The process is repeated until all clusters merge into a single cluster. As evident in its name, it is a constrained technique—only clusters that are stratigraphically adjacent to each other are considered for merging.

The results of the cluster analyses were plotted as dendrograms using the R packages ggdendro (de Vries & Ripley, 2020) and ggplot2 (Wickham, 2016). Finally, a broken stick model (Bennett, 1996) was implemented with the rioja package (Juggins, 2020) and used to determine the number of significant zones.

4.4.2 Ordination

Ordination is a group of techniques used to identify and summarise patterns in multivariate data sets. Coined and first applied within an ecological context by Goodall (1954), the term is simply defined by Legendre & Birks (2012:202) as a way "to arrange objects in some order". Observations within a data set (e.g. lacustrine core samples) can be arranged in an order according to their value for a particular variable (e.g. the abundance of a particular diatom taxon). When there are many variables in a data set (as is the case with species assemblage compositional data, where each taxon is a variable) the data can be difficult to summarise. Ordination is able to reduce much of the variation across the numerous variables into just two or three synthetic variables (also known as latent variables), which can be plotted as coordinate axes (Legendre & Birks, 2012). Within this ordination space of reduced dimensionality, observations that are similar to each other will plot close together, whilst those that are different to each other will plot far apart (Gauch, 1982). In an ecological context, the synthetic variables used to create the coordinate axes represent hypothetical environmental variables that are yet to be elucidated (Birks, 2010). An environmental interpretation of the ordination results (i.e. deducing what the hypothetic environmental gradients represent) can be

proposed if the patterns that surface in the ordination space are compared with environmental information (Gauch, 1982).

In order to achieve a useful ordination result, it is necessary to consider the type of relationship that exists between the diatom species and the latent environmental variables. Most organisms exhibit unimodal responses to environmental variables, but if the sampled environmental gradient is not very long, then a true unimodal response would appear linear (Smol, 2008; Figure 4.5). In such a case, an ordination technique with a linear response model would be appropriate (ter Braak, 1995). If, however, there is a long environmental gradient within which multiple species have their optima, then non-linear methods are appropriate (ter Braak & Prentice, 1988).
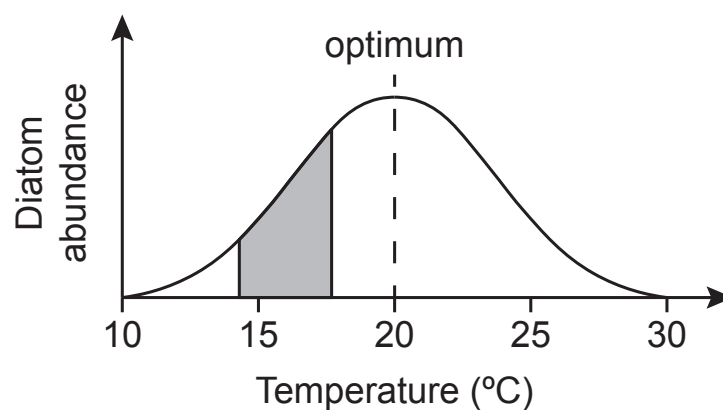
Figure 4.5: Example of a hypothetical unimodal diatom abundance response. If the environment gradient is short, for example the shaded temperature range, the diatom response appears linear.

Detrended correspondence analysis is an ordination technique suited to unimodal species responses. When a DCA is performed, the resulting component axes represent environmental gradients in standard deviation (SD) units. A normal species distribution, like that illustrated in Figure 4.5, is expected to occur over 4 SD units along such an axis (Waite, 2000). If the length of the longest axis is less than 3 SD units, a linear ordination method might be more appropriate (Leps & Šmilauer, 2003).

Principal components analysis (PCA) assumes linear species responses to the latent variables, each of which is represented by a principal component axis. As PCA is an eigenvector technique, it produces an eigenvalue for each axis (Gauch, 1982). These indicate the proportion of the total variance in the dataset that each axis accounts for, with more important axes having higher eigenvalues (ter Braak & Prentice, 1988). The first principal component will explain the largest proportion of the variance with successive components explaining increasingly small proportions.

In this thesis, the data were initially subjected to a DCA to identify whether linear or unimodal ordination techniques were appropriate. If the length of the longest DCA axis was <3 SD units, a PCA was performed. These analyses were carried out in R (R Core Team, 2021) with the assistance of the tidyverse packages (Wickham et al., 2019) and the vegan package (Oksanen et al., 2019).

4.4.3 Data presentation

Diatom count data were converted to percentage relative abundances and plotted as stratigraphic diagrams using R (R Core Team, 2021) with the aid of several R packages including the tidyverse collection (Wickham et al., 2019), tidypaleo (Dunnington, 2021) and cowplot (Wilke, 2020).

Chapter 5 | Lake Ioannina results

This chapter presents the new diatom record for the I-284 core from Lake Ioannina. Existing pollen and sedimentological data are subsequently introduced. They are used to aid the interpretation of the new diatom record and the reconstruction palaeoenvironmental change at Lake Ioannina during the glacial–interglacial cycles corresponding to MIS 7–9.

5.1 Results

A total of 176 samples were examined from the I-284 core between depths of 282.82 m and 138.02 m, a section spanning 144.8 m (45.4% of the whole I-284 core). Other than a missing 6.2 m-long section of the core spanning 271.02–264.82 m, a sample was examined approximately every 0.8 m (providing an estimated temporal resolution of approximately 650 years). A minimum count of 300 diatom valves was achieved for all samples except three with very low diatom concentrations, for which a minimum of 100 valves were counted, and eleven that contained too few diatom valves to make viable counts.

In total, 187 diatom taxa (10 planktonic, 12 facultative planktonic and 165 benthic) were identified within this section of the I-284 core. Twelve diatom assemblage zones, here termed Ioannina diatom zones (IDZs), can be recognised from the CONISS cluster analysis (Appendix B). IDZ 12 has been further split into subzones to aid description. The diatom assemblage of each zone is shown on Figure 5.1 and described in Table 5.1 alongside other key features of the diatom record.

Despite being the least diverse group, planktonic taxa comprise 77.4% of all valves counted, with facultative planktonic and benthic taxa comprising 7.2% and 15.4% respectively. This dominance of planktonic taxa is a key feature of the record. Shifts in the abundance of planktonic taxa are generally subtle,
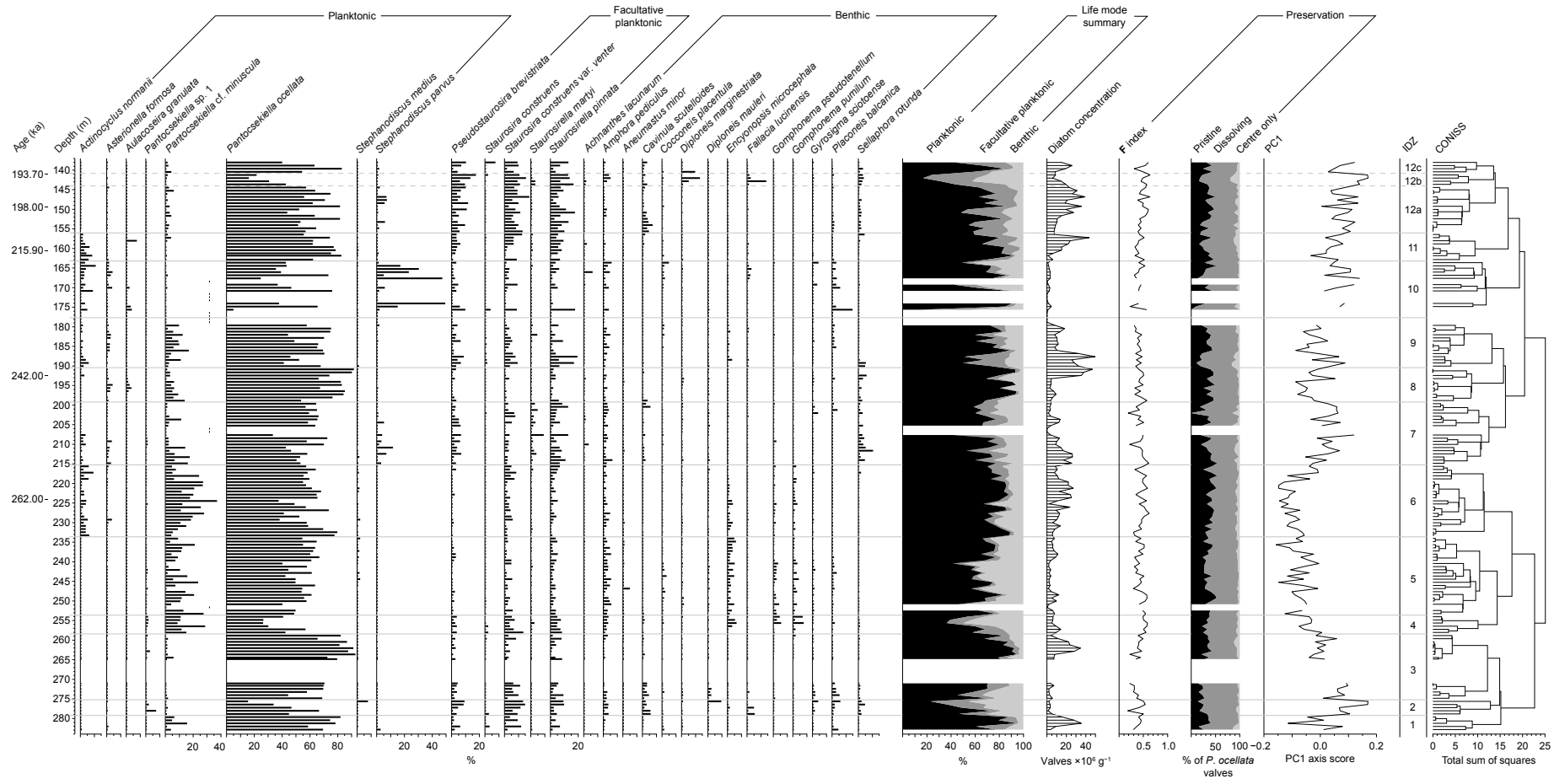
Figure 5.1: Summary diatom stratigraphy of core I 284 displayed as relative abundances by depth for taxa present at ≥4% in at least one. The diatom assemblage is summarised by life mode. Diatom concentration is displayed as the total number of diatom valves present per gram of dry sediment. Diatom preservation is represented by the **F** index based on all valves counted and by the dissolution of *Pantocsekiella ocellata* valves. Axis scores of the first principal component (PC1) are displayed. The record is split into IDZs based on the results of the CONISS cluster analysis, which are also presented.

Table 5.1: Summary of the diatom results for the Lake Ioannina I-284 core.

Zone	Depth (m)	Estimated age[a]	Description of diatom results
IDZ 1	282.82–279.22	Older than 262 ka Probably MIS 9c or 9b	Planktonic abundance is high, reaching the record peak of 95% in this zone. *Pantocsekiella ocellata* dominates (59–82% abundance) with lower abundances of *Pantocsekiella minuscula* (<15%) and small Fragilariaceae (<30%). Benthic taxa comprise <16% of all taxa in any sample. The diatom concentration is relatively high in IDZ 1, forming a peak with a maximum value of 35.4×10^6 g^{-1} in the middle of the zone (281.22 m). Preservation is moderate with the proportion of pristine *P. ocellata* valves of around 35%. The **F** index reflects a similar level of preservation with a value of around 0.4. Both increase slightly from the base to the top of the zone. PC1 axis scores are relatively low, declining to below −0.10 before recovering across the boundary into IDZ 2.
IDZ 2	279.22–275.22	Older than 262 ka Probably MIS 9b	Planktonic taxa decline to very low abundances across IDZ 2, reaching as low as 23%. This is mainly due to a decrease in *P. ocellata* abundance, but *P.* cf. *minuscula* exhibits a decline as well. Facultative planktonic and benthic taxa are both present at similar abundances (up to 33% and 45% respectively), and the benthic taxa are diverse. The diatom concentration is very low (<6×10^6 g^{-1}). The **F** index reaches relatively high values, exceeding 0.5 for much of the zone except for a marked decrease to 0.2 at 278.02 m. However, the abundance of pristine *P. ocellata* valves is low (c. 20% throughout). PC1 axis scores are very high, almost reaching a value of c. 0.17 towards the top of the zone.
IDZ 3	275.22–258.42	Older than 262 ka Probably MIS 9b to 9a	IDZ 3 contains a section for which no core material was available. Planktonic abundance recovers during IDZ 3, reaching as high as 95% in the upper part of the zone. Both the facultative planktonic and benthic taxa decline in abundance, reaching very low abundances (<10%) after the gap in the record. *P. ocellata* dominates once again. Towards the top of the zone, the large morphotypes of *P. ocellata* are present at low abundances. The diatom concentration is very low at the start of the zone (<8×10^6 g^{-1}) but increases to form the second peak of the record after the gap. Concentrations reach as high as 35×10^6 g^{-1} before declining towards the top of the zone. Preservation is moderate and appears to be better after the gap in the record than before it. The **F** index declines before the gap in the record and recovers after it. The abundance of pristine *P. ocellata* valves is around 20% before the cap and around 35% afterwards. PC1 axis scores exhibit a declining trend across the zone, dropping to c. 0.00 at the boundary with IDZ 4.

Table 5.1 (continued)

Zone	Depth (m)	Estimated age[a]	Description of diatom results
IDZ 4	258.42–253.62	Older than 262 ka Probably late MIS 9a to early MIS 8	The planktonic abundance is relatively low in IDZ 4, declining below 40% in the middle of the zone. *P. ocellata* is still the most abundant planktonic taxa with the large, non-classic morphotypes also present at low abundances. *P.* cf. *minuscula* is also moderately abundant (9% to 29%). Benthic taxa are highly abundant and reach their highest abundance of the record in this zone (50%). They are diverse, although the most abundant include *Gomphonema* spp. and *Encyonopsis microcephala*. Diatom concentration is moderate with a relatively small peak at the start of the zone (14×10^6 g^{-1} at 257.22 m) before stabilising at around 6×10^6 g^{-1}. Preservation is moderate with an **F** index of around 0.5, although *P. ocellata* preservation is slightly worse with around 30% of valves unaffected by dissolution. PC1 axis scores are variable but continue the declining trend from IDZ 3.
IDZ 5	253.62–233.62	Older than 262 ka Early MIS 8	Planktonic abundances are moderate but variable in IDZ 5. After recovering from the low in IDZ 4, they fluctuate around 60% to 80% before reaching a low of 42% at 240.42 m. They recover rapidly to >70% after this and maintain high abundances for the rest of the zone. *P. ocellata* remains the most abundant taxon and is present at around 50% abundance. *P.* cf. *minuscula* continues to persist at values similar to IDZ 4 but its abundance is highly variable, ranging between 1% and 24%. Facultative planktonic taxa are rare, generally below 10% abundance. Benthic taxa maintain their high abundance from IDZ 4. In the lower two thirds of the zone they range between 13% and 49% abundance, declining to around 20% in the upper third. They maintain their diversity, and *Gomphonema* spp. and *Encyonopsis microcephala* remain the most abundant benthic taxa. Concentration is low ($2–12 \times 10^6$ g^{-1}). One sample did not contain enough diatoms to make a viable count. Both preservation indices indicate moderate preservation. PC1 axis scores are relatively low but variable (between 0.00 and −1.50), and they continue to exhibit a declining trend.
IDZ 6	233.62–215.22	Base just older than 262 ka Top just younger than 262 ka Mid. MIS 8	IDZ 6 is characterised by a high planktonic abundance of around 70% to 80%. Facultative planktonic taxa are rare, and benthic taxa have abundances of around 10% to 25%. Although *P. ocellata* remains the most abundant taxon, this zone is characterised by relatively high abundances of *P.* cf. *minuscula*, which reaches its peak abundance of 37% in this zone (at 224.42 m). Although present at low abundances (<10%), *Actinocyclus normanii* appears at the start of the zone and maintain a consistent presence throughout. The diatom concentration is moderate at the start of the zone (c. $5–15 \times 10^6$ g^{-1}) and increases to relatively high values in the

Table 5.1 (continued)

Zone	Depth (m)	Estimated age[a]	Description of diatom results
IDZ 6 (continued)			middle of the zone (20–25×10^6 g^{-1}) before returning to values similar to those at the start of the zone.
			The quality of the diatom preservation is similar to IDZ 5 and is not very variable.
			PC1 axis scores are low. They reach some of their lowest values of the record (c. -1.50) near the top of the zone before increasing across the zone boundary in to IDZ 7.
IDZ 7	215.22–199.22	Base just younger than 262 ka Top c. 246 ka Late MIS 8	Planktonic abundances are around 55% to 65%, slightly lower than IDZ 6. *P.* cf. *minuscula* is present at lower abundances that IDZ 6 and there are some moderate abundances of *Stephanodiscus parvus* for the first time. The is an expansion of small Fragilariaceae at the start of this zone. There is also a shift in the most abundant benthic taxa, with *Gomphonema* spp. and *E. microcephala* no longer more abundant than any other benthic taxa and relatively high abundances of *Sellaphora rotunda* of up to 11%.
			Concentration is moderately high at the start of the zone (c. 25×10^6 g^{-1}) but declines to low values by the top of the zone (c. 4×10^6 g^{-1}). There are a couple of samples in the middle of the zone that contained too few diatom valves to count.
			The preservation quality is moderate but variable, with both preservation indices exhibiting a couple of short-lived declines.
			PC1 axis scores are high, reaching values >1.00.
IDZ 8	199.22–190.42	c. 246–240 ka Late MIS 8 to 7e	IDZ 8 is characterised by a very high planktonic abundance around 90% with some low abundances of benthic taxa. *P. ocellata* dominates, although there are some low abundances of *Asterionella formosa* and *Aulacoseira granulata* in the middle of the zone and *P.* cf. *minuscula* increases in abundance slightly from IDZ 7.
			The diatom concentration is low to start but exhibits a marked increase in the upper half the zone, increasing from 4 to 36×10^6 g^{-1} from one sample to the next and reaching a peak of 47×10^6 g^{-1} in the final sample of the zone.
			Preservation is moderate, the **F** index consistently around 0.4 and the proportion of pristine valves of *P. ocellata* at around 35%.
			PC1 axis scores decline to relatively low values in this zone of c. -0.07, then they start to recover towards the top of the zone.
IDZ 9	190.42–177.62	c. 240–237 ka Mid. MIS 7e to early 7d	The start of IDZ 9 is marked by a decrease in the abundance of *P. ocellata*, although they are still present at between 40% and 75%. *P.* cf. *minuscula* and *A. formosa* persist at similar abundances to IDZ 8, and *A. normanii* returns at low abundances. The small Fragilariaceae have relatively high abundances at the start of the zone, with a combined abundance of up to 38%.

Table 5.1 (continued)

Zone	Depth (m)	Estimated age[a]	Description of diatom results
IDZ 9 (continued)			The diatom concentration is very high in the lower third of the zone ($26–50 \times 10^6$ g^{-1}) and then exhibits a marked decline to around 10×10^6 g^{-1}. The samples at the top of the zone did not contain many diatom valves.
			The **F** index is consistently around 0.4, while the preservation of *P. ocellata* valves declines in the lower part of the zone. This is reflected by both a decrease in the abundance of pristine valves and a small increase in the abundance of heavily dissolved valves with only their central areas remaining. Their preservation recovers by a depth of around 186 m, which coincides with the decline in concentration.
			PC1 axis scores are in the middle of the range of PC1 axis values but are very variable.
IDZ 10	177.62–163.22	c.237–217 ka MIS 7d	IDZ 10 is charactered by variable but sometimes high abundances of *S. parvus* (up to 49%). In some samples it is more abundant than *P. ocellata*. Other planktonic taxa present but at low abundances include *A. normanii*, *A. formosa* and *A. granulata*. *P.* cf. *minuscula* is almost absent, being present at extremely low abundances.
			The diatom concentration is very low throughout this zone (<5×10^6 g^{-1}). Multiple samples contained too few diatom valves to make viable counts.
			The **F** index continues to indicate moderate preservation, however there are some samples with very low abundances of pristine *P. ocellata* valves. The top of the zone is generally better preserved than the lower part.
			The PC1 axis scores in IDZ 10 are quite high, sometimes exceeding 0.10.
IDZ 11	163.22–156.02	c. 217–210 ka Early MIS 7c	The start of IDZ 11 is marked by an increase in planktonic abundance. This is due to high abundances of *P. ocellata*. *A. normanii* persists at low abundances from IDZ 10. *S. parvus* is no longer abundant. Facultative planktonic taxa increase in abundance across the zone. This marks the start of a long term increasing trend that continues to the top of the record.
			Diatom concentration is low at the start of the zone but increases to a high peak of 44×10^6 g^{-1} at 157.22 m, which is followed by an abrupt decline to 8×10^6 g^{-1} by 156.42 m.
			Both indices indicate moderate preservation, although across the zone, there is a slight decline in the proportion of pristine *P. ocellata* valves and a slight increase in the proportion of those with only their central areas remaining.
			PC1 axis scores are moderate at the start of the zone (c. 0.03) but increase towards the upper zone boundary with IDZ 12 (to c. 0.08).

Table 5.1 (continued)

Zone	Depth (m)	Estimated age[a]	Description of diatom results
IDZ 12a	156.02–144.02	c. 210–195 ka Late MIS 7c, MIS 7b and MIS 7a	IDZ 12 is characterised by moderately high abundances of planktonic taxa (mainly *P. ocellata* but there are low abundances of *P.* cf. *minuscula* and *S. parvus*), which exhibit a declining trend that is punctuated by multiple small fluctuations. Facultative planktonic taxa gradually increase in abundance while benthic taxa are generally at low abundances. *Cavinula scutelloides* and *S. rotunda* are the most abundant benthic taxa. Diatom concentrations are low at the start of the zone (c. 10×10^6 g^{-1} up to 152.42 m) then increase to over 20×10^6 g^{-1}, reaching a maximum of 39×10^6 g^{-1} at 146.82 m. The **F** index remains at around 0.4 and the abundance of pristine valves of *P. ocellata* increases slightly in this zone, back to around 30%. PC1 axis scores are high, between c. 0.05 and c. 0.15.
IDZ 12b	144.02–140.82	c. 195–194 ka Early MIS 6	IDZ 12b is characterised by low abundances of *P. ocellata*. The small Fragilariaceae are abundant (c. 45% combined abundance), as the benthic taxa, with relatively high abundance of *Diploneis marginestriata* (up to 13%) and *Fallacia lucinensis* (up to 14%). The diatom concentration declines across the zone, reaching relatively low values of around 8×10^6 g^{-1} by 142.02 m. There is a small decline in the abundance of *P. ocellata* valves that are pristine and an increase in the number that have only their central areas remaining, suggesting a slight decline in preservation. The **F** index exhibits a similar decline, but it is not as marked. PC1 axis scores are very high in IDZ 12b, peaking at >1.50.
IDZ 12c	140.82–138.02	c. 194–191 ka Early MIS 6	IDZ 12c is characterised by a return to high abundances of *P. ocellata*, which reach as high as 85% abundance at 139.62 m before declining towards the top of the record as the small Fragilariaceae increase in abundance to 42%. The concentration increases at the start of the subzone to reach a moderate peak of 25.8×10^6 g^{-1} at 138.82 m. It declines slightly to 15.2×10^6 g^{-1} by the final sample of the record. Both the **F** index and dissolution of *P. ocellata* valves indicate moderate preservation. PC1 axis scores decline from IDZ 12b into IDZ 12c (to just below 0.05) before increasing to >0.10 by the top of the zone.

[a] Ages estimated from published age control points (Table 4.1), Ioannina pollen record and a comparison with the Ohrid diatom record (for the latter see Chapter 7).

which is remarkable considering the length of the record and that it encompasses a glacial–interglacial cycle.

Eurytopic, planktonic *Pantocsekiella ocellata* dominates the assemblage with relative abundances (hereafter abbreviated to abundance) exceeding 50% in most (146 out of 165) samples (Figure 5.1). This taxon exhibits a large degree of morphological variability, with large, non-classic morphotypes (section 4.3.2) present mainly within IDZs 3–5 and 12 (Figure 5.2). Other abundant planktonic taxa include small-celled *Pantocsekiella* cf. *minuscula,* which is particularly abundant throughout the middle of the record (IDZ 4–9), and mesotrophic *Stephanodiscus parvus,* which is particularly abundant within IDZ 10. The distribution of facultative planktonic taxa is concentrated within certain parts of the record. Multiple samples with a facultative planktonic abundance exceeding 30% can be found in IDZ 2, at the start of IDZ 9 and across IDZ 12, with a gentle increasing trend discernible across the upper zones of the record (IDZ 10–12). In contrast, facultative planktonic taxa are particularly scarce throughout IDZ 5–6 and in IDZ 8. Small taxa of the Fragilariaceae family (*Staurosirella pinnata, Staurosira construens* var. *venter* and *Pseudostaurosira brevistriata*) are the most abundant facultative planktonic taxa. The abundance of any individual benthic taxon rarely exceeds 10%. Those that do include *Placoneis balcanica* (14.7% at 175.62 m, a poorly preserved sample), *Fallacia luncinensis* (13.7% at 142.82 m), *Diploneis marginestriata* (13.1% at 142.02) and *Sellaphora rotunda* (10.5% at 211.62 m). In all instances, the relatively high abundance is not maintained beyond a single sample.

The diatom concentration ranges from samples where no countable diatom valves are present up to a maximum concentration of 49.6×10^6 valves per gram of dry sediment. The record is clearly defined, exhibiting several distinct periods of high diatom concentration that are clearly separated by periods of lower concentration. The greatest peaks, which all exceed concentrations of $30 \times 10^6 \text{ g}^{-1}$, occur in zones 1, 3, 8–9, 11 and 12a. Moderately high concentrations exceeding $20 \times 10^6 \text{ g}^{-1}$ are reached in two other parts of the record: spanning
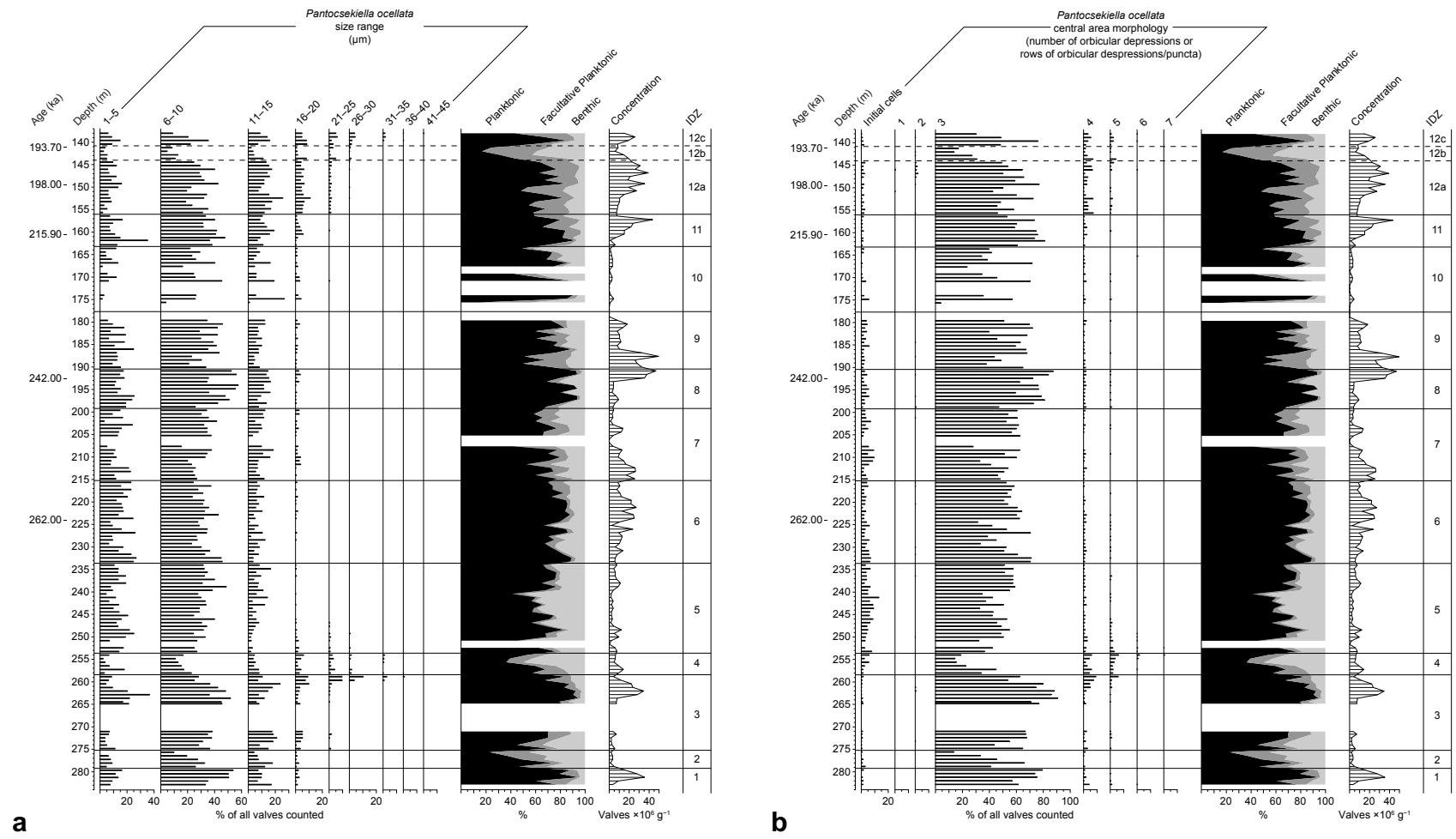
Figure 5.2: A breakdown of the relative abundances of *Pantocsekiella ocellata* valves according to their valve diameters (**a**) and the morphology of their central areas (**b**). Relative abundances are expressed as a percentage of all diatom valves counted in a sample. They are displayed alongside a summary of the diatom assemblage and concentration. Valves with unknown diameters or unknown central area morphologies are not shown.

zones 6–7 and within IDZ 12c. The latter is a short-lived peak reaching 25.8×10^6 g^{-1}. However, the former exhibits a notably different outline to any other part of the record, increasing and decreasing gradually (albeit overprinted by shorter-term fluctuations) over a long section of the core and possessing no single peak but several samples with concentrations of around 25×10^6 g^{-1}. Very low diatom concentrations of $<5 \times 10^6$ g^{-1} are mainly found within four parts of the record: spanning zones 2–3 (278.82–271.02 m), throughout most of IDZ 5 (251.62–239.62 m), spanning the upper half of IDZ 7 and the bottom half of IDZ 8 (207.62–193.22 m), and from the top of IDZ 9 to the bottom of IDZ 11 (178.82–161.22 m). Within the latter, numerous samples have such low diatom concentrations that there were not enough diatoms present to make viable diatom counts. Other such samples are found in the low concentration zones of IDZ 5 and IDZ 7.

Across all countable samples, there is a mean **F** index of 0.44 with a standard deviation of 0.09, indicating moderate preservation quality that does not vary much throughout the record. The mean proportion of pristine *P. ocellata* valves is 32.9% ($SD = 10.4\%$). This is lower than that of all taxa, reflecting their higher susceptibility to dissolution than some other taxa in the record. Whilst a large proportion of *P. ocellata* valves exhibit a small degree of dissolution, as represented by the relative abundance of valves with striae that are dissolving ($M = 61.7\%$, $SD = 9.6\%$), very few have experienced such extreme dissolution that only their central areas remain ($M = 5.5\%$, $SD = 3.8\%$). These very low abundances of valves (of a relatively dissolution-susceptible taxa) in the end stages of dissolution indicate that the integrity of the diatom assemblage record is maintained despite evidence that some dissolution has taken place. The *P. ocellata* dissolution categories exhibit more variation than the **F** index of all taxa and better reflect the preservation variation observed across the samples.

Unconstrained ordination methods performed on untransformed data did not provide a useful result as PC1 (explaining 59% of the variation in the record) was highly correlated with the abundance of *P. ocellata* ($\rho = -0.999$, p <0.001;

Appendix C). This highlights the dominance of *P. ocellata* in the record, but it is of little help in investigating the underlying variability and any environmental parameters that could be driving species compositional change. Ordination methods were subsequently performed on square root transformed data to reduce the influence of the highly dominant *P. ocellata,* with linear techniques being deemed appropriate. PC1 explains 26% of the variance and is plotted on Figure 5.1. Samples with low PC1 axis scores are associated with relatively high abundances of *P.* cf. *minuscula,* whilst samples with high PC1 axis scores are associated with relatively high abundances of the small Fragilariaceae (Figure C.6). As detailed in Table 2.1, both *P.* cf. *minuscula* and the small Fragilariaceae have high growth rates, enabling them to tolerate low nutrient and light availability. They are both also tolerant of a large range of nutrient conditions. The only major way in which their environmental associations differ is by mixing regime. While *P.* cf. *minuscula* has slow sinking rates and is associated with a stable stratified water column, the small Fragilariaceae are characteristic of unstable environments and physical disturbance. On this basis, PC1 is interpreted as reflecting the mixing regime of the lake, with low PC1 axis scores associated with stable stratified conditions and high PC1 axis scores associated with a turbulent, well mixed water column. The positions of the other taxa along PC1 are in agreement with this. Several of the other taxa that plot with high values on PC1 (e.g. *Aulacoseira granulata* and *S. parvus*) have been associated with turbulent, disturbed or stressed environments. Those associated with low PC1 scores alongside *P.* cf. *minuscula* include *Gomphonema* spp. and *Encyonopsis microcephala*. These taxa tend to form branching colonies from mucilage stalks and are associated with macrophytes (Table 2.1), so a low energy environment is probably more conducive for their growth than high water turbulence (Passy, 2007). PC1 axis scores are highest in IDZ 2, IDZ 10 and IDZ 12, while they are lowest in IDZ 5–6. They exhibit a declining trend during the lower half of the record before increasing across the IDZ 6–7 boundary, which is identified by the CONISS cluster analysis as the most important of the record.

5.2 Data and results from previous investigations

Pollen and sedimentological data from earlier work are used to aid the interpretation of the diatom record and ascertain a more complete understanding of environmental and climatic conditions during MIS 7–9 at Ioannina. The data are displayed alongside a summary of the diatom results in Figure 5.3 and detailed below.

Pollen

Pollen data are available for the top half of the diatom record at a 20 cm resolution and span 210.0–130.9 m, a section of the core equivalent to the interglacial complex of MIS 7 (Roucoux et al., 2008). AP and AP–PJB percentages and concentrations are displayed in Figure 5.3 and reflect four forested intervals (Zitsa I–IV), which are separated by periods of predominately open vegetation during which arboreal pollen still persists but at lower percentages. Zitsa I, corresponding to MIS 7e, represents a truncated forested interval, the relatively short duration of which is also evident in other records (e.g. Roucoux et al., 2006). It is followed by the contraction of temperate forests to close to their fully glacial extent. Zitsa II, corresponding to MIS 7c, is the most floristically diverse forested interval. There is a minor, short-lived forest contraction prior to Zitsa III. AP–PJB percentages represent temperate tree populations and reach a similar value in all intervals except Zitsa IV, which is relatively short and of a smaller magnitude than the others. Pollen concentrations are highest in Zitsa I and lower in each successive forested interval.

Many IDZ boundaries coincide with those of the pollen zones or are very close, indicating concomitant shifts in the diatom assemblage and catchment vegetation. However some major boundaries in the pollen record are not evident in the diatom assemblage, including the start of Zitsa I and the start of Zitsa III. The diatom concentration follows the same pattern as the pollen
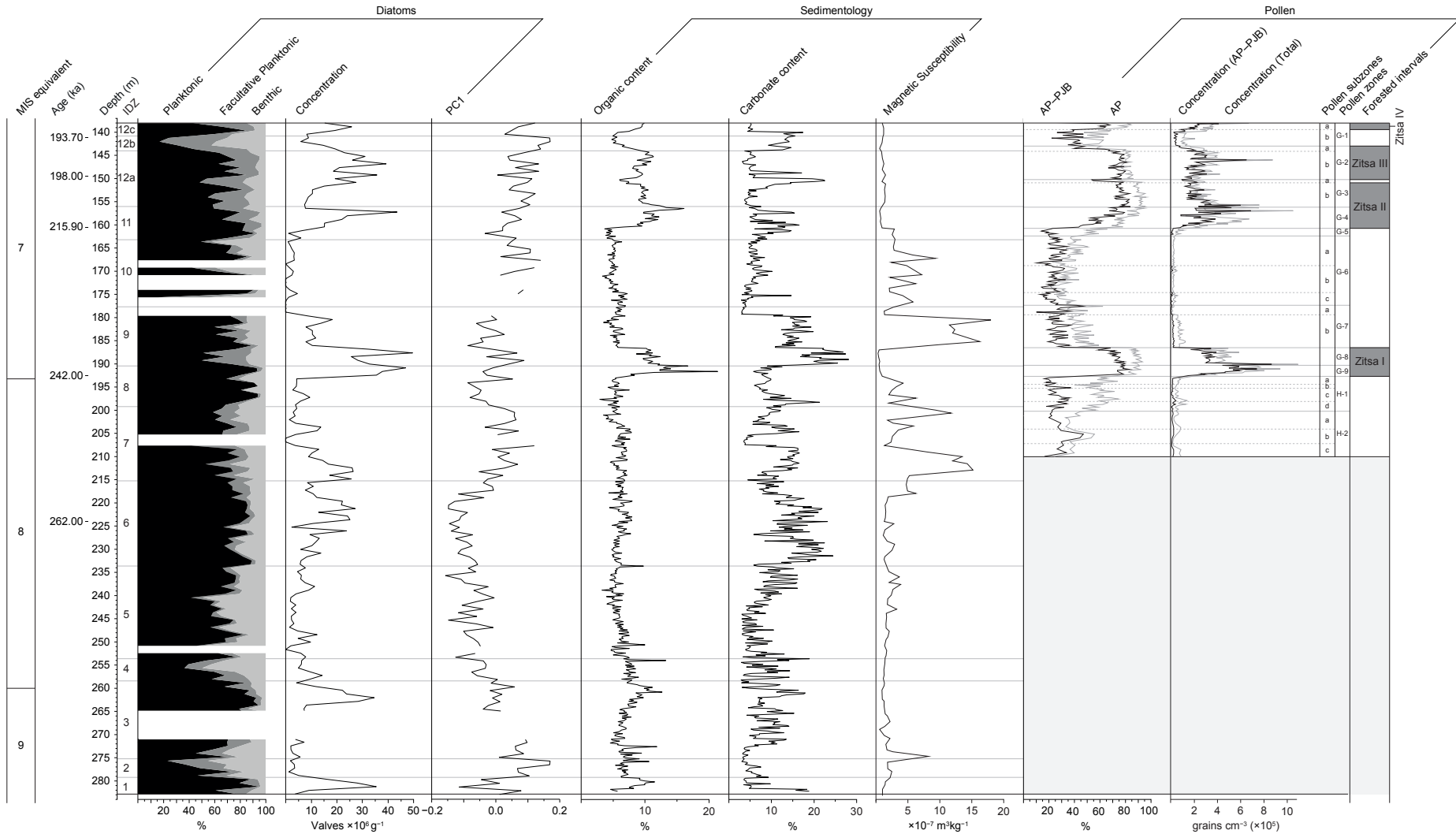
Figure 5.3: Summary diatom record plotted alongside sedimentological data (Frogley, 1997) and summary pollen data (Roucoux et al., 2008).

concentration, with the highest concentrations occurring in IDZ 8–9 during the first forested interval of MIS 7, and with a major peak occurring in each successive forested interval that gets smaller each time.

Organic content

An estimate of the organic content of the sediment is provided by the percentage mass loss-on-ignition (LOI) at 550°C, carried out at 20 cm resolution (Frogley, 1997). The mean organic content of the sediment for this section of the I-284 core is 6.8% (*SD* = 2.1%). There are sections with sustained elevated organic content of over 10% within IDZ 1, IDZ 3, IDZ 8–9 and IDZ 11–12. These tend to be associated with moderate to high diatom concentrations, although the opposite is not true as high diatom concentrations still occur when organic content is not elevated (e.g. in IDZ 6 and IDZ 7). Previous investigations on the I-284 core have demonstrated that the organic content broadly corresponds with the pollen record during the Lateglacial–Holocene (Lawson et al., 2004), MIS 5 (Frogley, 1997) and MIS 7 (Roucoux et al., 2008), with peaks in the percentage of organic content correlating with high pollen concentrations and arboreal pollen percentages. Roucoux et al. (2008) attributed the highest peaks in organic content to a combination of both a high input of organic material from the catchment and high productivity within the lake itself. Where pollen data are not yet available, the consideration of the organic content alongside the diatom concentration can cautiously be used as an indicator for catchment productivity.

Carbonate content

An estimate of the calcium carbonate content of the sediment is derived from the percentage mass LOI at 950°C, carried out at 20 cm resolution (Frogley, 1997). The values are more variable than those of the organic content, ranging between 2.9% and 28.1% with a mean of 9.7% (*SD* = 5.1%). The broad-scale carbonate curve is overprinted by shorter-term fluctuations, which are of greater amplitude than those of the organic content curve. In terms of the

broad-scale changes, the carbonate content is generally low in the bottom and top thirds of the record. Within the central third of the record, which spans IDZ 6 to IDZ 9, there are several extended periods with elevated carbonate percentages and values rarely decline to the overall curve baseline of around 5%.

As detailed in section 2.2.5, there are numerous possible sources of the carbonate in lacustrine sediments. Due to the profundal location of the core site, the lack of a fluvial input and a lack of evidence for the mass movement of sediment via turbidity currents, Frogley (1997) reasoned that the carbonate of the I-284 core is predominantly authigenic (precipitated within the lake itself) rather than detrital carbonate from the catchment. This was confirmed through scanning electron microscopy (SEM) analyses, which also ruled out any carbonate dissolution (Frogley, 1997). However, this is not the case throughout the entirety of the core. Based on SEM analyses and a comparison of isotopic data with magnetic susceptibility, Leng et al. (2010) demonstrated that the upper 30 m of the core lacks significant authigenic carbonate and contains detrital carbonate washed in from the catchment. Clearly both processes have been at work in Lake Ioannina and must be considered during interpretations.

Magnetic susceptibility

Magnetic susceptibility (χ) measurements were made at approximately 1 m intervals along the I-284 core (Frogley, 1997). Values are low throughout most of the core (generally below 3×10^{-7} m^3kg^{-1}) except for a section spanning approximately 220–165 m where they peak at almost 19×10^{-7} m^3kg^{-1}. This section of the core is associated with high concentrations of small, black, aggregated, iron-rich nodules with diameters of approximately 1–2 mm, the magnetic susceptibility of which yields values similar to the iron-oxide minerals magnetite (Fe_3O_4) and maghaemite (γ-Fe_3O_4) (Frogley, 1997). These minerals can result from pedogenesis (Maxbauer et al., 2016) and the present

day soils of the Ioannina catchment also contain magnetic minerals (haematite and goethite; Frogley, 1997. The magnetic susceptibility record at Ioannina has therefore been considered a proxy for soil inwash (Frogley, 1997; Roucoux et al., 2008). The low values that persist throughout most of the I-284 core would therefore reflect low initial concentrations of magnetic minerals in the catchment soils and/or the distal location of the core site from the lake margin throughout most of the lake's history.

5.3 Interpretations

5.3.1 Life mode response

In more recent climatic cycles, variations in the relative abundances of planktonic versus facultative planktonic taxa have been interpreted as reflecting lake level changes, productivity shifts or both (section 2.2.6). Lake level was confirmed as the primary driver, at least for the late glacial and Holocene (Jones et al., 2013). Although it is important to consider that the primary driver could vary through time, there is little evidence for nutrient-driven productivity shifts influencing the relative abundance of planktonic taxa. Phases with the highest planktonic abundances are dominated by *P. ocellata* rather than eutrophic taxa such as *Aulacoseira* spp., which dominate the planktonic habitat in the present-day hyper-eutrophic Lake Ioannina (Wilson et al., 2013) and during MIS 5a in nearby and similarly shallow Lake Prespa (Cvetkoska et al., 2015). Therefore, lake level change is probably also the primary driver of change in the ratio of planktonic versus facultative planktonic and benthic taxa, rather than nutrient-driven productivity shifts, during this time interval.

5.3.2 Morphological variability of *P. ocellata*

Many of the taxa in the sediments of Lake Ioannina are eurytopic, which makes interpretations difficult. It is particularly problematic that the record is

dominated by a single eurytopic taxon, *P. ocellata*. In more recent climatic cycles, it has been interpreted as representing oligotrophic–mesotrophic conditions, particularly when the large, "non-classic" forms are also present (Wilson et al., 2015). This interpretation is supported by their similar morphologies to recently described large *Pantocsekiella* taxa in other Mediterranean lakes, which have been associated with low nutrient availability (Cvetkoska et al., 2014a; Cvetkoska et al., 2015; Vossel et al., 2015; Vossel et al., 2018). The large morphotypes have also been used to infer deep water phases at Ioannina (Wilson et al., 2008; Jones et al., 2013). However, this is in the context of fluctuations between very shallow, turbid, turbulent conditions and deeper water. The lake is not inferred to have been extremely shallow during any part of the time interval under investigation here, so lake level is unlikely to have been a limiting factor in their growth. Furthermore, their presence seems unrelated to variations in water depth within a persistent deeper water setting as they are present in this record when planktonic abundance is both high (e.g. IDZ 3) and low (e.g. IDZ 4). This demonstrates that different factors have controlled their presence throughout the lake's history.

Similar observations and conclusions were reached by Luethje and Snyder (2021) in an investigation into the morphological variation of *Pantocsekiella* valves in Lake El'gygytgyn (northeastern Russia) over the last c. 1.2 Ma. They found an inconsistent trend towards larger *Pantocsekiella* valves during warm intervals, suggesting interspecific competition or niche partitioning between planktonic taxa as other possible controls on size. One hypothesis is that a larger genus could be limiting the size of *Pantocsekiella* valves during some parts of the Lake El'gygytgyn diatom record. This is also a possibility in Lake Ioannina. In the new record presented here, another large planktonic taxon, *Actinocyclus normanii*, co-occurs with the smaller valves of *P. ocellata* but not with the large morphotypes. As large *P. ocellata* morphotypes are probably indicative of low nutrient availability and *A. normanii* prefers nutrient enriched

conditions (Table 2.1), it is possible that the two taxa occupy a similar niche but under different trophic states.

Another possible control on the valve size of *P. ocellata* is temperature. It has long been recognised that the size of an individual organism can potentially reflect the ambient temperature at which it grew. Organisms of a certain species, living in relatively colder environments such as at higher altitudes or higher latitudes, tend to have larger body sizes than organisms of the same species residing in relatively warmer environments. The phenomenon, which has been observed in both endotherms and ectotherms, was first described by Bergmann (1847). A recent review provides strong evidence that freshwater phytoplankton conform to Bergmann's Rule (Zohary et al., 2021). This is at odds with the trend towards larger valve sizes during warmer intervals that was observed by Luethje and Snyder (2021). However, as discussed in section 2.2.3, the direct effects of temperature on diatoms are often superseded by changes in the other lacustrine variables that it controls. Still, it is worth considering the possible role temperature might play in controlling *P. ocellata* valve size in this record.

5.3.3 Interpretations by diatom zone

IDZ 1 (282.82–279.22 m)

The dominance of planktonic taxa and the large concentration peak within IDZ 1 are indicative of a deep, productive lake. These features are unlikely to be the result of high nutrient-driven productivity because there is a lack of eutrophic taxa that would be expected to flourish under such conditions. The record is instead dominated by *P. ocellata* and accompanied by lower abundances of *P.* cf. *minuscula*, a small planktonic taxon that is particularly competitive under low nutrient availability (Winder et al., 2009). This interpretation is consistent with the low magnetic susceptibility values, which indicate low detrital input (and therefore nutrient delivery) from the catchment. Although pollen data are not yet available for this section of the

core, the organic content is relatively high and peaks after the diatom concentration peak. It is therefore likely that the catchment was substantially vegetated, which would have resulted in low catchment erosion and detrital input. Although the source of the carbonate is not known, there is a low percentage of carbonate in the sediment throughout most of IDZ 1. Depending on its source, this is consistent with either low detrital input or a deep fresh system, both of which are inferred to have occurred during IDZ 1.

Overall, the lake was deep, oligotrophic and productive during IDZ 1. The lake level is inferred to have increased in the lower half of IDZ 1, likely reaching its maximum level at around 281.22 m when the abundance of planktonic taxa and the diatom concentration reach their peaks concurrently. By the top of IDZ 1, the lake level had started to decline. The catchment was probably substantially vegetated, which resulted in a low input of detrital material to the lake during this time.

IDZ 2 (279.22–275.22 m)

The declines in planktonic abundance and diatom concentration suggest a decrease in lake level and high PC1 axis scores indicate increased lake mixing. The diatom assemblage provides evidence of enhanced nutrient availability. There are several heavily silicified taxa, such *Pantocsekiella* sp. 1 and *Diploneis mauleri*, which indicate a plentiful Si supply. *D. mauleri* is also considered mesotrophic (Zhang et al., 2014b), and it co-occurs with mesotrophic *Stephanodiscus medius* in a sample towards the top of the zone. This increase in nutrient availability is consistent with the inferred increase in lake mixing, which could have enhanced the circulation of nutrients from the hypolimnion and sediments. The restriction of the mesotrophic taxa to a sample with low planktonic abundance also supports the interpretation that lake level is the primary driver of change in the relative abundance of planktonic versus facultative planktonic and benthic taxa rather than nutrient-driven productivity shifts. If productivity change were driving the change in

planktonic abundance, mesotrophic or eutrophic taxa would be expected to flourish when the planktonic abundance was high rather than at a minimum.

IDZ 3 (275.22–258.42 m)

A notable feature of IDZ 3 is the 6.2 m hiatus in the diatom record that spans the central portion of the zone. This is due to a misplaced segment of the core so is not an artefact of the diatom record itself. To aid in the description of this zone, it is considered in three parts—below the hiatus, the hiatus itself and above the hiatus.

From the low of 23% at the end of IDZ 2, the planktonic abundance recovers throughout the lower third of IDZ 3. Planktonic taxa comprise around 70% of the diatom assemblage just prior to the hiatus in the diatom record. This is much lower than the previous peak of 95% in IDZ 1, so although the lake level has increased, it is unlikely to have fully recovered to the very high levels experienced in IDZ 1 by this point. The diatom concentration remains low, persisting at values similar to those of IDZ 2 up to the gap in the diatom record. This indicates the continuation of low productivity from IDZ 2 into the lower part of IDZ 3. There is evidence that this low productivity also persists throughout the hiatus in the diatom record.

The hiatus in the diatom record spans from 271.02 m to 264.82 m. As the sedimentological analyses were carried out before this section of the core was misplaced, data on the organic content, carbonate content and magnetic susceptibility of the sediment are available. Of particular use is the organic content, which remains low throughout. Although this alone is not enough to provide a thorough determination of the lake status, it does indicate that it is unlikely that the lake and catchment were highly productive. Throughout this record, all peaks in diatom concentration exceeding $30 \times 10^6 \text{ g}^{-1}$ are associated with organic content percentages that are elevated above the baseline of around 5% to 6%. The organic content during the hiatus in the diatom record

ranges between 5% and 8%, which is not sufficiently elevated above the baseline to suggest very high productivity.

When the diatom record resumes, high planktonic abundances suggest that the lake was deep with high lake levels, similar to those of IDZ 1. The diatom concentration also increases and does so rapidly. Unlike IDZ 1, the peak planktonic abundance is reached before the increase in diatom concentration, indicating that high lake levels were established prior to an increase of within-lake productivity. In turn, the peak in diatom concentration occurs just prior to a period of sustained elevated organic content percentages, demonstrating a more rapid response to forcing mechanisms of the lake than the catchment.

Towards the end of IDZ 3, decreases in both the abundance of planktonic taxa and diatom concentration provide evidence for declining lake levels and within-lake productivity. This is accompanied by an increase in the morphological diversity of *P. ocellata*, possibly indicating reduced detrital input. This would be consistent with the inferred development of the catchment vegetation, which would have stabilised the catchment soils.

In summary, IDZ 3 represents a deepening of the lake from the lower lake levels at the end of IDZ 2. Only once a deep lake is established does the within-lake productivity then start to increase. It reaches a peak rapidly then declines with the lake level at the top of the zone. There is evidence that the catchment productivity increases during IDZ 3, peaking after the lake level and within-lake productivity and resulting in low detrital input.

IDZ 4 (258.42–253.62 m)

The marked increase in the abundance of benthic taxa, at the expense of planktonic taxa, is indicative of a decline in lake level. Planktonic abundance is not as low as in more recent climatic cycles, so it was probably not extremely shallow. The increase in *P.* cf. *minuscula* is probably indicative of an oligotrophic and a stratified water column. The presence of large *P. ocellata*

valves supports the inference of low nutrient availability, and the benthic assemblage is comprised of taxa associated with low energy environments (*Encyonopsis microcephala*, *Gomphonema pseudotenellum* and *Gomphonema pumilum*), further supporting the interference of stratified conditions. The relatively high benthic abundance indicates that light availability was not a limiting factor to their growth, so the water column is inferred to have been relatively clear.

IDZ 5 (253.62–233.62 m)

IDZ 5 reflects very similar conditions to IDZ 4 with an oligotrophic, clear and stratified water column inferred. The major difference in the assemblage from the preceding zone is an increase in the abundance of *P. ocellata* at the expense of small Fragilariaceae, which hints towards a slight increase in lake level and/or a further decrease in lake mixing. Although the very low diatom concentration could be indicative of a high sedimentation rate, it probably reflects low productivity as the sedimentological record does not provide any evidence for elevated sedimentation rates when the diatom concentration is at its lowest. Furthermore, increased magnetic susceptibility values and carbonate content percentages at the top of the zone suggest increased detrital input but coincide with higher diatom concentrations, indicating that sedimentation rate is not the dominant control on diatom concentration in this zone. The higher diatom concentration towards the top of the zone could be due to an increase in the delivery of nutrients as a result of the increased detrital input. Organic content is also very low towards the top of the zone, possibly indicating low catchment productivity, which supports the inference of increased detrital input as a result of reduced catchment stability.

IDZ 6 (233.62–215.22 m)

The increase in planktonic abundance from IDZ 5 to IDZ 6 reflects a further increase in lake level, resulting in the persistence of a relatively deep lake throughout IDZ 6. Low PC1 axis scores, very low abundances of facultative

planktonic taxa and relatively high abundances of *P.* cf. *minuscula* indicate that the stable lake conditions of IDZ 5 persist into IDZ 6, at least up to a depth of 219.62 m. Above this depth there is a small increase in the abundance of facultative planktonic taxa, which could indicate an increase in water turbulence, turbidity or both. This interpretation is supported by the magnetic susceptibility values, which are elevated during this part of the zone and suggest increased detrital input.

The increasing diatom concentration indicates an increasingly productive lake. The start of IDZ 6 is marked by the appearance of *A. normanii*, which persists at low abundances throughout the zone. Although it does not dominate the diatom assemblage, its presence and preference for nutrient enrichment (Table 2.1) could indicate a slight increase in nutrient availability from IDZ 5.

IDZ 7 (215.22–199.22 m)

The dominance of planktonic taxa indicates that the lake remains moderately deep, although the elevated abundances of facultative planktonic taxa could suggest a relative decline from the previous zone and/or increased lake mixing. This interpretation is supported by the decline in the abundance of *P.* cf. *minuscula*, which probably loses its competitive advantage as the water column becomes more well-mixed. The presence of several taxa with a preference for nutrient enrichment (e.g. *A. normanii*, *A. formosa* and *S. parvus*) further supports the interpretation of an unstable water column as a higher degree of mixing can release and redistribute more nutrients from the lake sediments. Furthermore, magnetic susceptibility is high, which could indicate enhanced delivery of detrital material from the catchment. Despite this, the lake remains oligotrophic with the diatom assemblage still dominated by *P. ocellata*.

IDZ 8 (199.22–190.42 m)

High planktonic abundances indicate a deep lake throughout this zone,

possibly the deepest of the record. Fragilariaceae decline to their lowest abundances of the record, their scarcity suggesting a stable lake with clear water. This is consistent with the pollen record, which indicates the development of a pioneer succession with the potential to stabilise the catchment soils and decrease detrital input to the lake. The continued dominance of *P. ocellata* indicates that the lake remains oligotrophic. Some taxa with preferences for nutrient enrichment and high silica availability (*A. granulata*, *A. formosa* and *S. parvus*) return at very low abundances in the middle of the zone, suggesting a slight increase in nutrient availability. This is again consistent with the pollen record, a decrease in arboreal pollen percentage across pollen subzones H-1-c to H-1-b representing a brief reversal to the development of the pioneer succession and the potential for increased erosion and nutrient delivery to the lake.

The large increase in diatom concentration towards the top of the zone is suggestive of a large and rapid productivity increase. It coincides with a return to low magnetic susceptibility values and a marked increase in arboreal pollen percentage that represents the onset of the Zitsa I forested interval. The increase in diatom concentration is not accompanied by an ecological shift in diatom species assemblage composition, other than the loss of rare taxa with higher nutrient preferences, indicating that the productivity increase is probably not related to an increase in nutrient availability. Nor is it likely to be related to an increase in lake level. The lake is already deep, with only a minor increase in planktonic abundance while the productivity increases. Clearly other factors that are not reflected by an assemblage composition change (e.g. temperature) must be driving this large productivity increase.

IDZ 9 (190.42–177.62 m)

The continued dominance of *P. ocellata* indicates that the lake remains oligotrophic and at least moderately deep throughout IDZ 9. However, across the lower third of the zone, there are elevated abundances of small

Fragilariaceae at the expense of *P. ocellata*. This coincides with a reduction in the preservation quality of *P. ocellata* valves. As no equivalent decline is recorded in the **F** index, it is possible that the relative decline in planktonic taxa could partly be an artefact of selective valve destruction. The interval of enhanced *P. ocellata* dissolution and increased small Fragilariaceae abundance exactly coincides with a period of elevated carbonate content. The high arboreal pollen percentages and concentration indicate that the catchment remains vegetated, and low magnetic susceptibility values suggest low detrital input. Therefore, the carbonate is probably not of detrital origin. The high diatom concentration indicates that within-lake productivity is high, so it could have been produced as a result of the drawdown of CO_2, or it could perhaps be linked to water temperature (section 2.2.3), which could also explain the enhanced diatom dissolution.

As the planktonic abundance recovers, within-lake productivity starts to decline. This exactly coincides with the end of the Zitsa I forested interval and a marked, large increase in magnetic susceptibility values, possibly reflecting the input of unstable catchment soils. Despite this enhanced detrital input, the lake remains oligotrophic. Small populations of *A. formosa* and *P.* cf. *minuscula* suggest the water column is still stratified. The lake remains oligotrophic, deep and moderately productive to the top of the zone, at least up to 179.62 m, above which the samples do not contain enough diatom valves to make viable counts.

The deficiency of diatom valves in the uppermost samples of the zone could indicate poor preservation or low within-lake productivity, with both probably acting as contributory factors. The small quantity of valves that are present (<10 valves per 300 microspheres counted per sample) represent taxa from all life modes but are highly fragmented and dissolved (except for some robust Fragilariaceae), indicating that diatoms do remain present across all lake habitats and that the complete destruction of valves could have taken place. Low within-lake productivity is probably also a factor in the low diatom

concentration and is consistent with the low catchment productivity inferred from very low pollen concentrations.

In summary, the lake is oligotrophic and deep throughout IDZ 9, except perhaps for the uppermost part of the zone where too few diatoms are present to make viable counts. Within-lake productivity declines in a step-like manner across the zone, reflecting similar declines in catchment productivity.

IDZ 10 (177.62–163.22 m)

Poor preservation hinders the interpretation of the assemblage in IDZ 10, which is punctuated by sections containing too few diatom valves to make viable counts. Where the record is available, variable planktonic abundances suggest the occurrence of relatively large lake level shifts. A very low planktonic abundance of 15.7% at 175.62 m indicates that the lake is shallow. However, enhanced destruction of *P. ocellata* valves and a relatively high **F** index suggests this could be an underestimation of lake depth. The planktonic abundance increases to 90.6% by 174.02 m, probably reflecting both an increase in lake level and an improvement in the preservation quality of *P. ocellata* valves. Following the subsequent hiatus in the diatom assemblage record, lake levels decline, a moderately deep lake persisting for the rest of the zone.

The diatom assemblage also indicates a shift in the trophic status of the lake during IDZ 10; the lake is probably at its most nutrient enriched during this zone. There are relatively high abundances of mesotrophic–eutrophic *S. parvus*, which is occasionally more abundant than *P. ocellata*. Other taxa with preferences for nutrient enrichment (*A. granulata*, *A. formosa* and *A. normanii*) are also present. Moderate and variable magnetic susceptibility values indicate pulses of enhanced soil erosion throughout the zone, which could account for some of the nutrient supply.

As with those at the end of IDZ 9, the uncountable samples in IDZ 10 contain a small number of diatom valves and fragments, most being too poorly preserved to identify. This indicates the persistent presence of diatoms in the lake and makes it difficult to determine whether the lack of valves is due to low productivity or reduced preservation quality. Where enough valves are present, the diatom concentrations are very low. Whilst some of these samples exhibit reduced preservation quality, those that are well-preserved also exhibit low diatom concentrations, indicating that low concentrations cannot just be an artefact of reduced preservation quality and that within-lake productivity is indeed low. This is consistent with low catchment productivity that is inferred from the pollen record. The abundance of taxa with preferences for nutrient enrichment demonstrates that the low within-lake productivity cannot be the result of low nutrient availability. Neither does it seem to be related to lake level; most of the zone exhibits moderate to high planktonic abundances. As with IDZ 8, there is clearly another factor driving diatom productivity at this point in the record, one that is also impacting catchment productivity.

IDZ 11 (163.22–156.02 m)

High planktonic abundances and low diatom concentrations indicate a deep and relatively unproductive lake at the start of the zone. The dominance of *P. ocellata* indicates the return of oligotrophic conditions following the slight nutrient enrichment of IDZ 10. Planktonic abundance declines across the zone as the abundance of small Fragilariaceae increases. The trend is punctuated by several oscillations and continues into the following zone. Each phase of planktonic abundance decrease is associated with a minor decline in AP–PJB. This is interpreted as a gradual and punctuated increase in lake mixing. The increase in diatom concentration mirrors that of the pollen, indicating increased within-lake productivity concurrent with increased catchment productivity and development of the Zitsa II forested interval. Low magnetic susceptibility values reflect low detrital input from the vegetated, stable catchment.

IDZ 12a (156.02–144.02 m)

Limnetic conditions across the lower half of IDZ 12a are inferred to be similar to those of IDZ 11, although with lower within-lake productivity. The more stable planktonic abundance in the upper half of the subzone coincides with the Zitsa III forested interval. At this point the lake is deep and productive. The relatively high abundance of facultative planktonic taxa and the high PC1 axis indicate that it is probably also well mixed.

IDZ 12b (144.02–140.82 m)

The marked declines in planktonic abundance and diatom concentration probably reflect a decrease in lake level and productivity. The diatom record is in accord with interpretations previously made from the pollen record. The decline in lake level and within-lake productivity is accompanied by a reduction in the forested extent of the catchment. IDZ 12b corresponds with the very end of the Zitsa III forest interval (pollen zone G-2-a) and a subsequent period of tree population decline with open grassland expansion (the lower half of pollen zone G-1-b). Despite this reduction in forest extent, the persistent vegetation coverage on the catchment would have ensured minimal soil erosion (Roucoux et al., 2008). This would have encouraged clear waters that, combined with the shallow water depth, would have enabled the growth of the relatively large benthic diatom population that is present at this time. The inference of a low lake level is also supported by the carbonate content, which is elevated exactly when planktonic abundance is low. As the catchment is stable, this is probably not a result of detrital input, and as within-lake productivity is low, it is probably not a result of the drawn down of CO_2.

IDZ 12c (140.82–138.02 m)

IDZ 12c reflects a brief return to higher lake levels and increased within-lake productivity. The increase in facultative planktonic taxa at the top of the zone could indicate increased mixing, lake shallowing or both. Again this agrees

with the pollen record, which reflects the final but relatively subdued forested interval of Zitsa IV.

5.3.4 Palaeoenvironmental summary

The palaeoenvironmental interpretations are summarised in Figure 5.4 alongside a series of schematic diagrams that illustrate the reconstructed palaeoenvironmental conditions at Lake Ioannina during each diatom zone.

5.4 Summary

Diatom analysis of a long section of the I-284 core from Lake Ioannina has revealed a dominance of planktonic taxa, indicating that a relatively deep lake persisted throughout most of the time period spanning the glacial–interglacial cycles equivalent to MIS 7–9. Previous investigations of diatom responses to changing environmental conditions during more recent climatic cycles have revealed that shifts in the diatom assemblage primarily reflect changing lake levels rather than nutrient-driven productivity shifts. Whilst this still holds true for MIS 7–9, the persistence of a deep lake with only subtle variations in lake level unveils diatom responses to changes in mixing regime.

IDZ 1
282.82–279.22 m
Older than 262 ka, probably MIS 9c or 9b

Deep and oligotrophic.

IDZ 2
279.22–275.22 m
Older than 262 ka, probably MIS 9b

Moderate lake levels. Increased lake mixing.
Evidence for slight nutrient enrichment. Low
within-lake and catchment productivity.

IDZ 3
275.22–258.42 m
Older than 262 ka, probably MIS 9b to 9a

Lake levels increase whilst productivity
remains low. Deep, oligotrophic conditions
then resume before productivity increases
abruptly.

IDZ 4
258.42–253.62 m
Older than 262 ka, probably late MIS 9a to
early MIS 8

Moderate lake levels. Oligotrophic, clear and
stratified water column.

IDZ 5
253.62–233.62 m
Older than 262 ka, early MIS 8

Moderate lake levels. Oligotrophic, clear and
stratified water column. Increased detrital
input from an unstable catchment leads to a
slight increase in productivity towards the top
of the zone.

Figure 5.4: Schematic diagrams illustrating the reconstructed palaeoenvironmental conditions at Lake Ioannina during each diatom zone. Core depths, estimated ages and written summaries are also provided.

IDZ 6
233.62–215.22 m
Base just older than 262 ka, top just younger than 262 ka, mid. MIS 8

Deep, productive lake. Stratified water column but increased mixing towards the top of the zone, coinciding with increased catchment erosion and detrital input.

IDZ 7
215.22–199.22 m
Base just younger than 262 ka, top c. 246 ka, late MIS 8

High lake levels with enhanced water column mixing. Slight increase in nutrient availability due to release from the lake sediments under increased mixing and/or delivery of detrital material from the catchment.

IDZ 8
199.22–190.42 m
c. 246–240 ka, late MIS 8 to 7e

High lake levels with a stable, stratified water column. A large, marked increase in within-lake productivity coincides with the onset of Zitsa I and appears unrelated to lake level or nutrient shifts. It could reflect a direct response to warming in a lake that is already deep and stratified.

IDZ 9
190.42–177.62 m
c. 240–237 ka, mid. MIS 7e to early 7d

Deep, oligotrophic conditions. High within-lake productivity, which decreases in a stepwise manner across the zone.

IDZ 10
177.62–163.22 m
c.237–217 ka, MIS 7d

Enhanced nutrient availability. Large fluctuations in lake level. Poor preservation could indicate high energy environment (i.e. turbulent mixing).

Figure 5.4 (continued)

IDZ 11
163.22–156.02 m
c. 217–210 ka, early MIS 7c

Deep, oligotrophic conditions resume. Within-lake productivity increases in line with catchment productivity. Increased water mixing and/or shallowing across the zone.

IDZ 12a
156.02–144.02 m
c. 210–195 ka, late MIS 7c, MIS 7b and MIS 7a

Deep, oligotrophic conditions resume. The water column continues to be well mixed. Low within-lake productivity increases at the top of the zone during the Zitsa III forested interval.
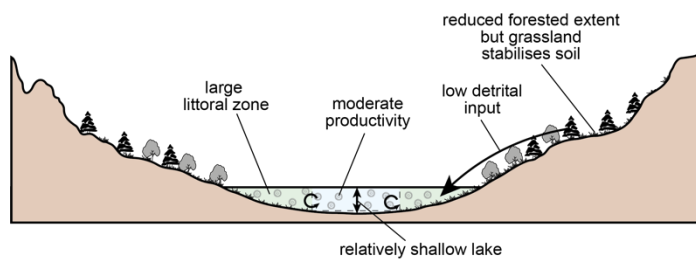
IDZ 12b
144.02–140.82 m
c. 195–194 ka, early MIS 6

Low lake levels and within-lake productivity. Clear waters with low detrital input.
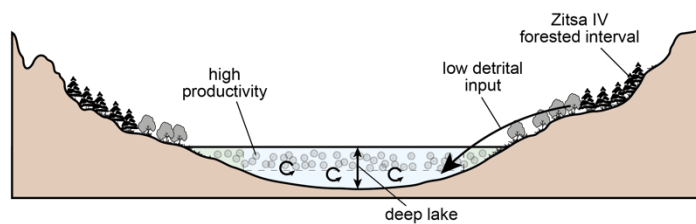
IDZ 12c
140.82–138.02 m
c. 194–191 ka, early MIS 6

Brief return to high lake levels and productivity before returning to shallower conditions at the top of the record.

Figure 5.4 (continued)

Chapter 6 | Lake Ohrid results

This chapter presents the new diatom record for the DEEP core from Lake Ohrid spanning MIS 7. After the description of the diatom results, existing pollen and geochemical data from the DEEP core are presented alongside the new diatom record. These data are then used to aid the interpretation of the diatom response and the reconstruction of palaeoenvironmental change at Lake Ohrid during MIS 7.

6.1 Results

A total of 80 samples were counted at 32 cm intervals between depths of 105.71 m and 80.42 m in the DEEP core, a section spanning 25.29 m. This provides a c. 56 kyr-long record spanning 241.3–185.5 ka and with a mean temporal resolution of approximately 700 years. A minimum count of 300 diatom valves was achieved for all samples.

In total, 100 diatom taxa (9 planktonic, 3 facultative planktonic and 88 benthic) were identified within this section of the DEEP core. Four diatom assemblage zones, here termed Ohrid diatom zones (ODZs), can be recognised from the CONISS cluster analysis (Appendix D). ODZ 3 has been further split into subzones, which have not been identified as significant, in order to aid description. The diatom assemblage of each zone is displayed on Figure 6.1 and described in Table 6.1.

Despite their low diversity, planktonic taxa dominate the assemblage, comprising 96.6% of all valves counted. The most abundant are *Cyclotella fottii* var. 1, *Pantocsekiella ocellata* and *Pantocsekiella minuscula*. *Cyclotella cavitata* is also abundant but only at the base of the record. It is absent from the record above a depth of c. 96 m. Diatom concentration is high, with all samples containing more than 10×10^7 valves per gram of dry sediment. Note that
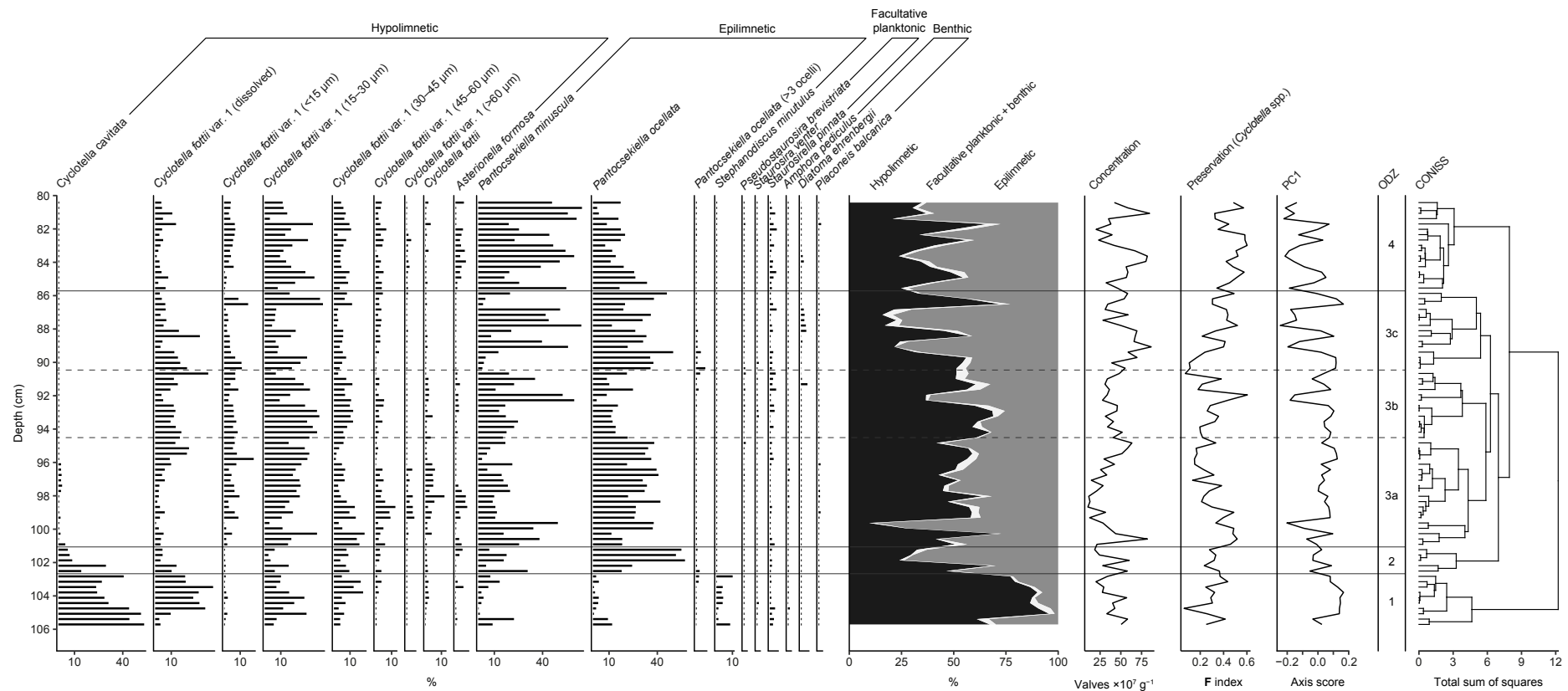
Figure 6.1: Summary diatom stratigraphy of the DEEP core displayed as percentage relative abundances by depth. Only taxa present at ≥1% in at least one sample are displayed. The diatom taxa are grouped by life mode with the planktonic taxa further categorised according to water depth. Diatom concentration is displayed as the total number of diatom valves present per gram of dry sediment. Diatom preservation is represented by the **F** index of *Cyclotella* spp. (*C. cavitata*, *C. fottii* and *C. fottii* var. 1) valves. Axis scores of the first principal component (PC1) are also displayed. The record is split into 4 Ohrid diatom zones (ODZ), and the results of the CONISS cluster analysis are displayed.

Table 6.1: Summary of the diatom results for the Lake Ohrid DEEP core.

Zone	Depth (m)	Age (ka)	Description of diatom results
ODZ 1	105.7–102.7	241.3–234.9	Hypolimnetic taxa dominate (c. 57% to 96%), with *Cyclotella fottii* var. 1 and *Cyclotella cavitata* the most abundant. This zone is also characterised by the presence of mesotrophic *Stephanodiscus minutulus* at up to 10% abundance.
			Concentration is moderately high and variable, exhibiting a downward trend from the base to the top of zone.
			Preservation is moderate, although a single sample has a very low **F** index of 0.06, the lowest of the record.
			PC1 axis scores are the highest of the record and track the high abundance of hypolimnetic taxa.
ODZ 2	102.7–101.1	234.9–231.4	ODZ 2 is characterised by an increase in epilimnetic taxa from ODZ 1, particularly *P. ocellata*, which reaches almost 58% abundance by the middle of the zone. *C. cavitata* exhibits a declining trend and is present at only 6% abundance by the top of the zone.
			Concentration is moderate but variable and declines to relatively low values towards the top of the zone ($<25 \times 10^7\,\text{g}^{-1}$).
			Preservation remains similar to that of ODZ 1.
			PC1 axis scores exhibit moderate values and continue to exhibit a similar trend to the hypolimnetic abundance.
ODZ 3a	101.1–94.7	231.4–212.7	ODZ 3a is characterised by almost equal abundances of hypolimnetic and epilimnetic taxa. Hypolimnetic taxa briefly recover in abundance at the base of the zone before becoming established at around 50% abundance by 99.3 m (c. 228 ka), around the same point that there is a slight increase in the abundance of facultative planktonic and benthic taxa. *C. fottii* var. 1 is the dominant hypolimnetic taxon with the last appearance of *C. cavitata* occurring in this zone. *Asterionella formosa*, which had been present at low abundances (<8%) for most of the record so far, is not recorded in the upper third of ODZ 3a. *P. minuscula* reaches almost 50% abundance in the lower half of the zone, although declines shortly afterwards, and *P. ocellata* becomes the dominant epilimnetic taxon.
			Following an early peak of 82×10^7 valves g^{-1}, the diatom concentration declines to its lowest values of the record before increasing towards the top of the zone.
			Although the **F** index increases at the ODZ 2–3 boundary, it declines across ODZ 3a.
			PC1 axis scores remain moderate and continue to track hypolimnetic abundance, although they display relatively subdued variations in comparison.
ODZ 3b	94.7–90.5	212.7–202.2	ODZ 3b is characterised by reduced abundances of *P. ocellata*. *A. formosa* returns for the duration of the zone. Hypolimnetic abundances reach slightly higher values than in ODZ 3a, but not as high as in ODZ 1. There is a minor reversal in hypolimnetic abundance in the centre of the zone as a result of increased abundances of *P. minuscula*.

			Diatom concentration is slightly lower that the peak at the end of ODZ 3a.
			Preservation increases and peaks in the middle of the zone, coinciding with the reduced ratio of hypolimnetic to epilimnetic taxa. The **F** index declines to very low values by the top of the zone.
			PC1 axis scores remain moderate but do capture the marked decline hypolimnetic abundance in the middle of the zone.
ODZ 3c	90.5–85.7	202.2–193.7	There is an expansion of epilimnetic taxa in ODZ 3c, although this is punctuated rapid fluctuations in the ratio of hypolimnetic to epilimnetic taxa, which start in ODZ 3c and continue to the end of the record. *A. formosa* is once again almost disappears from the record for the duration of this zone.
			Concentration is high, rising to the record peak of 87×10^7 valves g^{-1} at 89.1 m (c. 200 ka).
			The preservation improves across the zone with the **F** index increasing to over 0.5.
			PC1 scores fluctuate markedly, reflecting the rapid fluctuations in the hypolimnetic to epilimnetic ratio.
ODZ 4	85.7–80.4	193.7–185.5	ODZ 4 is characterised by rapid fluctuations between the hypolimnetic and epilimnetic taxa that began in ODZ 3c. These fluctuations are primarily between *C. fottii* var. 1 and *P. minuscula*. *P. ocellata* declines in abundance and *A. formosa* returns.
			Diatom concentration is high in the lower half of the zone but does decline in the upper half.
			Preservation is relatively high for the duration of the zone.
			PC1 continues to reflect the rapid fluctuations in the ratio of hypolimnetic to epilimnetic valves.

concentrations are presented as $\times\,10^7$ to maintain consistency with the other intervals from Lake Ohrid and aid comparison. Preservation is moderate and variable throughout, the **F** index of *Cyclotella* spp. (representing the proportion of their valves unaffected by dissolution) ranging between 0.06 and 0.60 (M = 0.34, SD = 0.13). At 1.96 SD units, the length of the longest DCA axis indicated that PCA was appropriate (Appendix D). PC1 explains 51% of the total variation in the record and reflects the ratio of hypolimnetic to epilimnetic taxa. PC1 values become more variable in the top half of the record.

6.2 Previously published data

The diatom record is compared with previously published pollen and sedimentological data from the DEEP core to strengthen the diatom interpretation. These data are presented in Figure 6.2.

Pollen

Pollen data are available at a 64 cm resolution (c. 1400-year temporal resolution) and are displayed as the percentage of arboreal pollen minus *Pinus* (Sadori et al., 2016). The pollen record reflects three forest expansions during MIS 7 (c. 245, 217 and 204 ka), although this record commences after the first forest expansion once AP has increased to high percentages. Changes in the ratio of hypolimnetic to epilimnetic planktonic taxa, which is primarily a result of variations in the relative abundance of *Cyclotella fottii* var. 1 during this part of the Ohrid record, broadly track variations in AP. The hypolimnetic taxa are at higher abundances when AP is higher. This is evident in both long-term trends and on shorter timescales. This demonstrates that hypolimnetic productivity varies with catchment productivity.

Biogenic silica content

The percentage of biogenic silica (bSi) is available at a 32 cm resolution (c. 700-year temporal resolution; Francke et al., 2016), which is the same as that of the
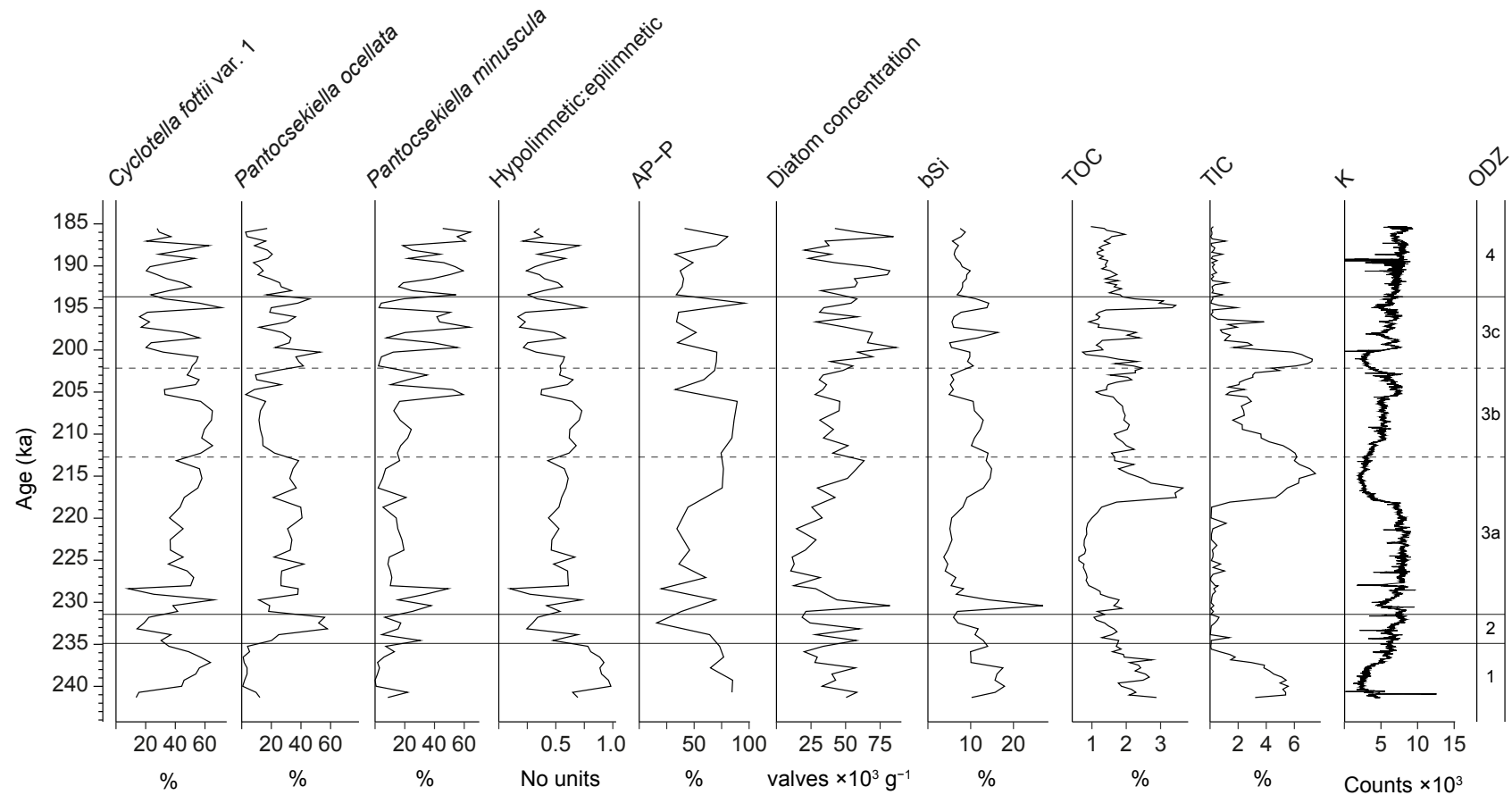
Figure 6.2: Comparison of Lake Ohrid diatom data from MIS 7 with existing data from the DEEP core. The new diatom data include the relative abundances of selected diatom taxa, a summary of the planktonic assemblage as the ratio of hypolimnetic to epilimnetic taxa and the diatom concentration. Previously published data include the percentage of arboreal pollen minus *Pinus* (AP; Sadori et al., 2016) and sedimentological data, including the biogenic silica content (bSi), total organic carbon (TOC) content, total inorganic carbon (TIC) content and K intensity (Francke et al., 2016).

new diatom record. It reflects the proportion of the sediment that is composed of diatom frustules, although sponge spicules can also contribute to the bSi content (Vogel et al., 2010). Therefore, bSi content should closely match the diatom concentration. This is the case in the lower part of the record.; the diatom concentration exhibits the same general pattern as bSi throughout ODZ 1–3b, although the diatom concentration exhibits more variability from one sample to the next than bSi does. The synchronicity of the bSi and diatom concentration records breaks down in ODZ 3c and ODZ 4. This is probably due to the large fluctuations that occur throughout these diatom zones in the relative abundances of two taxa that have very different valve sizes (*Pantocsekiella minuscula*, with valve sizes of c. 4–7 µm, and *C. fottii* var. 1, which exhibits valve sizes of up to 80 µm).

Carbon content

The total organic carbon (TOC) content and total inorganic carbon (TIC) content are also available at a 32 cm resolution (Francke et al., 2016). The TOC content reflects the amount of finely dispersed organic matter, which is an indicator of the primary productivity of the lake. The TIC content tends to consist of calcite during intervals with high TIC (interglacials and interstadials) and siderite during intervals with low TIC (glacials and stadials; Lacey et al., 2016). As the precipitation of calcite is believed to be associated with increased temperatures and the photosynthetic removal of CO_2 within the epilimnion, this has been used as a proxy for temperature-induced productivity at Lake Ohrid (Zhang et al., 2016). Three distinct periods of TIC are evident and occur just after each forest expansion episode mentioned above. TOC exhibits a similar pattern, but it is more variable with more frequent, higher-amplitude peaks towards the top of the record than in the TIC content.

Potassium intensities

Potassium (K) intensities obtained from high-resolution XRF scanning are also provided and can vary as a result of changes in catchment erosion (Francke et

al., 2016). For this reason, it has been used as an indicator for changes in catchment dynamics during previous diatom analyses at Ohrid (e.g. Cvetkoska et al., 2016; Zhang et al., 2016). K intensities exhibit an increasing trend from the base to the top of the record, with a major reduction occurring after each forest expansion episode.

6.3 Interpretations

The dominance of planktonic taxa, but high diversity of benthic taxa, is consistent with other records from Lake Ohrid and is explained by the great water depth at the coring site (243 m); the bottom of the lake where benthic taxa would reside is far below the optimal depth for diatoms (Cvetkoska et al., 2016). Any facultative planktonic or benthic taxa present at the DEEP site would have been transported from the lake margin, and for this reason, their presence at the DEEP site has been interpreted as an indicator of the intensity of lake circulation (Zhang et al., 2016). As with other lakes like Ioannina, small Fragilariaceae are also considered an indicator of cold water and winter lake ice cover at Ohrid.

The main shifts in the diatom record occur between three planktonic taxa: *Cyclotella fottii* var. 1, which differs from *Cyclotella fottii* sensu stricto by its more elliptical to rhombic valve outline, *Pantocsekiella ocellata* and *Pantocsekiella minuscula*. Preliminary diatom data generated from core catcher samples during the Lake Ohrid drilling campaign indicated clear shifts in the dominant planktonic taxa occurred on orbital timescales, although the responses were complex and varied between different parts of the core (Wagner et al., 2014; Zhang, 2015). During the most recent climatic cycles (MIS 1–6), hypolimnetic taxa tend to dominate in the glacial phases with epilimnetic taxa dominating during the interglacials (Reed et al., 2010; Cvetkoska et al., 2016). The opposite response was noted for the interval under investigation here (Wagner et al., 2014; Zhang, 2015). The new diatom record is

in agreement with these initial observations from the low-resolution core catcher data. Hypolimnetic taxa are more abundant during intervals with higher AP and hence more interglacial-like conditions, whilst epilimnetic taxa are more abundant during forest contractions associated with stadials and the start of the penultimate glacial towards the top of the record. However, despite general trends being evident, Zhang et al. (2016) demonstrated that the diatom response is not always a linear response to temperature. Studies on the present-day Lake Ohrid have indicated that whilst temperature is the primary control on the vertical distribution of diatom taxa in the lake, other contributors include water mixing and the availability of nutrients and light (Stanković, 1960; Allen & Ocevski, 1976). These factors were also implicated in indirect diatom responses to temperature change during the late glacial and Holocene (Zhang et al., 2016).

Two of the very abundant taxa in this interval (*C. fottii* var. 1 and *C. cavitata*) are endemic, fossil taxa. As noted in section 2.2.4, this is one of the difficulties associated with diatom analyses in ancient lakes. They are inferred to be hypolimnetic based on their morphological similarities with *Cyclotella fottii* sensu stricto. However, many aspects of their ecology might differ from the latter, and interpretations must make use of evidence from other proxy indicators. Based on the very clear association between AP and the relative abundance of hypolimnetic taxa, particularly *C. fottii* var. 1, the diatoms exhibit a strong response to temperature. The diatom response is now explored further throughout MIS 7.

6.3.1 MIS 7e (c. 242–235 ka; ODZ 1)

High abundances of *Cyclotella cavitata* and *C. fottii* var. 1 are present at the start of the record, which coincides with the start of MIS 7e and high AP. As the latter is suggestive of warm temperatures, the dominance of hypolimnetic taxa could be due to strong thermal stratification, which would reduce the mixing-induced, upward nutrient supply into the epilimnion and limit the abundance

of epilimnetic *P. ocellata,* which is usually indicative of increased nutrient availability in this oligotrophic lake. The high AP indicates a forested and stable catchment, which is supported by low K intensities, and suggests low erosion-induced nutrient delivery from the catchment. It is worth noting that the sample with a low **F** index does not exhibit a decline in *Cyclotella* spp., indicating that the reduction in preservation has not affected the integrity of the record.

6.3.2 MIS 7d (c. 235–218 ka; ODZ 2 to mid ODZ 3a)

The increase in the abundance of *P. ocellata* at the start of MIS 7d coinsides with a marked reduction in AP. *P. ocellata* occupies the epilimnion at Lake Ohrid and in the more recent climatic cycles, it is usually associated with enhanced temperature-driven productivity in the epilimnion (Reed et al., 2010). However, its increase in abundance here, during a cooler period with reduced forest extent, could represent a similar situation to that in the Holocene, when its populations unexpectedly expanded during the thermal decline of the 8.2 ka event (Zhang et al., 2016). Its increase in abundance could be due to enhanced nutrient availability in the epilimnion. This is possibly due to increased erosion-induced nutrient delivery from the less stable catchment following the forest contraction suggested by declining AP. However K intensities don't increase much at this time. Another possibility is increased nutrient redistribution from the hypolimnion, which would be expected as a result of weaker stratification and increased water mixing expected under declining temperatures.

A brief increase in the abundance of hypolimnetic *C. fottii* var. 1 occurs in the middle of ODZ 7d and possibly suggests another period of strengthened thermal stratification. It is associated with an increase in AP, which suggests warmer conditions. There is subsequently a marked increase in epilimnetic taxa, particularly of *P. minuscula*. Again, this is associated with a reduction in AP and could reflect enhanced nutrient delivery to the epilimnion from the

catchment and redistribution from the hypolimnion. The higher abundance of *P. minuscula* than *P. ocellata* is probably related to its ability to tolerate unstable environments with high detrital input and low light availability (see entry for *P. minuscula* in Table 2.1). It suggests this second cold period at 228 ka might have been more extreme than the first at ca 232 ka.

After 228 ka, there is a marked recovery in the abundance of hypolimnetic *C. fottii* var. 1, which is accompanied by moderate abundances of *P. ocellata*, and AP recovers from the earlier low values but remains below 50% up to 218 ka. The balance between the relative abundances of *C. fottii* var. 1 and *P. ocellata* reflects cooler conditions than MIS 7e with weaker stratification and the higher detrital input of nutrients, as indicated by the higher K intensities during MIS 7d than MIS 7e.

6.3.3 MIS 7c to MIS 7a (c. 218–194 ka; mid ODZ 3a to ODZ 3c)

The start of MIS 7c is remarkably subtle in the diatom assemblage. There is a very small increase in the abundance of *C. fottii* var. 1 and a loss of their largest valves (>60 µm). This coincides with increasing AP and bSi, as well as marked increases in both TOC and TIC, all of which point to increasing catchment and within-lake productivity. A marked decline in *P. ocellata* at c. 212 ka is associated with minor increases in both *C. fottii* var. 1 and *P. minuscula* as well as slight reductions in diatom concentration and bSi. This could reflect enhanced thermal stratification with reduced nutrient availability in the epilimnion. AP reaches high values and indicates some of the warmest conditions probably persisted at this time.

The highest *C. fottii* var. 1 abundances coincide with the highest AP at around 207 ka. This is followed by a large expansion of *P. minuscula* at c. 205 ka, which probably represents a minor response to MIS 7b. This is associated with a forest contraction and reduced bSi, indicating both within-lake and catchment productivity declined at this time. K intensities indicate enhanced detrital input associated with the less stable catchment.

The recovery in *C. fottii* var. 1 abundances at c. 204 ka represents the start of MIS 7a and coincides with the forest expansion indicated by increasing AP. Both indicators exhibit lower percentages than the peak values at the end of MIS 7c, suggesting cooler conditions during MIS 7a than MIS 7c. At 202 ka, the abundance of *P. ocellata* increases, coinciding with a slight increase in bSi and a large increase in TIC, indicating enhanced epilimnetic productivity. This marks the start of large fluctuations in the relative abundances of hypolimnetic versus epilimnetic taxa, primarily between *C. fottii* var. 1 and *P. minuscula.* This indicates unstable conditions and large temperature fluctuations, some of which are also associated with changes in AP.

6.3.4 MIS 6 (c. 294–185 ka; ODZ 4)

The large fluctuations between *C. fottii* var. 1 and *P. minuscula* continue from the end of MIS 7a into MIS 6, reflecting catchment and thermal instability at the onset of the penultimate glacial. Low bSi, TOC and TIC all indicate low productivity.

6.3.5 Palaeoenvironmental summary

The palaeoenvironmental interpretations are summarised in Figure 6.3 alongside a series of schematic diagrams that illustrate the changing palaeoenvironmental conditions at Lake Ohrid during the substages of MIS 7.

6.4 Summary

High-resolution diatom analysis of the DEEP core from Lake Ohrid has revealed an indirect temperature-driven diatom response during MIS 7. This response is probably related to changes in the intensity of lake stratification and variations in detrital input, which control nutrient availability in the epilimnion.
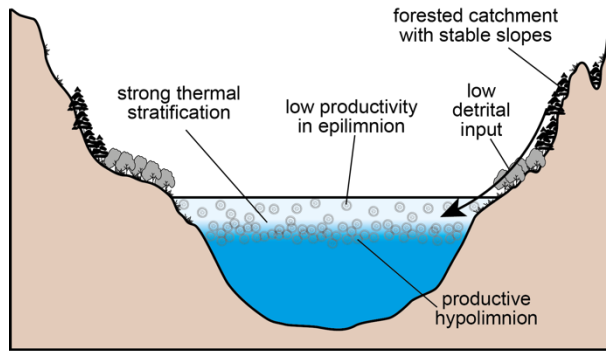
MIS 7e
c. 242–235 ka
ODZ 1

Strong thermal stratification limits upward transport of nutrients from the hypolimnion into the epilimnion. Well-vegetated catchment stabilises slopes and limits nutrient delivery from the catchment to the epilimnion.
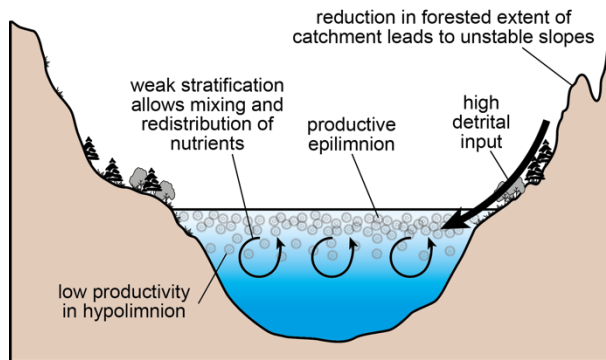
MIS 7d
c. 235–218 ka
ODZ 2 to mid ODZ 3a

Reduced forested extent leads to unstable slopes with increased detrital input and nutrient delivery to the epilimnion. Weak stratification allows more frequent mixing and the redistribution of nutrients from the hypolimnion into the epilimnion.
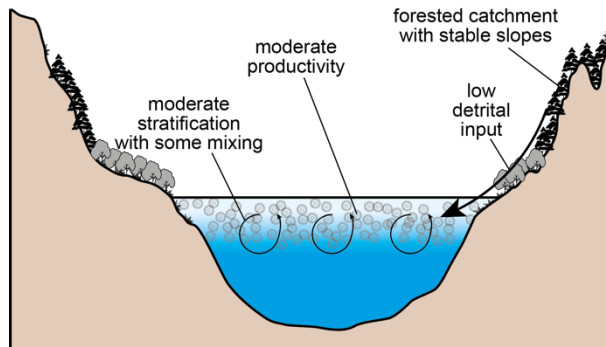
MIS 7c–7a
c. 218–194 ka
Mid ODZ 3a to ODZ 3c

Forest expansion following the contraction of MIS 7d. Slopes stabilise and detrital input reduces. Moderate productivity that is equal throughout the epilimnion and hypolimnion. Stratification is moderate but weakens at times, particularly during MIS 7b.
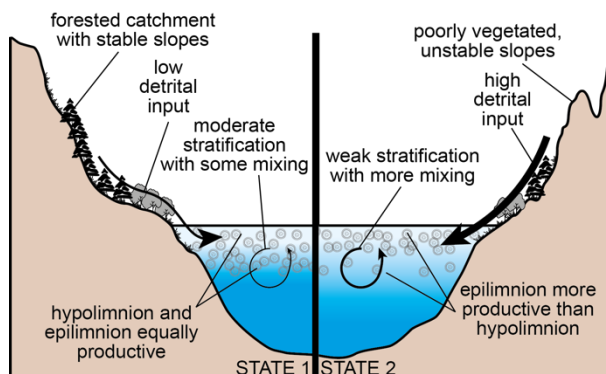
MIS 6
c. 294–185 ka
ODZ 4

Low productivity throughout. Unstable conditions. Alternates between a more stratified state with low detrital input and a more mixed state with high detrital input.

Figure 6.3: Schematic diagrams illustrating the reconstructed palaeoenvironmental conditions at Lake Ohrid during each substage of MIS 7 and the start of MIS 6. Age ranges and written summaries are also provided.

Chapter 7 | Discussion

This thesis has set out to achieve two aims. The first (to improve our understanding of how diatom communities respond to changing environmental conditions in Lake Ioannina and Lake Ohrid) has been addressed within the two preceding chapters. Attention is now turned to the second aim of this thesis. The palaeoenvironmental reconstructions generated in Chapter 5 and Chapter 6 are considered alongside other records to improve our understanding of palaeoclimatic change in the northeastern Mediterranean during the glacial–interglacial cycles equivalent to MIS 7–9.

7.1 Chronological control at Lake Ioannina

In order to compare high resolution palaeoenvironmental records between different depositional systems, robust age controls are required. As detailed in section 4.1.1 and Chapter 5, the published pollen data and associated age model for Lake Ioannina do not currently extend to the base of the new I-284 diatom record presented in Chapter 5. This is most clearly evident in Figure 5.3. Despite this, some initial palaeoclimate interpretations can still be made from the palaeoenvironmental reconstruction. It is also possible to make some broad comparisons between the Lake Ioannina record and other palaeoclimate records by using the limited chronological data that are currently available (detailed in section 4.1.1) and through a comparison with the well dated Lake Ohrid record (section 4.1.2).

Between c. 265 m and c. 190 m, the diatom concentration of Lake Ioannina broadly tracks the biogenic silica (bSi) percentage of Lake Ohrid over c. 290–240 ka (Figure 7.1). Some distinct peaks and dips are observed in both, including the marked decline and subsequent increase around the Ioannina 262 ka age tie point. Although bSi content and diatom concentration are affected by various processes such as sedimentation rate and dissolution, the
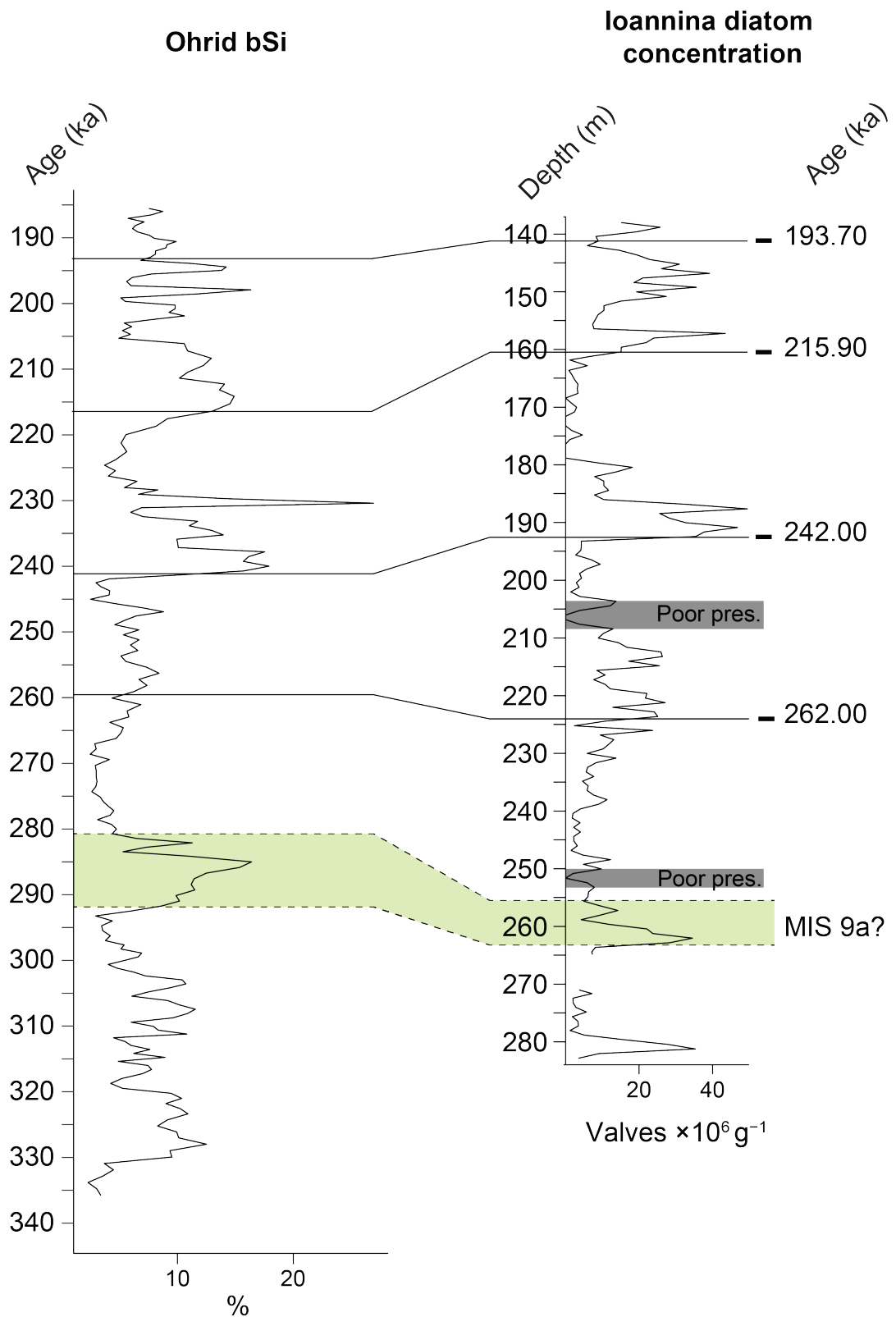
Figure 7.1: Comparison of the diatom concentration of the Lake Ioannina I-284 core with the bSi content of the Lake Ohrid DEEP core (Francke et al., 2016). The solid lines indicate age tie points from the Ioannina MIS 7 age model (Table 4.1; Roucoux et al., 2008). The dotted line indicates the hypothesised match in diatom productivity during MIS 9a.

broad correspondence means that it is with reasonable confidence that the peak in diatom concentration in the Lake Ioannina record at c. 263 m corresponds to a peak in bSi content exhibited in Lake Ohrid during MIS 9a at c. 285 ka.

Although this approach is far from ideal, it provides a tentative age control for the lower part of the new Ioannina diatom record to enable broad, initial palaeoclimate interpretations to be examined within the context of existing palaeoclimate records from other archives. The extended pollen record and astronomically tuned age model covering the base of the I-284 core is eagerly anticipated and will allow more detailed analyses of the diatom data. Recent chronostratigraphic advances at Ioannina provide the exciting possibility of being able to further improve the age control of the sediments from this lake and evaluate uncertainties related to sediment reworking. Although tephra layers were not originally identified in the I-284 core (4.1.1), developments over the last couple of decades have enabled the processing of smaller glass shards of volcanic origin (cryptotephras; Blockley et al., 2005). These have been identified in another core from Lake Ioannina (I–08) and used to constrain changes during the last glacial (McGuire et al., 2022).

7.2 Northeastern Mediterranean palaeoclimate during MIS 7–9

The following subsections consider the results and interpretations of the Lake Ioannina diatom record (Chapter 5) for each MIS in the context of other records. For MIS 7, where the diatom record has been produced for Lake Ohrid (Chapter 6), the subsection is further divided based on marine isotope substages, and comparisons are made between the records from the contrasting lakes.

7.2.1 MIS 9

Although the highest Antarctic surface air temperatures, CO_2 concentrations and CH_4 concentrations of the last 800 kyr occurred within MIS 9e (Past Interglacials Working Group of PAGES, 2016), MIS 9 in the northeastern Mediterranean was cooler than the preceding interglacial (MIS 11) and relatively wet (Francke et al., 2016; Lacey et al., 2016). One way in which the northeastern Mediterranean records do agree with Antarctic records is their structure. They exhibit the tripartite structure that is evident in many ice and marine records during MIS 9 (Lang & Wolff, 2011). Following the peak interglacial conditions of MIS 9e, the region experienced colder and drier conditions during the stadial of MIS 9d, warmer and wetter conditions during the MIS 9c interstadial, colder and drier conditions during the MIS 9b stadial, and warmer and wetter conditions once more during the MIS 9a interstadial (Fletcher et al., 2013; Lacey et al., 2016).

Stable isotope data from Lake Ohrid indicate that the onset of full interglacial conditions during MIS 9e was relatively rapid (Lacey et al., 2016), which is consistent with warming at the start of MIS 9 reflected in pollen records from Tenaghi Philippon in northeastern Greece (Tzedakis et al., 2006). The stable isotope data also indicate that peak interglacial conditions on the Balkan Peninsula were reached c. 327 ka during MIS 9e (Lacey et al., 2016). This is corroborated by pollen data from Lake Ohrid, with high arboreal pollen percentages (>90%) reached at around the same time (Sadori et al., 2016). The interglacial peak at Ohrid is short-lived (c. 3.7 ka; Lacey et al., 2016), which is in agreement with observations of a short interglacial peak in Antarctica (Past Interglacials Working Group of PAGES, 2016). This early interglacial part of MIS 9 is not present in the Lake Ioannina diatom record. Based on the organic content, carbonate content and diatom concentration (Figure 7.1), the base of the new Lake Ioannina diatom record presented in Chapter 6 probably corresponds to the end of MIS 9c or an interstadial of MIS 9b. Either way, it falls under the antepenultimate glacial period, the inception of which occurred

at the MIS 9e–9d boundary at c. 320 ka (Hughes et al., 2020). A speleothem recovered from an unsurveyed cave located at an altitude of c. 1130 m within hills c. 16 km to the northeast of Lake Ohrid (stalagmite OH2) corroborates this timing of the glacial inception, recording decreased precipitation in the northeastern Mediterranean from c. 321 ka (Regattieri et al., 2018).

IDZ 2 is probably equivalent to the stadial of MIS 9b. The interpretation of a relatively shallow, well-mixed water column indicates that dry conditions persisted at Ioannina, and the slight nutrient-enrichment suggests the increased delivery of detrital material from an unstable catchment. This is consistent with records from Lake Ohrid, where multiple proxies (e.g. the presence of siderite, low total inorganic carbonate, low biogenic silica and low AP) indicate low catchment and within-lake productivity and an extended period of cold and dry conditions (Francke et al., 2016; Lacey et al., 2016; Sadori et al., 2016). These cold and dry conditions are widespread. A brief, moderate incursion of polar waters at the Portuguese margin and a pronounced tree population collapse in southwest Portugal are indicative of cooler and drier conditions extending to the Atlantic (Roucoux et al., 2006).

The interval spanning IDZ 1 to just after the start of IDZ 3 exhibits rapid fluctuations in planktonic abundance, including two peaks centred on 278 m and 275 m. As these marked changes occur from one sample to the next, a higher resolution is required to resolve them. However, they could represent rapid lake level fluctuations similar to those observed at Ioannina during MIS 6, which have been attributed to changing conditions in the North Atlantic (Wilson et al., 2021). Comparisons have been drawn between millennial-scale variability during the interval spanning c. 310–290 ka and the D–O variability of MIS 3 (Siddall et al., 2007). Records from the Iberian margin justify this comparison with millennial-scale variability detected in SSTs (Martrat et al., 2007) and terrestrial vegetation (Desprat et al., 2009). Furthermore, rapid oscillations are evident in the stable isotope record of Lake Ohrid towards the end of MIS 9c (c. 310 ka; Lacey et al., 2016). However, in the northeastern

Mediterranean, a high-resolution pollen record from Tenaghi Philippon reveals a series of long interstadials rather than clusters of millennial-scale events (Fletcher et al., 2013). As diatoms respond more rapidly to climate and demonstrate more sensitivity than vegetation (Wilson et al., 2013), the fluctuations in the Ioannina diatom record could represent the more rapid fluctuations that were hypothesised for this interval and warrant further investigation.

The higher lake levels inferred for IDZ 3 indicate wetter conditions and are probably equivalent to the interstadial of MIS 9a. At Ioannina, lake levels were high prior to the marked productivity increase, suggesting wet conditions prevailed before warming. Planktonic abundances reach their second highest value of the entire record during this interval (94.5%). However, some records in the northeastern Mediterranean point towards MIS 9a being relatively dry. The OH2 speleothem from near Lake Ohrid stopped growing just prior to the start of this interstadial (Regattieri et al., 2018), and the Lake Ohrid pollen record indicates the presence of semi-deciduous *Quercus cerris* type forests during substage 9a, as opposed to deciduous *Quercus rober* type forests in MIS 9c and 9e, suggesting drier conditions than those earlier substages (Sadori et al., 2016). However, stable isotope records from Lake Ohrid demonstrate a fresh lake system with a high P–E ratio (Lacey et al., 2016) and the deposition of sapropel *S'* in the Mediterranean Sea suggests enhanced precipitation (Ziegler et al., 2010). Lacey (2016) attributed the discrepancy between the dryness indicated by the vegetation and the wet conditions indicated by the isotopes at Ohrid to a strong seasonality in precipitation whereby the peak summer insolation drives summer dryness, but there is enhanced winter precipitation. The diatom results from Ioannina corroborate these existing data from Ohrid and provide further evidence for wet winters in the northeastern Mediterranean during MIS 9a. These wet winters were probably the result of a dominance of negative NAO phases. Low pressure contrasts in the North Atlantic would have resulted in the southwards shift of the mid-latitude westerlies, increasing precipitation

in the Mediterranean and leading to dry conditions in northern Europe (section 3.1.2). Further supporting this interpretation is evidence for dry conditions in the Western Carpathians (north of the study region) during MIS 9a (Błaszczyk & Hercman, 2022).

7.2.2 MIS 8

MIS 8 has been identified as a relatively weak glacial period based on ice and marine records (Lang & Wolff, 2011; see section 2.1.3). Existing records from the northeastern Mediterranean also reflect the weak nature of this glacial. In the Ohrid record, MIS 8 is somewhat warmer than many other glacials, occasionally exhibiting interglacial-like conditions (Francke et al., 2016). The moderate lake levels inferred from the Lake Ioannina diatom record in the early part of MIS 8 (c. 255–240 m core depth, IDZ 4–5) suggest drier conditions than during the preceding interstadial of MIS 9a. This is in agreement with regional and some global records. Most marine isotope records suggest that the largest ice volumes of the antepenultimate glacial occur towards the end of MIS 8 (Hughes & Gibbard, 2018). However, in Antarctic records, the strongest glacial values in MIS 8 are found early in the interval (c. 270 ka) as opposed to just prior to the termination; the latter is the more usual pattern for the climatic-cycles of the last c. 450 kyr (Lang & Wolff, 2011). Dust flux over Antarctica, indicating dry conditions, was particularly high during MIS 8 and peaked at c. 272 ka (Lambert et al., 2012). At Tenaghi Philippon, early MIS 8 (c. 277–265 ka) is associated with intense cold and dry conditions (Fletcher et al., 2013). While at the Portuguese margin, the lowest SSTs of MIS 7–9 are recorded during this time interval, and pollen from the same record indicates extensive steppe vegetation with reduced tree populations in southwest Portugal (Roucoux et al., 2006).

The diatom assemblage was interpreted as reflecting a stable, stratified lake during this time. This is in stark contrast to the dominance of small Fragilariaceae during the strongest glacial conditions of MIS 6 (Wilson et al.,

2021). The presence of taxa associated with macrophytes and those that grow as branched colonies indicates a longer ice-free period and warmer summer growing season than assemblages dominated by adnate taxa (Douglas & Smol, 2010). Their presence at Ioannina during the most extreme glacial conditions of MIS 8 (as suggested by the records discussed above) highlights the relatively weak nature of this glacial in comparison to the last and penultimate glacials. The relatively high and persistent abundance of planktonic taxa through this interval indicates that MIS 8 was wetter than these other glacials. Between depths of c. 240 m and c. 220 m, the increasing planktonic abundance indicates an increase in moisture availability and rising lake levels, which peak just after the age tie point of 262 ka. This is again in agreement with several other records including an increase in pollen-inferred water depth at Tenaghi Philippon c. 265 ka (Fletcher et al., 2013) and an expansion of tree populations in southwest Portugal between c. 265 and 252 ka (Roucoux et al., 2006). The OH2 speleothem from near Lake Ohrid also started to grow again between c. 264 and 248 ka (Regattieri et al., 2018).

Following this wetter interval, conditions at Ioannina deteriorated, with increased detrital input to the lake as well as increased water mixing and/or a slight lake level decrease during IDZ 7. The increased abundance of small Fragilariaceae at Ioannina is indicative of colder, glacial climates and extended seasonal ice cover (Wilson et al., 2021), although they do only form a small proportion of the assemblage. Some marine records indicate that the largest global ice volumes and lowest sea levels occurred during this later stage of MIS 8 (Lisiecki & Raymo, 2005; Shakun et al., 2015). However, based on regional records, it is unexpected that the end of MIS 8 appears to indicate more extensive/longer seasonal ice cover than the early part of MIS 8. These conditions end abruptly with an almost complete loss of small Fragilariaceae from the diatom record at the start of IDZ 8 and very high lake levels just prior to Termination III (TIII). This points to very wet conditions at Ioannina from c. 246 ka, which is in agreement with the onset of speleothem growth at

Spannagel cave in Austria at 247.3 ka (Wendt et al., 2021). Although there is little change in the diatom assemblage, reduced diatom concentrations just prior to TIII coincide with reduced AP and could reflect a minor response to the later of two millennial-scale aridity events (S8.1, 244.7–241 ka) recorded in the western Mediterranean region (Roucoux et al., 2006; Pérez-Mejías et al., 2017).

7.2.3 MIS 7

MIS 7 has been described as a weak interglacial with a strength more comparable to interglacials prior to 450 ka (Lang & Wolff, 2011). It exhibits a bipartite or tripartite structure in many ice and marine records, with the interglacial intervals being assigned the substages 7e, 7c and 7a (see section 2.1.3). This same structure is evident in northeastern Mediterranean records. Warmer and wetter conditions identified from Lake Ohrid stable isotope data correspond to MIS substages 7e, 7c and 7a (Lacey et al., 2016). These substages are also reflected by the presence of forested intervals at Ioannina (Roucoux et al., 2008).

MIS 7e

High diatom-inferred lake levels at Ioannina during the start of MIS 7e (c. 242 ka, IDZ 8) indicate that the wet conditions just prior to TIII persisted into this interglacial. The start of the interglacial is marked by a rapid increase in diatom concentration at Ioannina, which is coincident with the onset of the Zitsa I forested interval (Roucoux et al., 2008). This probably reflects a direct response to warming as the diatoms indicate no change in trophic status and the lake level was already high. The strong thermal stratification inferred from the high abundance of hypolimnetic taxa in Lake Ohrid during ODZ I supports the inference of warm conditions in the northeastern Mediterranean during this time.

The Lake Ioannina diatom record indicates that these very wet conditions at the start of the interglacial were quickly interrupted by a reduction in moisture availability lasting from c. 240 ka to 237 ka. At a depth of 190 m in the I-284 core (c. 240 ka), there is an increase in the abundance of small Fragilariaceae, a marked increase in carbonate content and a change in the pollen assemblage (marking the start of pollen assemblage zone G-8). These three aspects of the Lake Ioannina record all point to reduced moisture availability, an interpretation that is supported by a speleothem record from Ejulve cave (eastern Spain) where increased $\delta^{13}C$ values, which are an indicator of increased aridity, span c. 240.5–239 ka (Pérez-Mejías et al., 2017). This is further supported by stable isotope data from Lake Ohrid, which reflect a drying trend throughout MIS 7e (Lacey et al., 2016).

The Spannagel cave speleothem indicates only a minor temperature decrease at c. 240 ka following peak $\delta^{18}O$ values at 240.5 ±0.3 ka (Wendt et al., 2021). This is perhaps reflected at Lake Ohrid by the very minor reduction in AP during this time. There is also a very slight reduction in the abundance of hypolimnetic taxa, but this is barely discernible and probably within any errors associated with diatom counting. This demonstrates the success of the method of comparing contrasting diatom responses in deep versus shallow lakes and has enabled the identification of a reduction in moisture availability alongside the persistence of warm temperatures.

MIS 7d

During MIS 7d (IDZ 10), the Ioannina diatom record indicates initially wet conditions with high lake levels and moderate productivity spanning c. 186–180 m (c. 237–232 ka). This is followed by a period of extremely low within-lake productivity and poor diatom preservation spanning c. 180–162 m (c. 232–217 ka). The latter could be related to very low lake levels and increased turbulence, as indicated by marked shifts in the diatom assemblage and occasionally low planktonic abundance.

The Ioannina diatom record is in complete agreement with the Ioannina pollen record during this interval. During MIS 7d the pollen record indicates that temperate forests contracted to close to their full glacial extent (Roucoux et al., 2008). The earlier wet interval corresponds exactly with pollen assemblage zone G-7 and the later drier interval corresponds exactly with pollen assemblage zone G-6; the difference between these two pollen zones is a higher abundance of *Artemisia* and *Ephedra* in the latter, indicating drier conditions (Roucoux et al., 2008). What is most interesting about this interval is the very strong response exhibited by the diatoms in contrast to the early part of MIS 8. Whilst this response is expected in MIS 7d, it serves to emphasise the very stable and mild conditions exhibited during the early antepenultimate glacial.

A comparison of the contrasting diatom responses at Ohrid and Ioannina during MIS 7d once again demonstrates the success of this approach in disentangling changes in temperature versus moisture availability. The diatom response at Ohrid indicates that the coldest temperatures of MIS 7d occurred between c. 233 and 228 ka, when the Ioannina record still records relatively high planktonic abundances, indicating the persistence of cold but wet conditions. Between c. 228 and 221 ka (180–167 m depth in the I-284 core) Lake Ioannina records fluctuating lake levels and very poor diatom preservation, indicating a reduction in moisture availability. In contrast, Lake Ohrid records a thermal improvement. MIS 7d is therefore inferred to have been initially cold and wet, then cool and dry.

This interpretation is in agreement with regional records. The Spannagel cave speleothem records an abrupt drop in temperature between 236 and 234.4 (±0.3) ka (Wendt et al., 2021), corresponding to the decline in catchment and within-lake productivity at the start of MIS 7d at Ioannina. Furthermore, Sardinian speleothems indicate the persistence of humid conditions until 230.1 ±1.6 ka (Columbu et al., 2019), corresponding with the inferred wetter interval of MIS 7d at Ioannina. A marked decline in planktonic abundance that suggests a short period of reduced lake level is evident at the

end of IDZ 10 (c. 163 m, 218 ka). This could reflect drier conditions as a result of a major meltwater pulse in the North Atlantic at c. 216.9 ±0.5 ka (Channell et al., 2012; Wendt et al., 2021), which would have reduced the amount of moisture carried by storm tracks into the Mediterranean.

MIS 7c–7a

Very high planktonic abundances in the Ioannina diatom record at 162 m (217 ka) indicate wet conditions immediately prior to the temperate forest expansion of the Zitsa II forested interval. It was suggested that low $\delta^{18}O_{calcite}$ at Lake Ohrid during the onset of MIS 7c was either due to isotopically fresher glacial lake water (as a result of precipitation falling as snow) or a particularly wet climate, with changes in $\delta^{13}C$ possibly indicating the former was more likely (Lacey, 2016). However, the evidence from the Lake Ioannina diatoms supports the inference of very wet conditions at the start of MIS 7c. High lake levels are inferred to have persisted at Ioannina from MIS 7c through to MIS 7a (c. 162–144 m, c. 217–191 ka, IDZ 11–12a) and indicate that wet conditions persisted during the forested intervals of Zitsa II and III. However, the increasing abundance of facultative planktonic taxa suggests drying as the period progressed.

Interestingly, the pattern of fluctuations exhibited by the Ioannina planktonic abundance during MIS 7c–7a is a close match for the pattern exhibited by proxy records from the Portuguese margin (Roucoux et al., 2006). Both sites record four minor but clear peaks within MIS 7c (IDZ 11 and the start of IDZ 12a) before increasing to higher and more stable values for the duration of MIS 7a (c. 202–195 ka, c. 150–144 m depth in the I-284 core, the end of IDZ 12a). Very minor changes in AP–PJB at Ioannina can just about be discerned at some of these intervals, demonstrating the relatively more sensitive response of the diatoms than the catchment. A similar relationship is also exhibited at the subsequent glacial inception (Wilson et al., 2013). The minor fluctuations in lake level at Ioannina are probably a result of regional climatic variations that

were connected to changes in the North Atlantic. A similar pattern of fluctuations is also exhibited in the isotope record from Lake Ohrid (Lacey et al., 2016) but not in the Lake Ohrid diatom record. There is only one notable reduction in hypolimnetic abundance in the Ohrid diatom record during MIS 7c (centred on 213 ka), indicating that these changes in the northeastern Mediterranean probably reflect variations in moisture availability rather than temperature.

Both diatom records record a response to the stadial of MIS 7b that is relatively subtle. In the Ioannina diatom record, MIS 7b is marked by planktonic abundances of c. 50% (c. 151 m, c. 201 ka), which is not much lower than other parts of MIS 7c. At Lake Ohrid, a slight increase in the abundance of epilimnetic taxa within ODZ 3b suggests a minor temperature reduction. These findings suggest that MIS 7b is a relatively short period of minor cooling and drying, and they support the inference from the Ioannina pollen record that MIS 7b is only a minor event in the northeastern Mediterranean (Roucoux et al., 2008). The persistence of calcite precipitation at Ohrid also demonstrates the mild nature of this interval.

Following the end of MIS 7a, both diatom records exhibit large fluctuations. The large decline in lake level at Ioannina inferred for IDZ 12b marks the end of the Zitsa III forested interval and reflects dry conditions at the inception of the penultimate glacial period (MIS 6). A subsequent increase in lake level indicates wet conditions that coincide with the short Zitsa IV forested interval before dry conditions resume once more. At Lake Ohrid, the strong, high-frequency diatom response is perhaps surprising considering it had demonstrated a much more subtle response to changing conditions up to this point. The large fluctuations exhibited by both diatom records demonstrate increasing climate instability at the start of the penultimate glacial and suggest variability in both moisture and temperature availability at this time.

7.3 Comparison of MIS 7–9 at Lake Ioannina with other intervals

Variations in the diatom assemblage at Lake Ioannina throughout MIS 7–9 are remarkably muted, especially considering the interval spans a glacial–interglacial cycle. This is even more evident when it is compared with previously published diatom data from the I-284 core for the more recent climatic cycles (Figure 7.2). Although the previously published I-284 records are of a higher resolution than the new long record presented in Chapter 5, it is clear that there are no phases in MIS 7–9 with the same character as that of the late glacial (MIS 2) or the younger part of MIS 6, where facultative planktonic taxa often dominate. The closest the new record comes to an assemblage like these is in MIS 9b, where there are rapid fluctuations in planktonic abundance from one sample to the next and other regional records demonstrate millennial-scale variability.

Unlike during MIS 6 (Wilson et al., 2021), the lake system is clearly not close to crossing environmental thresholds during MIS 8. The persistent dominance of planktonic taxa and the inference of a relatively deep lake over such a long period of time does raise the question as to whether tectonic factors, for example increased subsidence rates, could have influenced the evolution of the lake during this interval. It would be interesting to investigate the oldest samples of the I-284 core, which are believed to date to the glacial period of MIS 10, to see if these demonstrate evidence for lower lake levels. Nevertheless, the lake conditions in MIS 9b do indicate that slightly lower lake levels did persist at some point prior to the long deep phase of the lake's history (MIS 7–8), and the fact that the diatom record corresponds well with regional palaeoclimate records lends more to the original hypothesis that climate is the controlling factor on lake depth rather than tectonic evolution. The deep conditions and muted diatom response during MIS 8 and MIS 7 attests to the

weaker nature of these climatic cycles and demonstrates a level of resilience to weaker climate forcing.
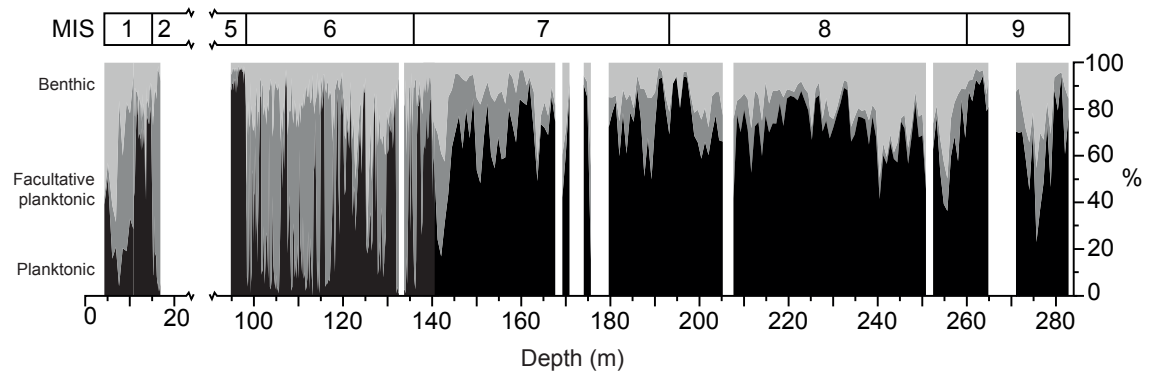
Figure 7.2: Percentage relative abundance of planktonic, facultative planktonic and benthic diatom taxa for the new record presented here (MIS 7–9) alongside previously published data for MIS 6 (Wilson et al., 2013; Wilson et al., 2021), MIS 5 (Wilson et al., 2015) and the late glacial to Holocene (Wilson et al., 2008; Jones et al., 2013).

Chapter 8 | Conclusions

Two new high-resolution diatom records have been produced from shallow Lake Ioannina and deep Lake Ohrid, two proximal ancient lakes in the northeastern Mediterranean. The diatom record of Lake Ioannina spans an interval equivalent to MIS 7–9 and reveals a diatom response primarily driven by lake level variations and changes in lake mixing. In contrast, the diatom record of Lake Ohrid spans MIS 7 and reveals a diatom response to temperature-induced changes in lake stratification and the delivery of nutrients to the epilimnion.

The diatom record from Lake Ioannina demonstrates the remarkable dominance of planktonic taxa throughout most of the interval under investigation. This lake persisted with relatively high lake levels for much of MIS 7–9, including during early MIS 8, when records from other Mediterranean sites exhibit the most extreme cold and dry conditions of the antepenultimate glacial. This is in stark contrast to the glacial periods of the more recent climatic cycles, which demonstrate shallower lake conditions. Although the start of MIS 8 was comparatively dry in relation to the preceding interstadial of MIS 9a, it appears to have been wetter at Ioannina than the penultimate and last glacial periods. The diatom record indicates an increase in moisture availability in the middle of MIS 8, in agreement with regional palaeoclimate records, before returning to drier conditions at the end of MIS 8. The contrasting diatom response recorded at Lake Ohrid and Lake Ioannina has enabled temperature and precipitation changes to be more clearly separated during MIS 7. MIS 7e was warm and initially wet but became drier. Conditions became cold but remained wet at the start of MIS 7d before very dry conditions set in. The start of MIS 7c was warm and initially very wet but the Ioannina diatom record demonstrates increased aridity on the approach into the penultimate glacial. Marked variability in both temperature and moisture availability characterise the glacial inception.

This study has demonstrated the success of examining the contrasting diatom responses in deep versus shallow lakes in separating temperature from precipitation change. It has also highlighted intervals in MIS 8 and MIS 9 that deserve further attention. Examples include MIS 9b, which demonstrates some initial evidence for millennial-scale variability, and the early part of MIS 8, which appears to be rather mild at Ioannina.

References

Albrecht, C., Trajanovski, S., Kuhn, K., Streit, B. & Wilke, T. (2006) Rapid evolution of an ancient lake species flock: freshwater limpets (Gastropoda: Ancylidae) in the Balkan Lake Ohrid. *Organisms Diversity & Evolution*, 6, 294–307.

Albrecht, C., Salzburger, W., Tolo, C. U. & Stelbrink, B. (2020) Speciation in Ancient Lakes 8 – celebrating 25 years and moving towards the future. *Journal of Great Lakes Research*, 46, 1063–1066.

Alexakis, D., Kagalou, I. & Tsakiris, G. (2013) Assessment of pressures and impacts on surface water bodies of the Mediterranean. Case study: Pamvotis Lake, Greece. *Environmental Earth Sciences*, 70, 687–698.

Allen, H. L. & Ocevski, B. T. (1976) Limnological studies in a large, deep, oligotrophic lake (Lake Ohrid, Yugoslavia): evaluation of nutrient availability and control of phytoplankton production through in situ radiobioassay procedures. *Archiv für Hydrobiologia*, 77, 1–21.

Amataj, S., Anovski, T., Benischke, R., Eftimi, R., Gourcy, L. L., Kola, L., Leontiadis, I., Micevski, E., Stamos, A. & Zoto, J. (2007) Tracer methods used to verify the hypothesis of Cvijić about the underground connection between Prespa and Ohrid Lake. *Environmental Geology*, 51, 749–753.

Ampel, L., Wohlfarth, B., Risberg, J., Veres, D., Leng, M. J. & Tillman, P. K. (2010) Diatom assemblage dynamics during abrupt climate change: the response of lacustrine diatoms to Dansgaard–Oeschger cycles during the last glacial period. *Journal of Paleolimnology*, 44, 397–404.

Angeli, N. & Cantonati, M. (2005) Depth-distribution of surface sediment diatoms in Lake Tovel, Italy. *Verhandlungen der Internationalen Vereinigung Limnologie*, 29, 539–544.

Anovski, T., Andonovski, B. & Minčeva, B. (1991) Study of the hydrological relationship between lakes Ohrid and Prespa. *Proceedings of an IAEA international symposium.* Vienna, 11–15 March.

Barker, P., Fontes, J. C., Gasse, F. & Druart, J.-C. (1994) Experimental dissolution of diatom silica in concentrated salt solutions and implications for paleoenvironmental reconstruction. *Limnology and Oceanography*, 39, 99–110.

Barker, S., Knorr, G., Edwards, R. L., Parrenin, F., Putnam, A. E., Skinner, L. C., Wolff, E. & Ziegler, M. (2011) 800,000 years of abrupt climate variability. *Science*, 334, 347–351.

Battarbee, R. W. & Kneen, M. (1982) The use of electronically counted microspheres in absolute diatom analysis. *Limnology and oceanography*, 27, 184–188.

Battarbee, R. W. (1986) Diatom analysis. In Berglund, B. E. (ed) *Handbook of palaeoecology and palaeohydrology*. Chichester: John Wiley & Sons, 527–570.

Battarbee, R. W., Jones, V. J., Flower, R. J., Cameron, N. G., Bennion, H., Carvalho, L. & Juggins, S. (2001) Diatoms. In Smol, J. P., Birks, H. J. B. & Last, W. M. (eds) *Tracking environmental change using lake sediments, Volume 3: terrestrial, algal, and siliceous indicators*. Dordrecht: Kluwer Academic Publishers, 155–202.

Battarbee, R. W., Mackay, A., Jewson, D., Ryves, D. & Sturm, M. (2005) Differential dissolution of Lake Baikal diatoms: correction factors and implications for palaeoclimatic reconstruction. *Global and Planetary Change*, 46, 75–86.

Bennett, K. D., Tzedakis, P. C. & Willis, K. J. (1991) Quaternary refugia of North European trees. *Journal of Biogeography*, 18, 103–115.

Bennett, K. D. (1996) Determination of the number of zones in a biostratigraphical sequence. *New Phytologist*, 132, 155–170.

Bennett, K. D. & Willis, K. J. (2001) Pollen. In Smol, J. P., Birks, H. J. B. & Last, W. M. (eds) *Tracking environmental change using lake sediments, Volume 3: terrestrial, algal, and siliceous indicators*. Dordrecht: Kluwer Academic Publishers, 5–32.

Bennion, H. (1995) Surface-sediment diatom assemblages in shallow, artificial, enriched ponds, and implications for reconstructing trophic status. *Diatom Research*, 10, 1–19.

Bennion, H., Appleby, P. G. & Phillips, G. L. (2001) Reconstructing nutrient histories in the Norfolk Broads, UK: implications for the role of diatom-total phosphorus transfer functions in shallow lake management. *Journal of Paleolimnology*, 26, 181–204.

Berends, C. J., Köhler, P., Lourens, L. J. & van de Wal, R. S. W. (2021) On the cause of the Mid-Pleistocene transition. *Reviews of Geophysics*, 59, e2020RG000727.

Bergmann, C. (1847) Über die verhältnisse der wärmeokönomie der thiere zu ihrer grösse. *Göttinger Studien*, 3, 595–708.

Bintanja, R. & van der Linden, E. C. (2013) The changing seasonal climate in the Arctic. *Scientific Reports*, 3, 1556.

Birks, H. H. & Birks, H. J. B. (2006) Multi-proxy studies in palaeolimnology. *Vegetation History and Archaeobotany*, 15, 235–251.

Birks, H. J. B. & Birks, H. H. (1980) *Quaternary palaeoecology*. London: Edward Arnold.

Birks, H. J. B. & Gordon, A. D. (1985) *Numerical Methods in Quaternary Pollen Analysis*. London: Academic Press.

Birks, H. J. B. (1986) Numerical zonation, comparison and correlation of Quaternary pollen-stratigraphical data. In Berglund, B. E. (ed) *Handbook of palaeoecology and palaeohydrology*. Chichester: John Wiley & Sons, 743–774.

Birks, H. J. B. (2010) Numerical methods for the analysis of diatom assemblage data. In Smol, J. P. & Stoermer, E. F. (eds) *The diatoms: applications for the environmental and earth sciences, 2nd edition*. Cambridge: Cambridge University Press.

Birks, H. J. B. (2012) Analysis of stratigraphical data. In Birks, H. J. B., Lotter, A. F., Juggins, S. & Smol, J. P. (eds) *Tracking environmental change using lake sediments, Volume 5: Data handling and numerical techniques*. Dordrecht: Springer, 201–248.

Birks, H. J. B. & Berglund, B. E. (2018) One hundred years of Quaternary pollen analysis 1916–2016. *Vegetation History and Archaeobotany*, 27, 271–309.

Birner, B., Hodell, D. A., Tzedakis, P. C. & Skinner, L. C. (2016) Similar millennial climate variability on the Iberian margin during two early Pleistocene glacials and MIS 3. *Paleoceanography*, 31, 203–217.

Błaszczyk, M. & Hercman, H. (2022) Palaeoclimate in the Low Tatras of the Western Carpathians during MIS 11–6: Insights from multiproxy speleothem records. *Quaternary Science Reviews*, 275, 107290.

Blockley, S. P. E., Pyne-O'Donnell, S. D. F., Lowe, J. J., Matthews, I. P., Stone, A., Pollard, A. M., Turney, C. S. M. & Molyneux, E. G. (2005) A new and less destructive laboratory procedure for the physical separation of distal glass tephra shards from sediments. *Quaternary Science Reviews*, 24, 1952–1960.

Bond, G., Heinrich, H., Broecker, W., Labeyrie, L., McManus, J., Andrews, J., Huon, S., Jantschik, R., Clasen, S. & Simet, C. (1992) Evidence for massive discharges of icebergs into the North Atlantic ocean during the last glacial period. *Nature*, 360, 245–249.

Bond, G., Broecker, W., Johnsen, S., McManus, J., Labeyrie, L., Jouzel, J. & Bonani, G. (1993) Correlations between climate records from North Atlantic sediments and Greenland ice. *Nature*, 365, 143–147.

Bond, G., Showers, W., Cheseby, M., Lotti, R., Almasi, P., deMenocal, P., Priore, P., Cullen, H., Hajdas, I. & Bonani, G. (1997) A pervasive millennial-scale cycle in North Atlantic Holocene and glacial climates. *Science*, 278, 1257–1266.

ter Braak, C. J. F. & Prentice, I. C. (1988) A theory of gradient analysis. *Advances in Ecological Research*, 18, 271–317.

ter Braak, C. J. F. (1995) Ordination. In Jongman, R. H. G., ter Braak, C. J. F. & van Tongeren, O. F. R. (eds) *Data analysis in community and landscape ecology, 2nd edition*. Cambridge: Cambridge University Press.

Broecker, W. S., Bond, G., Klas, M., Bonani, G. & Wolfli, W. (1990) A salt oscillator in the glacial Atlantic? 1. The concept. *Paleoceanography*, 5, 469–477.

Brown, L. C. & Duguay, C. R. (2010) The response and role of ice cover in lake-climate interactions. *Progress in Physical Geography*, 34, 671–704.

Bruesewitz, D. A., Carey, C. C., Richardson, D. C. & Weathers, K. C. (2015) Under-ice thermal stratification dynamics of a large, deep lake revealed by high-frequency data. *Limnology and Oceanography*, 60, 347–359.

Burchfiel, B. C., Nakov, R., Dumurdzanov, N., Papanikolaou, D., Tzankov, T., Serafimovski, T., King, R. W., Kotzev, V., Todosov, A. & Nurce, B. (2008) Evolution and dynamics of the Cenozoic tectonics of the South Balkan extensional system. *Geosphere*, 4, 919–938.

Campbell, I. D., McDonald, K., Flannigan, M. D. & Kringayark, J. (1999) Long-distance transport of pollen into the Arctic. *Nature*, 399, 29–30.

Candy, I., Schreve, D. C., Sherriff, J. & Tye, G. J. (2014) Marine Isotope Stage 11: palaeoclimates, palaeoenvironments and its role as an analogue for the current interglacial. *Earth-Science Reviews*, 128, 18–51.

Cantonati, M., Scola, S., Angeli, N., Guella, G. & Frassanito, R. (2009) Environmental controls of epilithic diatom depthdistribution in an oligotrophic lake characterized by marked water-level fluctuations. *European Journal of Phycology*, 44, 15–29.

Cavazza, W. & Wezel, F. C. (2003) The Mediterranean region—a geological primer. *Episodes*, 26, 160–168.

Channell, J. E. T., Hodell, D. A., Romero, O., Hillaire-Marcel, C., de Vernal, A., Stoner, J. S., Mazaud, A. & Röhl, U. (2012) A 750-kyr detrital-layer stratigraphy for the North Atlantic (IODP Sites U1302–U1303, Orphan Knoll, Labrador Sea). *Earth and Planetary Science Letters*, 317–318, 218–230.

Chen, D., Rojas, M., Samset, B. H., Cobb, K., Diongue Niang, A., Edwards, P., Emori, S., Faria, S. H., Hawkins, E., Hope, P., Huybrechts, P., Meinshausen, M., Mustafa, S. K., Plattner, G.-K. & Tréguier, A.-M. (2021) Framing, context, and methods. In Masson-Delmotte, V., Zhai, P., Pirani, A., Connors, S. L., Péan, C., Berger, S., Caud, N., Chen, Y., Goldfarb, L., Gomis, M. I., Huang, M., Leitzell, K., Lonnoy, E., Matthews, J. B. R., Maycock, T. K., Waterfield, T., Yelekçi, O., Yu, R. & Zhou, B. (eds) *Climate change 2021: the physical science basis. Contribution of Working Group I to the Sixth Assessment Report of the Intergovernmental Panel on Climate Change.* Cambridge University Press. In Press.

Chen, J., Liu, J., Rühland, K. M., Smol, J. P., Zhang, X., Zhang, Z., Zhou, A., Shen, Z. & Chen, F. (2021) Aquatic ecosystem responses to environmental and climatic changes in NE China since the last deglaciation (~17, 500 cal yr BP) tracked by diatom assemblages from Lake Moon. *Quaternary Science Reviews*, 272, 107218.

Cheng, H., Sinha, A., Wang, X., Cruz, F. W. & Edwards, R. L. (2012) The Global Paleomonsoon as seen through speleothem records from Asia and the Americas. *Climate Dynamics*, 39, 1045–1062.

Cherepanova, M. V., Usol'tseva, M. V., Pushkar, V. S. & Dubrovina, Y. F. (2010) Morphogenesis in *Cyclotella ocellata* – Complex from Lake El'gygytgyn (Chukchi Peninsula) during the Pleistocene–Holocene. *Paleontological Journal*, 44, 1252–1261.

Chevalier, M., Davis, B. A. S., Heiri, O., Seppä, H., Chase, B. M., Gajewski, K., Lacourse, T., Telford, R. J., Finsinger, W., Guiot, J., Kühl, N., Maezumi, S. Y., Tipton, J. R., Carter, V. A., Brussel, T., Phelps, L. N., Dawson, A., Zanon, M., Vallé, F., Nolan, C., Mauri, A., de Vernal, A., Izumi, K., Holmström, L., Marsicek, J., Goring, S., Sommer, P. S., Chaput, M. & Kupriyanov, D. (2020) Pollen-based climate reconstruction techniques for late Quaternary studies. *Earth-Science Reviews*, 210, 103384.

Clark, P. U., Archer, D., Pollard, D., Blum, J. D., Rial, J. A., Brovkin, V., Mix, A. C., Pisias, N. G. & Roy, M. (2006) The middle Pleistocene transition: characteristics, mechanisms, and implications for long-term changes in atmospheric pCO_2. *Quaternary Science Reviews*, 25, 3150–3184.

Clews, J. E. (1989) Structural controls on basin evolution: Neogene to Quaternary of the Ionian zone, Western Greece. *Journal of the Geological Society*, 146, 447–457.

Cohen, A. S. (2003) *Paleolimnology: the history and evolution of lake systems.* Oxford: Oxford University Press.

Cohen, A. S. (2012) Scientific drilling and biological evolution in ancient lakes: lessons learned and recommendations for the future. *Hydrobiologia*, 682, 3–25.

Columbu, A., Spötl, C., De Waele, J., Yu, T.-L., Shen, C.-C. & Gázquez, F. (2019) A long record of MIS 7 and MIS 5 climate and environment from a western Mediterranean speleothem (SW Sardinia, Italy). *Quaternary Science Reviews*, 220, 230–243.

Conispoliatis, N., Panagos, A., Perissoratis, C. & Varnavas, S. (1986) Geological and sedimentological patterns in the Lake Pamvotis (Ioannina), NW Greece. *Annales G!eologiques des Pays Helleniques*, 33, 269-285.

Cox, E. J. (2011) Morphology, cell wall, cytology, ultrastructure and morphogenetic studies. In Seckbach, J. & Kociolek, J. P. (eds) *The diatom world. Cellular Origin, Life in Extreme Habitats and Astrobiology Volume 19.* Dordrecht: Springer, 23–45.

Cox, E. J. (2014) Diatom identification in the face of changing species concepts and evidence of phenotypic plasticity. *Journal of Micropalaeontology*, 33, 111–120.

Cramer, W., Guiot, J., Fader, M., Garrabou, J., Gattuso, J.-P., Iglesias, A., Lange, M. A., Lionello, P., Llasat, M. C., Paz, S., Peñuelas, J., Snoussi, M., Toreti, A., Tsimplis, M. N. & Xoplaki, E. (2018) Climate change and interconnected risks to sustainable development in the Mediterranean. *Nature Climate Change*, 8, 972–980.

Cremer, H. & Wagner, B. (2003) The diatom flora in the ultra-oligotrophic Lake El'gygytgyn, Chukotka. *Polar Biology*, 26, 105–114.

Cremer, H., Wagner, B., Juschus, O. & Melles, M. (2005) A microscopical study of the diatom phytoplankton in deep crater Lake El'gygytgyn, Northeast Siberia. *Algological Studies*, 116, 147–169.

Cushing, E. J. (1963) *Late-Wisconsin pollen stratigraphy in east central Minnesota*. PhD thesis. University of Minnesota.

Cvetkoska, A., Levkov, Z., Reed, J. M. & Wagner, B. (2014a) Late Glacial to Holocene climate change and human impact in the Mediterranean: the last ca. 17 ka diatom record of Lake Prespa (Macedonia/Albania/Greece). *Palaeogeography, Palaeoclimatology, Palaeoecology*, 406, 22–32.

Cvetkoska, A., Hamilton, P. B., Ognjanova–Rumenova, N. & Levkov, Z. (2014b) Observations of the genus *Cyclotella* (Kützing) Brébisson in ancient lakes Ohrid and Prespa and a description of two new species *C. paraocellata* sp. nov. and *C. prespanensis* sp. nov. *Nova Hedwigia*, 98, 313–340.

Cvetkoska, A., Levkov, Z., Reed, J. M., Wagner, B., Panagiotopoulos, K., Leng, M. J. & Lacey, J. H. (2015) Quaternary climate change and Heinrich events in the southern Balkans: Lake Prespa diatom palaeolimnology from the last interglacial to present. *Journal of Paleolimnology*, 53, 215–231.

Cvetkoska, A., Jovanovska, E., Francke, A., Tofilovska, S., Vogel, H., Levkov, Z., Donders, T. H., Wagner, B. & Wagner-Cremer, F. (2016) Ecosystem regimes and responses in a coupled ancient lake system from MIS 5b to present: the diatom record of lakes Ohrid and Prespa. *Biogeosciences*, 13, 3147–3162.

Cvetkoska, A., Pavlov, A., Jovanovska, E., Tofilovska, S., Blanco, S., Ector, L., Wagner-Cremer, F. & Levkov, Z. (2018) Spatial patterns of diatom diversity and community structure in ancient Lake Ohrid. *Hydrobiologia*, 819, 197–215.

Cvetkoska, A., Jovanovska, E., Hauffe, T., Donders, T. H., Levkov, Z., van de Waal, D. B., Reed, J. M., Francke, A., Vogel, H., Wilke, T., Wagner, B. & Wagner-Cremer, F. (2021) Drivers of phytoplankton community structure change with ecosystem ontogeny during the Quaternary. *Quaternary Science Reviews*, 265, 107046.

Cvijic, J. (1906) *Fundamentals of Geography and Geology of Macedonia and Old Serbia*. Belgrade: Serbian Academy of Sciences.

Dansgaard, W., Johnsen, S. J., Clausen, H. B., Dahl-Jensen, D., Gundestrup, N., Hammer, C. U. & Oeschger, H. (1984) North Atlantic climatic oscillations revealed by deep Greenland ice cores. In Hansen, J. E. & Takahashi, T. (eds) *Climate processes and climate sensitivity. Geophysical Monograph Series Volume 29*. Washington D.C.: American Geophysical Union, 288–298.

Dansgaard, W., Johnsen, S. J., Clausen, H. B., Dahl-Jensen, D., Gundestrup, N. S., Hammer, C. U., Hvidberg, C. S., Steffensen, J. P., Sveinbjörnsdottir, A. E., Jouzel, J. & Bond, G. (1993) Evidence for general instability of past climate from a 250-kyr ice-core record. *Nature*, 364, 218–220.

Dean, J. R., Jones, M. D., Leng, M. J., Noble, S. R., Metcalfe, S. E., Sloane, H. J., Sahy, D., Eastwood, W. J. & Roberts, C. N. (2015) Eastern Mediterranean hydroclimate over the late glacial and Holocene, reconstructed from the sediments of Nar lake, central Turkey, using stable isotopes and carbonate mineralogy. *Quaternary Science Reviews*, 124, 162–174.

Dean, W. E. (1981) Carbonate minerals and organic matter in sediments of modern north temperate hard-water lakes. *Society of Economic Palaeontologists and Mineralogists Special Publication*, 31, 213–231.

Dearing, J. A. & Foster, I. D. L. (1986) Lake sediments and palaeohydrological studies. In Berglund, B. E. (ed) *Handbook of palaeoecology and palaeohydrology*. Chichester: John Wiley & Sons, 67–90.

Desprat, S., Sánchez Goñi, M., McManus, J. F., Duprat, J. & Cortijo, E. (2009) Millennial-scale climatic variability between 340 000 and 270 000 years ago in SW Europe: evidence from a NW Iberian margin pollen sequence. *Climate of the Past*, 5, 53–72.

Donders, T., Panagiotopoulos, K., Koutsodendris, A., Bertini, A., Mercuri, A. M., Masi, A., Combourieu-Nebout, N., Joannin, S., Kouli, K., Kousis, I., Peyron, O., Torri, P., Florenzano, A., Francke, A., Wagner, B. & Sadori, L. (2021) 1.36 million years of Mediterranean forest refugium dynamics in response to glacial–interglacial cycle strength. *Proceedings of the National Academy of Sciences*, 118, e2026111118.

Douglas, M. S. V. & Smol, J. P. (2010) Freshwater diatoms as indicators of environmental change in the High Arctic. In Smol, J. P. & Stoermer, E. F. (eds) *The diatoms: applications for the environmental and earth sciences, 2nd edition*. Cambridge: Cambridge University Press, 249–266.

Douville, H., Raghavan, K., Renwick, J., Allan, R. P., Arias, P. A., Barlow, M., Cerezo-Mota, R., Cherchi, A., Gan, T. Y., Gergis, J., Jiang, D., Khan, A., Pokam Mba, W., Rosenfeld, D., Tierney, J. & Zolina, O. (2021) Water cycle changes. In Masson-Delmotte, V., Zhai, P., Pirani, A., Connors, S. L., Péan, C., Berger, S., Caud, N., Chen, Y., Goldfarb, L., Gomis, M. I., Huang, M., Leitzell, K., Lonnoy, E., Matthews, J. B. R., Maycock, T. K., Waterfield, T., Yelekçi, O., Yu, R. & Zhou, B. (eds) *Climate change 2021: the physical science basis. Contribution of Working Group I to the Sixth Assessment Report of the Intergovernmental Panel on Climate Change*. Cambridge University Press. In Press.

Dumurdzanov, N., Serafimovski, T. & Burchfiel, B. C. (2004) *Evolution of the Neogene-Pleistocene Basins of Macedonia*. Boulder: Geological Society of America.

Dumurdzanov, N., Serafimovski, T. & Burchfiel, B. C. (2005) Cenozoic tectonics of Macedonia and its relation to the South Balkan extensional regime. *Geosphere*, 1, 1–22.

Dunnington, D. (2021) *tidypaleo: tidy tools for paleoenvironmental archives* [Software]. Available online: https://CRAN.R-project.org/package=tidypaleo.

Dwyer, J. G., Biasutti, M. & Sobel, A. H. (2012) Projected changes in the seasonal cycle of surface temperature. *Journal of Climate*, 25, 6359–6374.

Eftimi, R., Skende, P. & Zoto, J. (2002) Isotope study of the connection of Ohrid and Prespa lakes. *Geologica Balanica*, 32, 43–49.

Elkibbi, M. & Rial, J. A. (2001) An outsider's review of the astronomical theory of the climate: is the eccentricity-driven insolation the main driver of the ice ages? *Earth-Science Reviews*, 56, 161–177.

Elliot, M., Labeyrie, L., Dokken, T. & Manthé, S. (2001) Coherent patterns of ice-rafted debris deposits in the Nordic regions during the last glacial (10–60 ka). *Earth and Planetary Science Letters*, 194, 151–163.

EPICA Community Members (2006) One-to-one coupling of glacial climate variability in Greenland and Antarctica. *Nature*, 444, 195–198.

Finné, M., Woodbridge, J., Labuhn, I. & Roberts, C. N. (2019) Holocene hydro-climatic variability in the Mediterranean: A synthetic multi-proxy reconstruction. *The Holocene*, 29, 847–863.

Fletcher, W. J., Sánchez Goñi, M. F., Allen, J. R. M., Cheddadi, R., Combourieu-Nebout, N., Huntley, B., Lawson, I., Londeix, L., Magri, D., Margari, V., Müller, U. C., Naughton, F., Novenko, E., Roucoux, K. & Tzedakis, P. C. (2010) Millennial-scale variability during the last glacial in vegetation records from Europe. *Quaternary Science Reviews*, 29, 2839–2864.

Fletcher, W. J., Müller, U. C., Koutsodendris, A., Christanis, K. & Pross, J. (2013) A centennial-scale record of vegetation and climate variability from 312 to 240 ka (Marine Isotope Stages 9c–a, 8 and 7e) from Tenaghi Philippon, NE Greece. *Quaternary Science Reviews*, 78, 108–125.

Flower, R. J. (1993) Diatom preservation: experiments and observations on dissolution and breakage in modern and fossil material. *Hydrobiologia*, 473–484.

Flower, R. J. & Ryves, D. B. (2009) Diatom preservation: differential preservation of sedimentary diatoms in two saline lakes. *Acta Botanica Croatica*, 68, 381–399.

Follieri, M., Magri, D. & Sadori, L. (1988) 250,000-year pollen record from Valle di Castiglione (Roma). *Pollen et Spores*, 30, 329–356.

Francke, A., Wagner, B., Just, J., Leicher, N., Gromig, R., Baumgarten, H., Vogel, H., Lacey, J. H., Sadori, L., Wonik, T., Leng, M. J., Zanchetta, G., Sulpizio, R. & Giaccio, B. (2016) Sedimentological processes and environmental variability at Lake Ohrid (Macedonia, Albania) between 637 ka and the present. *Biogeosciences*, 13, 1179–1196.

Francke, A., Dosseto, A., Panagiotopoulos, K., Leicher, N., Lacey, J. H., Kyrikou, S., Wagner, B., Zanchetta, G., Kouli, K. & Leng, M. J. (2019) Sediment residence time reveals Holocene shift from climatic to vegetation control on catchment erosion in the Balkans. *Global and Planetary Change*, 177, 186–200.

Fritz, S. C., Cumming, B. F., Gasse, F. & Laird, K. R. (2010) Diatoms as indicators of hydrologic and climatic change in saline lakes. In Smol, J. P. & Stoermer, E. F. (eds) *The diatoms: applications for the environmental and earth sciences, 2nd edition.* Cambridge: Cambridge University Press, 186–208.

Frogley, M. R. (1997) *The biostratigraphy, palaeoecology and geochemistry of a long lacustrine sequence from NW Greece*. PhD thesis. University of Cambridge.

Frogley, M. R., Tzedakis, P. C. & Heaton, T. H. E. (1999) Climate variability in northwest Greece during the Last Interglacial. *Science*, 285, 1886–1888.

Frogley, M. R., Griffiths, H. I. & Heaton, T. H. E. (2001) Historical biogeography and Late Quaternary environmental change of Lake Pamvotis, Ioannina (north-western Greece): evidence from ostracods. *Journal of Biogeography*, 28, 745–756.

Furlan, D. (1977) The climate of southeast Europe. In Wallén, C. C. (ed) *Climates of Central and Southern Europe. World Survey of Climatology, Volume 6*. Amsterdam: Elsevier, 185–235.

Gauch, H. G. (1982) *Multivariate analysis in community ecology*. Cambridge: Cambridge University Press.

Genkal, S. I. & Popovskaya, G. I. (2008) Morphological variability of *Cyclotella ocellata* from Lake Khubsugul (Mongolia). *Diatom Research*, 23, 75–91.

Giaccio, B., Leicher, N., Mannella, G., Monaco, L., Regattieri, E., Wagner, B., Zanchetta, G., Gaeta, M., Marra, F. & Nomade, S. (2019) Extending the tephra and palaeoenvironmental record of the Central Mediterranean back to 430 ka: A new core from Fucino Basin, central Italy. *Quaternary Science Reviews*, 225, 106003.

Gibbard, P. & Head, M. J. (2009a) IUGS ratification of the Quaternary System/Period and the Pleistocene Series/Epoch with a base at 2.58 Ma. *Quaternaire*, 20, 411–412.

Gibbard, P. & Head, M. J. (2009b) The definition of the Quaternary System/Era and the Pleistocene Series/Epoch. *Quaternaire*, 20, 125–133.

Gibbard, P. L. & Hughes, P. D. (2021) Terrestrial stratigraphical division in the Quaternary and its correlation. *Journal of the Geological Society*, 178, jgs2020-134.

Giorgi, F. (2006) Climate change hot-spots. *Geophysical Research Letters*, 33, L08707.

Giorgi, F., Coppola, E. & Raffaele, F. (2014) A consistent picture of the hydroclimatic response to global warming from multiple indices: models and observations. *Journal of Geophysical Research: Atmospheres*, 119, 11695–11708.

Giorgi, F., Raffaele, F. & Coppola, E. (2019) The response of precipitation characteristics to global warming from climate projections. *Earth System Dynamics*, 10, 73–89.

Glushchenko, A., Kulikovskiy, M., Okhapkin, A. & Kociolek, J. P. (2017) *Aneumastus laosica* sp. nov. and *A. genkalii* sp. nov. — two new diatom species from Laos (Southeast Asia) with comments on the biogeography of the genus. *Cryptogamie, Algologie*, 38, 183–199.

Goodall, D. W. (1954) Objectives methods for the classification of vegetation. III. An essay on the use of factor analysis. *Australian Journal of Botany*, 2, 304–324.

Gordon, A. D. & Birks, H. J. B. (1972) Numerical methods in Quaternary palaeoecology. I. Zonation of pollen diagrams. *New Phytologist*, 71, 961–979.

Grant, K., Rohling, E., Bar-Matthews, M., Ayalon, A., Medina-Elizalde, M., Ramsey, C. B., Satow, C. & Roberts, A. (2012) Rapid coupling between ice volume and polar temperature over the past 150,000 years. *Nature*, 491, 744–747.

Greene, C. H. (2012) The winters of our discontent. *Scientific American*, 307, 5055.

Grimm, E., C. (2011) *Tilia version 2.6.1* [Software]. Available online: https://www.tiliait.com.

Grimm, E. C. (1987) CONISS: A FORTRAN 77 program for stratigraphically constrained cluster analysis by the method of incremental sum of squares. *Computers & Geosciences*, 13, 13–35.

Gulev, S. K., Thorne, P. W., Ahn, J., Dentener, F. J., Domingues, C. M., Gerland, S., Gong, D., Kaufman, D. S., Nnamchi, H. C., Quaas, J., Rivera, J. A., Sathyendranath, S., Smith, S. L., Trewin, B., von Schuckmann, K. & Vose, R. S. (2021) Changing state of the climate system. In Masson-Delmotte, V., Zhai, P., Pirani, A., Connors, S. L., Péan, C., Berger, S., Caud, N., Chen, Y., Goldfarb, L., Gomis, M. I., Huang, M., Leitzell, K., Lonnoy, E., Matthews, J. B. R., Maycock, T. K., Waterfield, T., Yelekçi, O., Yu, R. &

Zhou, B. (eds) *Climate change 2021: the physical science basis. Contribution of Working Group I to the Sixth Assessment Report of the Intergovernmental Panel on Climate Change*. Cambridge University Press. In Press.

Haberyan, K. A. (1985) The role of eopepod fecal pellets in the deposition of diatoms in Lake Tanganyika. *Limnology and Oceanography*, 30, 1010–1023.

Håkansson, H. (1990) A comparison of *Cyclotella krammeri* sp. nov. and *C. schumannii* Håkansson stat. nov. with similar species. *Diatom Research*, 5, 261–271.

Håkansson, H. (1993) Morphological and taxonomic problems in four *Cyclotella* species (Bacillariophyceae). *Diatom Research*, 8, 309–316.

Håkansson, H. (2002) A compilation and evaluation of species in the general *Stephanodiscus*, *Cyclostephanos* and *Cyclotella* with a new genus in the family Stephanodiscaceae. *Diatom Research*, 17, 1–139.

Hall, R. I. & Smol, J. P. (2010) Diatoms as indicators of lake eutrophication. In Smol, J. P. & Stoermer, E. F. (eds) *The diatoms: applications for the environmental and earth sciences, 2nd edition*. Cambridge: Cambridge University Press, 122–151.

van der Hammen, T., Wijmstra, T. A. & Zagwyn, W. H. (1971) The floral record of the late Cenozoic of Europe. In Turekian, K. K. (ed) *The late Cenozoic glacial ages*. New Haven: Yale University Press, 391–424.

Hampton, S. E., Galloway, A. W. E., Powers, S. M., Ozersky, T., Woo, K. H., Batt, R. D., Labou, S. G., O'Reilly, C. M., Sharma, S., Lottig, N. R., Stanley, E. H., North, R. L., Stockwell, J. D., Adrian, R., Weyhenmeyer, G. A., Arvola, L., Baulch, H. M., Bertani, I., Bowman Jr., L. L., Carey, C. C., Catalan, J., Colom-Montero, W., Domine, L. M., Felip, M., Granados, I., Gries, C., Grossart, H.-P., Haberman, J., Haldna, M., Hayden, B., Higgins, S. N., Jolley, J. C., Kahilainen, K. K., Kaup, E., Kehoe, M. J., MacIntyre, S., Mackay, A. W., Mariash, H. L., McKay, R. M., Nixdorf, B., Nõges, P., Nõges, T., Palmer, M., Pierson, D. C., Post, D. M., Pruett, M. J., Rautio, M., Read, J. S., Roberts, S. L., Rücker, J., Sadro, S., Silow, E. A., Smith, D. E., Sterner, R. W., Swann, G. E. A.,

Timofeyev, M. A., Toro, M., Twiss, M. R., Vogt, R. J., Watson, S. B., Whiteford, E. J. & Xenopoulos, M. A. (2017) Ecology under lake ice. *Ecology letters*, 20, 98–111.

Hania, A., Eichner, M., Norici, A., Prášil, O. & Giordano, M. (2021) Does growth rate affect diatom compositional response to temperature? *Phycologia*, 60, 462–472.

Harding, A. E., Palutikof, J. & Holt, T. (2009) The climate system. In Woodward, J. C. (ed) *The Physical Geography of the Mediterranean*. Oxford: Oxford University Press, 69–88.

Hassan, G. S. (2015) On the benefits of being redundant: low compositional fidelity of diatom death assemblages does not hamper the preservation of environmental gradients in shallow lakes. *Paleobiology*, 41, 154–173.

Havinga, A. J. (1967) Palynology and pollen preservation. *Review of Palaeobotany and Palynology*, 2, 81–98.

Haworth, E. Y. (1976) Two late-glacial (Late Devensian) diatom assemblage profiles from northern Scotland. *New Phytologist*, 227–256.

Hays, J. D., Imbrie, J. & Shackleton, N. J. (1976) Variations in the Earth's orbit: pacemaker of the ice ages. *Science*, 194, 1121–1132.

Head, M. J. & Gibbard, P. L. (2015) Early–Middle Pleistocene transitions: linking terrestrial and marine realms. *Quaternary International*, 389, 7–46.

Hegewald, E. & Hindáková, A. (1997) Variability of a natural population and clones of the *Cyclotella ocellata*-complex (Bacillariophyceae) from the Gallberg-pond, NW-Germany. *Algological Studies*, 86, 17–37.

Heinrich, H. (1988) Origin and consequences of cyclic ice rafting in the northeast Atlantic Ocean during the past 130,000 years. *Quaternary Research*, 29, 142–152.

Hellenic National Meteorological Service (2020) *Climatic data for selected stations in Greece.* Available online:

http://www.hnms.gr/emy/en/climatology/climatology_city?perifereia=Epirus&poli=Io annina [Accessed 2020-10-07].

Hellström, T. (1991) The effect of resuspension on algal production in a shallow lake. *Hydrobiologia*, 213, 183–190.

Higgs, E. S., Vita-Finzi, C., Harris, D. R., Fagg, A. E. & Bottema, S. (1967) The climate, environment and industries of Stone Age Greece: Part III. *Proceedings of the Prehistoric Society*, 33, 1–29.

Hijmans, R. J., Cameron, S. E., Parra, J. L., Jones, P. G. & Jarvis, A. (2005) Very high resolution interpolated climate surfaces for global land areas. *International Journal of Climatology*, 25, 1965–1978.

Hobbs, W. O., Telford, R. J., Birks, H. J. B., Saros, J. E., Hazewinkel, R. R., Perren, B. B., Saulnier-Talbot, É. & Wolfe, A. P. (2010) Quantifying recent ecological changes in remote lakes of North America and Greenland using sediment diatom assemblages. *PloS one*, 5, e10026.

Hoffmann, N., Reicherter, K., Fernandez-Steeger, T. & Grutzner, C. (2010) Evolution of ancient Lake Ohrid: a tectonic perspective. *Biogeosciences*, 7, 3377–3386.

Houk, V., Klee, R. & Tanaka, H. (2010) Atlas of freshwater centric diatoms with a brief key and descriptions. Part III. Stephanodiscaceae A: *Cyclotella, Tertiarius, Discostella*. *Fottea (Supplement)*, 10, 1–498.

Hughes, P. D. & Gibbard, P. L. (2018) Global glacier dynamics during 100 ka Pleistocene glacial cycles. *Quaternary Research*, 90, 222–243.

Hughes, P. D., Gibbard, P. L. & Ehlers, J. (2020) The "missing glaciations" of the Middle Pleistocene. *Quaternary Research*, 96, 161–183.

Hurrell, J. W., Hoerling, M. P. & Folland, C. K. (2002) Climatic variability over the North Atlantic. In Pearce, R. P. (ed) *International Geophysics*. New York: Academic Press, 143–151.

Hurrell, J. W. & Deser, C. (2009) North Atlantic climate variability: The role of the North Atlantic Oscillation. *Journal of Marine Systems*, 78, 28–41.

Imbrie, J., Berger, A., Boyle, E. A., Clemens, S. C., Duffy, A., Howard, W. R., Kukla, G., Kutzbach, J., Martinson, D. G., McIntyre, A., Mix, A. C., Molfino, B., Morley, J. J., Peterson, L. C., Pisias, N. G., Prell, W. L., Raymo, M. E., Shackleton, N. J. & Toggweiler, J. R. (1993) On the structure and origin of major glaciation cycles 2. The 100,000-year cycle. *Paleoceanography*, 8, 699–735.

Imeri, A., Mullaj, A., Gjeta, E., Kalajnxhiu, A., Kupe, L., Shehu, J. & Dodona, E. (2010) Preliminary results from the study of flora and vegetation of Ohrid lake. *Natura Montenegrina*, 9, 253–264.

IPCC (2021) Summary for policymakers. In Masson-Delmotte, V., Zhai, P., Pirani, A., Connors, S. L., Péan, C., Berger, S., Caud, N., Chen, Y., Goldfarb, L., Gomis, M. I., Huang, M., Leitzell, K., Lonnoy, E., Matthews, J. B. R., Maycock, T. K., Waterfield, T., Yelekçi, O., Yu, R. & Zhou, B. (eds) *Climate change 2021: the physical science basis. Contribution of Working Group I to the Sixth Assessment Report of the Intergovernmental Panel on Climate Change*. Cambridge University Press. In Press.

Jahn, R., Kusber, W. H. & Romero, O. E. (2009) *Cocconeis pediculus* Ehrenberg and *C. placentula* Ehrenberg var. *placentula* (Bacillariophyta): typification and taxonomy. *Fottea*, 9, 275–288.

Jardine, P. E., Hoorn, C., Beer, M. A., Barbolini, N., Woutersen, A., Bogota-Angel, G., Gosling, W. D., Fraser, W. T., Lomax, B. H. & Huang, H. (2021) Sporopollenin chemistry and its durability in the geological record: an integration of extant and fossil chemical data across the seed plants. *Palaeontology*, 64, 285–305.

Jewson, D. H., Lowry, S. F. & Bowen, R. (2006) Co-existence and survival of diatoms on sand grains. *European Journal of Phycology*, 41, 131–146.

Johnsen, S. J., Dansgaard, W., Clausen, H. B. & Langway, C. C. (1972) Oxygen isotope profiles through the Antarctic and Greenland ice sheets. *Nature*, 235, 429–434.

Johnsen, S. J., Clausen, H. B., Dansgaard, W., Fuhrer, K., Gundestrup, N., Hammer, C. U., Iversen, P., Jouzel, J., Stauffer, B. & steffensen, J. P. (1992) Irregular glacial interstadials recorded in a new Greenland ice core. *Nature*, 359, 311–313.

Jones, T. D. (2010) *A reconstruction of late Pleistocene and Holocene lake level change at Ioannina, northwest Greece*. PhD thesis. University of Leeds.

Jones, T. D., Lawson, I. T., Reed, J. M., Wilson, G. P., Leng, M. J., Gierga, M., Bernasconi, S. M., Smittenberg, R. H., Hajdas, I., Bryant, C. L. & Tzedakis, P. C. (2013) Diatom-inferred late Pleistocene and Holocene palaeolimnological changes in the Ioannina basin, northwest Greece. *Journal of Paleolimnology*, 49, 185–204.

Jouzel, J., Masson-Delmotte, V., Cattani, O., Dreyfus, G., Falourd, S., Hoffmann, G., Minster, B., Nouet, J., Barnola, J. M., Chappellaz, J., Fischer, H., Gallet, J. C., Johnsen, S., Leuenberger, M., Loulergue, L., Luethi, D., Oerter, H., Parrenin, F., Raisbeck, G., Raynaud, D., Schilt, A., Schwander, J., Selmo, E., Souchez, R., Spahni, R., Stauffer, B., Steffensen, J. P., Stenni, B., Stocker, T. F., Tison, J. L., Werner, M. & Wolff, E. W. (2007) Orbital and millennial Antarctic climate variability over the past 800,000 years. *Science*, 317, 793–796.

Jovanovska, E., Nakov, T. & Levkov, Z. (2013) Observations of the genus *Diploneis* from Lake Ohrid, Macedonia. *Diatom Research*, 28, 237–262.

Jovanovska, E., Levkov, Z. & Edlund, M. B. (2015) The genus *Diploneis* Ehrenberg *ex* Cleve (Bacillariophyta) from Lake Hövsgöl, Mongolia. *Phytotaxa*, 217, 201–248.

Jovanovska, E., Cvetkoska, A., Hauffe, T., Levkov, Z., Wagner, B., Sulpizio, R., Francke, A., Albrecht, C. & Wilke, T. (2016) Differential resilience of ancient sister lakes Ohrid and Prespa to environmental disturbances during the Late Pleistocene. *Biogeosciences*, 13, 1149–1161.

Jovanovska, E. & Levkov, Z. (2020) The diatom genus *Diploneis* in the Republic of North Macedonia. In Lange-Bertalot, H. (ed) *Freshwater Diploneis. Two studies. Diatoms of Europe 9*. Ruggell: A.R.G. Gantner Verlag K.G., 527–689.

Juggins, S. (2020) *rioja: Analysis of Quaternary Science Data* [Software]. Available online: https://cran.r-project.org/package=rioja.

Julius, M. L. & Theriot, E. C. (2010) The diatoms: a primer. In Smol, J. P. & Stoermer, E. F. (eds) *The diatoms: applications for the environmental and earth sciences, 2nd edition*. Cambridge: Cambridge University Press, 8–22.

Kagalou, I., Tsimarakis, G. & Paschos, I. (2001) Water chemistry and biology in a shallow lake (Lake Pamvotis—Greece). Present state and perspectives. *Global Nest*, 3, 85–94.

Kagalou, I., Papastergiadou, E. & Leonardos, I. (2008) Long term changes in the eutrophication process in a shallow Mediterranean lake ecosystem of W. Greece: response after the reduction of external load. *Journal of Environmental Management*, 87, 497–506.

Kageyama, M., Roche, D. M., Nebout, N. C. & Alvarez-Solas, J. (2021) Rapid climate variability: description and mechanisms. In Ramstein, G., Landais, A., Bouttes, N., Sepulchre, P. & Govin, A. (eds) *Paleoclimatology. Frontiers in Earth Sciences*. Cham, Switzerland: Springer.

Kaštovský, J., Hauer, T., Mareš, J., Krautová, M., Bešta, T., Komárek, J., Desortová, B., Heteša, J., Hindáková, A. & Houk, V. (2010) A review of the alien and expansive species of freshwater cyanobacteria and algae in the Czech Republic. *Biological Invasions*, 12, 3599–3625.

Kelly, M. G., Penny, C. J. & Whitton, B. A. (1995) Comparative performance of benthic diatom indices used to assess river water quality. *Hydrobiologia*, 302, 179–188.

Kelts, K. & Hsü, K. J. (1978) Freshwater carbonate sedimentation. In Lerman, A. (ed) *Lakes: geology, chemistry and physics*. New York: Springer-Verlag, 295–323.

Kilham, P., Kilham, S. S. & Hecky, R. E. (1986) Hypothesized resource relationships among African planktonic diatoms. *Limnology and Oceanography*, 31, 1169–1181.

Kilham, S. S. & Kilham, P. (1975) *Melosira granulata* (Ehr.) Ralfs: morphology and ecology of a cosmopolitan freshwater diatom. *Verhandlungen der Internationalen Vereinigung Limnologie*, 19, 2716–2721.

Kindler, P., Guillevic, M., Baumgartner, M., Schwander, J., Landais, A. & Leuenberger, M. (2014) Temperature reconstruction from 10 to 120 kyr b2k from the NGRIP ice core. *Climate of the Past*, 10, 887–902.

King, G. & Bailey, G. (1985) The palaeoenvironment of some archaeological sites in Greece: the influence of accumulated uplift in a seismically active region. *Proceedings of the Prehistoric Society*, 51, 273–282.

King, G., Bailey, G. & Sturdy, D. (1994) Active tectonics and human survival strategies. *Journal of Geophysical Research*, 99, 20063–20078.

Kirillin, G., Leppäranta, M., Terzhevik, A., Granin, N., Bernhardt, J., Engelhardt, C., Efremova, T., Golosov, S., Palshin, N., Sherstyankin, P., Zdorovennova, G. & Zdorovennov, R. (2012) Physics of seasonally ice-covered lakes: a review. *Aquatic Sciences*, 74, 659–682.

Kiss, K. T., Le Cohu, R., Coste, M., Genkal, S. I. & Houk, V. (1990) *Actinocyclus normanii* (Bacillariophyceae), in some rivers and lakes in Europe. Morphological examinations and quantitative relations. In Ricard, M. (ed) *Ouvrage dédié à la mémoire du Professeur Henry Germain*. Königstein: Koeltz Scientific, 111–123.

Kiss, K. T., Rojo, C. & Alvarez Cobelas, M. (1996) Morphological variability of a *CyclotelIa ocellata* (Bacillariophyceae) population in the Lake Las Madres (Spain). *Algological Studies*, 82, 37–55.

Kiss, K. T., Klee, R. & Hegewald, E. (1999) Reinvestigation of the original material of *Cyclotella ocellata* Pantocsek (Bacillariophyceae). *Algological Studies*, 93, 39–53.

Kiss, K. T., Klee, R., Ector, L. & Ács, É. (2012) Centric diatoms of large rivers and tributaries in Hungary: morphology and biogeographic distribution. *Acta Botanica Croatica*, 71, 311–363.

Krammer, K. & Lange-Bertalot, H. (1986) *Süsswasserflora von Mitteleuropa. Bacillariophyceae. 1. Teil: Naviculaceae (Vol. 2/1)*. Stuttgart: Gustav Fischer Verlag.

Krammer, K. & Lange-Bertalot, H. (1988) *Süsswasserflora von Mitteleuropa. Bacillariophyceae. 2. Teil: Epithemiaceae, Bacillariaceae, Surirellaceae (Vol. 2/2)*. Stuttgart: Gustav Fischer Verlag.

Krammer, K. & Lange-Bertalot, H. (1991a) *Süsswasserflora von Mitteleuropa. Bacillariophyceae. 3. Teil: Centrales, Fragilariaceae, Eunotiaceae (Vol. 2/3)*. Stuttgart: Gustav Fischer Verlag.

Krammer, K. & Lange-Bertalot, H. (1991b) *Süsswasserflora von Mitteleuropa. Bacillariophyceae. 4. Teil: Achnanthaceae (Vol. 2/4)*. Stuttgart: Gustav Fischer Verlag.

Krammer, K. & Lange-Bertalot, H. (2000) *Süsswasserflora von Mitteleuropa. Bacillariophyceae. 5. English and French translation of the keys (Vol. 2/5)*. Stuttgart: Gustav Fischer Verlag.

Lacey, J. H. (2016) *Late Quaternary palaeoenvironmental reconstruction from Lake Ohrid*. PhD thesis. University of Nottingham.

Lacey, J. H., Leng, M. J., Francke, A., Sloane, H. J., Milodowski, A., Vogel, H., Baumgarten, H., Zanchetta, G. & Wagner, B. (2016) Northern Mediterranean climate since the Middle Pleistocene: a 637 ka stable isotope record from Lake Ohrid (Albania/Macedonia). *Biogeosciences*, 13, 1801–1820.

Lacey, J. H. & Jones, M. D. (2018) Quantitative reconstruction of early Holocene and last glacial climate on the Balkan Peninsula using coupled hydrological and isotope mass balance modelling. *Quaternary Science Reviews*, 202, 109–121.

Lambert, F., Bigler, M., Steffensen, J. P., Hutterli, M. & Fischer, H. (2012) Centennial mineral dust variability in high-resolution ice core data from Dome C, Antarctica. *Climate of the Past*, 8, 609–623.

Landais, A., Sánchez Goñi, M. F., Toucanne, S., Rodrigues, T. & Naughton, F. (2022) Chapter 24 - Abrupt climatic variability: Dansgaard–Oeschger events. In Palacios, D., Hughes, P. D., García-Ruiz, J. M. & Andrés, N. (eds) *European glacial landscapes*. Oxford: Elsevier, 175–180.

Lang, N. & Wolff, E. W. (2011) Interglacial and glacial variability from the last 800 ka in marine, ice and terrestrial archives. *Climate of the Past*, 7, 361–380.

Lange-Bertalot, H., Hofmann, G., Werum, M. & Cantonati, M. (2017) *Freshwater Benthic Diatoms of Central Europe: Over 800 Common Species Used in Ecological Assessment. English edition with updated taxonomy and added species.* Oberreifenberg: Koeltz Botanical Books.

Lawson, I. T., Frogley, M. R., Bryant, C. L., Preece, R. C. & Tzedakis, P. C. (2004) The Lateglacial and Holocene environmental history of the Ioannina basin, north-west Greece. *Quaternary Science Reviews*, 23, 1599–1625.

Lee, J.-Y., Marotzke, J., Bala, G., Cao, L., Corti, S., Dunne, J. P., Engelbrecht, F., Fischer, E., Fyfe, J. C., Jones, C., Maycock, A., Mutemi, J., Ndiaye, O., Panickal, S. & Zhou, T. (2021) Future global climate: scenario-based projections and near-term information. In Masson-Delmotte, V., Zhai, P., Pirani, A., Connors, S. L., Péan, C., Berger, S., Caud, N., Chen, Y., Goldfarb, L., Gomis, M. I., Huang, M., Leitzell, K., Lonnoy, E., Matthews, J. B. R., Maycock, T. K., Waterfield, T., Yelekçi, O., Yu, R. & Zhou, B. (eds) *Climate change 2021: the physical science basis. Contribution of Working Group I to the Sixth Assessment Report of the Intergovernmental Panel on Climate Change*. Cambridge University Press. In Press.

Legendre, P. & Birks, H. J. B. (2012) From classical to canonical ordination. In Birks, H. J. B., Lotter, A. F., Juggins, S. & Smol, J. P. (eds) *Tracking environmental change using*

lake sediments, Volume 5: Data handling and numerical techniques. Dordrecht: Springer, 201–248.

Legendre, P. & Legendre, L. (2012) *Numerical Ecology*. Developments in Environmental Modelling, Third English Edition edition. Oxford: Elsevier.

Leicher, N., Zanchetta, G., Sulpizio, R., Giaccio, B., Wagner, B., Nomade, S., Francke, A. & Carlo, P. D. (2016) First tephrostratigraphic results of the DEEP site record from Lake Ohrid (Macedonia and Albania). *Biogeosciences*, 13, 2151–2178.

Leng, M. J., Jones, M. D., Frogley, M. R., Eastwood, W. J., Kendrick, C. P. & Roberts, C. N. (2010) Detrital carbonate influences on bulk oxygen and carbon isotope composition of lacustrine sediments from the Mediterranean. *Global and Planetary Change*, 71, 175–182.

Leps, J. & Šmilauer, P. (2003) *Multivariate Analysis of Ecological Data using CANOCO*. Cambridge: Cambridge University Press.

Levkov, Z. & Williams, D. M. (2006) Two new species of *Diatoma* from Lakes Ohrid and Prespa, Macedonia. *Diatom Research*, 21, 281–296.

Levkov, Z., Krstic, S., Metzeltin, D. & Nakov, T. (2007a) *Diatoms of Lakes Prespa and Ohrid. About 500 taxa from ancient lake system*. Iconographia diatomologica, volume 16. Ruggell: A.R.G. Gantner Verlag K.G.

Levkov, Z., Blanco, S., Krstic, S., Nakov, T. & Ector, L. (2007b) Ecology of benthic diatoms from Lake Macro Prespa (Macedonia). *Algological Studies*, 124, 71–83.

Levkov, Z. & Williams, D. M. (2011) Fifteen new diatom (Bacillariophyta) species from Lake Ohrid, Macedonia. *Phytotaxa*, 30, 1–41.

Li, Y.-L., Gong, Z.-J., Wang, C.-C. & Shen, J. (2010) New species and new records of diatoms from Lake Fuxian, China. *Journal of Systematics and Evolution*, 48, 65–72.

Lindhorst, K., Krastel, S., Reicherter, K., Stipp, M., Wagner, B. & Schwenk, T. (2015) Sedimentary and tectonic evolution of Lake Ohrid (Macedonia/Albania). *Basin Research*, 27, 84–101.

Lionello, P. & Scarascia, L. (2018) The relation between climate change in the Mediterranean region and global warming. *Regional Environmental Change*, 18, 1481–1493.

Lisiecki, L. E. & Raymo, M. E. (2005) A Pliocene-Pleistocene stack of 57 globally distributed benthic $\delta^{18}O$ records. *Paleoceanography*, 20, PA1003.

Litt, T., Pickarski, N., Heumann, G., Stockhecke, M. & Tzedakis, P. C. (2014) A 600,000 year long continental pollen record from Lake Van, eastern Anatolia (Turkey). *Quaternary Science Reviews*, 104, 30–41.

Liu, Y., Fu, C., Wang, Q. & Stoermer, E. F. (2010) A new species, *Diatoma rupestris*, from the Great Xing'an Mountains, China. *Diatom Research*, 25, 337–347.

Lolis, C. J. & Kotsias, G. (2020) The use of weather types in the definition of seasons: the case of southern Balkans. *Theoretical and Applied Climatology*, 142, 1199–1219.

Lorenschat, J., Zhang, X., Anselmetti, F. S., Reed, J. M., Wessels, M. & Schwalb, A. (2014) Recent anthropogenic impact in ancient Lake Ohrid (Macedonia/Albania): a palaeolimnological approach. *Journal of Paleolimnology*, 52, 139–154.

Lotter, A. F., Pienitz, R. & Schmidt, R. (2010) Diatoms as indicators of environmental change in subarctic and alpine regions. In Smol, J. P. & Stoermer, E. F. (eds) *The diatoms: applications for the environmental and earth sciences, 2nd edition*. Cambridge: Cambridge University Press, 231–248.

Lowe, J. & Walker, M. (2015) *Reconstructing quaternary environments*. London: Routledge.

Luethje, M. & Snyder, J. (2021) Climate-related morphological changes in *Pantocsekiella* (Mediophyceae) spanning 0–1.2 Ma in the Lake El'gygytgyn,

northeastern Russia including *Pantocsekiella elgygytgynensis* sp. nov. *Phytotaxa*, 478, 67–91.

Mackay, A. W., Edlund, M. B. & Khursevich, G. (2010) Diatoms in ancient lakes. In Smol, J. P. & Stoermer, E. F. (eds) *The diatoms: Applications for the environmental and earth sciences, 2nd edition*. Cambridge: Cambridge University Press, 209–228.

Magny, M., Combourieu-Nebout, N., de Beaulieu, J. L., Bout-Roumazeilles, V., Colombaroli, D., Desprat, S., Francke, A., Joannin, S., Ortu, E., Peyron, O., Revel, M., Sadori, L., Siani, G., Sicre, M. A., Samartin, S., Simonneau, A., Tinner, W., Vanniere, B., Wagner, B., Zanchetta, G., Anselmetti, F., Brugiapaglia, E., Chapron, E., Debret, M., Desmet, M., Didier, J., Essallami, L., Galop, D., Gilli, A., Haas, J. N., Kallel, N., Millet, L., Stock, A., Turon, J. L. & Wirth, S. (2013) North-south palaeohydrological contrasts in the central Mediterranean during the Holocene: tentative synthesis and working hypotheses. *Climate of the Past*, 9, 2043–2071.

Magri, D. (1994) Late-Quaternary changes of plant biomass as recorded by pollen-stratigraphical data: a discussion of the problem at Valle di Castiglione, Italy. *Review of Palaeobotany and Palynology*, 81, 313–325.

Magri, D. & Tzedakis, P. C. (2000) Orbital signatures and long-term vegetation patterns in the Mediterranean. *Quaternary International*, 73, 69–78.

Magri, D., Di Rita, F., Aranbarri, J., Fletcher, W. & González-Sampériz, P. (2017) Quaternary disappearance of tree taxa from Southern Europe: timing and trends. *Quaternary Science Reviews*, 163, 23–55.

Margari, V., Gibbard, P. L., Bryant, C. L. & Tzedakis, P. C. (2009) Character of vegetational and environmental changes in southern Europe during the last glacial period; evidence from Lesvos Island, Greece. *Quaternary Science Reviews*, 28, 1317–1339.

Margari, V., Skinner, L. C., Tzedakis, P. C., Ganopolski, A., Vautravers, M. & Shackleton, N. J. (2010) The nature of millennial-scale climate variability during the past two glacial periods. *Nature Geoscience*, 3, 127–131.

Margari, V., Skinner, L. C., Hodell, D. A., Martrat, B., Toucanne, S., Grimalt, J. O., Gibbard, P. L., Lunkka, J. P. & Tzedakis, P. C. (2014) Land-ocean changes on orbital and millennial time scales and the penultimate glaciation. *Geology*, 42, 183–186.

Martrat, B., Grimalt, J. O., Lopez-Martinez, C., Cacho, I., Sierro, F. J., Flores, J. A., Zahn, R., Canals, M., Curtis, J. H. & Hodell, D. A. (2004) Abrupt temperature changes in the Western Mediterranean over the past 250,000 years. *Science*, 306, 1762–1765.

Martrat, B., Grimalt, J. O., Shackleton, N. J., de Abreu, L. , Hutterli, M. A. & Stocker, T. F. (2007) Four climate cycles of recurring deep and surface water destabilizations on the Iberian margin. *Science*, 317, 502–507.

Maslin, M. (2016) Forty years of linking orbits to ice ages. *Nature*, 540, 208–209.

Maslin, M. A. & Brierley, C. M. (2015) The role of orbital forcing in the Early Middle Pleistocene Transition. *Quaternary International*, 389, 47–55.

Matevski, V., Čarni, A., Avramovski, O., Juvan, N., Kostadinovski, M., Košir, P., Marinšek, A., Paušic, A. & Šilc, U. (2011) *Forest Vegetation of the Galicica Mountain Range in Macedonia*. Ljubljana: Založba ZRC.

Matzinger, A., Veljanoska-Sarafiloska, E., Jordanoski, M. & Naumoski, T. (2004) Lake Ohrid—a unique ecosystem endangered by eutrophication? *International Conference on Water Observation and Information System for Decision Support.* Ohrid, 25–29 May.

Matzinger, A., Spirkovski, Z., Patceva, S. & Wuest, A. (2006a) Sensitivity of ancient Lake Ohrid to local anthropogenic impacts and global warming. *Journal of Great Lakes Research*, 32, 158–179.

Matzinger, A., Jordanoski, M., Veljanoska-Sarafiloska, E., Sturm, M., Muller, B. & Wuest, A. (2006b) Is Lake Prespa jeopardizing the ecosystem of ancient Lake Ohrid? *Hydrobiologia*, 553, 89–109.

Matzinger, A., Schmid, M., Veljanoska-Sarafiloska, E., Patceva, S., Guseska, D., Wagner, B., Muller, B., Sturm, M. & Wuest, A. (2007) Eutrophication of ancient Lake Ohrid: global warming amplifies detrimental effects of increased nutrient inputs. *Limnology and Oceanography*, 52, 338–353.

Maxbauer, D. P., Feinberg, J. M. & Fox, D. L. (2016) Magnetic mineral assemblages in soils and paleosols as the basis for paleoprecipitation proxies: a review of magnetic methods and challenges. *Earth-Science Reviews*, 155, 28–48.

McGuire, A. M., Lane, C. S., Roucoux, K. H., Albert, P. G. & Kearney, R. (2022) The dating and correlation of an eastern Mediterranean lake sediment sequence: a 46–4 ka tephrostratigraphy for Ioannina (NW Greece). *Journal of Quaternary Science*, 1–19.

McManus, J. F., Oppo, D. W. & Cullen, J. L. (1999) A 0.5-million-year record of millennial-scale climate variability in the North Atlantic. *Science*, 283, 971–975.

Menviel, L. C., Skinner, L. C., Tarasov, L. & Tzedakis, P. C. (2020) An ice–climate oscillatory framework for Dansgaard–Oeschger cycles. *Nature Reviews Earth & Environment*, 1, 677–693.

Merkel, A. (2018) *Climate Data for Cities Worldwide—Ohrid Climate (Macedonia)*. Available online: https://en.climate-data.org/europe/macedonia/ohrid/ohrid-715042/ [Accessed 2018-05-24].

Meyers, P. A. & Teranes, J. L. (2001) Sediment organic matter. In Last, W. M. & Smol, J. P. (eds) *Tracking environmental change using lake sediments, Volume 2: physical and geochemical methods*. Dordrecht: Springer, 239–269.

Michel, B. & Ramseier, R. O. (1971) Classification of river and lake ice. *Canadian Geotechnical Journal*, 8, 36–45.

Müller, U. (1999) The vertical zonation of adpressed diatoms and other epiphytic algae on *Phragmites australis*. *European Journal of Phycology*, 34, 487–496.

North Greenland Ice Core Project members (2004) High-resolution record of Northern Hemisphere climate extending into the last interglacial period. *Nature*, 431, 147–151.

North Greenland Ice Core Project members (2007) *50 year means of oxygen isotope data from ice core NGRIP*, PANGAEA. Available online: https://doi.org/10.1594/PANGAEA.586886 [Accessed 2021-12-22].

Obrochta, S. P., Crowley, T. J., Channell, J. E. T., Hodell, D. A., Baker, P. A., Seki, A. & Yokoyama, Y. (2014) Climate variability and ice-sheet dynamics during the last three glaciations. *Earth and Planetary Science Letters*, 406, 198–212.

Oksanen, J., Blanchet, F. G., Friendly, M., Kindt, R., Legendre, P., McGlinn, D., Minchin, P. R., O'Hara, R. B., Simpson, G. L., Solymos, P., Stevens, M. H. H., Szoecs, E. & Wagner, H. (2019) *vegan: Community Ecology Package* [Software]. Available online: https://CRAN.R-project.org/package=vegan.

Oppo, D. W., McManus, J. F. & Cullen, J. L. (2006) Evolution and demise of the Last Interglacial warmth in the subpolar North Atlantic. *Quaternary Science Reviews*, 25, 3268–3277.

Panagiotopoulos, K. (2013) *Late Quaternary ecosystem and climate interactions in SW Balkans inferred from Lake Prespa sediments*. Universität zu Köln.

Pantocsek, J. (1902) A Balatoni kovamoszatok [The diatoms of Lake Balaton]. In Lóczy, L. (ed) *A Balaton tudományos tanulmányozásának eredményei II. Kötet: A Balaton tónak és partjainak biologiája [Results of the scientific study of Lake Balaton, Volume 2: Biology of Lake Balaton and its shores]*. Budapest: A Magyar Földrajzi Társaság Balaton-Bizottsága [The Balaton Committee of the Hungarian Geographical Society].

Passy, S. I. (2007) Diatom ecological guilds display distinct and predictable behavior along nutrient and disturbance gradients in running waters. *Aquatic botany*, 86, 171–178.

Past Interglacials Working Group of PAGES (2016) Interglacials of the last 800,000 years. *Reviews of Geophysics*, 54, 162–219.

Peltier, W. R. & Vettoretti, G. (2014) Dansgaard‑Oeschger oscillations predicted in a comprehensive model of glacial climate: a "kicked" salt oscillator in the Atlantic. *Geophysical Research Letters*, 41, 7306–7313.

Peppa, M., Vasilakos, C. & Kavroudakis, D. (2020) Eutrophication monitoring for Lake Pamvotis, Greece, using Sentinel-2 data. *International Journal of Geo-Information*, 9, 143.

Pérez-Martínez, C. & Cruz-Pizarro, L. (1992) Auxosporulation in *Cyclotella ocellata* (Bacillariophyceae) under natural and experimental conditions. *Journal of Phycology*, 28, 608–615.

Pérez-Mejías, C., Moreno, A., Sancho, C., Bartolomé, M., Stoll, H., Cacho, I., Cheng, H. & Edwards, R. L. (2017) Abrupt climate changes during Termination III in Southern Europe. *Proceedings of the National Academy of Sciences of the United States of America*, 114, 10047–10052.

Petit, J. R., Jouzel, J., Raynaud, D., Barkov, N. I., Barnola, J. M., Basile, I., Bender, M., Chappellaz, J., Davis, M., Delaygue, G., Delmotte, M., Kotlyakov, V. M., Legrand, M., Lipenkov, V. Y., Lorius, C., Pépin, L., Ritz, C., Saltzman, E. & Stievenard, M. (1999) Climate and atmospheric history of the past 420,000 years from the Vostok ice core, Antarctica. *Nature*, 399, 429–436.

Pillans, B. & Naish, T. (2004) Defining the Quaternary. *Quaternary Science Reviews*, 23, 2271–2282.

Pithan, F. & Mauritsen, T. (2014) Arctic amplification dominated by temperature feedbacks in contemporary climate models. *Nature Geoscience*, 7, 181–184.

Popovska, C. & Bonacci, O. (2007) Basic data on the hydrology of Lakes Ohrid and Prespa. *Hydrological Processes*, 21, 658–664.

Potapova, M. & Snoeijs, P. (1997) The natural life cycle in wild populations of *Diatoma moniliformis* (Bacillariophyceae) and its disruption in an aberrant environment. *Journal of Phycology*, 33, 924–937.

Prentice, I. C. (1985) Pollen representation, source area, and basin size: toward a unified theory of pollen analysis. *Quaternary Research*, 23, 76–86.

Pross, J., Christanis, K., Fischer, T., Fletcher, W. J., Hardiman, M., Kalaitzidis, S., Knipping, M., Kotthoff, U., Milner, A. M. & Muller, U. C. (2015) The 1.35-Ma-long terrestrial climate archive of Tenaghi Philippon, northeastern Greece: evolution, exploration, and perspectives for future research. *Newsletters on Stratigraphy*, 48, 253–276.

Punning, J.-M. & Puusepp, L. (2007) Diatom assemblages in sediments of Lake Juusa, Southern Estonia with an assessment of their habitat. *Hydrobiologia*, 586, 27–41.

R Core Team (2021) *R: a language and environment for statistical computing* [Software]. Available online: https://www.R-project.org/.

Rahmstorf, S. (2002) Ocean circulation and climate during the past 120,000 years. *Nature*, 419, 207–214.

Raicich, F., Pinardi, N. & Navarra, A. (2003) Teleconnections between Indian monsoon and Sahel rainfall and the Mediterranean. *International Journal of Climatology*, 23, 173–186.

Rasmussen, S. O., Bigler, M., Blockley, S. P., Blunier, T., Buchardt, S. L., Clausen, H. B., Cvijanovic, I., Dahl-Jensen, D., Johnsen, S. J., Fischer, H., Gkinis, V., Guillevic, M., Hoek, W. Z., Lowe, J. J., Pedro, J. B., Popp, T., Seierstad, I. K., Steffensen, J. P.,

Svensson, A. M., Vallelonga, P., Vinther, B. M., Walker, M. J. C., Wheatley, J. J. & Winstrup, M. (2014) A stratigraphic framework for abrupt climatic changes during the Last Glacial period based on three synchronized Greenland ice-core records: refining and extending the INTIMATE event stratigraphy. *Quaternary Science Reviews*, 106, 14–28.

Reavie, E. D. & Cai, M. (2019) Consideration of species-specific diatom indicators of anthropogenic stress in the Great Lakes. *PloS one*, 14, e0210927.

Reed, J. M. (1998) Diatom preservation in the recent sediment record of Spanish saline lakes: implications for palaeoclimate study. *Journal of Paleolimnology*, 19, 129–137.

Reed, J. M., Krystufek, B. & Eastwood, W. J. (2004) The physical geography of the Balkans and nomenclature of place names. In Griffiths, H. I., Kryštufek, B. & Reed, J. M. (eds) *Balkan Biodiversity: Pattern and Process in the European Hotspot*. Dordrecht: Kluwer Academic Publishers, 9–22.

Reed, J. M., Cvetkoska, A., Levkov, Z., Vogel, H. & Wagner, B. (2010) The last glacial-interglacial cycle in Lake Ohrid (Macedonia/Albania): testing diatom response to climate. *Biogeosciences*, 7, 3083–3094.

Regattieri, E., Zanchetta, G., Isola, I., Bajo, P., Perchiazzi, N., Drysdale, R. N., Boschi, C., Hellstrom, J. C., Francke, A. & Wagner, B. (2018) A MIS 9/MIS 8 speleothem record of hydrological variability from Macedonia (FYROM). *Global and planetary change*, 162, 39–52.

Reicherter, K., Hoffmann, N., Lindhorst, K., Krastel, S., Fernandez-Steeger, T., Grutzner, C. & Wiatr, T. (2011) Active basins and neotectonics: morphotectonics of the Lake Ohrid Basin (FYROM and Albania). *Zeitschrift Der Deutschen Gesellschaft Fur Geowissenschaften*, 162, 217–234.

Reille, M., Andrieu, V., de Beaulieu, J.-L., Guenet, P. & Goeury, C. (1998) A long pollen record from Lac du Bouchet, Massif Central, France: for the period ca. 325 to 100 ka BP (OIS 9c to OIS 5e). *Quaternary Science Reviews*, 17, 1107–1123.

Rimet, F., Druart, J.-C. & Anneville, O. (2009) Exploring the dynamics of plankton diatom communities in Lake Geneva using emergent self-organizing maps (1974–2007). *Ecological Informatics*, 4, 99–110.

Roberts, N., Jones, M. D., Benkaddour, A., Eastwood, W. J., Filippi, M. L., Frogley, M. R., Lamb, H. F., Leng, M. J., Reed, J. M., Stein, M., Stevens, L., Valero-Garcés, B. & Zanchetta, G. (2008) Stable isotope records of Late Quaternary climate and hydrology from Mediterranean lakes: the ISOMED synthesis. *Quaternary Science Reviews*, 27, 2426–2441.

Roberts, N., Eastwood, W. J., Kuzucuoğlu, C., Fiorentino, G. & Caracuta, V. (2011a) Climatic, vegetation and cultural change in the eastern Mediterranean during the mid-Holocene environmental transition. *The Holocene*, 21, 147–162.

Roberts, N., Brayshaw, D., Kuzucuoğlu, C., Perez, R. & Sadori, L. (2011b) The mid-Holocene climatic transition in the Mediterranean: causes and consequences. *The Holocene*, 21, 3–13.

Roberts, N., Moreno, A., Valero-Garcés, B. L., Corella, J. P., Jones, M., Allcock, S., Woodbridge, J., Morellón, M., Luterbacher, J., Xoplaki, E. & Türkeş, M. (2012) Palaeolimnological evidence for an east–west climate see-saw in the Mediterranean since AD 900. *Global and Planetary Change*, 84–85, 23–34.

Rodrigues, T., Alonso-García, M., Hodell, D. A., Rufino, M., Naughton, F., Grimalt, J. O., Voelker, A. H. L. & Abrantes, F. (2017) A 1-Ma record of sea surface temperature and extreme cooling events in the North Atlantic: a perspective from the Iberian Margin. *Quaternary Science Reviews*, 172, 118–130.

Roelofs, A. K. & Kilham, P. (1983) The diatom stratigraphy and palaeoecology of Lake Ohrid, Yugoslavia. *Palaeogeography, Palaeoclimatology, Palaeoecology*, 42, 225–245.

Romero, J. R., Kagalou, I., Imberger, J., Hela, D., Kotti, M., Bartzokas, A., Albanis, T., Evmirides, N., Karkabounas, S., Papagiannis, J. & Bithava, A. (2002) Seasonal water

quality of shallow and eutrophic Lake Pamvotis, Greece: implications for restoration. *Hydrobiologia*, 474, 91–105.

Roucoux, K. H., de Abreu, L., Shackleton, N. J. & Tzedakis, P. C. (2005) The response of NW Iberian vegetation to North Atlantic climate oscillations during the last 65 kyr. *Quaternary Science Reviews*, 24, 1637–1653.

Roucoux, K. H., Tzedakis, P. C., de Abreu, L. & Shackleton, N. J. (2006) Climate and vegetation changes 180,000 to 345,000 years ago recorded in a deep-sea core off Portugal. *Earth and Planetary Science Letters*, 249, 307–325.

Roucoux, K. H., Tzedakis, P. C., Frogley, M. R., Lawson, I. T. & Preece, R. C. (2008) Vegetation history of the marine isotope stage 7 interglacial complex at Ioannina, NW Greece. *Quaternary Science Reviews*, 27, 1378–1395.

Roucoux, K. H., Tzedakis, P. C., Lawson, I. T. & Margari, V. (2011) Vegetation history of the penultimate glacial period (Marine Isotope Stage 6) at Ioannina, northwest Greece. *Journal of Quaternary Science*, 26, 616–626.

Round, F. E., Crawford, R. M. & Mann, D. G. (1990) *The Diatoms. Biology and morphology of the genera*. Cambridge: Cambridge University Press.

Rühland, K. M., Paterson, A. M. & Smol, J. P. (2015) Lake diatom responses to warming: reviewing the evidence. *Journal of Paleolimnology*, 54, 1–35.

Ryves, D. B., Juggins, S., Fritz, S. C. & Battarbee, R. W. (2001) Experimental diatom dissolution and the quantification of microfossil preservation in sediments. *Palaeogeography, Palaeoclimatology, Palaeoecology*, 172, 99–113.

Ryves, D. B., Jewson, D. H., Sturm, M., Battarbee, R. W., Flower, R. J., Mackay, A. W. & Granin, N. G. (2003) Quantitative and qualitative relationships between planktonic diatom communities and diatom assemblages in sedimenting material and surface sediments in Lake Baikal, Siberia. *Limnology and Oceanography*, 48, 1643–1661.

Ryves, D. B., Battarbee, R. W., Juggins, S., Fritz, S. C. & Anderson, N. J. (2006) Physical and chemical predictors of diatom dissolution in freshwater and saline lake sediments in North America and West Greenland. *Limnology and Oceanography*, 51, 1355–1368.

Sadori, L., Koutsodendris, A., Panagiotopoulos, K., Masi, A., Bertini, A., Combourieu-Nebout, N., Francke, A., Kouli, K., Joannin, S., Mercuri, A. M., Peyron, O., Torri, P., Wagner, B., Zanchetta, G., Sinopoli, G. & Donders, T. H. (2016) Pollen-based paleoenvironmental and paleoclimatic change at Lake Ohrid (southeastern Europe) during the past 500 ka. *Biogeosciences*, 13, 1423–1437.

Santer, B. D., Po-Chedley, S., Zelinka, M. D., Cvijanovic, I., Bonfils, C., Durack, P. J., Fu, Q., Kiehl, J., Mears, C., Painter, J., Pallotta, G., Solomon, S., Wentz, F. J. & Zou, C.-Z. (2018) Human influence on the seasonal cycle of tropospheric temperature. *Science*, 361, eaas8806.

Saros, J. E., Michel, T. J., Interlandi, S. J. & Wolfe, A. P. (2005) Resource requirements of Asterionella formosa and Fragilaria crotonensis in oligotrophic alpine lakes: implications for recent phytoplankton community reorganizations. *Canadian Journal of Fisheries and Aquatic Sciences*, 62, 1681–1689.

Saros, J. E., Clow, D. W., Blett, T. & Wolfe, A. P. (2011) Critical nitrogen deposition loads in high-elevation lakes of the western US inferred from paleolimnological records. *Water, Air, & Soil Pollution*, 216, 193–202.

Saros, J. E. & Anderson, N. J. (2015) The ecology of the planktonic diatom *Cyclotella* and its implications for global environmental change studies. *Biological Reviews*, 90, 522–541.

Sayer, C. D. (2001) Problems with the application of diatom-total phosphorus transfer functions: examples from a shallow English lake. *Freshwater Biology*, 46, 743–757.

Schallenberg, M. & Burns, C. W. (2004) Effects of sediment resuspension on phytoplankton production: teasing apart the influences of light, nutrients and algal entrainment. *Freshwater Biology*, 49, 143–159.

Scheffer, M. & van Nes, E. H. (2007) Shallow lakes theory revisited: various alternative regimes driven by climate, nutrients, depth and lake size *Shallow lakes in a changing world* Springer, 455–466.

Schlegel, I. & Scheffler, W. (1999) Seasonal development and morphological variability of *Cyclotella ocellata* (Bacillariophyceae) in the eutrophic Lake Dagow (Germany). *International Review of Hydrobiology*, 84, 469–478.

Schulz, H., von Rad, U. & Erlenkeuser, H. (1998) Correlation between Arabian Sea and Greenland climate oscillations of the past 110,000 years. *Nature*, 393, 54–57.

Seneviratne, S. I., Donat, M. G., Pitman, A. J., Knutti, R. & Wilby, R. L. (2016) Allowable CO_2 emissions based on regional and impact-related climate targets. *Nature*, 529, 477–483.

Serôdio, J. (2021) Diatom motility: mechanisms, control and adaptive value. In Cohn, S. A., Manoylov, K. M. & Gordon, R. (eds) *Diatom gliding motility. Diatoms: biology and applications*. Beverly, MA, USA: Scrivener Publishing, 159–184.

Shackleton, N. J. (1967) Oxygen isotope analyses and Pleistocene temperatures re-assessed. *Nature*, 215, 15–17.

Shakun, J. D., Lea, D. W., Lisiecki, L. E. & Raymo, M. E. (2015) An 800-kyr record of global surface ocean $\delta^{18}O$ and implications for ice volume-temperature coupling. *Earth and Planetary Science Letters*, 426, 58–68.

Siddall, M., Stocker, T. F., Blunier, T., Spahni, R., Schwander, J., Barnola, J. M. & Chappellaz, J. (2007) Marine Isotope Stage (MIS) 8 millennial variability stratigraphically identical to MIS 3. *Paleoceanography*, 22, PA1208.

Sivarajah, B., Rühland, K. M., Labaj, A. L., Paterson, A. M. & Smol, J. P. (2016) Why is the relative abundance of *Asterionella formosa* increasing in a Boreal Shield lake as nutrient levels decline? *Journal of Paleolimnology*, 55, 357–367.

Smol, J. P. (1988) Paleoclimate proxy data from freshwater arctic diatoms. *Verhandlungen der Internationalen Vereinigung Limnologie*, 23, 837–844.

Smol, J. P., Birks, H. J. B. & Last, W. M. (2001) Using biology to study long-term environmental change. In Smol, J. P., Birks, H. J. B. & Last, W. M. (eds) *Tracking environmental change using lake sediments, Volume 3: terrestrial, algal, and siliceous indicators*. Dordrecht: Kluwer Academic Publishers, 2–3.

Smol, J. P. (2008) *The pollution of lakes and rivers: a paleoenvironmental perspective*. 2nd edition. Oxford: Blackwell.

Smol, J. P. & Stoermer, E. F. (2010) Applications and uses of diatoms: prologue. In Smol, J. P. & Stoermer, E. F. (eds) *The diatoms: applications for the environmental and earth sciences, 2nd edition*. Cambridge: Cambridge University Press, 3–7.

Spooner, I., Douglas, M. S. V. & Terrusi, L. (2002) Multiproxy evidence of an early Holocene (8.2 kyr) climate oscillation in central Nova Scotia, Canada. *Journal of Quaternary Science*, 17, 639–645.

Spratt, R. M. & Lisiecki, L. E. (2016) A Late Pleistocene sea level stack. *Climate of the Past*, 12, 1079–1092.

Stanković, S. (1960) *The Balkan Lake Ohrid and its living world*. Monographiae biologicae, volume IX. The Hague, Netherlands: Dr. W. Junk.

Stefanidis, K. & Papastergiadou, E. (2007) Aquatic vegetation and related abiotic environment in a shallow urban lake of Greece. *Belgian Journal of Botany*, 140, 25–38.

Stelbrink, B., Jovanovska, E., Levkov, Z., Ognjanova-Rumenova, N., Wilke, T. & Albrecht, C. (2018) Diatoms do radiate: evidence for a freshwater species flock. *Journal of Evolutionary Biology*, 31, 1969–1975.

Stone, J. R. & Fritz, S. C. (2004) Three-dimensional modeling of lacustrine diatom habitat areas: improving paleolimnological interpretation of planktic : benthic ratios. *Limnology and Oceanography*, 49, 1540–1548.

Stone, J. R., Westover, K. S. & Cohen, A. S. (2011) Late Pleistocene paleohydrography and diatom paleoecology of the central basin of Lake Malawi, Africa. *Palaeogeography, Palaeoclimatology, Palaeoecology*, 303, 51–70.

Sutton, R. T., Dong, B. & Gregory, J. M. (2007) Land/sea warming ratio in response to climate change: IPCC AR4 model results and comparison with observations. *Geophysical Research Letters*, 34, L02701.

Talevska, M., Petrovic, D., Milosevic, D., Talevski, T., Maric, D. & Talevska, A. (2009) Biodiversity of macrophyte vegetation from Lake Prespa, Lake Ohrid and Lake Skadar. *Biotechnology & Biotechnological Equipment*, 23, 931–935.

Teubner, K. (1995) A light microscopical investigation and multivariate statistical analyses of heterovalvar cells of *Cyclotella*-species Bacillariophyceae) from lakes of the Berlin-Brandenburg region. *Diatom Research*, 10, 191–205.

Thompson, R., Battarbee, R. W., O'Sullivan, P. E. & Oldfield, F. (1975) Magnetic susceptibility of lake sediments. *Limnology and Oceanography*, 20, 687–698.

Thompson, R., Bloemendal, J., Dearing, J. A., Oldfield, F., Rummery, T. A., Stober, J. C. & Turner, G. M. (1980) Environmental applications of magnetic measurements. *Science*, 207, 481–486.

Thompson, R. & Oldfield, F. (1986) *Environmental magnetism*. London: Allen & Unwin.

Tiffany, M. A. & Lange, C. B. (2002) Diatoms provide attachment sites for other diatoms: a natural history of epiphytism from southern California. *Phycologia*, 41, 116–124.

Tiffany, M. A. (2011) Epizoic and epiphytic diatoms. In Seckbach, J. & Kociolek, J. P. (eds) *The diatom world. Cellular origin, life in extreme habitats and astrobiology volume 19.* Dordrecht: Springer, 195–209.

Tofilovska, S., Cvetkoska, A., Jovanovska, E., Ognjanova-Rumenova, N. & Levkov, Z. (2016) Two new fossil *Cyclotella* (Kützing) Brébisson species from Lake Ohrid, Macedonia/Albania. *Fottea*, 16, 218–233.

Tzedakis, P. C. (1993) Long-term tree populations in northwest Greece through multiple Quaternary climatic cycles. *Nature*, 364, 437–440.

Tzedakis, P. C. (1994) Vegetation change through glacial–interglacial cycles: a long pollen sequence perspective. *Philosophical Transactions of the Royal Society B. Biological Sciences.*, 345, 403–432.

Tzedakis, P. C., Andrieu, V., de Beaulieu, J.-L., Crowhurst, S., Follieri, M., Hooghiemstra, H., Magri, D., Reille, M., Sadori, L. & Shackleton, N. J. (1997) Comparison of terrestrial and marine records of changing climate of the last 500,000 years. *Earth and Planetary Science Letters*, 150, 171–176.

Tzedakis, P. C. (2000) Vegetation variability in Greece during the last interglacial. *Netherlands Journal of Geosciences*, 79, 355–367.

Tzedakis, P. C., Lawson, I. T., Frogley, M. R., Hewitt, G. M. & Preece, R. C. (2002a) Buffered tree population changes in a Quaternary refugium: evolutionary implications. *Science*, 297, 2044–2047.

Tzedakis, P. C., Lawson, I. T., Frogley, M. R., Hewitt, G. M. & Preece, R. C. (2002b) Buffered tree population changes in a Quaternary refugium: evolutionary implications. *Science*, 297, 2044–2047.

Tzedakis, P. C., Frogley, M. R. & Heaton, T. H. E. (2002c) Duration of Last Interglacial conditions in northwestern Greece. *Quaternary Research*, 58, 53–55.

Tzedakis, P. C., Frogley, M. R. & Heaton, T. H. E. (2003) Last Interglacial conditions in southern Europe: evidence from Ioannina, northwest Greece. *Global and Planetary Change*, 36, 157–170.

Tzedakis, P. C., Hooghiemstra, H. & Pälike, H. (2006) The last 1.35 million years at Tenaghi Philippon: revised chronostratigraphy and long-term vegetation trends. *Quaternary Science Reviews*, 25, 3416–3430.

Tzedakis, P. C. (2009) Cenozoic climate and vegetation change. In Woodward, J. C. (ed) *The physical geography of the Mediterranean*. Oxford: Oxford University Press, 89–137.

Tzedakis, P. C., Raynaud, D., McManus, J. F., Berger, A., Brovkin, V. & Kiefer, T. (2009a) Interglacial diversity. *Nature Geoscience*, 2, 751–755.

Tzedakis, P. C., Palike, H., Roucoux, K. H. & de Abreu, L. (2009b) Atmospheric methane, southern European vegetation and low-mid latitude links on orbital and millennial timescales. *Earth and Planetary Science Letters*, 277, 307–317.

Tzedakis, P. C., Crucifix, M., Mitsui, T. & Wolff, E. W. (2017) A simple rule to determine which insolation cycles lead to interglacials. *Nature*, 542, 427–432.

Verosub, K. L. & Roberts, A. P. (1995) Environmental magnetism: past, present, and future. *Journal of Geophysical Research*, 100, 2175–2192.

Vidaković, D., Krizmanić, J., Subakov-Simić, G. & Karadžić, V. (2016) Distribution of invasive species *Actinocyclus normanii* (Hemidiscaceae, Bacillariophyta) in Serbia. *Studia Botanica Hungarica*, 47, 201–212.

Vidal, L. A., Castro, L. E., Rodríguez-Barrios, J., Vélez, M. I. & Rangel, O. (2018) Sizes of the centric diatom *Actinocyclus normanii* as salinity function, a new tool for the assessment of paleoenvironments. *Revista de la Academia Colombiana de Ciencias Exactas, Físicas y Naturales*, 42, 330–342.

Voelker, A. H. L. (2002) Global distribution of centennial-scale records for Marine Isotope Stage (MIS) 3: a database. *Quaternary Science Reviews*, 21, 1185–1212.

Vogel, H., Wagner, B., Zanchetta, G., Sulpizio, R. & Rosén, P. (2010) A paleoclimate record with tephrochronological age control for the last glacial-interglacial cycle from Lake Ohrid, Albania and Macedonia. *Journal of Paleolimnology*, 44, 295–310.

Vossel, H., Reed, J. M., Houk, V., Cvetkoska, A. & Van de Vijver, B. (2015) *Cyclotella paleo–ocellata*, a new centric diatom (Bacillariophyta) from Lake Kinneret (Israel). *Fottea*, 15, 63–75.

Vossel, H., Roeser, P., Litt, T. & Reed, J. M. (2018) Lake Kinneret (Israel): New insights into Holocene regional palaeoclimate variability based on high-resolution multi-proxy analysis. *The Holocene*, 28, 1395–1410.

de Vries, A. & Ripley, B. D. (2020) *ggdendro: Create Dendrograms and Tree Diagrams Using 'ggplot2'* [Software]. Available online: https://CRAN.R-project.org/package=ggdendro.

Waelbroeck, C., Lougheed, B. C., Vazquez Riveiros, N., Missiaen, L., Pedro, J., Dokken, T., Hajdas, I., Wacker, L., Abbott, P., Dumoulin, J.-P., Thil, F., Eynaud, F., Rossignol, L., Fersi, W., Albuquerque, A. L., Arz, H., Austin, W. E. N., Came, R., Carlson, A. E., Collins, J. A., Dennielou, B., Desprat, S., Dickson, A., Elliot, M., Farmer, C., Giraudeau, J., Gottschalk, J., Henderiks, J., Hughen, K., Jung, S., Knutz, P., Lebreiro, S., Lund, D. C., Lynch-Stieglitz, J., Malaizé, B., Marchitto, T., Martínez-Méndez, G., Mollenhauer, G., Naughton, F., Nave, S., Nürnberg, D., Oppo, D., Peck, V., Peeters, F. J. C., Penaud, A., Portilho-Ramos, R. d. C., Repschläger, J., Roberts, J., Rühlemann, C., Salgueiro, E., Sanchez Goni, M. F., Schönfeld, J., Scussolini, P., Skinner, L. C., Skonieczny, C., Thornalley, D., Toucanne, S., Rooij, D. V., Vidal, L., Voelker, A. H. L., Wary, M., Weldeab, S. & Ziegler, M. (2019) Consistently dated Atlantic sediment cores over the last 40 thousand years. *Scientific Data*, 6, 165.

Wagner, B., Reicherter, K., Daut, G., Wessels, M., Matzinger, A., Schwalb, A., Spirkovski, Z. & Sanzhaku, M. (2008) The potential of Lake Ohrid for long-term palaeoenvironmental reconstructions. *Palaeogeography, Palaeoclimatology, Palaeoecology*, 259, 341–356.

Wagner, B., Wilke, T., Krastel, S., Zanchetta, G., Sulpizio, R., Reicherter, K., Leng, M. J., Grazhdani, A., Trajanovski, S., Francke, A., Lindhorst, K., Levkov, Z., Cvetkoska, A., Reed, J. M., Zhang, X., Lacey, J. H., Wonik, T., Baumgarten, H. & Vogel, H. (2014) The SCOPSCO drilling project recovers more than 1.2 million years of history from Lake Ohrid. *Scientific Drilling*, 17, 19–29.

Wagner, B., Wilke, T., Francke, A., Albrecht, C., Baumgarten, H., Bertini, A., Combourieu-Nebout, N., Cvetkoska, A., D'Addabbo, M., Donders, T. H., Foeller, K., Giaccio, B., Grazhdani, A., Hauffe, T., Holtvoeth, J., Joannin, S., Jovanovska, E., Just, J., Kouli, K., Koutsodendris, A., Krastel, S., Lacey, J. H., Leicher, N., Leng, M. J., Levkov, Z., Lindhorst, K., Masi, A., Mercuri, A. M., Nomade, S., Nowaczyk, N., Panagiotopoulos, K., Peyron, O., Reed, J. M., Regattieri, E., Sadori, L., Sagnotti, L., Stelbrink, B., Sulpizio, R., Tofilovska, S., Torri, P., Vogel, H., Wagner, T., Wagner-Cremer, F., Wolff, G. A., Wonik, T., Zanchetta, G. & Zhang, X. S. (2017) The environmental and evolutionary history of Lake Ohrid (FYROM/Albania): interim results from the SCOPSCO deep drilling project. *Biogeosciences*, 14, 2033–2054.

Wagner, B., Vogel, H., Francke, A., Friedrich, T., Donders, T., Lacey, J. H., Leng, M. J., Regattieri, E., Sadori, L. & Wilke, T. (2019) Mediterranean winter rainfall in phase with African monsoons during the past 1.36 million years. *Nature*, 573, 256–260.

WAIS Divide Project Members (2015) Precise interpolar phasing of abrupt climate change during the last ice age. *Nature*, 520, 661–665.

Waite, S. (2000) *Statistical ecology in practice: a guide to analysing environmental and ecological data*. Harlow: Prentice Hall.

Wang, Q., Yang, X., Hamilton, P. B. & Zhang, E. (2012) Linking spatial distributions of sediment diatom assemblages with hydrological depth profiles in a plateau deep–water lake system of subtropical China. *Fottea*, 12, 59–73.

Watzin, M. C., Puka, V. & Naumoski, T. B. (2002) *Lake Ohrid and its watershed, state of the environment report*. Tirana, Macedonia: Lake Ohrid Conservation Project.

Wendt, K. A., Li, X., Edwards, R. L., Cheng, H. & Spötl, C. (2021) Precise timing of MIS 7 substages from the Austrian Alps. *Climate of the Past*, 17, 1443–1454.

Wetzel, R. G. (2001) *Limnology*. London: Academic Press.

Wickham, H. (2016) *ggplot2: Elegant Graphics for Data Analysis* [Software]. Available online: https://ggplot2.tidyverse.org.

Wickham, H., Averick, M., Bryan, J., Chang, W., McGowan, L. D. A., François, R., Grolemund, G., Hayes, A., Henry, L., Hester, J., Kuhn, M., Pedersen, T. L., Miller, E., Bache, S. M., Müller, K., Ooms, J., Robinson, D., Seidel, D. P., Spinu, V., Takahashi, K., Vaughan, D., Wilke, C., Woo, K. & Yutani, H. (2019) Welcome to the Tidyverse. *Journal of Open Source Software*, 4, 1686.

Wilke, C. O. (2020) *cowplot: streamlined plot theme and plot annotations for 'ggplot2'. R package version 1.1.1* [Software]. Available online: https://CRAN.R-project.org/package=cowplot.

Wilke, T., Wagner, B., Van Bocxlaer, B., Albrecht, C., Ariztegui, D., Delicado, D., Francke, A., Harzhauser, M., Hauffe, T. & Holtvoeth, J. (2016) Scientific drilling projects in ancient lakes: integrating geological and biological histories. *Global and Planetary Change*, 143, 118–151.

Wilson, G. P., Reed, J. M., Lawson, I. T., Frogley, M. R., Preece, R. C. & Tzedakis, P. C. (2008) Diatom response to the Last Glacial–Interglacial Transition in the Ioannina basin, northwest Greece: implications for Mediterranean palaeoclimate reconstruction. *Quaternary Science Reviews*, 27, 428–440.

Wilson, G. P., Frogley, M. R., Roucoux, K. H., Jones, T. D., Leng, M. J., Lawson, I. T. & Hughes, P. D. (2013) Limnetic and terrestrial responses to climate change during the onset of the penultimate glacial stage in NW Greece. *Global and Planetary Change*, 107, 213–225.

Wilson, G. P., Reed, J. M., Frogley, M. R., Hughes, P. D. & Tzedakis, P. C. (2015) Reconciling diverse lacustrine and terrestrial system response to penultimate deglacial warming in southern Europe. *Geology*, 43, 819–822.

Wilson, G. P., Frogley, M. R., Hughes, P. D., Roucoux, K. H., Margari, V., Jones, T. D., Leng, M. J. & Tzedakis, P. C. (2021) Persistent millennial-scale climate variability in Southern Europe during Marine Isotope Stage 6. *Quaternary Science Advances*, 3, 1–10.

Winder, M., Reuter, J. E. & Geoffrey Schladow, S. (2009) Lake warming favours small-sized planktonic diatom species. *Proceedings of the Royal Society B. Biological Sciences.*, 276, 427–435.

Wolff, E. W., Chappellaz, J., Blunier, T., Rasmussen, S. O. & Svensson, A. (2010) Millennial-scale variability during the last glacial: the ice core record. *Quaternary Science Reviews*, 29, 2828–2838.

Wolin, J. A. & Stone, J. R. (2010) Diatoms as indicators of water-level changes in freshwater lakes. In Smol, J. P. & Stoermer, E. F. (eds) *The diatoms: applications for the environmental and earth sciences, 2nd edition*. Cambridge: Cambridge University Press, 174–185.

Woodward, J. (2014) *The ice age: a very short introduction*. Oxford: Oxford University Press.

Yehoshua, Y. & Alster, A. (2011) The diatom algae of Lake Kinneret, Israel. In Seckbach, J. & Kociolek, J. P. (eds) *The diatom world. Cellular Origin, Life in Extreme Habitats and Astrobiology Volume 19*. Dordrecht: Springer, 385–400.

Yin, Q. Z., Wu, Z. P., Berger, A., Goosse, H. & Hodell, D. (2021) Insolation triggered abrupt weakening of Atlantic circulation at the end of interglacials. *Science*, 373, 1035–1040.

Zacharias, I., Bertachas, I., Skoulikidis, N. & Koussouris, T. (2002) Greek lakes: limnological overview. *Lakes and Reservoirs: Research and Management*, 7, 55–62.

Zachos, J., Pagani, M., Sloan, L., Thomas, E. & Billups, K. (2001) Trends, rhythms and aberrations in global climate 65Ma to present. *Science*, 292, 686–693.

Zachos, J. C., Dickens, G. R. & Zeebe, R. E. (2008) An early Cenozoic perspective on greenhouse warming and carbon-cycle dynamics. *Nature*, 451, 279–283.

Zalat, A. & Vildary, S. S. (2005) Distribution of diatom assemblages and their relationship to environmental variables in the surface sediments of three northern Egyptian lakes. *Journal of Paleolimnology*, 34, 159–174.

Zaova, D., Beszteri, B., Cvetkoska, A., Jovanovska, E., Mitic-Kopanja, D. & Levkov, Z. (2021) Intraspecific variability in *Cyclotella cavitata* - an adaptation to environmental changes during the mid-Pleistocene Transition (MPT) in Lake Ohrid. *International Diatom Symposium.* Japan (online).

Zhang, X., Lohmann, G., Knorr, G. & Purcell, C. (2014a) Abrupt glacial climate shifts controlled by ice sheet changes. *Nature*, 512, 290–294.

Zhang, X., Reed, J., Wagner, B., Francke, A. & Levkov, Z. (2014b) Lateglacial and Holocene climate and environmental change in the northeastern Mediterranean region: diatom evidence from Lake Dojran (Republic of Macedonia/Greece). *Quaternary Science Reviews*, 103, 51–66.

Zhang, X., Knorr, G., Lohmann, G. & Barker, S. (2017) Abrupt North Atlantic circulation changes in response to gradual CO2 forcing in a glacial climate state. *Nature Geoscience*, 10, 518–523.

Zhang, X., Barker, S., Knorr, G., Lohmann, G., Drysdale, R., Sun, Y., Hodell, D. & Chen, F. (2021) Direct astronomical influence on abrupt climate variability. *Nature Geoscience*, 14, 819–826.

Zhang, X. S. (2015) *Diatom-based reconstruction of multi-timescale climate and environmental change from Lakes Dojran and Ohrid in the northeastern Mediterranean region*. PhD thesis. University of Hull.

Zhang, X. S., Reed, J. M., Lacey, J. H., Francke, A., Leng, M. J., Levkov, Z. & Wagner, B. (2016) Complexity of diatom response to Lateglacial and Holocene climate and environmental change in ancient, deep and oligotrophic Lake Ohrid (Macedonia and Albania). *Biogeosciences*, 12, 1351–1365.

Ziegler, M., Tuenter, E. & Lourens, L. J. (2010) The precession phase of the boreal summer monsoon as viewed from the eastern Mediterranean (ODP Site 968). *Quaternary Science Reviews*, 29, 1481–1490.

Zielhofer, C., Köhler, A., Mischke, S., Benkaddour, A., Mikdad, A. & Fletcher, W. J. (2019) Western Mediterranean hydro-climatic consequences of Holocene ice-rafted debris (Bond) events. *Climate of the Past*, 15, 463–475.

Zohary, T., Flaim, G. & Sommer, U. (2021) Temperature and the size of freshwater phytoplankton. *Hydrobiologia*, 848, 143–155.

Appendix A | Determining the number of diatom valves to count per sample of the Lake Ioannina MIS 7–9 diatom record using R

A.1 Introduction

It is necessary to decide upon the minimum number of diatom valves to count per sample so as to achieve an acceptable level of accuracy whilst optimising efficiency. This document reports on the analyses undertaken to determine how many diatom valves should be counted per sample of the Lake Ioannina MIS 7-9 diatom record.

Battarbee (1986) explains that the number of diatom valves that should be counted per sample varies according to the purpose of the analysis and the ability to achieve statistical precision, the latter being a function of the structure of the diatom assemblage itself (e.g. a sample dominated by a single taxon would require a higher count in order for low numbers of rare taxa to be statistically reliable). Based on the relationship between the change in percentage abundance of individual taxa and the number of valves counted, Battarbee (1986) goes on to recommend a count of 300–600 valves per sample for routine analyses. There has been no change to this recommended count over the years; Battarbee et al. (2001) also recommend a count of 300–600 valves per sample for most analyses, and this has remained the standard practice across palaeolimnological investigations.

However, there have been some further attempts to identify the minimum number of valves required to produce an adequate result for specific lakes/regions or to address specific questions. For example, using the efficiency metric of Pappas and Stoermer (1996), which represents the probability of encountering a new species as the count progresses, Bate and Newall (2001) concluded that a count of 200 valves was sufficient for bioassessment of water quality in the Kiewa River catchment, Australia. (A short review of various counts used specifically for the assessment of environmental quality is provided by Stevenson et al. (2010)). In another example, a minimum count of 300 valves has been shown to be adequate for palaeolimnological studies in tropical systems even with diverse assemblages (Soeprobowati et al., 2016). Similarly, a 300-valve count was adequate for most samples of a Late Quaternary diatom record from Lake Hayk, Ethiopia (Loakes, 2016; Loakes et al. 2018). In contrast, previous diatom analyses at Lake

Ioannina have used a minimum count of 500 valves per sample without justifying why this number was chosen, other than stating that the preservation allowed it (Wilson et al., 2008; Jones, 2010; Wilson et al., 2013; Wilson et al., 2015; Wilson et al., 2021). The analyses here will investigate whether 500 valves is actually the optimum number for the Lake Ioannina sediments in order to balance accuracy and counting efficiency or whether a different number of valves is preferable.

Two types of data have been collected:

- Detailed counts were obtained for three slides chosen at random, whereby the taxon name of each valve was recorded in the order it was counted.

- An initial low-resolution "skeleton" record of 15 samples was counted to gain some early insights into what the diatom record would look like. Based on previous diatom analyses of the I-284 core, a minimum of 500 valves were counted for each of these samples. As it was thought that the full count of 500 valves might not be necessary, these counts were tallied at three stages: after 300, 400 and 500 valves had been counted.

A.2 Import packages and data

```r
library(readxl)
library(purrr)
library(readr)
library(tools)
library(ggplot2)
library(dplyr)
library(tidyr)

# Create function that reads in a worksheet from an excel file then writes
# it to csv for longevity.
read_then_csv <- function(sheet, path) {
  path %>%
    read_excel(sheet = sheet) %>%
    write_csv(paste0("data/csv/imported-", sheet, ".csv"))
}

# Execute function and iterate over all worksheets in excel file.
path <- "data/count-justification-data.xlsx"

imported <- path %>%
  excel_sheets() %>%
  set_names() %>%
  map(read_then_csv, path = path)

# Set ggplot theme.
theme_set(theme_minimal(8))
theme_update(
  legend.box.background = element_rect(fill = "white",
                                       colour = "lightgrey"),
  legend.key.height = unit(0.4, "cm"),
  legend.key.width = unit(1, "cm")
)
```

A.3 Analyses

Two types of data exploration have been performed on these data:

- how relative abundances of individual taxa vary as the number of valves counted is increased.

- how relative abundances of each life mode (planktonic, facultative planktonic and benthic) varies as the number of valves counted is increased.

A.3.1 Individual taxa

These analyses investigate whether the percentage relative abundances of selected taxa vary as the valve count is increased. This is the same analysis that Battarbee (1986) used to illustrate that 300 to 600 valves should be counted per sample. It is helpful to perform this analysis on the I-284 data as there could be an underlying assemblage structure specific to the Ioannina diatom assemblage that influences the point at which the abundances stabilise, which would dictate whether the lower or higher end of the recommended range should be used here.

Breakdown of results per valve counted

As figures A.1, A.2 and A.3 demonstrate, there is some movement in the percentage relative abundances as the count progresses right up to 500 valves. However, between counts of 300 and 500 valves, these movements are very small, in the order of a few percentage points. The point at which the percentages stabilise varies across samples with sample 529 requiring the largest count before stabilising (Figure A.3).

```
# Plot sample 17.
# ---------------

imported$s_17 %>%
  # Wrangle data to long (tidy) format.
  select(., all_of(c("valve_no",
                     "p_oc_pc",
                     "p_brev_pc",
                     "s_con_pc",
                     "s_pin_pc",
                     "a_ped_pc",
                     "s_rot_pc"))) %>%
  pivot_longer(., all_of(c("p_oc_pc",
                           "p_brev_pc",
                           "s_con_pc",
                           "s_pin_pc",
                           "a_ped_pc",
                           "s_rot_pc")),
               names_to = "taxon",
               names_transform = list(taxon = as.factor),
               values_to = "pc") %>%
```

```r
  # Plot.
  ggplot(aes(x = valve_no,
             y = pc,
             colour = taxon)) +
  geom_line() +
  scale_colour_viridis_d(
    option = "C",
    begin = 0.1,
    end = 0.9,
    labels = c(expression(italic("Ampora pediculus")),
               expression(italic("Pseudostaurosira brevistriata")) ,
               expression(italic("Pantocsekiella ocellata")),
               expression(paste(italic("Staurosira construens"),
                                " var. ",
                                paste(italic("venter")))),
               expression(italic("Staurosirella pinnata")),
               expression(italic("Sellaphora rotunda")))) +
  labs(title = paste("Variation in relative abundance of selected taxa as valve",
                     "count increases"),
       subtitle = "Sample 17 (141.22 m)",
       colour = "Taxon") +
  xlab("Number of valves counted") +
  ylab("Relative abundance (%)") +
  theme(
    legend.position = c(0.97, 0.97),
    legend.justification = c("right", "top"),
  )


# Plot sample 33.
# ---------------

imported$s_33 %>%
  # Wrangle data to long (tidy) format.
  select(., all_of(c("valve_no",
                     "p_oc_pc",
                     "p_brev_pc",
                     "s_con_pc",
                     "s_pin_pc",
                     "a_ped_pc",
                     "s_rot_pc"))) %>%
  pivot_longer(., all_of(c("p_oc_pc",
                           "p_brev_pc",
                           "s_con_pc",
                           "s_pin_pc",
                           "a_ped_pc",
                           "s_rot_pc")),
               names_to = "taxon",
               names_transform = list(taxon = as.factor),
               values_to = "pc") %>%
  # Plot.
  ggplot(aes(x = valve_no,
             y = pc,
             colour = taxon)) +
  geom_line() +
  scale_colour_viridis_d(
    option = "C",
    begin = 0.1,
    end = 0.9,
    labels = c(expression(italic("Ampora pediculus")),
               expression(italic("Pseudostaurosira brevistriata")) ,
               expression(italic("Pantocsekiella ocellata")),
               expression(paste(italic("Staurosira construens"),
                                " var. ",
                                paste(italic("venter")))),
               expression(italic("Staurosirella pinnata")),
               expression(italic("Sellaphora rotunda")))) +
  labs(title = paste("Variation in relative abundance of selected taxa as valve",
```

```
                         "count increases"),
         subtitle = "Sample 33 (144.42 m)",
         colour = "Taxon") +
  xlab("Number of valves counted") +
  ylab("Relative abundance (%)") +
  theme(
    legend.position = c(0.97, 0.5),
    legend.justification = c("right", "center"),
  )


# Plot sample 529.
# ---------------

imported$s_529 %>%
  # Wrangle data to long (tidy) format.
  select(., all_of(c("valve_no",
                     "p_min_pc",
                     "p_oc_pc",
                     "s_con_pc",
                     "s_pin_pc",
                     "a_ped_pc",
                     "e_mic_pc"))) %>%
  pivot_longer(., all_of(c("p_min_pc",
                           "p_oc_pc",
                           "s_con_pc",
                           "s_pin_pc",
                           "a_ped_pc",
                           "e_mic_pc")),
               names_to = "taxon",
               names_transform = list(taxon = as.factor),
               values_to = "pc") %>%
  # Plot.
  ggplot(aes(x = valve_no,
             y = pc,
             colour = taxon)) +
  geom_line() +
  scale_colour_viridis_d(
    option = "C",
    begin = 0.1,
    end = 0.9,
    labels = c(expression(italic("Ampora pediculus")),
               expression(italic("Encyonopsis microcephala")) ,
               expression(paste(italic("Pantocsekiella"),
                                " cf. ",
                                paste(italic("minuscula")))),
               expression(italic("Pantocsekiella ocellata")),
               expression(paste(italic("Staurosira construens"),
                                " var. ",
                                paste(italic("venter")))),
               expression(italic("Staurosirella pinnata")))) +
  labs(title = paste("Variation in relative abundance of selected taxa as valve",
                     "count increases"),
       subtitle = "Sample 529 (243.62 m)",
       colour = "Taxon") +
  xlab("Number of valves counted") +
  ylab("Relative abundance (%)") +
  theme(
    legend.position = c(0.97, 0.55),
    legend.justification = c("right", "center"),
  )
```

V

Breakdown of results at 300, 400 and 500 valves counted

A less granular breakdown across numerous samples is displayed on a facet plot (Figure A.4). The relatively straight lines of the plots demonstrate that there is little change in the percentages as counting progresses.

```
imported$hundreds_taxa %>%
  ggplot(aes(x = count,
             y = pc_ab,
             colour = taxon)) +
  geom_line() +
  scale_colour_viridis_d(
    option = "C",
    labels = c(expression(italic("Amphora pediculus")),
               expression(italic("Pantocsekiella ocellata")),
               expression(italic("Staurosirella pinnata"))),
    begin = 0.1,
    end = 0.9) +
  facet_wrap("sample_no", ncol = 5) +
  scale_x_continuous(limits = c(300, 500),
                     breaks = seq(300, 500, 100)) +
  scale_y_continuous(limits = c(0, 100),
                     breaks = seq(0, 100, 20)) +
  labs(title = paste("Change in relative abundance of selected taxa as count",
                     "increases across several samples"),
       colour = "Taxon") +
  xlab("Valves counted") +
  ylab("Relative abundance (%)") +
  theme(
    legend.position = "top",
    axis.text.x = element_text(angle = 270)
  )
```

For each line on the facet plots, the changes in relative abundance between a count of 300 to 400 valves, a count of 400 to 500 valves and a count of 300 to 500 valves have been calculated. The changes are summarised by the statistics below. There is a mean difference in the relative abundances of these taxa of only 1.3 percentage points between a count of 300 valves and a count of 500 valves. The largest difference is 4.1 percentage points, which is very small and would probably not change any interpretation that might be made from an analysis of the assemblage.

```
dif_300_400 <- with(imported$hundreds_taxa,
                    abs(pc_ab[count=="400"] - pc_ab[count=="300"]))

dif_400_500 <- with(imported$hundreds_taxa,
                    abs(pc_ab[count=="500"] - pc_ab[count=="400"]))

dif_300_500 <- with(imported$hundreds_taxa,
                    abs(pc_ab[count=="500"] - pc_ab[count=="300"]))

differences_taxa <- tibble("300 to 400 valves" = dif_300_400,
                           "400 to 500 valves" = dif_400_500,
                           "300 to 500 valves" = dif_300_500)

summary(differences_taxa)

##  300 to 400 valves 400 to 500 valves 300 to 500 valves
##  Min.   :0.07363   Min.   :0.02168   Min.   :0.1164
##  1st Qu.:0.33208   1st Qu.:0.17678   1st Qu.:0.3870
##  Median :0.62303   Median :0.42639   Median :1.0587
```

```
##  Mean    :0.99016   Mean    :0.72305   Mean    :1.2912
##  3rd Qu.:1.54902   3rd Qu.:1.09963   3rd Qu.:1.8404
##  Max.    :3.21124   Max.    :3.92647   Max.    :4.0570
```

A.3.2 Life mode

The intention is for the results of the diatom analysis to be used to reconstruct the past lake environment with a particular emphasis on lake level change. The variations in the relative abundances of planktonic, facultative planktonic and benthic taxa (i.e. diatom life mode or habitat) are most useful in reconstructing such changes. It was therefore deemed useful to see how these abundances vary as a function of number of valves counted.

Breakdown of results per valve counted

Figures A.5, A.6 and A.7 show that the relative abundances all stabilise by a count of 250 valves, but that this number also varies between samples. Whilst a count of 250 valves would have been required for sample 17, counts of only 200 and 100 would have been sufficient for samples 33 and 529 respectively.

```r
# Plot sample 17.
# ---------------

imported$s_17 %>%
  # Wrangle data to long (tidy) format.
  select(., all_of(c("valve_no", "p_pc", "fp_pc", "b_pc"))) %>%
  pivot_longer(., all_of(c("p_pc", "fp_pc", "b_pc")),
              names_to = "life_mode",
              names_transform = list(life_mode = as.factor),
              values_to = "pc") %>%
  # Plot.
  ggplot(aes(x = valve_no,
            y = pc,
            colour = life_mode)) +
  geom_line() +
  scale_colour_viridis_d(
    option = "C",
    begin = 0.9,
    end = 0.1,
    labels = c("Benthic", "Faculative Planktonic", "Planktonic"),
    guide = guide_legend(reverse = TRUE)) +
  labs(title = paste("Variation in relative abundance of planktonic, facultative",
                    "planktonic and benthic diatom taxa as valve count increases"),
      colour = "Life Mode") +
  xlab("Number of valves counted") +
  ylab("Relative abundance (%)") +
  theme(
    legend.position = c(0.97, 0.97),
    legend.justification = c("right", "top"),
  )


# Plot sample 33.
# ---------------

imported$s_33 %>%
  # Wrangle data to long (tidy) format.
  select(., all_of(c("valve_no", "p_pc", "fp_pc", "b_pc"))) %>%
  pivot_longer(., all_of(c("p_pc", "fp_pc", "b_pc")),
              names_to = "life_mode",
```

```
            names_transform = list(life_mode = as.factor),
            values_to = "pc") %>%
  # Plot data.
  ggplot(aes(x = valve_no,
             y = pc,
             colour = life_mode)) +
geom_line() +
scale_colour_viridis_d(
  option = "C",
  begin = 0.9,
  end = 0.1,
  labels = c("Benthic", "Faculative Planktonic", "Planktonic"),
  guide = guide_legend(reverse = TRUE)) +
labs(title = paste("Variation in relative abundance of planktonic, facultative",
                   "planktonic and benthic diatom taxa as valve count increases"),
     subtitle = "Sample 33 (144.42 m)",
     colour = "Life Mode") +
xlab("Number of valves counted") +
ylab("Relative abundance (%)") +
theme(
  legend.position = c(0.97, 0.97),
  legend.justification = c("right", "top"),
)


# Plot sample 529.
# ----------------

imported$s_529 %>%
  # Wrangle data to long (tidy) format.
  select(., all_of(c("valve_no", "p_pc", "fp_pc", "b_pc"))) %>%
  pivot_longer(., all_of(c("p_pc", "fp_pc", "b_pc")),
               names_to = "life_mode",
               names_transform = list(life_mode = as.factor),
               values_to = "pc") %>%
  # Plot data.
  ggplot(aes(x = valve_no,
             y = pc,
             colour = life_mode)) +
geom_line() +
scale_colour_viridis_d(
  option = "C",
  begin = 0.9,
  end = 0.1,
  labels = c("Benthic", "Faculative Planktonic", "Planktonic"),
  guide = guide_legend(reverse = TRUE)) +
labs(title = paste("Variation in relative abundance of planktonic, facultative",
                   "planktonic and benthic diatom taxa as valve count increases"),
     subtitle = "Sample 529 (243.62 m)",
     colour = "Life Mode") +
xlab("Number of valves counted") +
ylab("Relative abundance (%)") +
theme(
  legend.position = c(0.97, 0.97),
  legend.justification = c("right", "top"),
)
```

Breakdown of results at 300, 400 and 500 valves counted

The results above demonstrated that a count of 250 valves should be sufficient to obtain an accurate representation of the percentage abundances of diatom taxa grouped by life mode. However, it also showed that the point at which the percentages stabilised varies across samples. It is sensible to check whether

the percentages are stable across increasing valve counts in more samples before deciding if a lower count is going to be acceptable.

A less granular breakdown of counts (at 300, 400 and 500 valves) was carried out on 15 samples throughout the length of the core section. Figure 8 shows that the percentage relative abundance is very stable across counts of 300, 400 and 500 valves. Relative abundances of planktonic, facultative planktonic and benthic taxa vary by only a few percentage points as the count progresses.

```r
imported$hundreds_life_mode %>%
  ggplot(aes(x = count,
             y = pc_ab,
             colour = life_mode)) +
  geom_line() +
  scale_colour_viridis_d(
    option = "C",
    begin = 0.9,
    end = 0.1,
    labels = c("Benthic", "Faculative Planktonic", "Planktonic"),
    guide = guide_legend(reverse = TRUE)) +
  facet_wrap("sample_no", ncol = 5) +
  scale_x_continuous(limits = c(300, 500),
                     breaks = seq(300, 500, 100)) +
  scale_y_continuous(limits = c(0, 100),
                     breaks = seq(0, 100, 20)) +
  labs(title = paste("Change in life mode relative abundance as count increases",
                     "across several samples"),
       colour = "Life Mode") +
  xlab("Valves counted") +
  ylab("Relative abundance (%)") +
  theme(
    legend.position = "top",
    axis.text.x = element_text(angle = 270)
  )
```

For each line on the facet plots, the changes in relative abundance between a count of 300 to 400 valves, a count of 400 to 500 valves and a count of 300 to 500 valves have been calculated. The changes are summarised by the statistics below. These statistics confirm that the relative abundances remain stable as the count progresses. There is a mean change across all variables of only 1.7 percentage points as the count is increased from 300 to 500 valves. The maximum change is 4.7 percentage points, which is so small that it would not affect any interpretation of past lake level from the planktonic to benthic ratio.

```r
dif_300_400 <- with(imported$hundreds_life_mode,
                    abs(pc_ab[count=="400"] - pc_ab[count=="300"]))

dif_400_500 <- with(imported$hundreds_life_mode,
                    abs(pc_ab[count=="500"] - pc_ab[count=="400"]))

dif_300_500 <- with(imported$hundreds_life_mode,
                    abs(pc_ab[count=="500"] - pc_ab[count=="300"]))

differences_life_mode <- tibble("300 to 400 valves" = dif_300_400,
                    "400 to 500 valves" = dif_400_500,
                    "300 to 500 valves" = dif_300_500)

summary(differences_life_mode)
```

```
##   300 to 400 valves 400 to 500 valves  300 to 500 valves
##  Min.   :0.01425   Min.   :0.006228   Min.   :0.02118
##  1st Qu.:0.47436   1st Qu.:0.339730   1st Qu.:0.72507
##  Median :1.06607   Median :0.715180   Median :1.70691
##  Mean   :1.55891   Mean   :0.900081   Mean   :1.68788
##  3rd Qu.:2.42511   3rd Qu.:1.440707   3rd Qu.:2.36352
##  Max.   :5.27076   Max.   :3.035093   Max.   :4.72818
```

A.4 Conclusion

This document has investigated changes in the percentage relative abundances of selected diatom taxa and changes in the percentage relative abundances of all diatom taxa grouped by life mode as the number of diatom valves counted is increased. It demonstrates that a diatom valve count of 300 valves per sample is sufficient to achieve the aims of the diatom analyses.

The abundances of taxa grouped by life mode stabilise by a count of 250 valves in the three samples investigated in detail. Less granular counts (at 300, 400 and 500 valves) of multiple samples also showed little change in the relative abundances of taxa grouped by life mode. These samples were taken from the full length of the core section so probably encapsulate the majority of the diatom assemblage variation to be found in the new diatom record. However, it is still possible that some samples might have an assemblage that requires a higher count so it is best to be cautious and count the minimum 300 valves recommended by Battarbee (1986) rather than 250.

A.5 References

Battarbee, R. W. (1986) Diatom analysis. In Berglund, B. E. (ed) Handbook of Holocene palaeoecology and palaeohydrology. Chichester: John Wiley & Sons.

Battarbee, R. W., Jones, V. J., Flower, R. J., Cameron, N. G., Bennion, H., Carvalho, L. & Juggins, S. (2001) Diatoms. In Smol, J. P., Birks, H. J. B. & Last, W. M. (eds) Tracking environmental change using lake sediments, Volume 3: Terrestrial, algal, and siliceous indicators. Dordrecht: Kluwer Academic Publishers, 155–202.

Jones, T. D. (2010) A reconstruction of late Pleistocene and Holocene lake level change at Ioannina, northwest Greece. PhD thesis. University of Leeds.

Loakes, K. L., (2015) Late Quaternary palaeolimnology and environmental change in the South Wollo Highlands, Ethiopia. PhD thesis. Loughborough University.

Loakes, K. L., Ryves, D. B., Lamb, H. F., Schäbitz, F., Dee, M., Tyler, J. J., Mills, K. & McGowan, S. (2018) Late Quaternary climate change in the north-eastern

highlands of Ethiopia: a high resolution 15,600 year diatom and pigment record from Lake Hayk. Quaternary Science Reviews, 202, 166–181.

Soeprobowati, T. R., Tandjung, S. D., Sutikno, S., Hadissusanto, S., & Gell, P. (2016) The minimum number of valves for diatom identification in Rawapening Lake, central Java. Biotropia, 23, 96–104.

Stevenson, R. J., Pan, Y. & van Dam, H. (2010) Assessing environmental conditions in rivers and streams with diatoms. In Smol, J. P. & Stoermer, E. F. (eds) The Diatoms: applications for the Environmental and Earth Sciences, Cambridge: Cambridge University Press, 57–85.

Wilson, G. P., Reed, J. M., Lawson, I. T., Frogley, M. R., Preece, R. C. & Tzedakis, P. C. (2008) Diatom response to the Last Glacial–Interglacial Transition in the Ioannina basin, northwest Greece: implications for Mediterranean palaeoclimate reconstruction. Quaternary Science Reviews, 27, 428–440.

Wilson, G. P., Frogley, M. R., Roucoux, K. H., Jones, T. D., Leng, M. J., Lawson, I. T. & Hughes, P. D. (2013) Limnetic and terrestrial responses to climate change during the onset of the penultimate glacial stage in NW Greece. Global and Planetary Change, 107, 213–225.

Wilson, G. P., Reed, J. M., Frogley, M. R., Hughes, P. D. & Tzedakis, P. C. (2015) Reconciling diverse lacustrine and terrestrial system response to penultimate deglacial warming in southern Europe. Geology, 43(9), 819–822.

Wilson, G. P., Frogley, M. R., Hughes, P. D., Roucoux, K. H., Margari, V., Jones, T. D., Leng, M. J. & Tzedakis, P. C. (2021) Persistent millennial-scale climate variability in Southern Europe during Marine Isotope Stage 6. Quaternary Science Advances, 3, 1–10.
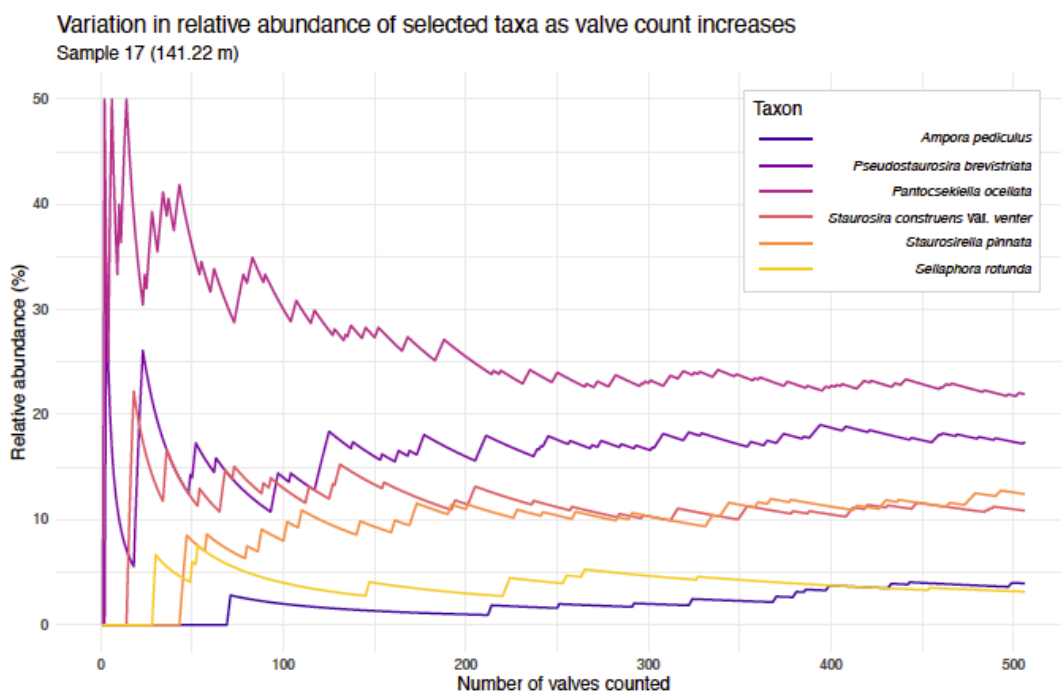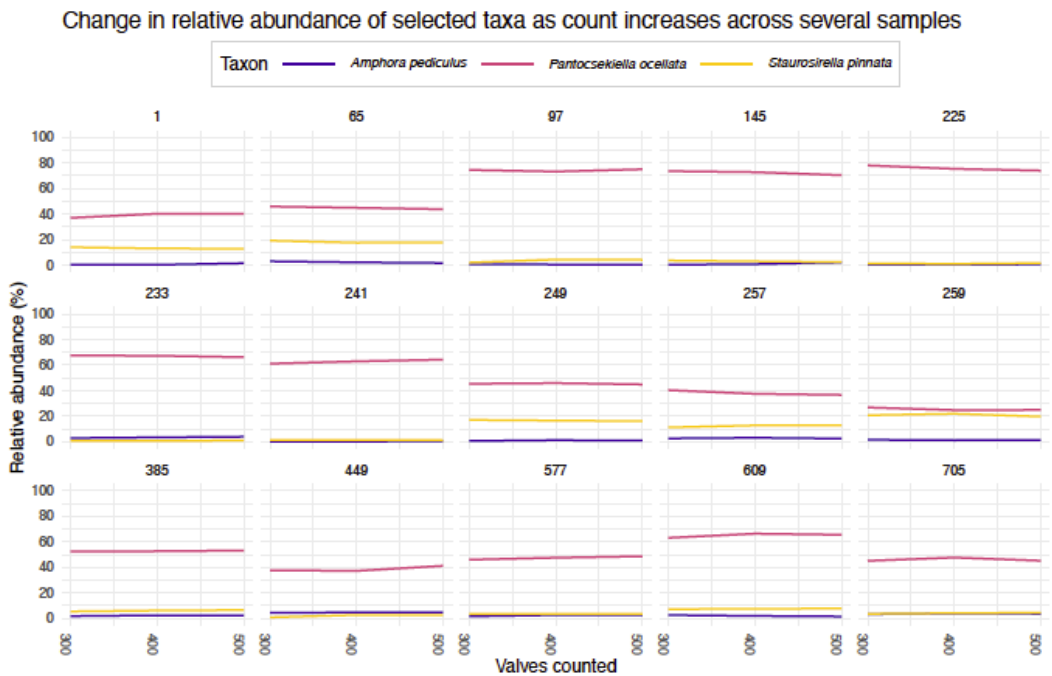
Figure A.1: Variation in the percentage relative abundance of selected taxa as the number of valves counted is increased for I-284 core sample 17 (141.22 m).
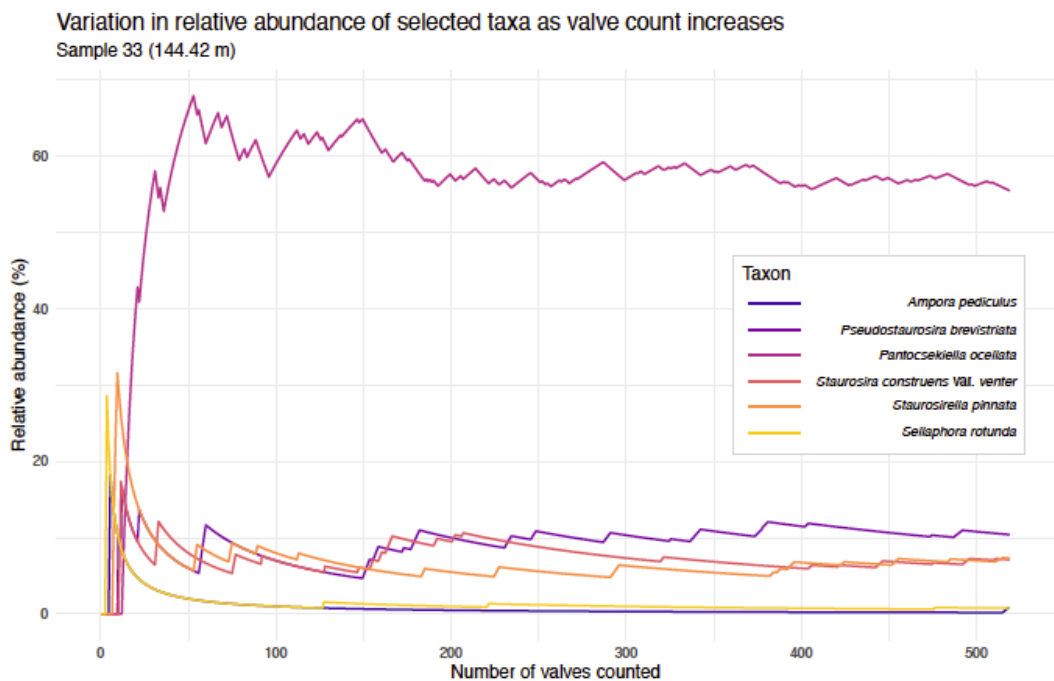
Figure A.2: Variation in the percentage relative abundance of selected taxa as the number of valves counted is increased for I-284 core sample 33 (144.42 m).
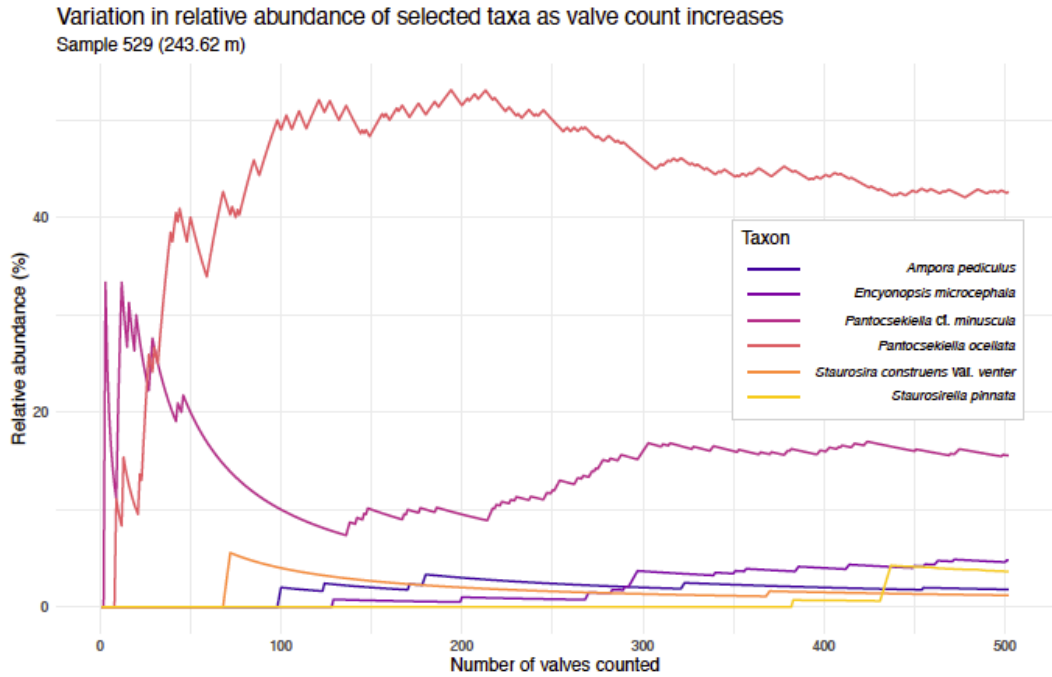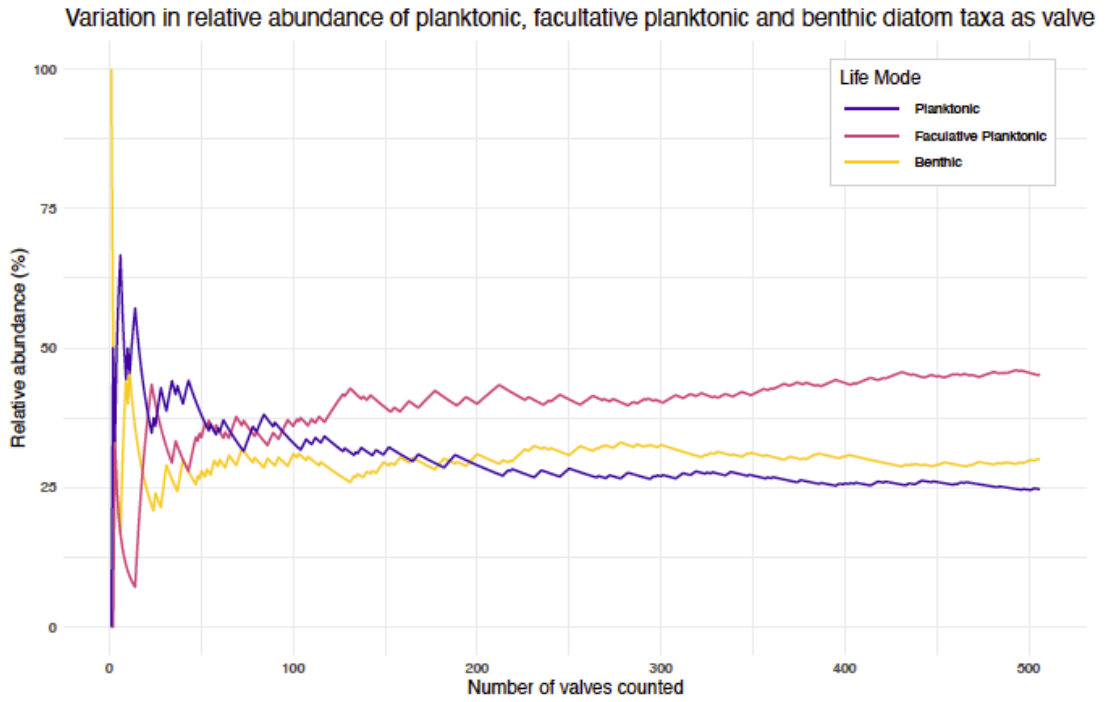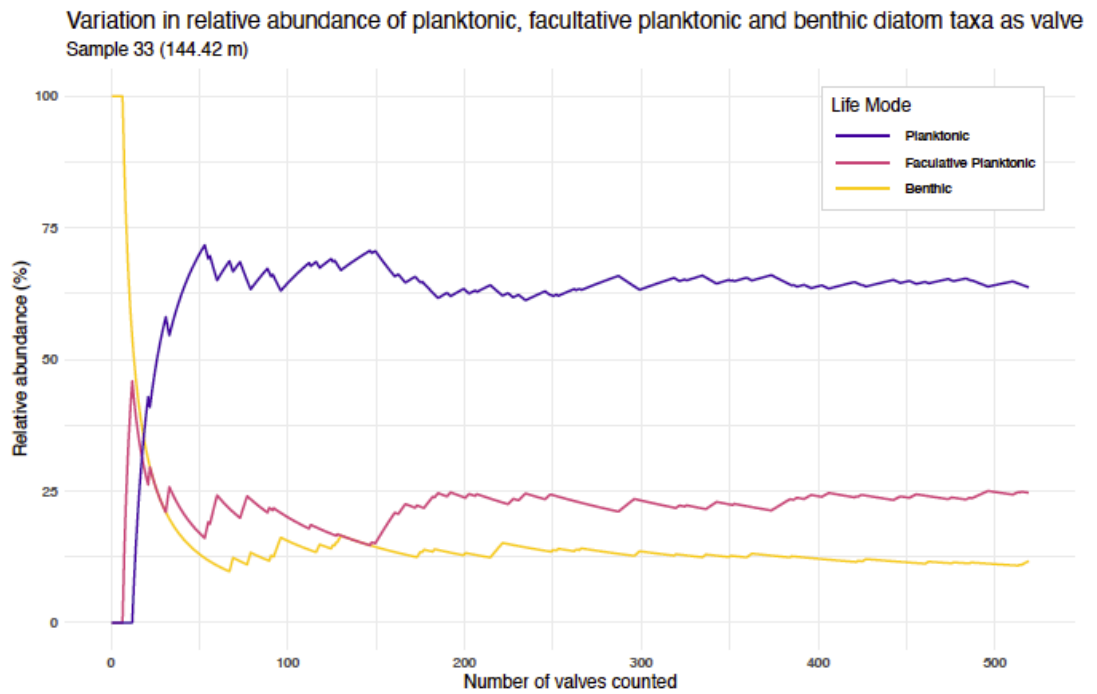
Figure A.3: Variation in the percentage relative abundance of selected taxa as the number of valves counted is increased for I-284 core sample 529 (243.62 m).

Figure A.4: Variation in the percentage relative abundance of selected taxa as the number of valves counted is increased from 300 to 400 to 500 valves for selected I-284 core samples.

Figure A.5: Variation in the percentage relative abundance of selected taxa as the number of valves counted is increased from 300 to 400 to 500 valves for selected I-284 core samples.
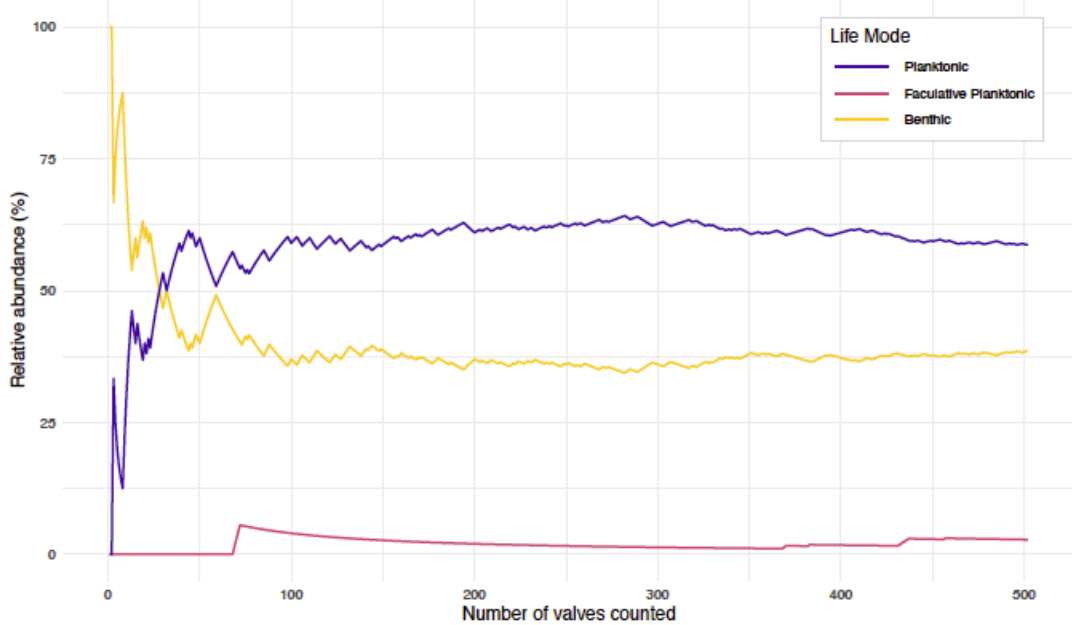

Figure A.6: Variation in the percentage relative abundance of all diatom taxa grouped by life mode as the number of valves counted is increased for I-284 core sample 33 (144.42 m).
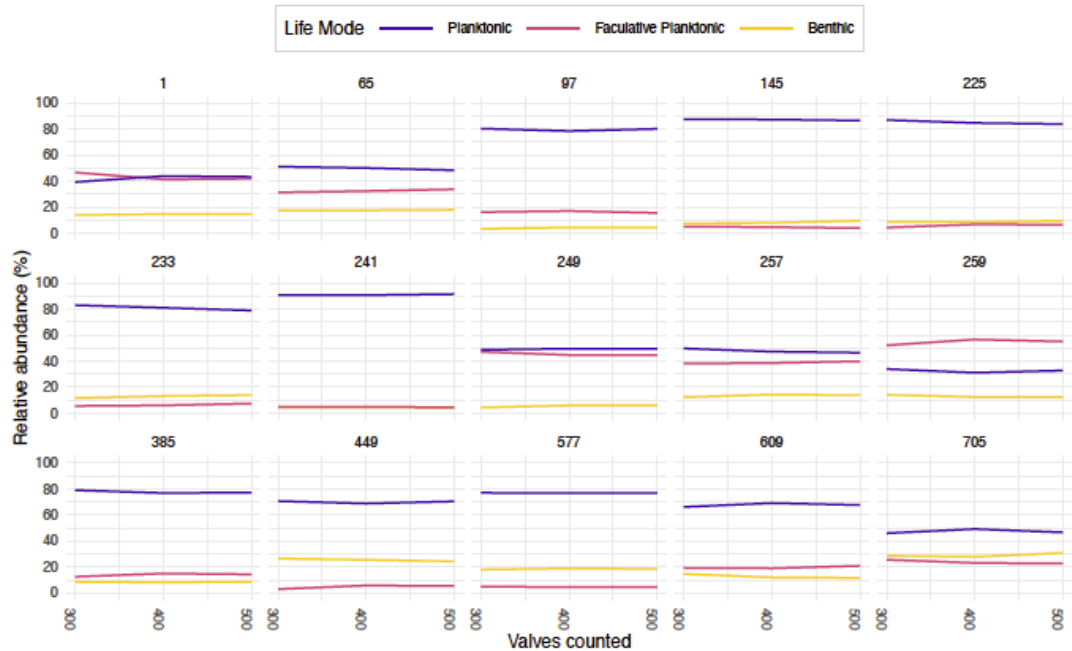
Figure A.7: Variation in the percentage relative abundance of all diatom taxa grouped by life mode as the number of valves counted is increased for I-284 core sample 529 (243.62 m).

Figure A.8: Variation in the percentage relative abundance of all taxa grouped by life mode as the number of valves counted is increased from 300 to 400 to 500 valves for selected I-284 core samples.

Appendix B | Zonation of the Lake Ioannina diatom data using R

B.1 Introduction

This document outlines the steps taken to split the Lake Ioannina MIS 7-9 diatom record into diatom assemblage zones, and it contains the R code used to do so. The reason for splitting the record into zones is to delineate sections of the record that share a similar diatom assemblage, helping to identify major changes in the record and making it easier to describe (the results can be written up by zone).

B.1.1 Clustering algorithm choice

A constrained cluster analysis is required in order to group samples together that are stratigraphically adjacent. The specific cluster analysis chosen is the Constrained Incremental Sum of Squares (CONISS) method, as outlined by Grimm (1987).

First, a matrix of dissimilarities between samples is computed. The CONISS algorithm then computes a statistic known as the *sum of squares** between each pair of adjacent samples (each sample can be considered a cluster of just one sample at this stage). The pair with the smallest sum of squares is joined into a cluster, and then the sum of squares is recalculated for all samples with these newly joined samples receiving one sum of squares value for their cluster. The clusters with the smallest sum of squares is joined and the sum of squares recalculated. This process continues, clustering samples into successively larger groups (it is therefore an agglomerative technique).

*The sum of squares is the squared difference between the value of a taxon in one sample of a cluster divided by the average value of that taxon across all samples in that cluster, which is then summed for each taxon, which is then summed for each sample in the cluster.

B.2 Import packages and data

```r
library(dplyr)
library(tibble)
library(ggplot2)
library(vegan) # designdist, decostand
library(rioja) # chclust
library(ggdendro) # dendro_data

source("scripts/borders-for-ggplot2.R") # custom theme to remove borders
```

XVI

```
imported_counts <- read.csv("data/csv/counts.csv")
taxa_life_modes <- read.csv("data/csv/taxa-life-modes.csv") %>%
  transmute(
    taxon = taxon,
    type = as.factor(type)
  )
```

B.3 Prepare data

The following steps are taken to prepare the data specifically for the analyses in this document:

1. Remove samples with no diatoms and an outlier, which contains some diatoms but is poorly preserved.

2. Discard rare taxa. These analyses are performed on taxa that are present at ≥4% in at least one sample. This decision was taken based on the following review of the literature.

3. Gordon and Birks (1972) suggest that the cluster analysis should only be run on taxa present at ≥5% in at least one sample as the low abundance taxa are of little numerical importance. Grimm (1987) eliminated those present at <3% at every level and noted that eliminating rare taxa has little effect on the analysis. Bennett (1996) also uses only taxa present at >5% in at least one sample and then goes on to assess the effect of decreasing and increasing the threshold for taxa inclusion. In an example using the CONISS algorithm, Bennett (1996) identified 6 zones with the threshold set at 0-5%, 1%, 2% or 5%, and identified 5 zones with the threshold set at 10% or 20%—a difference of only one zone.

4. Eliminating the rare taxa doesn't seem to make much difference, however Birks (1986) explains that although rare taxa could be of ecological importance, the counts of rare taxa are associated with a high relative error so are poorly estimated numerically unless very large counts are made.

5. Obviously, the work cited so far is quite old, so I have looked around to see if there has been any progression on this. Birks (2012:357) states that the basic principles "remain largely unchanged" since they were established in Gordon and Birks (1972) and Birks and Gordon (1985).

6. Convert raw diatom valve counts into relative proportions (out of 1.0).

7. Square-root transform the data.

```
# Get names of taxa present at ≥4%.
abundant_taxa <- imported_counts %>%
  column_to_rownames("depth") %>%
```

```
  decostand(method = "total", na.rm = TRUE) %>%
  select_if(~any(. >= 0.04)) %>%
  select(-contains("spp")) %>%
  colnames()

# Filter and transform data.
coniss_data <- imported_counts %>%
  filter(rowSums(select(., !matches("depth"))) > 0 & depth != 175.62) %>%
  column_to_rownames("depth") %>%
  select(all_of(abundant_taxa)) %>%
  decostand(method = "hellinger", na.rm = "TRUE") # sqrt of rel. proportions
```

B.4 Cluster analysis

Creating the zones involves three steps:

1. Calculate a distance matrix.

2. Run the cluster analysis.

3. Determine the number of significant zones.

First, a distance matrix of the squared Euclidean distance between samples is calculated. This dissimilarity index is the one used by the Tilia program. The CONISS cluster analysis is then performed on this distance matrix.

A broken stick model (Bennett, 1996) is used to determine the number of significant zones in the record. The plot in Figure B.1 shows that after splitting the record into 12 groups (zones), the observed reduction in within-group sum of squares (black line) drops (and remains) below that expected from the broken stick model (red line). Therefore, there are 12 significant zones in this record.

B.5 Plot results

The results of the cluster analysis can be plotted as a dendrogram (Figure B.2).

```
# Extract data for plotting
ddata<- dendro_data(coniss_results, type = "rectangle")
# Modify x values so leaves are plotted by depth in core rather than in
# sequential order
new_x <- approxfun(ddata$labels$x,
                   as.numeric(as.character(ddata$labels$label)))
ddata$segments$x <- new_x(ddata$segments$x)
ddata$segments$xend <- new_x(ddata$segments$xend)

# Create plot
ggplot(segment(ddata)) +
    geom_vline(xintercept = c(156.02, 163.22, 177.62, 190.42, 199.22, 215.22,
                              233.62, 253.62, 258.42, 275.22, 279.22),
               colour = "lightgrey") +
  geom_segment(aes(x = x, y = y, xend = xend, yend = yend)) +
```

```
coord_flip() +
scale_y_continuous() +
scale_x_reverse(breaks = seq(135, 285, 5)) +
labs(x = "Depth (m)",
     y = "Total sum of squares") +
theme_bw(10) +
theme(aspect.ratio = 3,
      legend.position = "none",
      panel.grid = element_blank(),
      panel.border = theme_border(c("left", "bottom")),
      panel.background = element_rect(fill = "transparent"),
      plot.background = element_rect(fill = "transparent")) +
geom_hline(yintercept = 14,
           linetype = 2)
```

B.6 Summary

CONISS cluster analysis has identified 12 significant zones in the I-284 diatom record.

B.7 References

Bennett, K. D. (1996) Determination of the number of zones in a biostratigraphical sequence. New Phytologist, 132, 155–170.

Birks, H. J. B. (1986) Numerical zonation, comparison and correlation of Quaternary pollen-stratigraphical data. In Berglund, B. E. (ed) Handbook of Palaeoecology and Palaeohydrology. Chichester: John Wiley & Sons.

Birks, H. J. B. (2012) Analysis of stratigraphical data. In Birks, H. J. B., Lotter, A. F., Juggins, S. & Smol, J. P. (eds) Tracking Environmental Change using Lake Sediments. Volume 5: Data Handling and Numerical Techniques. Dordrecht: Springer.

Birks, H. J. B. & Gordon, A. D. (1985) Numerical methods in Quaternary pollen analysis. London: Academic Press.

Gordon, A. D. & Birks, H. J. B. (1972) Numerical methods in Quaternary palaeoecology. I. Zonation of pollen diagrams. New Phytologist, 71, 961–979.

Grimm, E. C. (1987) CONISS: A Fortran 77 program for stratigraphically constrained cluster analysis by the method of incremental sum of squares. Computers & Geosciences, 13, 13–35.

Grimm, E. C. (2011) Tilia version 1.7.16 [Software]. Illinois State Museum, Springfield.
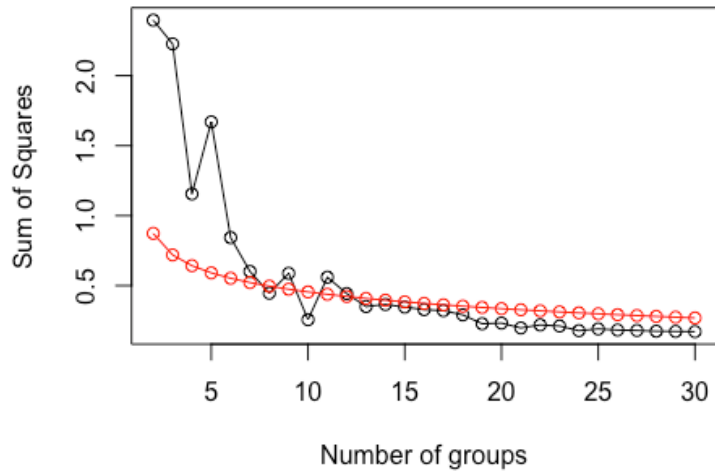
Figure B.1: Comparison of the CONISS results with a broken stick model. The observed reduction in within-group sum of squares is represented by the black line and the model is represented by the red line.
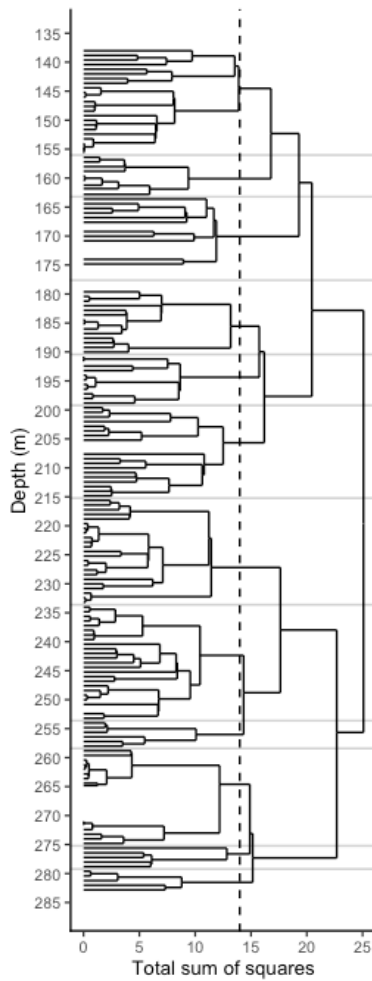
Figure B.2: Dendrogram of CONISS results. The vertical dashed line indicates the total sum of squares value that splits the record into the 12 significant zone. The horizonal grey lines delineate the resulting zones.

XX

Appendix C | Ordination of the Lake Ioannina MIS 7–9 diatom data using R

C.1 Introduction

This document outlines the ordination analyses of the Lake Ioannina I-284 core diatom record. Ordination is an exploratory technique that rotates the data in order to identify the gradients of greatest variation. It is done here to pick out these gradients and to see if any underlying latent environmental variables responsible for the variation can be identified.

C.2 Import packages and data

```
library(dplyr)
library(tidyr)
library(readr)
library(tibble)
library(ggplot2)
library(tidypaleo)
library(patchwork)
library(knitr)
library(vegan)

imported_counts <- read_csv("data/csv/counts.csv")
zones <- read_csv("data/csv/imported-zones.csv")
```

C.3 Ordination of relative abundance data

C.3.1 Prepare data

The analyses are performed on only abundant taxa present at ⩾4% in at least one sample. This removes the influence of very rare taxa, the abundances of which are poorly estimated.

```
# Get names of abundant taxa.
abundant_taxa <- imported_counts %>%
  column_to_rownames("depth") %>%
  decostand(method = "total", na.rm = TRUE) %>%
  select_if(~any(. >= 0.04)) %>%
  select(-contains("spp")) %>%
  colnames()

# Filter and transform data.
ord_data <- imported_counts %>%
  filter(rowSums(select(., !matches("depth"))) > 0 & depth != 175.62) %>%
  column_to_rownames("depth") %>%
  select(all_of(abundant_taxa)) %>%
  decostand(method = "total", na.rm = "TRUE") * 100
```

C.3.2 DCA

Following the approach of Leps and Šmilauer (2003), a preliminary detrended correspondence analysis (DCA) is first performed in order to determine the most appropriate ordination method for these data based on whether the species responses to the latent variables are linear or unimodal. If the DCA indicates that the species responses are unimodal, the DCA is deemed appropriate. If the DCA indicates that the species responses are linear, the linear ordination method of principal component analysis (PCA) is more appropriate for the data.

The results of the DCA are displayed in Table C.1. At less than three standard deviation units, the length of the longest axis (DCA1) indicates linear species responses as a result of low beta diversity (species turnover). A linear-based ordination is therefore most appropriate for these data.

```
# Run DCA.
dca <- decorana(ord_data)

# Extract results.
dca_results <- tibble(
  "Axis" = c("DCA1", "DCA2", "DCA3", "DCA4"),
  "Eigenvalues" = dca$evals,
  "Decorana values" = dca$evals.decorana,
  "Axis lengths" = apply(scores(dca), 2, max) - apply(scores(dca), 2, min)
  )

# Plot table.
kable(dca_results, caption="Summary results of the DCA performed on the Lake Ioannina co
re I-284 diatom assemblage relative species abundances.")
```

C.3.3 PCA

As linear ordination methods are most appropriate, a principal component analysis (PCA) is performed. The results are displayed in Table C.2. A large proportion of the variance is explained by the first two principal component axes, which can be plotted as a biplot (Figure C.1).

```
# Run PCA.
pca <- rda(ord_data)

# Extract results.
pca_results <- tibble(
  "Axis" = c("PC1", "PC2", "PC3", "PC4"),
  "Eigenvalues" = pca$CA$eig[1:4],
  "Cumulative percentage variance explained" = c(
    signif(sum((as.vector(pca$CA$eig) / sum(pca$CA$eig))[1]) * 100, 4),
    signif(sum((as.vector(pca$CA$eig) / sum(pca$CA$eig))[1:2]) * 100, 4),
    signif(sum((as.vector(pca$CA$eig) / sum(pca$CA$eig))[1:3]) * 100, 4),
    signif(sum((as.vector(pca$CA$eig) / sum(pca$CA$eig))[1:4]) * 100, 4)
  )
)

# Plot table.
kable(pca_results, caption="Summary results of the PCA performed on the Lake Ioannina co
re I-284 diatom assemblage relative species abundances.")
```

```r
# Plot biplot.
# -----------

# Provide names of select taxa to plot (need to be in original order).
pca_taxa <- c("Pantocsekiella minuscula",
              "Pantocsekiella ocellata",
              "Stephanodiscus parvus",
              "Pseudostaurosira brevistriata",
              "Staurosira venter",
              "Staurosirella pinnata",
              "Amphora pediculus",
              "Diploneis marginestriata",
              "Encyonopsis microcephala",
              "Gomphonema pumilum",
              "Placoneis balcanica",
              "Sellaphora rotunda")

text_positions <- c(1, 2, 3, 2, 4, 4, 4, 4, 4, 2, 2, 3)

# Create labels for plot.
labels <- c(expression(italic("Pantocsekiella minuscula")),
            expression(italic("Pantocsekiella \n ocellata")),
            expression(italic("Stephanodiscus parvus")),
            expression(italic("Pseudostaurosira brevistriata")),
            expression(paste(italic("Staurosira construens"),
                             " var. ",
                             italic("venter"))),
            expression(italic("Staurosirella pinnata")),
            expression(italic("Amphora pediculus")),
            expression(italic("Diploneis marginestriata")),
            expression(italic("Encyonopsis microcephala")),
            expression(italic("Gomphonema pumilum")),
            expression(italic("Placoneis balcanica")),
            expression(italic("Sellaphora rotunda")))

# Put axis scores in separate dataframes.
all_scrs <- scores(pca, display = c("sites", "species"), scaling = 2)

species_scrs <- all_scrs$species %>%
  as.data.frame() %>%
  rownames_to_column("taxon") %>%
  filter(taxon %in% pca_taxa)

sites_scrs <- all_scrs$sites %>%
  as.data.frame() %>%
  rownames_to_column("depth")

# Build plot.
xlim <- range(all_scrs[["species"]][,1], all_scrs[["sites"]][,1])
ylim <- range(all_scrs[["species"]][,2], all_scrs[["sites"]][,2])
plot.new()
plot.window(xlim = xlim, ylim = ylim, asp = 1)
abline(h = 0, lty = "dotted")
abline(v = 0, lty = "dotted")
axis(side = 1)
axis(side = 2)
title(xlab = "PC1", ylab = "PC2")
box()

points(sites_scrs$PC2~sites_scrs$PC1,
       pch = 19,
       cex = 0.5,
       col = "lightgrey")

arrows(0, 0, species_scrs$PC1, species_scrs$PC2,
       length = 0.05,
       angle = 30)
```

XXIII

```
text(species_scrs$PC2~species_scrs$PC1,
     labels = labels,
     cex = 0.8,
     col = "black",
     pos = text_positions)
```

However, a comparison of the results with a broken stick model indicates that the first three principal components are significant (Figure C.2).

```
screeplot(pca, bstick = TRUE, type = "l", main = NULL)
```

The axis scores of these principal components can be plotted by depth to explore variation through the core (Figure C.3).

```
sig_axes <- data.frame(scores(pca,
                              choices = c(1, 2, 3),
                              display = "sites",
                              scaling = 0)) %>%
  mutate(depth = as.numeric(row.names(.)))

plot_pc1 <- ggplot(sig_axes, aes(x = depth, y = PC1)) +
  geom_line() +
  coord_flip() +
  scale_x_reverse(breaks = seq(120, 290, 20)) +
  scale_y_continuous(breaks = seq(-0.4, 0.6, 0.1)) +
  labs(x = "Depth (m)",
       y = "PC1 axis score") +
  theme_minimal(10) +
  theme(
    panel.grid.major = element_line(colour = "gray 95"),
    panel.grid.minor = element_line(colour = "gray 96"),
    axis.text.x = element_text(angle = 45, hjust = 1))

plot_pc2 <- ggplot(sig_axes, aes(x = depth, y = PC2)) +
  geom_line() +
  coord_flip() +
  scale_x_reverse(breaks = seq(120, 290, 20)) +
  scale_y_continuous(breaks = seq(-0.4, 0.6, 0.1)) +
  labs(x = element_blank(),
       y = "PC2 axis score") +
  theme_minimal(10) +
  theme(
    panel.grid.major = element_line(colour = "gray 95"),
    panel.grid.minor = element_line(colour = "gray 96"),
    axis.text.x = element_text(angle = 45, hjust = 1),
    axis.ticks.y = element_blank(),
    axis.text.y = element_blank())

plot_pc3 <- ggplot(sig_axes, aes(x = depth, y = PC3)) +
  geom_line() +
  coord_flip() +
  scale_x_reverse(breaks = seq(120, 290, 20)) +
  scale_y_continuous(breaks = seq(-0.4, 0.6, 0.1)) +
  labs(x = element_blank(),
       y = "PC3 axis score") +
  theme_minimal(10) +
  theme(
    panel.grid.major = element_line(colour = "gray 95"),
    panel.grid.minor = element_line(colour = "gray 96"),
    axis.text.x = element_text(angle = 45, hjust = 1),
    axis.ticks.y = element_blank(),
    axis.text.y = element_blank())

plot_pc1 + plot_pc2 + plot_pc3
```

Variation in the principal component axis 1 (PC1) scores across the samples is driven by the relative abundance of *Pantocsekiella ocellata*. This taxon plots at an extremely low value on PC1, while all other taxa have relatively high PC1 axis scores (Figure C.1). Furthermore, the *P. ocellata* species arrow almost exactly aligns with PC1 (Figure C.1), demonstrating that it is highly correlated with this axis and resulting in the PC1 axis scores of the samples almost exactly reflecting the relative abundance of this taxon (Figure C.4). Correlation analysis confirms there is a significant, strong, negative association between the relative abundance of *P. ocellata* and PC1 axis scores ($\rho = -0.999$, $p < 0.001$; Figure C.5).

Whilst this emphasises the dominance of *P. ocellata* in the record, it means that PC1 offers no new information that could be useful for making interpretations of change in the diatom assemblage. As *P. ocellata* is eurytopic and there are no other taxa that have much of an influence on PC1 axis scores, suggesting an environmental parameter that could be driving the variation along PC1 is difficult. PC2 and PC3 axis scores are also each highly influenced by a single taxon, *P. minuscula* and *S. parvus* respectively.

An ordination performed on transformed data that reduces the influence of the very dominant taxa should be able to better pick out variation in moderately abundant taxa and identify if any tend to co-occur with the dominant ones. This could provide more information on drivers of variation in the record than examining variation in one dominant taxon can allow and better enable the identification of latent environmental variables that are driving change in the assemblage.

```r
sig_axes$poc <- ord_data$`Pantocsekiella ocellata`

ggplot(sig_axes, aes(x = poc, y = PC1)) +
  geom_point() +
  labs(x = "P. ocellata (%)") +
  theme_minimal()

# Test for normality
# -----------------
# Null hypothesis - distribution is not different from normal distribution
shapiro.test(sig_axes$poc) # p ≤ 0.05, reject null hypothesis

##
##  Shapiro-Wilk normality test
##
## data:  sig_axes$poc
## W = 0.97401, p-value = 0.003519
shapiro.test(sig_axes$PC1) # p ≤ 0.05, reject null hypothesis
##
##  Shapiro-Wilk normality test
##
## data:  sig_axes$PC1
## W = 0.97275, p-value = 0.002534

# Shapiro-Wilk test confirms non-normally distributed data.
# Must use non-parametric test.

# Spearmans's rank correlation
# ---------------------------
```

```
# Null hypothesis - there is no association
cor.test(sig_axes$PC1, sig_axes$poc,
         method = "spearman",
         exact = FALSE)

##
##  Spearman's rank correlation rho
##
## data:  sig_axes$PC1 and sig_axes$poc
## S = 1469368, p-value < 2.2e-16
## alternative hypothesis: true rho is not equal to 0
## sample estimates:
##        rho
## -0.9987866

# p ≤ 0.05, reject null hypothesis
```

C.3.4 Summary

A preliminary DCA on relative species abundances identified linear species responses and so a PCA was performed. Three significant principal component axes were identified. However, they are each heavily influenced by the relative abundance of an individual taxon. Therefore, they do not provide any new information, other than to highlight the dominance of these individual taxa in the diatom assemblage, particularly *P. ocellata*. Transforming the data to reduce the influence of the very dominant taxa should improve the results. This is performed in the section that follows.

C.4 Ordination of transformed data

C.4.1 Choice of transformation

A square root transformation of the relative species abundances (the combined process of which is known as the Hellinger transformation) was chosen as a compromise in order to reduce the influence of the very dominant taxa without up-weighting very rare taxa. It has an additional benefit over using relative species abundances in that it is not affected by the undesirable double zero problem whereby the absence of a taxon from two samples is considered a sign of similarity Legendre and Gallagher (2001). Although not detailed here, a log transformation produced similar results.

C.4.2 DAZ

Although it is technically not necessary to perform an initial DCA on data that has been transformed in this way (Legendre and Gallagher (2001); Zelený, 2019), the results of a DCA are provided in Table C.3 for clarity. The short length of the longest axis confirms that that a linear ordination method is appropriate.

```
# Run DCA.
dca <- decorana(sqrt(ord_data))

# Extract results.
dca_results <- tibble(
  "Axis" = c("DCA1", "DCA2", "DCA3", "DCA4"),
  "Eigenvalues" = dca$evals,
  "Decorana values" = dca$evals.decorana,
  "Axis lengths" = apply(scores(dca), 2, max) - apply(scores(dca), 2, min)
  )

# Plot table.
kable(dca_results, caption="Summary results of the DCA performed on square-root transfor
med relative species abundances.")
```

C.4.3 PCA

The results of the PCA performed on square root transformed species abundances are displayed in Table C.4. The first two principal component axes can be plotted as a biplot (Figure C.6).

```
# Run PCA.
sqrt_pca <- rda(sqrt(ord_data))

# Extract results.
sqrt_pca_results <- tibble(
  "Axis" = c("PC1", "PC2", "PC3", "PC4"),
  "Eigenvalues" = sqrt_pca$CA$eig[1:4],
  "Cumulative percentage variance explained" = c(
    signif(sum((as.vector(sqrt_pca$CA$eig) / sum(sqrt_pca$CA$eig))[1]) * 100, 4),
    signif(sum((as.vector(sqrt_pca$CA$eig) / sum(sqrt_pca$CA$eig))[1:2]) * 100, 4),
    signif(sum((as.vector(sqrt_pca$CA$eig) / sum(sqrt_pca$CA$eig))[1:3]) * 100, 4),
    signif(sum((as.vector(sqrt_pca$CA$eig) / sum(sqrt_pca$CA$eig))[1:4]) * 100, 4)
  )
)

# Plot table.
kable(sqrt_pca_results, caption="Summary results of the PCA performed on square-root tra
nsformed relative species abundances.")


# Biplot 1: taxa.
# ---------------

par(mfrow = c(2, 1))

# Provide names of select taxa to plot.
pca_taxa <- c("Actinocyclus normanii",
              "Asterionella formosa",
              "Aulacoseira granulata",
              "Pantocsekiella minuscula",
              "Pantocsekiella ocellata",
              "Stephanodiscus parvus",
              "Pseudostaurosira brevistriata",
              "Staurosira venter",
              "Staurosirella pinnata",
              "Achnanthes lacunarum",
              "Amphora pediculus",
              "Cavinula scutelloides",
              "Diploneis marginestriata",
              "Encyonopsis microcephala",
              "Gomphonema pseudotenellum",
              "Gomphonema pumilum",
              "Placoneis balcanica",
              "Sellaphora rotunda")
```

```r
# Create labels for plot.
labels <- c(expression(italic("Actinocyclus normanii")),
            expression(italic("Asterionella formosa")),
            expression(italic("Aulacoseira granulata")),
            expression(italic("Pantocsekiella minuscula")),
            expression(italic("Pantocsekiella ocellata")),
            expression(italic("Stephanodiscus parvus")),
            expression(italic("Pseudostaurosira brevistriata")),
            expression(paste(italic("Staurosira construens"),
                             " var. ",
                             italic("venter"))),
            expression(italic("Staurosirella pinnata")),
            expression(italic("Achnanthes lacunarum")),
            expression(italic("Amphora pediculus")),
            expression(italic("Cavinula scutelloides")),
            expression(italic("Diploneis marginestriata")),
            expression(italic("Encyonopsis microcephala")),
            expression(italic("Gomphonema pseudotenellum")),
            expression(italic("Gomphonema pumilum")),
            expression(italic("Placoneis balcanica")),
            expression(italic("Sellaphora rotunda")))

# Assign label positions.
text_positions <- c(2, 4, 4, 1, 2, 3, 4, 4, 1, 4, 1, 4, 1, 1, 1, 2, 4, 4)

# Put axis scores in separate dataframes.
all_scrs <- scores(sqrt_pca, display = c("sites", "species"), scaling = 2)

species_scrs <- all_scrs$species %>%
  as.data.frame() %>%
  rownames_to_column("taxon") %>%
  # Plot only some species to make it neater.
  filter(taxon %in% pca_taxa)

sites_scrs <- all_scrs$sites %>%
  as.data.frame() %>%
  rownames_to_column("depth")

# Build plot.
xlim <- range(all_scrs[["species"]][,1], all_scrs[["sites"]][,1])
ylim <- range(all_scrs[["species"]][,2], all_scrs[["sites"]][,2])
plot.new()
plot.window(xlim = xlim, ylim = ylim, asp = 1)
abline(h = 0, lty = "dotted")
abline(v = 0, lty = "dotted")
axis(side = 1)
axis(side = 2)
title(xlab = "PC1", ylab = "PC2")
box()

points(sites_scrs$PC2~sites_scrs$PC1,
       pch = 19,
       cex = 0.75,
       col = "gray80")

arrows(0, 0, species_scrs$PC1, species_scrs$PC2,
       col = "gray50",
       length = 0.05,
       angle = 30)

text(species_scrs$PC2~species_scrs$PC1,
     labels = labels,
     cex = 0.8,
     col = "black",
     pos = text_positions)
```

```r
# Biplot 2: samples by DAZ.
# ------------------------

# Assign zones to site scores.
sites_scrs_daz <- sites_scrs %>%
  merge(zones, by = "depth") %>%
  mutate(daz = as.factor(daz))

# Build plot.
xlim <- range(all_scrs[["species"]][,1], all_scrs[["sites"]][,1])
ylim <- range(all_scrs[["species"]][,2], all_scrs[["sites"]][,2])
plot.new()
plot.window(xlim = xlim, ylim = ylim, asp = 1)
abline(h = 0, lty = "dotted")
abline(v = 0, lty = "dotted")
axis(side = 1)
axis(side = 2)
title(xlab = "PC1", ylab = "PC2")
box()

points(sites_scrs_daz$PC2~sites_scrs_daz$PC1,
       col = c("red3",
               "orangered3",
               "darkorange3",
               "darkgoldenrod3",
               "yellowgreen",
               "olivedrab4",
               "seagreen",
               "turquoise4",
               "steelblue4",
               "slateblue3",
               "purple3",
               "violet")[as.factor(sites_scrs_daz$daz)],
       pch = c(0,1,2,3,4,5,6,8,15,16,17,18)[as.factor(sites_scrs_daz$daz)])


legend("topleft",
       legend = levels(sites_scrs_daz$daz),
       title = "DAZ",
       bty = 1,
       col = c("red3",
               "orangered3",
               "darkorange3",
               "darkgoldenrod3",
               "yellowgreen",
               "olivedrab4",
               "seagreen",
               "turquoise4",
               "steelblue4",
               "slateblue3",
               "purple3",
               "violet"),
       pch = c(0,1,2,3,4,5,6,8,15,16,17,18))
```

A comparison of the results with a broken stick model indicates that the first three principal components are significant (Figure C.7). The axis scores of the samples for the three significant principal components have been plotted by depth to explore variation through the core (Figure C.8).

```r
screeplot(sqrt_pca, bstick = TRUE, type = "l", main = NULL)

sig_axes <- data.frame(scores(sqrt_pca,
                              choices = c(1, 2, 3),
                              display = "sites",
                              scaling = 0)) %>%
  mutate(depth = as.numeric(row.names(.)))
```

```r
plot_pc1 <- ggplot(sig_axes, aes(x = depth, y = PC1)) +
  geom_line() +
  coord_flip() +
  scale_x_reverse(breaks = seq(120, 290, 20)) +
  scale_y_continuous(breaks = seq(-0.4, 0.6, 0.1)) +
  labs(x = "Depth (m)",
       y = "PC1 axis score") +
  theme_minimal(10) +
  theme(
    panel.grid.major = element_line(colour = "gray 95"),
    panel.grid.minor = element_line(colour = "gray 96"),
    axis.text.x = element_text(angle = 45, hjust = 1))

plot_pc2 <- ggplot(sig_axes, aes(x = depth, y = PC2)) +
  geom_line() +
  coord_flip() +
  scale_x_reverse(breaks = seq(120, 290, 20)) +
  scale_y_continuous(breaks = seq(-0.4, 0.6, 0.1)) +
  labs(x = element_blank(),
       y = "PC2 axis score") +
  theme_minimal(10) +
  theme(
    panel.grid.major = element_line(colour = "gray 95"),
    panel.grid.minor = element_line(colour = "gray 96"),
    axis.text.x = element_text(angle = 45, hjust = 1),
    axis.ticks.y = element_blank(),
    axis.text.y = element_blank())

plot_pc3 <- ggplot(sig_axes, aes(x = depth, y = PC3)) +
  geom_line() +
  coord_flip() +
  scale_x_reverse(breaks = seq(120, 290, 20)) +
  scale_y_continuous(breaks = seq(-0.4, 0.6, 0.1)) +
  labs(x = element_blank(),
       y = "PC3 axis score") +
  theme_minimal(10) +
  theme(
    panel.grid.major = element_line(colour = "gray 95"),
    panel.grid.minor = element_line(colour = "gray 96"),
    axis.text.x = element_text(angle = 45, hjust = 1),
    axis.ticks.y = element_blank(),
    axis.text.y = element_blank())

plot_pc1 + plot_pc2 + plot_pc3

par(mfrow=c(1,3))
ordiplot(sqrt_pca, choices = 1, display = "species")
ordiplot(sqrt_pca, choices = 2, display = "species")
ordiplot(sqrt_pca, choices = 3, display = "species")
```

Samples with high abundances of *P. minuscula* have low scores on PC1 while those with high abundances of Fragilariaceae have high PC1 axis scores. *P. minuscula* is able to tolerate low light and nutrient availability and has also been associated with stable, stratified lake conditions. The Fragilariaceae are considered pioneer taxa, tolerant of cold, turbulent and turbid conditions. It would seem that the distinguishing feature is the degree of water mixing that they represent.

P. minuscula, the Fragilariaceae and benthic taxa associated with macrophytes in the shallow littoral zone (e.g. *Encyonopsis* spp. and *Gomphonema* spp.) have the lowest PC2 axis scores while *P. ocellata* has the highest. A number of

mesotrophic-eutrophic taxa also plot quite highly along PC2, suggesting variation along this axis could reflect nutrient availability. However, eurytopic *P. ocellata* has the largest influence on this axis, which makes interpretation difficult.

PC3 is once again strongly influenced by *S. parvus*.

C.5 Summary

Ordination of the relative abundance data of the I-284 core produced results that did not aid interpretation of the diatom record. Subsequent ordination methods applied to square root transformed data revealed three significant principal components. PC1 appears to reflect the mixing regime of the lake, PC2 is largely driven by eurytopic *P. ocellata* and appears to reflect lake level or slight nutrient shifts, but it is difficult to interpret because of this taxon's wide environmental preferences. PC3 mainly reflects *S. parvus* abundance.

C.6 References

Legendre, P. & Gallagher, E. D. (2001) Ecologically meaningful transformations for ordination of species data. Oecologia, 129, 271–280.

Leps, J. & Šmilauer, P. (2003) *Multivariate Analysis of Ecological Data using CANOCO*. Cambridge: Cambridge University Press.

Zelený, D (2019) *Analysis of community ecology data in R: common confusions and mistakes*. Available online: https://www.davidzeleny.net/anadat-r/doku.php/en:confusions [Accessed 2021-12-03]
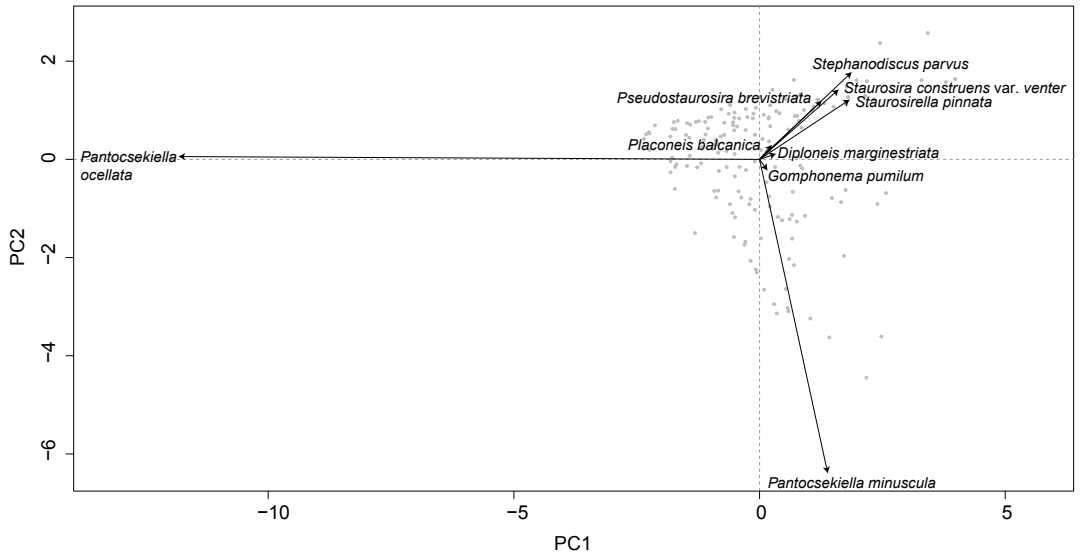
Figure C.1: Biplot of the first two principal component axes from the PCA of the Lake Ioannina diatom record performed on relative abundance data. Samples are plotted as points. Selected taxa are displayed with their axis scores scaled by eigenvalues so that the angles between the arrows represent species correlations and demonstrate which species tend to co-occur together.
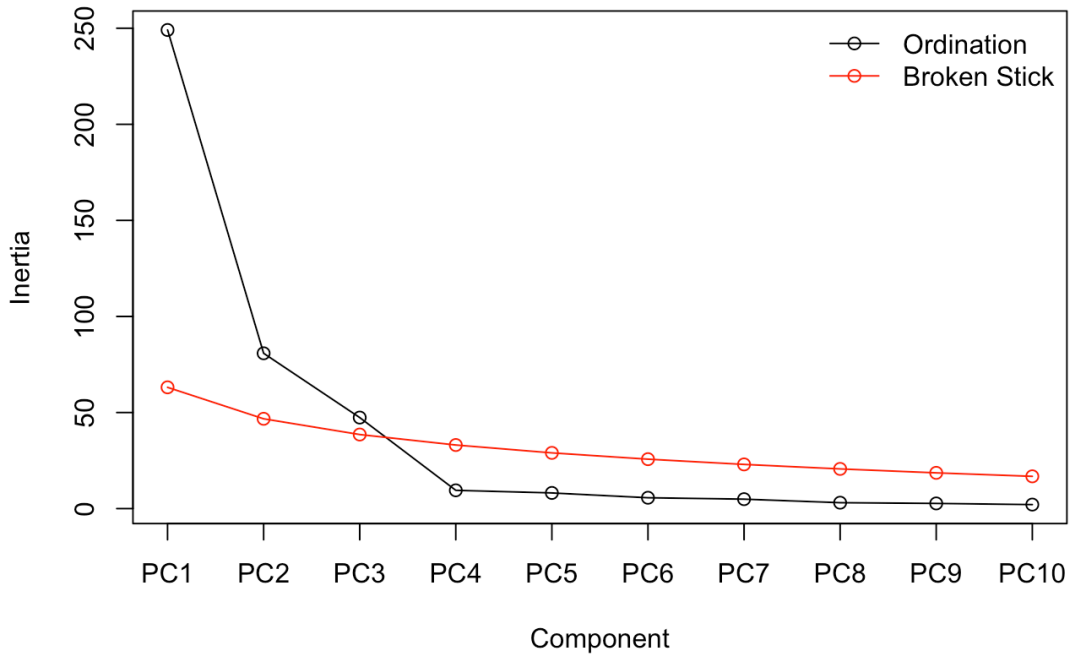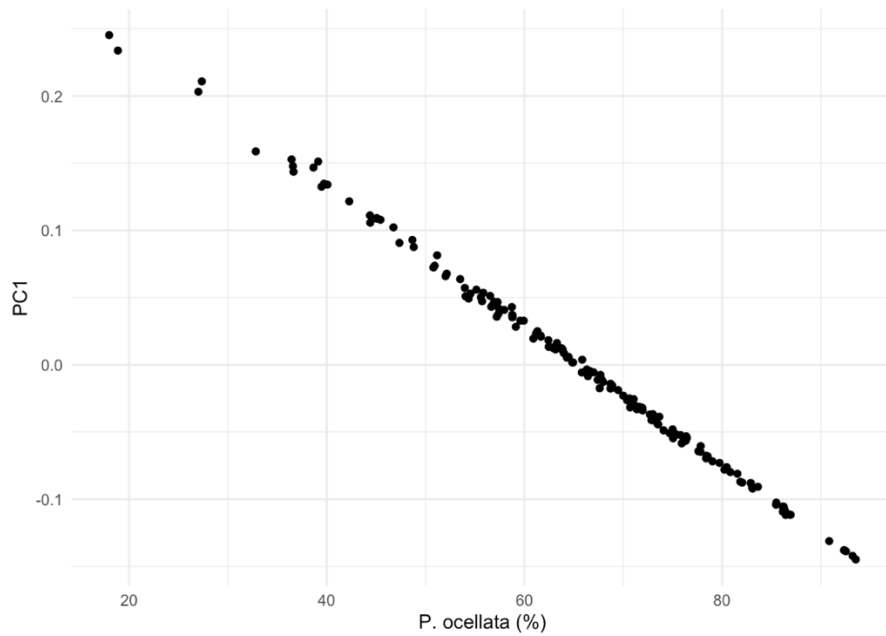

Figure C.2: Comparison of observed reduction in variance with a broken stick model for the PCA performed on relative abundance data.
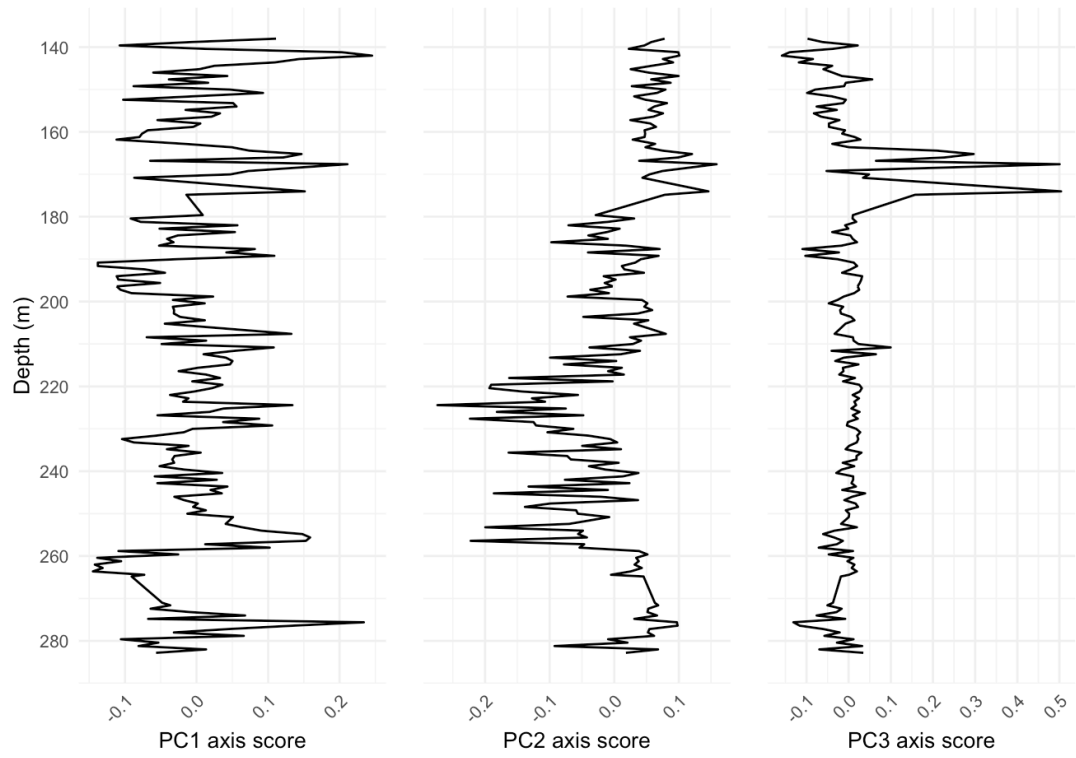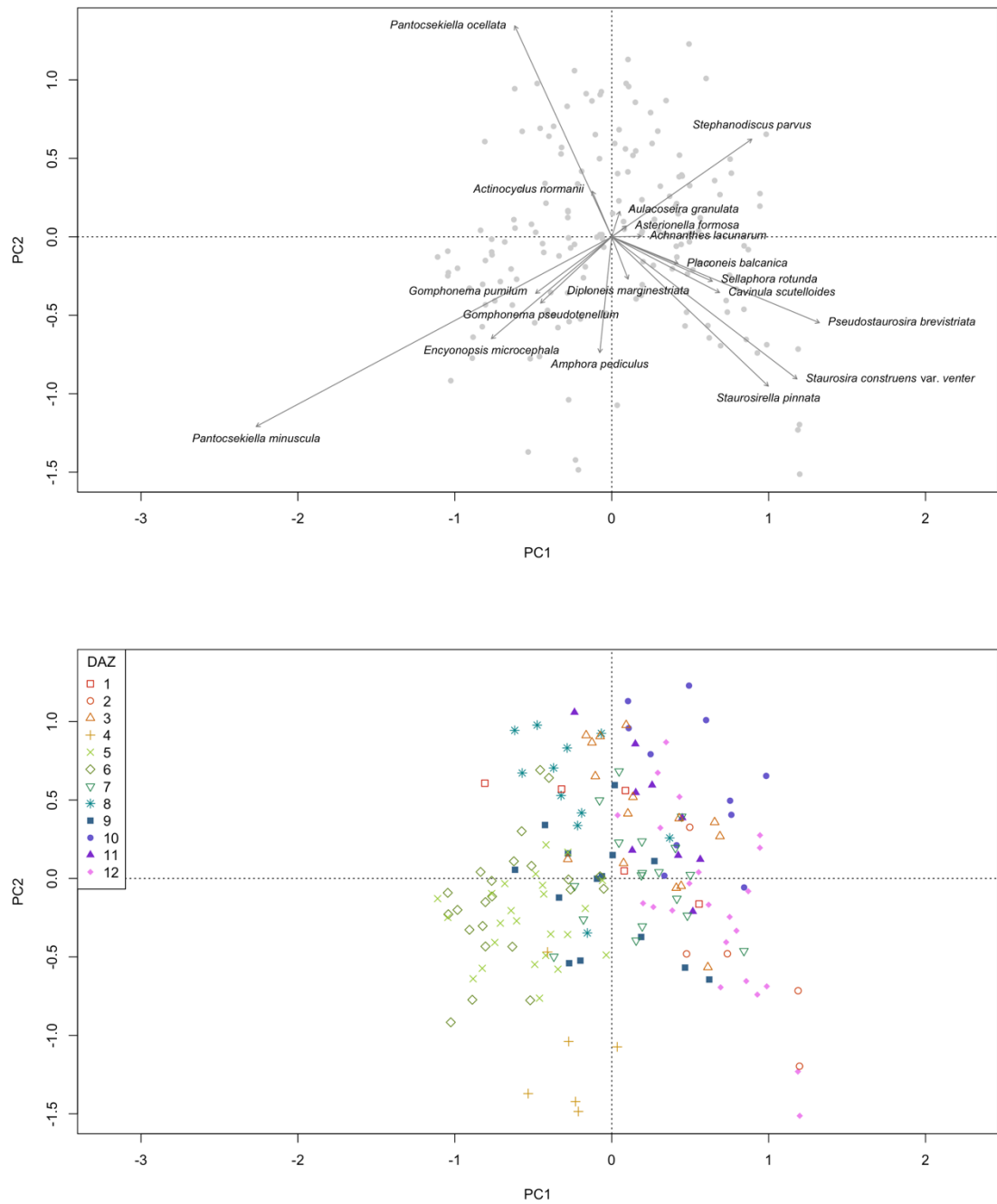
Figure C.3: Significant principal component axes scores plotted by core depth for the PCA performed on relative abundance data.
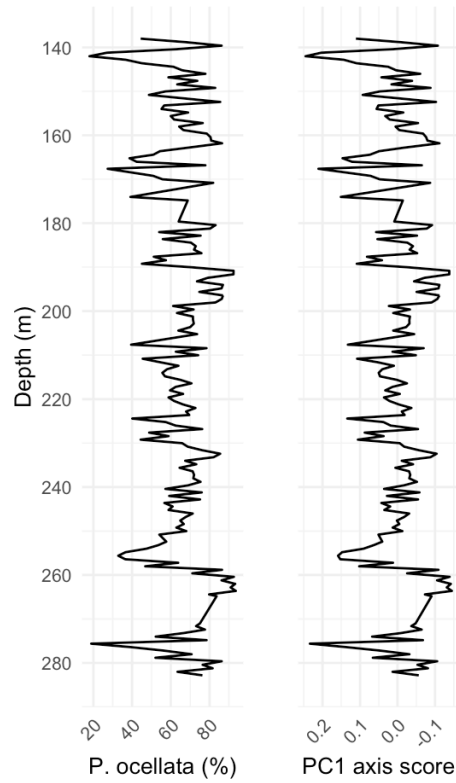
Figure C.4: Comparison of the percentage relative abundances of *P. ocellata* with PC1 axis scores from the PCA performed on relative abundance data.


Figure C.5: Relationship between P. ocellata abundance and PC1 axis scores across all samples for the PCA performed on relative abundance data.

Figure C.6: Biplots of PC1 and PC2 axis scores from the PCA performed on square root transformed data. The top plot displays the species scores while the bottom plot displays the samples by DAZ. Species scores are scaled by eigenvalues so that the angles between the arrows represent species correlations.
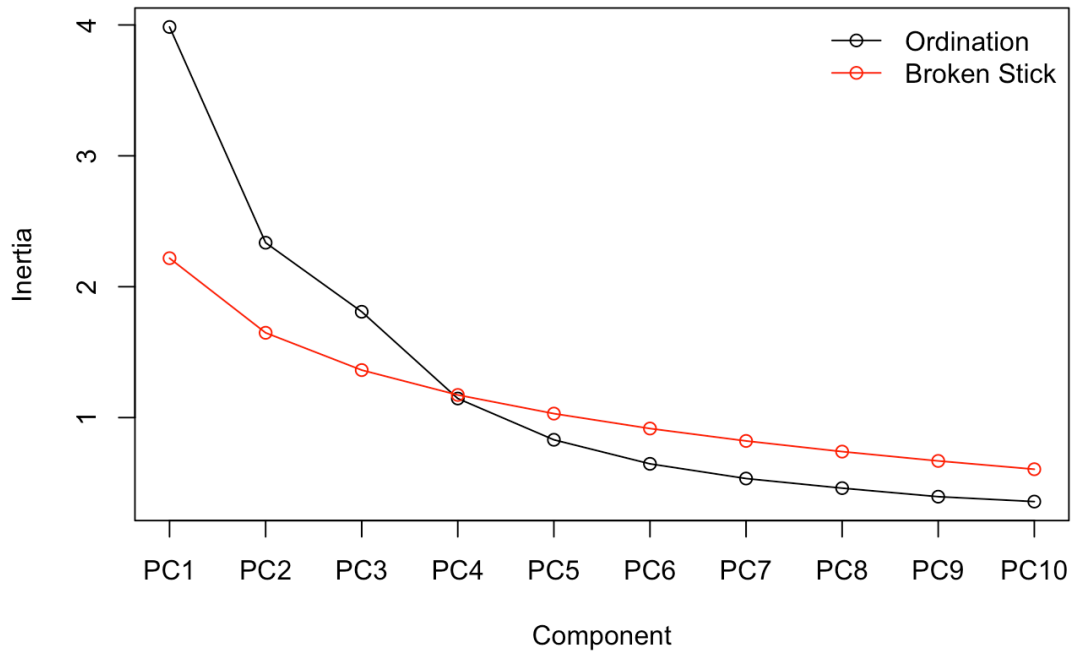
Figure C.7: Comparison of observed reduction in variance with a broken stick model for the PCA performed on square root transformed data.
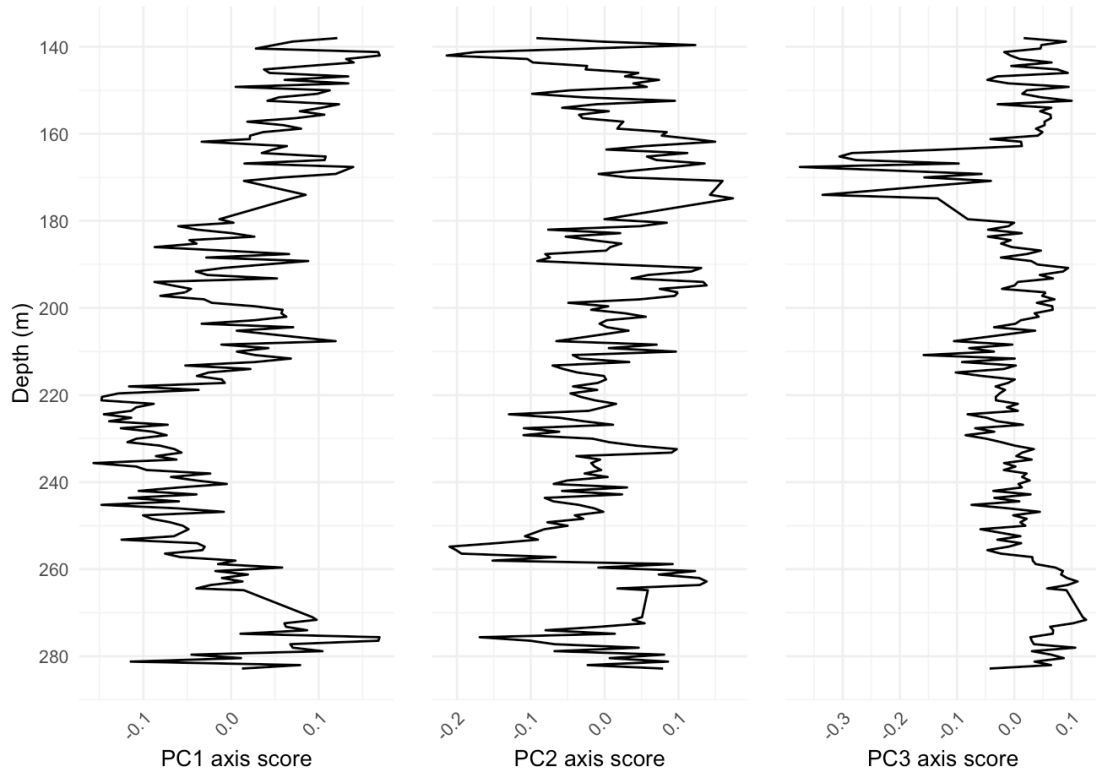
Figure C.8: Significant principal component axes scores plotted by core depth for the PCA performed on square root transformed data.
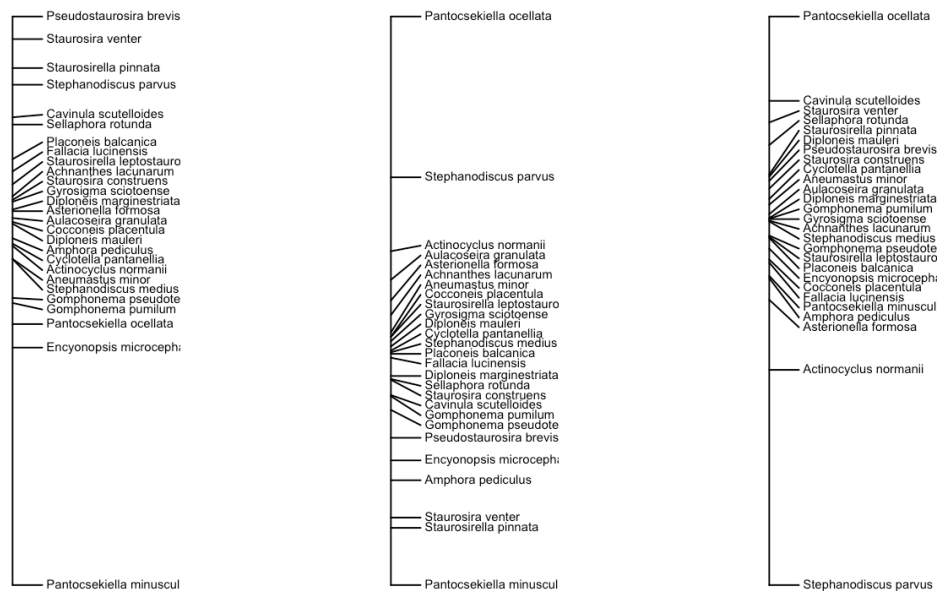
Figure C.9: Relative positions of taxa along the significant principal components for the PCA performed on square root transformed data.

XXXVII

Table C.1: Summary results of the DCA performed on relative species abundances.

Axis	Eigenvalues	Decorana values	Axis lengths
DCA1	0.777	0.266	1.99
DCA2	0.122	0.093	1.98
DCA3	0.071	0.052	1.04
DCA4	0.056	0.035	0.91

Table C.2: Summary results of the PCA performed on relative species abundances.

Axis	Eigenvalues	Cumulative percentage variance explained
PC1	249.09	58.51
PC2	80.83	77.49
PC3	47.89	88.62
PC4	9.51	90.86

Table C.3: Summary results of the DCA performed on square root transformed relative species abundances.

Axis	Eigenvalues	Decorana values	Axis lengths
DCA1	0.149	0.153	1.70
DCA2	0.088	0.078	1.38
DCA3	0.053	0.051	1.20
DCA4	0.06	0.044	1.21

Table C.4: Summary results of the PCA performed on square root transformed relative species abundances.

Axis	Eigenvalues	Cumulative percentage variance explained
PC1	3.98	25.89
PC2	2.34	41.08
PC3	1.81	52.83
PC4	1.15	60.27

Appendix D | Numerical analyses of the Lake Ohrid MIS 7 diatom data using R

D.1 Introduction

This document details the numerical analyses of the Lake Ohrid diatom assemblage during MIS 7, which was performed using R. A cluster analysis is performed in order to split the record into diatom assemblage zones. Ordination is then performed to explore the underlying variation in the diatom assemblage.

D.2 Import packages and data

```r
library(tidyverse)
library(vegan)
library(rioja)
library(ggdendro)
library(tidypaleo)
library(knitr)
library(patchwork)

source("scripts/borders-for-ggplot2.R") # custom theme to remove borders

# Import data
counts <- read_csv("data/csv/imported-counts.csv")
zones <- read_csv("data/csv/imported-zones.csv")

# Set plot theme
theme_set(theme_bw(8))
theme_update(legend.position = "none",
             panel.grid = element_blank(),
             panel.border = theme_border(c("left", "bottom"), size = 0.3),
             panel.background = element_rect(fill = "transparent"),
             plot.background = element_rect(fill = "transparent"))
```

D.3 Analyses

D.3.1 Isolated abundant taxa

The Lake Ohrid diatom assemblage is very diverse, but most taxa are present at extremely low abundances. The first step is to isolate only those that are abundant for these analyses.

```r
min_abundance <- 0.01  # Target proportion out of 1.0.
```

XXXIX

```
abundant_taxa <- counts %>%
  column_to_rownames("depth") %>%
  decostand(method = "total") %>%   # Convert to relative abundance.
  select_if(~any(. >= min_abundance)) %>%
  colnames()

abundant_taxa

##  [1] "Asterionella formosa"       "Cyclotella cavitata"
##  [3] "Cyclotella fottii"          "Cyclotella fottii var. nov."
##  [5] "Pantocsekiella minuscula"   "Pantocsekiella ocellata"
##  [7] "Stephanodiscus minutulus"   "Pseudostaurosira brevistriata"
##  [9] "Staurosira venter"          "Staurosirella pinnata"
## [11] "Amphora pediculus"          "Diatoma ehrenbergii"
## [13] "Placoneis balcanica"
```

D.3.2 Zonation

A CONISS cluster analysis is performed on only abundant taxa following Gordon and Birks (1972). Following Bennett (1996), a broken stick model is used to identify the number of significant zones (Figure D.1). The results indicate there are 4 significant zones. The results of the cluster analysis are plotted as a dendrogram (Figure D.2).

```
# Filter and transform data (into sqrt of relative abundance).
coniss_data <- counts %>%
  column_to_rownames("depth") %>%
  select(all_of(abundant_taxa)) %>%
  decostand(method = "hellinger")

# Calculate distance matrix.
dist_matrix <- designdist(coniss_data,
                          method = "A+B-2*J",
                          terms = "quadratic")

# Perform CONISS cluster analysis.
coniss_results <- chclust(dist_matrix,
                          method = "coniss")

# Plot broken stick model.
bstick(coniss_results, ng = 10)

# Extract data for plotting.
ddata<- dendro_data(coniss_results, type = "rectangle")

# Modify x values so leaves are plotted by depth in core rather than in
# sequential order.
new_x <- approxfun(ddata$labels$x,
                   as.numeric(as.character(ddata$labels$label)))
ddata$segments$x <- new_x(ddata$segments$x)
ddata$segments$xend <- new_x(ddata$segments$xend)

# Plot dendrogram.
ggplot(segment(ddata)) +
    geom_vline(xintercept = c(85.7, 101.1, 102.7),
               colour = "lightgrey") +
  geom_segment(aes(x = x, y = y, xend = xend, yend = yend)) +
  coord_flip() +
  scale_y_continuous() +
  scale_x_reverse(breaks = seq(80, 106, 1)) +
  labs(x = "Depth (m)",
       y = "Total sum of squares") +
  theme_bw(10) +
```

```
  theme(aspect.ratio = 3,
        legend.position = "none",
        panel.grid = element_blank(),
        panel.border = theme_border(c("left", "bottom")),
        panel.background = element_rect(fill = "transparent"),
        plot.background = element_rect(fill = "transparent")) +
  geom_hline(yintercept = 6.6,
             linetype = 2)
```

D.3.3 Ordination

Prepare data

The data are first filtered so that ordination is performed on only abundant taxa as those with low abundances are poorly estimated. They are then converted into percentage relative abundances.

```
ord_data <- counts %>%
  column_to_rownames("depth") %>%
  select(all_of(abundant_taxa)) %>%
  decostand(method = "total", na.rm = "TRUE") %>%
  "*"(100)
```

DCA

Following the approach of Leps and Šmilauer (2003), a preliminary DCA is performed first. The results of the DCA are displayed in Table D.1. At less than three standard deviation units, the length of the longest axis (DCA1) indicates linear species responses as a result of low beta diversity (species turnover). A linear-based ordination is therefore most appropriate for these data.

```
# Run DCA.
dca <- decorana(ord_data)

# Extract results.
dca_results <- tibble(
  "Axis" = c("DCA1", "DCA2", "DCA3", "DCA4"),
  "Eigenvalues" = dca$evals,
  "Decorana values" = dca$evals.decorana,
  "Axis lengths" = apply(scores(dca), 2, max) - apply(scores(dca), 2, min)
  )

# Plot table.
kable(dca_results, caption="Summary results of the DCA.")
```

PCA

The results of the PCA are displayed in Table D.2, and the first two axes are plotted as a biplot in Figure D.3. A comparison of the results with a broken stick model indicates that the first three principal components are significant (Figure D.4). The axis scores of the samples for the three significant principal components have been plotted by depth to explore variation through the core (Figure D.5). The positions of the species along the three significant principal components are plotted in Figure D.6.

Variation along PC1 is mainly driven by the abundances of *P. minuscula* versus *C. fottii* var. 1, as demonstrated by their low and high values respectively along PC1 and by their small angles to PC1 in the biplot of Figure D.3. Hypolimnetic *C. cavitata* also has a high score on PC1, although the large angle from PC1 indicates it does not explain a large proportion of the variation along this axis. With the longest arrow in Figure D.3, *P. minuscula* abundance explains more of the variation than *C. fottii* var. 1. As demonstrated in Figure D.6, all of the other taxa plot closely together near the middle of PC1, so do not explain much of the variation along this axis. Based on the ecology of the taxa explaining most of the variation, PC1 mainly reflects the ratio of hypolimnetic to epilimnetic taxa.

The plot of PC2 by depth (Figure D.5) closely tracks the relative abundance of *P. ocellata*. Samples with high abundances of *C. cavitata* have low values on this axis as *P. ocellata* is at low abundances in DAZ 1. However, *P. ocellata* is eurytopic and will need further investigation and comparison with other proxy data to identify the drivers of its abundance.

The most dominant taxa plot at equal intervals along PC3 (Figure D.3), making it a difficult axis to interpret. The plot of PC3 against depth most closely tracks the abundance of *C. fottii* var 1 with high PC3 scores associated with low *C. fottii* var. 1 abundances. The large decline in PC3 scores over the lower part of the record reflects the disappearance of *C. cavitata* from the record.

```r
# Run PCA.
# --------
pca <- rda(ord_data)

# Extract results.
pca_results <- tibble(
  "Axis" = c("PC1", "PC2", "PC3", "PC4"),
  "Eigenvalues" = pca$CA$eig[1:4],
  "Cumulative percentage variance explained" = c(
    signif(sum((as.vector(pca$CA$eig) / sum(pca$CA$eig))[1]) * 100, 4),
    signif(sum((as.vector(pca$CA$eig) / sum(pca$CA$eig))[1:2]) * 100, 4),
    signif(sum((as.vector(pca$CA$eig) / sum(pca$CA$eig))[1:3]) * 100, 4),
    signif(sum((as.vector(pca$CA$eig) / sum(pca$CA$eig))[1:4]) * 100, 4)
  )
)

# Plot table.
kable(pca_results, caption="Summary results of the PCA.")


# Plot biplot.
# -----------

# Prepare taxa labels.
pca_taxa <- c("Cyclotella cavitata",
              "Cyclotella fottii var. nov.",
              "Pantocsekiella minuscula",
              "Pantocsekiella ocellata")

labels <- c(expression(italic("C. cavitata")),
            expression(paste(italic("C. fottii"), " var. 1")),
            expression(italic("P. minuscula")),
            expression(italic("P. ocellata")))

text_positions <- c(1, 4, 2, 3)
```

```r
# Isolate PC1 and PC2 axis scores.
all_scrs <- scores(pca, display = c("sites", "species"), scaling = 2)

species_scrs <- all_scrs$species %>%
  as.data.frame() %>%
  rownames_to_column("taxon") %>%
  filter(taxon %in% pca_taxa)

sites_scrs <- all_scrs$sites %>%
  as.data.frame() %>%
  rownames_to_column("depth")

# Assign zones to site scores.
sites_scrs_daz <- sites_scrs %>%
  merge(zones, by = "depth") %>%
  mutate(daz = as.factor(daz))

# Plot blank axes.
xlim <- range(all_scrs[["species"]][,1], all_scrs[["sites"]][,1])
ylim <- range(all_scrs[["species"]][,2], all_scrs[["sites"]][,2])
plot.new()
plot.window(xlim = xlim, ylim = ylim, asp = 1)
abline(h = 0, lty = "dotted")
abline(v = 0, lty = "dotted")
axis(side = 1)
axis(side = 2)
title(xlab = "PC1", ylab = "PC2")
box()

# Plot biplot components.
points(sites_scrs_daz$PC2~sites_scrs_daz$PC1,
       col = c("palegreen3", "lightgoldenrod",
               "lightblue3", "salmon")[as.factor(sites_scrs_daz$daz)],
       pch = c(18, 16, 17, 15)[as.factor(sites_scrs_daz$daz)],
       cex = 1.5,)

legend("topleft",
       legend = levels(sites_scrs_daz$daz),
       title = "DAZ",
       bty = 1,
       col = c("palegreen3", "lightgoldenrod", "lightblue3", "salmon"),
       pch = c(18, 16, 17, 15),
       cex = 1.5,)

arrows(0, 0, species_scrs$PC1, species_scrs$PC2,
       col = "gray50",
       length = 0.05,
       angle = 30)

text(species_scrs$PC2~species_scrs$PC1,
     labels = labels,
     cex = 0.8,
     col = "black",
     pos = text_positions)


# Plot significant axes by depth.
# -----------------------------

sig_axes <- data.frame(scores(pca,
                              choices = c(1, 2, 3),
                              display = "sites",
                              scaling = 0)) %>%
  mutate(depth = as.numeric(row.names(.)))

plot_pc1 <- ggplot(sig_axes, aes(x = depth, y = PC1)) +
  geom_line() +
```

```r
  coord_flip() +
  scale_x_reverse(breaks = seq(80, 106, 2)) +
  labs(x = "Depth (m)",
       y = "PC1 axis score") +
  theme_minimal(10) +
  theme(
    panel.grid.major = element_line(colour = "gray 95"),
    panel.grid.minor = element_line(colour = "gray 96"),
    axis.text.x = element_text(angle = 45, hjust = 1))

plot_pc2 <- ggplot(sig_axes, aes(x = depth, y = PC2)) +
  geom_line() +
  coord_flip() +
  scale_x_reverse(breaks = seq(80, 106, 2)) +
  labs(x = element_blank(),
       y = "PC2 axis score") +
  theme_minimal(10) +
  theme(
    panel.grid.major = element_line(colour = "gray 95"),
    panel.grid.minor = element_line(colour = "gray 96"),
    axis.text.x = element_text(angle = 45, hjust = 1),
    axis.ticks.y = element_blank(),
    axis.text.y = element_blank())

plot_pc3 <- ggplot(sig_axes, aes(x = depth, y = PC3)) +
  geom_line() +
  coord_flip() +
  scale_x_reverse(breaks = seq(80, 106, 2)) +
  labs(x = element_blank(),
       y = "PC3 axis score") +
  theme_minimal(10) +
  theme(
    panel.grid.major = element_line(colour = "gray 95"),
    panel.grid.minor = element_line(colour = "gray 96"),
    axis.text.x = element_text(angle = 45, hjust = 1),
    axis.ticks.y = element_blank(),
    axis.text.y = element_blank())

plot_pc1 + plot_pc2 + plot_pc3


# Plot species scores along significant axes.
# ----------------------------------------

par(mfrow=c(1,3))
ordiplot(pca, choices = 1, display = "species", main = "PC1")
ordiplot(pca, choices = 2, display = "species", main = "PC2")
ordiplot(pca, choices = 3, display = "species", main = "PC3")
```

D.4 Summary

CONISS cluster analysis identified 4 significant diatom assemblage zones. A DCA showed linear ordination techniques were appropriate. A PCA identified 3 significant component axes, but all except the first were difficult to interpret. PC1 appears to reflect the ratio of hypolimnetic to epilimnetic taxa.

D.5 References

Bennett, K. D. (1996) Determination of the number of zones in a biostratigraphical sequence. *New Phytologist*, 132, 155–170.

Gordon, A. D. & Birks, H. J. B. (1972) Numerical methods in Quaternary palaeoecology. I. Zonation of pollen diagrams. *New Phytologist*, 71, 961–979.

Leps, J. & Šmilauer, P. (2003) *Multivariate Analysis of Ecological Data using CANOCO*. Cambridge: Cambridge University Press.
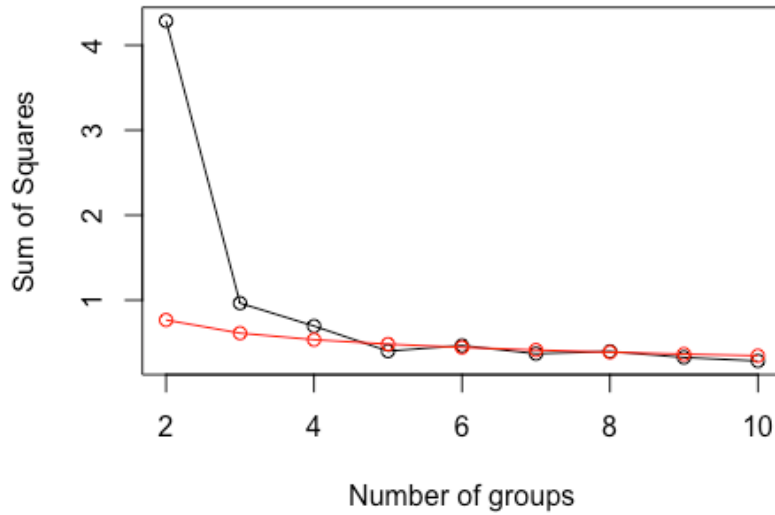
Figure D.1: Comparison of the CONISS results with a broken stick model. The observed reduction in within-group sum of squares is represented by the black line and the model is represented by the red line.
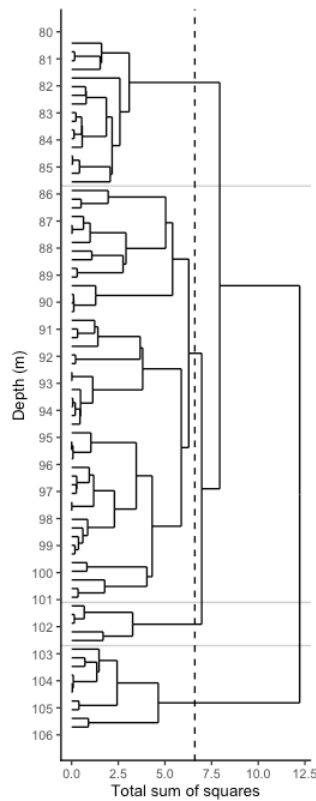

Figure D.2: Dendrogram of CONISS results. The vertical dashed line indicates the total sum of squares value that splits the record into the 4 significant zone. The horizonal grey lines delineate the resulting zones.
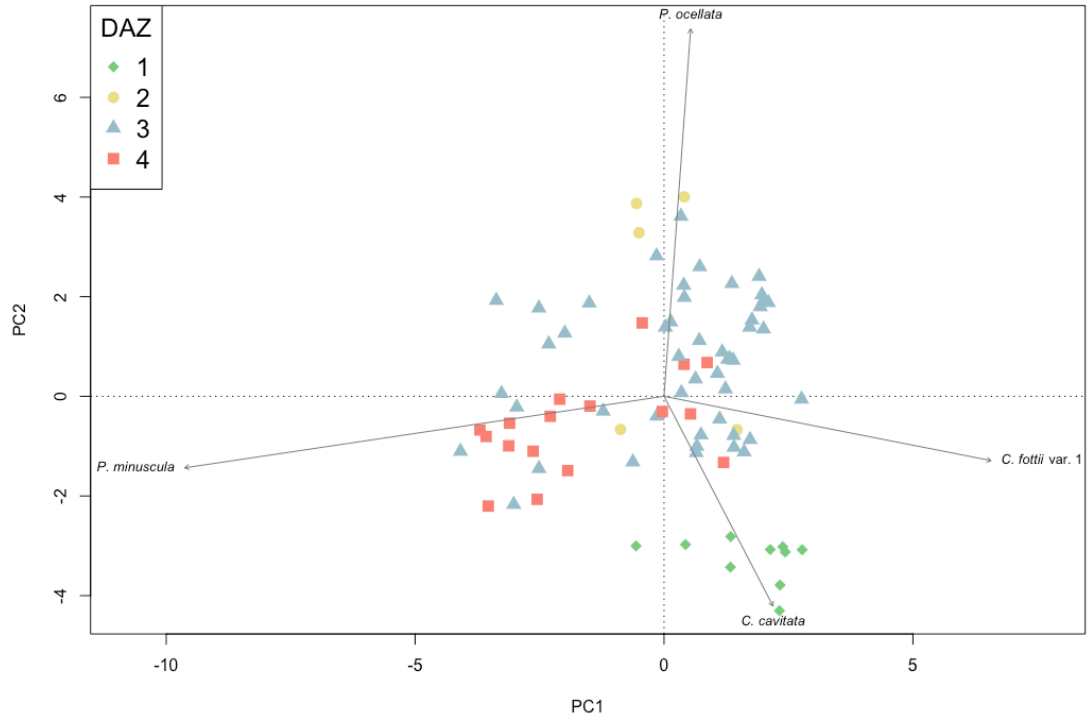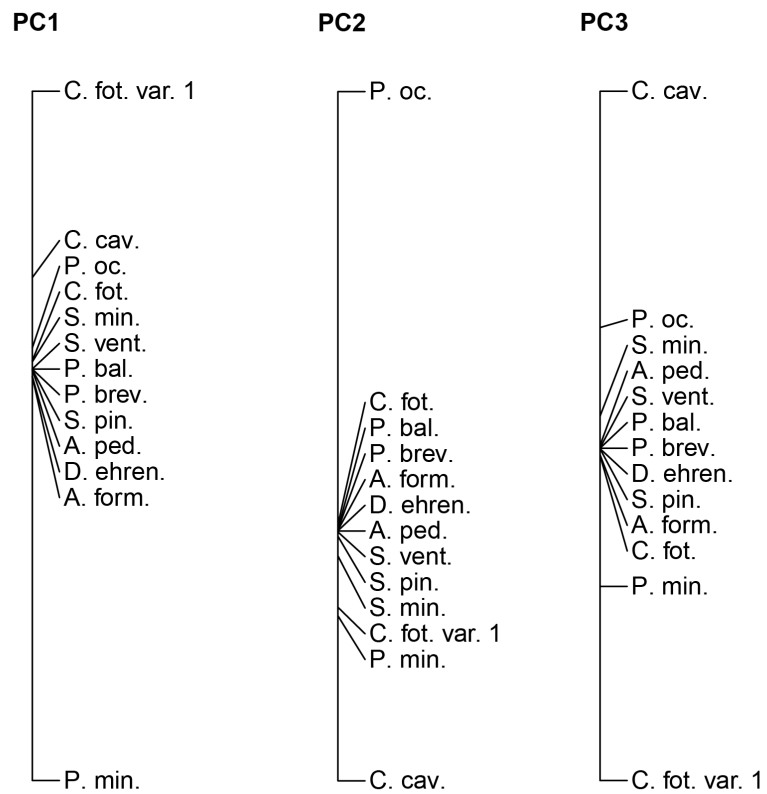
Figure D.3: Biplots of PC1 and PC2 axis scores from the PCA. Species scores are scaled by eigenvalues so that the angles between the arrows represent species correlations.
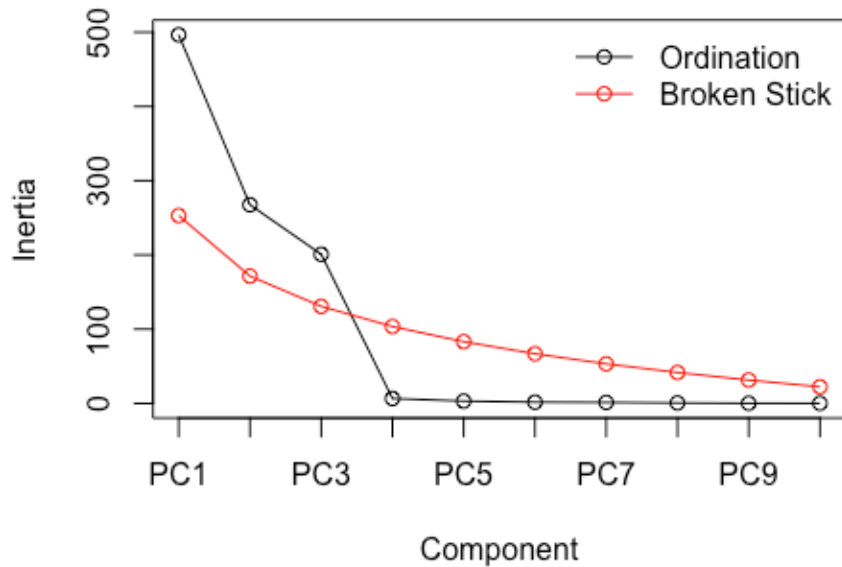
Figure D.4: Comparison of observed reduction in variance with a broken stick model.
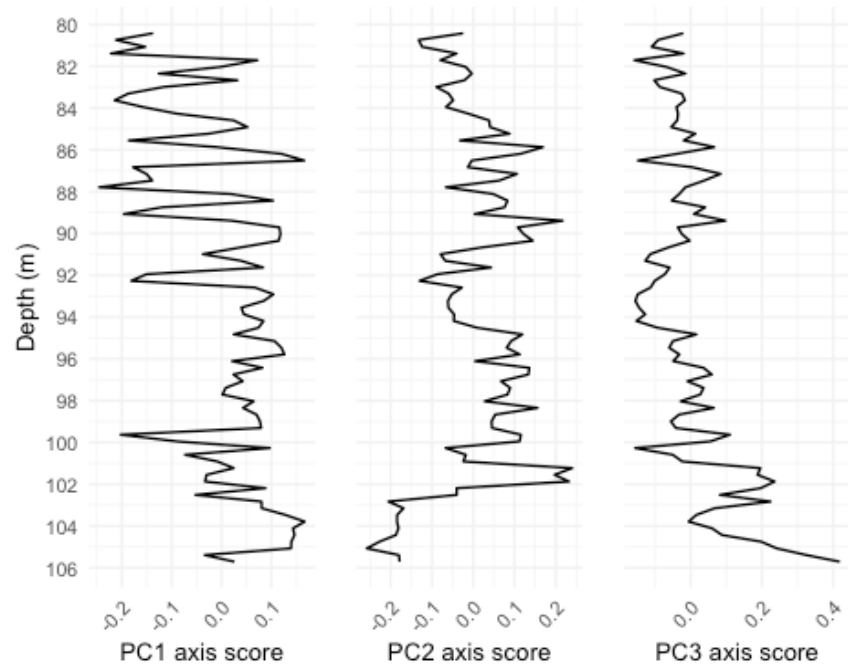
Figure D.5: Significant principal component axes scores plotted by core depth.

Figure D.6: Significant principal component axes scores plotted by core depth.

Table D.1: Summary results of the DCA.

Axis	Eigenvalues	Decorana values	Axis lengths
DCA1	0.268	0.373	1.96
DCA2	0.132	0.078	1.31
DCA3	0.141	0.026	1.56
DCA4	0.129	0.019	1.35

Table D.2: Summary results of the PCA.

Axis	Eigenvalues	Cumulative percentage variance explained
PC1	496.48	50.75
PC2	267.53	78.09
PC3	200.82	98.62
PC4	6.56	99.29